VOLUME XXVI OCTOBER, 1947 NO. 4

THE BELL SYSTEM TECHNICAL JOURNAL

DEVOTED TO THE SCIENTIFIC AND ENGINEERING ASPECTS OF ELECTRICAL COMMUNICATION

AMERICAN TELEPHONE AND TELEGRAPH COMPANY
NEW YORK

50¢ per copy *$1.50 per Year*

THE BELL SYSTEM TECHNICAL JOURNAL

Published quarterly by the
American Telephone and Telegraph Company
195 Broadway, New York, N. Y.

SUBSCRIPTIONS

Subscriptions are accepted at $1.50 per year. Single copies are 50 cents each. The foreign postage is 35 cents per year or 9 cents per copy.

PRINTED IN U. S. A.

The Bell System Technical Journal

Vol. XXVI *October, 1947* *No. 4*

The Radar Receiver

By L. W. MORRISON, JR.

TABLE OF CONTENTS

Introduction

THE spectacular development of radar during World War II remains an outstanding achievement in the history of communications and the allied electronic sciences. With military necessity furnishing the required driving force and through the full interchange of technical knowledge among all interested workers in this field, it has been possible to extend our visual senses far beyond the horizons considered quite inelastic only a few years ago. The potentialities of radar in the peacetime world and the future application of radar design principles and techniques to the communications and allied fields justify a review of some further details of this wartime development.

The performance and design aspects of radar receivers will be considered in this paper. For this purpose, the radar receiver will be defined as that assemblage of components within the radar system which is required to detect, amplify, and present the desired information as gathered at the radar location. The input signals to the radar receiver consist of radio-frequency pulses containing information regarding the area under observation by the radar system, together with coordinate data defining further characteristics of this observed area. The output of the radar receiver is most commonly an optical presentation of this composite information, but in certain applications the output is further converted into electrical or mechanical signals for specific use. In general, the output of a radar receiver is presented in a form capable of immediate analysis and use.

Though the functional boundaries of the radar receiver are by the above definition quite distinct, the exact detailed composition of the receiver and the specific component designs are influenced by a considerable number of factors. The successful performance of a radar receiver is dependent to a large degree on the nicety with which these individual components are assembled into the system as a whole.

A study of the principal factors which influence the design of the radar receiver is presented in the following sections, followed by a more detailed exposition of the principal design aspects of the various components associated within the receiver. Illustrative equipment descriptions are included

where military security permits. All of the specific equipment examples presented here have been chosen from radar systems that have been developed within the Bell Telephone Laboratories and manufactured for the services by the Western Electric Company. This latter limitation excludes many interesting experimental developments which have not been produced in quantity and which have not, therefore, been substantially employed by the services during the war period.

It should be observed that the rapid development and successful employment of radar systems during World War II have come about through the cooperation and coordination of various governmental and military agencies, many research and development organizations, and countless individual workers. It is, therefore, an impossible task to assign individual credit for the details of the development which is here described. Radar has reached its present state of development through the efforts of many, not only those employed specifically on radar projects during the war years, but also those technical workers in the communications and allied fields in the years prior to the war who so adequately supplied the firm basic foundation upon which to build.

1. Radar Receiver Design Considerations

1.1 *The Military Radar System*

The specific use and area of operation of the radar system are two basic factors which exercise a profound influence on the receiver design. It is, therefore, pertinent to consider some common classifications of radar systems as employed during the war years.

A convenient functional classification of military radar systems may be made as follows:

A. *Search or Navigation*

This classification may include warning of the presence of enemy surface vessels or aircraft, navigation by location of landmarks, and reconnaissance.

B. *Missile Control*

This function includes radar systems to control gunfire and release bombs or missiles.

C. *Aircraft Interception*

This classification may be considered as an airborne combination of search and missile control, but is separated here because of the special radar design problems encountered.

As the detailed electrical performance requirements are primarily in-

fluenced by the above functional classification of radar systems, the mechanical equipment design or arrangement is likewise considerably influenced by the area of use of the radar system. As an illustration of this factor, radar systems may be alternatively classified according to the area of operation as follows:

A. *Ground Equipment*

The equipment design of a ground radar system must include provisions for portability, protection against damage in movement over rough terrain, and for operation under extreme weather conditions.

B. *Naval Surface Vessel Equipment*

Radar equipment employed on surface vessels is subject to extreme atmospheric corrosive conditions, severe shock from gunfire and, in some cases, partial immersion in sea water. Large naval vessel installations often involve extreme distances between the location of the various components of the radar system.

C. *Airborne Equipment*

Mechanical equipment features for aircraft use must include provision for operation over rapidly fluctuating conditions of temperature and atmospheric pressure. Vibration conditions coupled with strict weight requirements result in many additional problems from the equipment designer's standpoint.

Figures 1, 2, and 3 indicate typical radar equipments employed on the ground, sea, and air, some component designs of which will be reviewed in later sections of this paper.

1.2 *The Function of the Radar Receiver*

The basic function of a radar receiver is to translate and present the information received at the radar location in a desirable form. This requires that the receiver contain provisions to enable:

A. Conversion of the received signals, originally of a microwave frequency character, to signals in a frequency region more convenient to utilize.

B. Amplification of the extremely low energy signals as received to amplitudes useful to the observer.

C. Correlation of all other available pertinent data with the received microwave signals to allow determination of the complete coordinates and other desired characteristics of the target under observation.

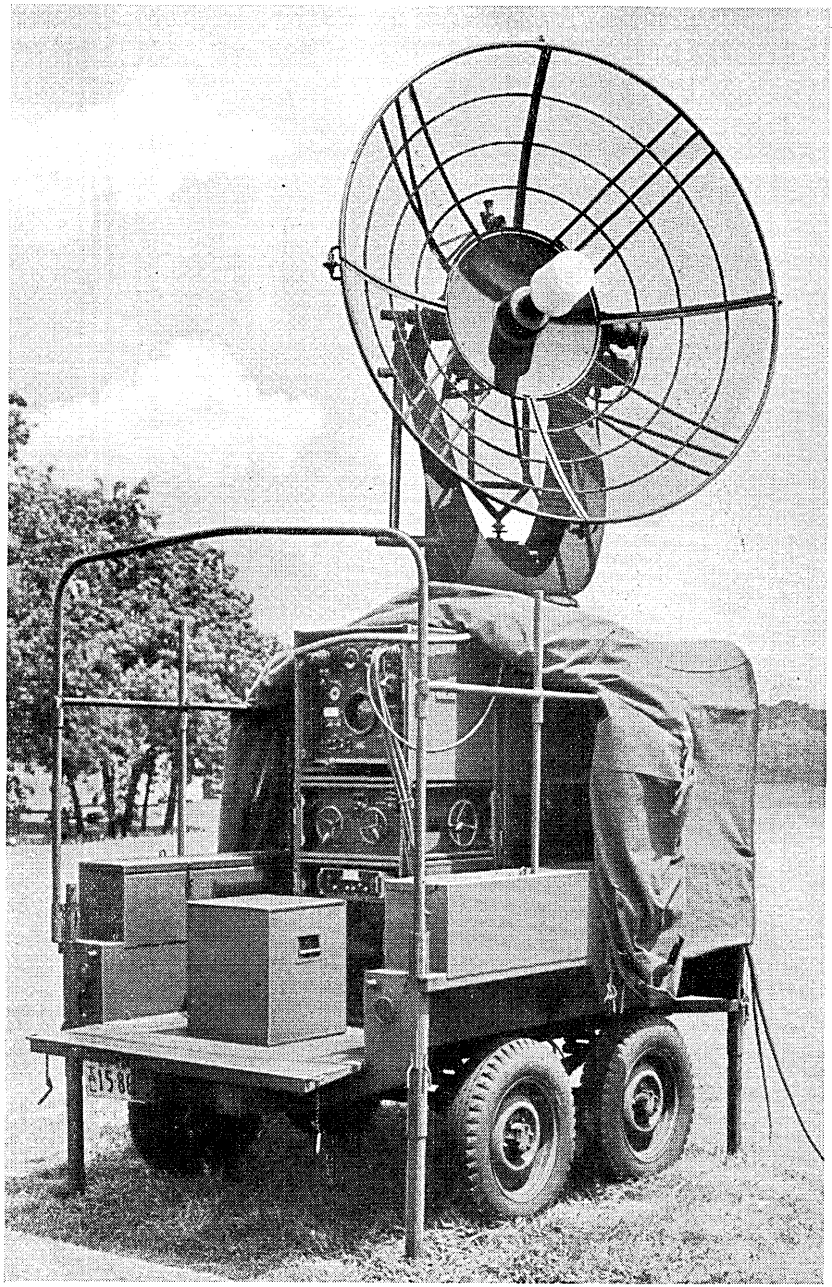

Fig. 1.—Radar Equipment—Mark 20. This mobile equipment operating at 1000 mc is employed for searchlight control purposes.

D. Presentation of all desired information to the observer in a form capable of immediate analysis and use.

With these functional requirements in mind, it is in order to examine the character of the information available at the input and that required at the output terminals of a radar receiver.

1.21 *Characteristics of the Radar Receiver Input Signal*

In general, the signal radiated by the radar transmitting antenna and received by the receiving antenna consists of intermittent pulses of energy

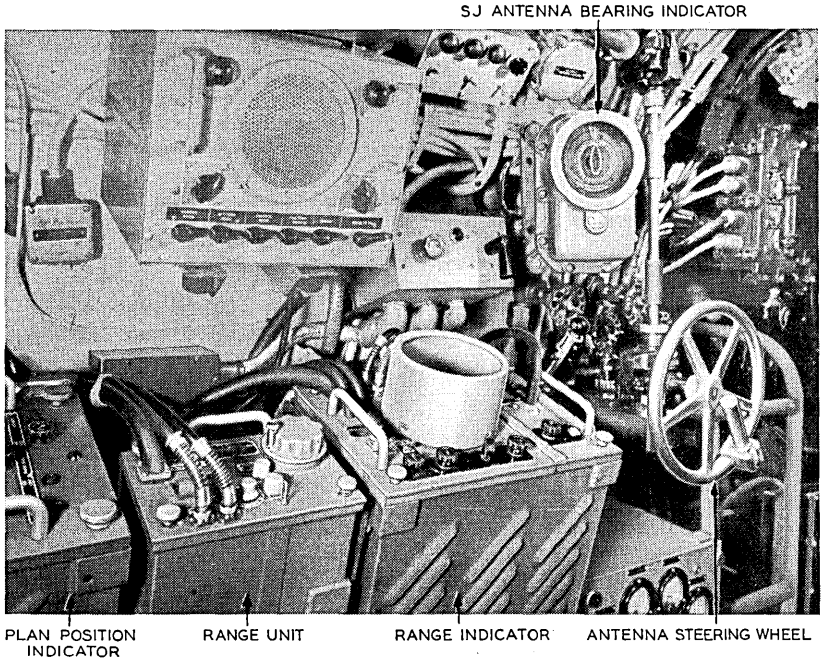

Fig. 2.—SJ Submarine Radar. Operating position of radar equipment in conning tower of U. S. Navy submarine.

at microwave frequencies. The methods employed in the generation and propagation of these radar microwave signals have been described elsewhere.[1, 2] For our purpose, it suffices to state that microwave frequencies extending from 700 mc to 10,000 mc are commonly employed. Pulse widths of 0.5 microsecond to 5 microseconds at repetition rates extending from 100 pps to 2000 pps are encountered in modern military radar systems, the

[1] "The Magnetron as a Generator of Centimeter Waves," J. B. Fisk, H. D. Hagstrum and P. L. Hartman, *Bell System Technical Journal*, Vol. XXV, April 1946.

[2] "Radar Antennas," H. T. Friis and W. D. Lewis, *Bell System Technical Journal*, Vol. XXVI, April 1947.

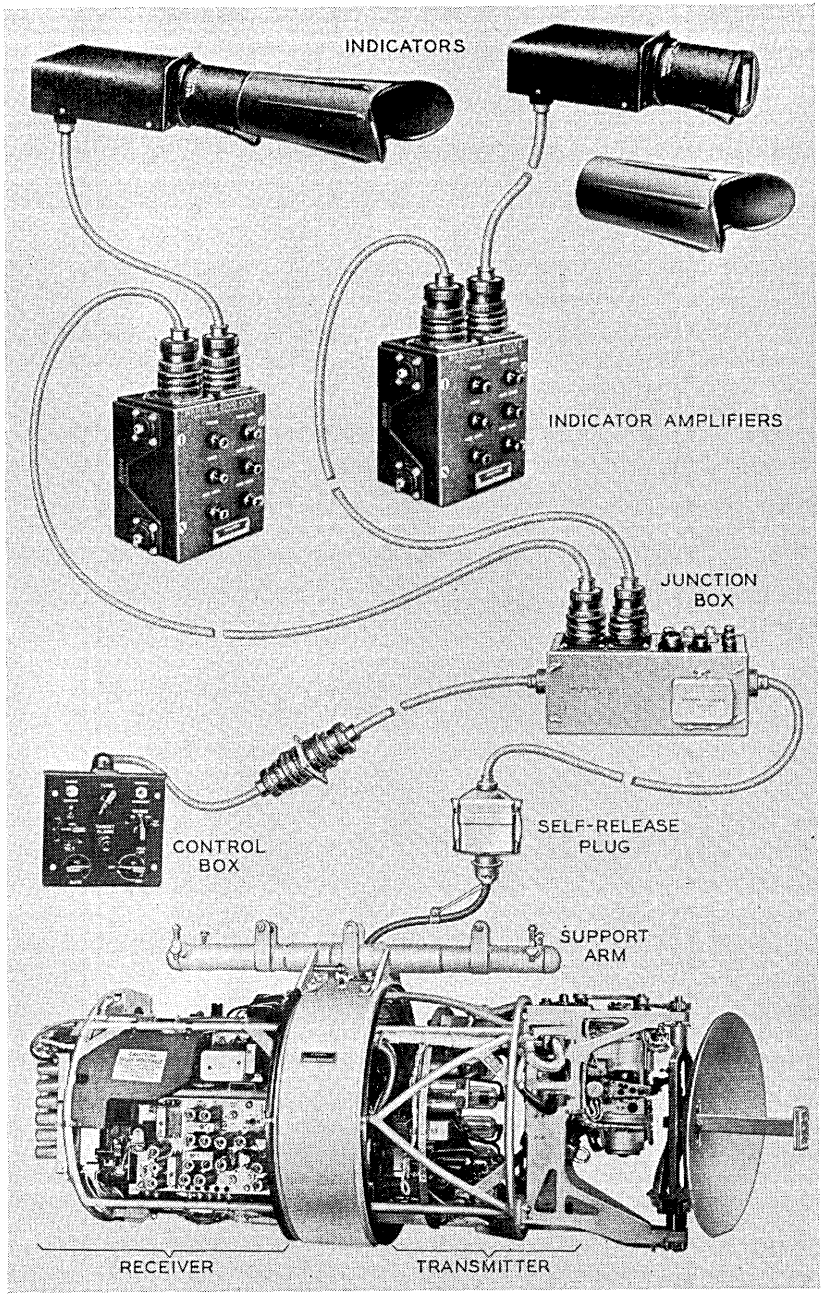

Fig. 3.—Components of Lightweight AN/APS-4. Airborne search and interception radar equipment.

exact choice of these parameters being dictated by the specific application of each type of equipment.

It has been customary to employ a common antenna system for both the transmitting and receiving functions, the necessary protection of the sensitive receiver input circuits from the high power transmitted pulse being furnished by a TR switch or tube.[3] The gas discharge TR switch assembly attenuates the energy fed to the input terminals of the receiver for the duration of the microwave outgoing pulse. At the time of decay of this transmitting pulse, the TR switch is arranged to offer low attenuation between the antenna and the receiver to any received signal.

The received microwave signal will be found to fluctuate in amplitude between extremely wide limits. This amplitude characteristic of a received radar signal is affected by the size and composition of the target, the power of the radiated outgoing pulse, the distance or range to the target, and miscellaneous propagation effects. Military requirements necessitate designing the radar receiver to perform successfully with the minimum received signal, while not unduly compromising this performance when signals of relatively high energy content are encountered.

Other characteristics of the transmitted microwave signal, such as pulse shape and repetition rate, are chosen to enable maximum performance to be attained for the specific application to be covered. The proper treatment of these miscellaneous characteristics of the radar signal is of basic concern to the receiver designer.

The primary basic information which can be derived from the characteristics of the received radar signal itself consists of data concerning the range to the target under observation. This range data is made available by a measurement of the elapsed time between the departure of the outgoing pulse and its return after reflection from the target and consideration of the velocity of electromagnetic wave propagation.

To determine the complete coordinates of a radar target, correlation of the range information, as determined above, and the direction of radiation from the antenna is necessary. Signals containing information as to the instantaneous attitude of the antenna with respect to chosen reference axes are, therefore, to be considered as essential inputs to the radar receiver.

Though the natural coordinate system of radar is of a polar form, many specific applications of radar systems require conversion of this information into other forms more convenient of use. For example, while in gun-pointing radar applications, it is desirable to present the final information in a polar coordinate form, corresponding to the aiming axes of the guns in many airborne radar bombing systems, it is necessary that the presentation be

[3] "The Gas-Discharge Transmit-Receive Switch," A. L. Samuel, J. W. Clark and W. W. Mumford, *Bell System Technical Journal*, Vol. XXV, January 1946.

made in terms of rectangular or other convenient coordinate systems referred to the ground itself. In certain applications, the characteristics of the display or presentation device requires that coordinate conversion functions be included within the radar receiver. The conversion and proper presentation of all radar system coordinate information will, therefore, be considered a necessary function of the radar receiver.

Additional forms of radar receiver input signals encountered are those primarily associated with the specific application of the radar system. Reference coordinate axes data obtained from compasses or gyroscopes are among the most common of these. In gun-fire control and bombing applications a considerable quantity of computed data must be accepted by the receiver. These data may include predicted quantities which must be presented in addition to the usual received present-time radar information. In the case of airborne radar systems, provision must be included to properly display navigational beacon and identification signals. The beacon is operated by the radar transmitter in the aircraft and returns a coded signal at a frequency slightly removed from the normal radar band. All aircraft radar receivers are required to adequately detect and properly display this information. It has also become common practice to require provision within the radar receiver for display of interrogator-response signals as employed for military identification purposes. The identification equipment (IFF) proper is not a radar system component and, therefore, it will not be considered here.

1.22 *Character of the Output of a Radar Receiver*

The output of a radar receiver is required to be available to the observer in a form which will permit immediate analysis and use of a maximum of the received information. The consideration of some additional characteristics of the radar information available and the military applications will furnish a basis for choice of presentation means in the receiver.

Because of the inherent pace of the constantly changing tactical military scene, the basic requirements imposed upon the radar presentation device are severe. For example, the use of radar in an aircraft, or on the ground or sea directed against aircraft involves a process of obtaining information on targets having relative velocities upward of 500 feet per second. If the radar system under consideration is being employed to furnish data for the release of bombs or to direct gunfire, a fraction of a second represents dimensions comparable to the target size. Such considerations adequately emphasize the extreme importance of retaining the "immediacy" characteristic of the information through the presentation device.

Another factor influencing the design of the presentation components in a radar receiver is found in consideration of the extreme complexity of the

received radar information. This complexity is created out of the comparatively limited resolution available and from the military need for presentation of detailed information concerning large areas during small time intervals.

The effect of limited resolution on the choice of presentation means of a radar receiver can be appreciated by considering the following. The microwave pulse employed in modern radar systems has a duration in time corresponding in linear range dimensions of hundreds of feet, while the beam width of commonly employed radar antenna systems likewise includes hundreds of feet of target at useful ranges. Thus, the inherent radio-frequency "resolution" is limiting to an extent that, while it usually enables one to determine the coordinates of the centroid of the target, it will not furnish adequate information as regards the exact size or shape characteristics of the target. The radar response of an area of military interest is a function of electrical conductivity and other related characteristics, rather than of the military importance of the target. These factors indicate strongly that the human observer must be required to supply a certain function of interpretation, and that the chosen radar presentation means should be such that this is possible. An effective illustration of this situation is found in the descriptive term "navigation by constellation" which was common among the radar operators in the long-range bombing forces. Here the navigation to and the orientation with respect to the military objective was often possible only through the interpretation of strong radar responses from known landmarks. Offset bombing, where the bombing radar operator carried out his observations on a satisfactory radar target in the vicinity of the final objective and introduced the known offset coordinates in the computed release point so as to strike the military objective, was found to be a successful method of partially overcoming this basic limitation of World War II radar equipments.

Modern warfare is concerned with rapid movement and extremely large area operations. The display of continuous information regarding these large areas is a basic military requirement of the modern radar system. For specific military applications the radar viewpoint may often be restricted to selected limited areas with increased demands on detail and on reproduction of changing information during small time intervals.

The above considerations have led to a choice of presentation means for the military radar system which is of an optical nature and has the essential characteristics of motion pictures. Such a display of complex information, in general, allows the observer to concentrate his attention at any time on any desired region of interest, to orient himself with respect to the broad features of the complete area, and to be cognizant of changes in the scene as they occur.

The cathode-ray tube has been most universally employed as the display device in the modern radar system. The incoming electrical information from the various receiver inputs is here electronically converted into a visual form capable of being modified over small intervals of time as the change in the radar scene occurs. Multiple presentations having various map-scale factors are found in many modern radar systems to enable detailed examination of a small magnified target area, while retaining the ability to observe the broad area features at will.

The use of radar for the purpose of control of gunfire, release of bombs, or steering of a vessel or aircraft requires that essentially continuous coordinate information be transmitted from the radar observer to the device under his control. This is usually accomplished through the registration of mechanical or projected electronic markers upon the visual radar display, this process of successive alignment furnishing the required information to the controlled device. In the case where automatic means of maintaining coincidence between marker and target are employed it should be observed that the original selection of the target and the initial coincidence adjustment still remains a matter for interpretation on the part of the human operator, and here again the visual radar display form is desirable.

The presentation means of a radar receiver has, therefore, been chosen to allow complete display of the data as quickly as it is received and in a form most convenient to the understanding of the human operator. In a broad sense, the radar system output terminal conditions and requirements are similar to those encountered for any communication system i.e. to supply the human observer with all the information available to the system in a form which will permit maximum usefulness with a minimum of delay.

1.3 *Composition of the Radar Receiver*

For convenience in the discussion to follow, the generalized radar receiver will be partitioned as shown in Figure 4. This particular choice of component division is somewhat arbitrary, but is chosen because of its functional simplicity. Mechanical, and in some cases electrical, conditions encountered in any particular radar system design often indicate physical arrangements which will differ considerably from the arrangement illustrated.

The converter component of the radar receiver has, as its primary function, the conversion of the received microwave signal to an intermediate frequency region where further amplification and discrimination is possible. The converter consists of a beating oscillator operating in the microwave frequency region and a nonlinear element, which at the higher radar frequencies consists of a point-contact crystal element. At the lower radar

frequencies it is customary to employ vacuum tube radio-frequency amplifiers preceding the converter element, and in these cases, similar vacuum tubes are employed as the nonlinear element. The output frequency of the converter commonly ranges from 30 mc to 100 mc. Because of the comparative difficulties experienced in the transmission of microwave energy over transmission lines or waveguides as contrasted with the problem at the lower intermediate frequency region, it is standard practice to locate the converter in close proximity to the antenna and transmitter portions of the radar system.

The intermediate frequency (IF) amplifier and associated second detector unit following the converter in Fig. 4 is required to obtain the necessary

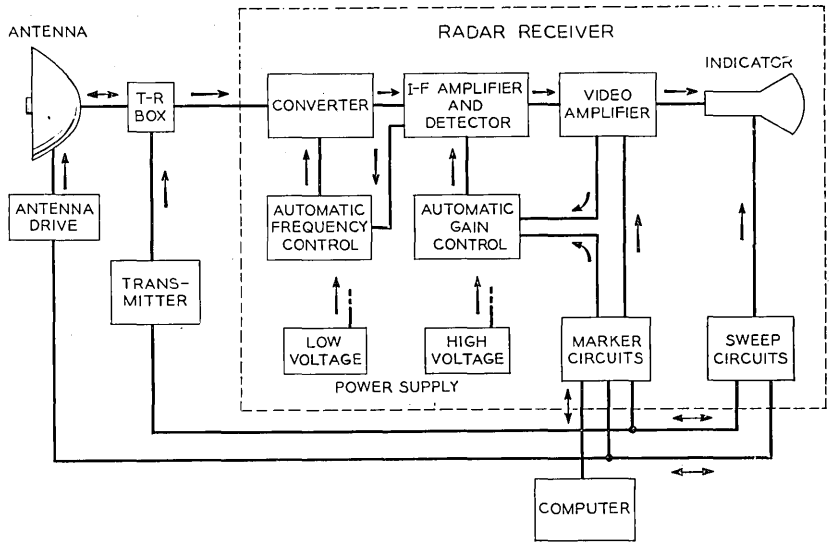

Fig. 4.—Schematic diagram of principal components of a military radar receiver.

amplification to the wanted signal, to supply discrimination against unwanted signals, and to finally convert the desired signal to a video form for presentation purposes. The usual gain required of a modern radar intermediate amplifier is of the order of 100 db. The band width of the IF amplifier is usually chosen between 1 mc and 10 mc depending on the specific radar system requirements. The techniques of construction developed for high gain radar IF amplifiers have resulted in compact component designs which are complete units in themselves, capable of being integrated into various radar systems.

The video amplifier characteristics are dependent to a large degree on the particular type of display system associated with it. Its primary func-

tion is to amplify the video signal output of the second detector, together with some other signals to be impressed on the cathode-ray tube. In this field the principles of design follow closely those developed for television prior to the war. Band widths of the order of 1 mc to 5 mc are commonly employed and output voltages ranging from 10 volts to 250 volts are required by the cathode-ray tube. Controllable nonlinear amplitude-gain characteristics are occasionally included in these video circuits to enhance the contrast or improve the apparent signal-to-noise performance.

The display device universally employed in modern military radar systems is the cathode-ray tube. The electro-optical response characteristics of this device may be chosen over quite wide limits to suit the specific needs of a particular system. In slow scanning systems, use of long time-decay optical characteristics of the sensitive screen is found to be advantageous, while in other cases of high-speed scanning, shorter persistence-type screens are employed. Screen diameters commonly employed range from 2″ to 12″ with a wide variety of color characteristics available to fit the detailed requirement of the radar system. A variety of radar presentation forms are employed to display most conveniently the received information for the specific application at hand. These display types differ primarily in the manner in which the radar field coordinates are presented. The deflection methods employed may be of an electrostatic or magnetic nature with combinations of each occasionally encountered.

The sweep circuit components of the radar receiver generate the electrical time wave forms necessary to display the received data properly. Here again the television art has supplied a technical background for these specialized electronic circuits. The great number of display types employed, requiring varied wave forms, has resulted in the development of a myriad of specialized sweep circuits whose apparent complexity is the result of varied combinations of elemental electronic circuits.

The range and time-marker circuits are required to interpret the coordinate data available to the receiver and to prepare this data for display in the desired form. Here again, television techniques have been employed and enlarged upon as the radar systems became more complex. A large number of specialized electronic circuit forms has resulted.

The automatic frequency control (AFC) and automatic gain control (AGC) components of a radar receiver have a function not unlike those elements found in most radio-communication systems. The automatic adjustments of the tuning and gain of the radar receiver has contributed greatly to the successful employment of radar under practical military conditions and have now become practically indispensable in the art. The circuit designs follow, in general, the techniques previously employed in radio communications though it will be observed that the character of the signal

and the close association of the receiver and the transmitter in the radar system introduces some additional new considerations.

The power supply components are shown divided into two types "low voltage" and "high voltage." This is a convenience which is desirable because of the different design problems encountered and the quite different equipment and circuits employed. The low d-c voltages required for the operation of the electronic components of a radar system vary from 100 volts to 500 volts with both polarities with respect to ground often required. The cathode-ray tube and "keep alive" circuits of the TR tube require voltages from 1000 to 7000 volts usually at low current. The voltage regulation of these power supply components to permit stable radar system operation under the extreme and variable military operating conditions encountered presents a problem of considerable magnitude to the radar receiver designer.

2. Radar Receiver Component Design

2.1 *The Radar Receiver Input Circuit*

The conversion of the received microwave radar signal to a lower frequency region where more efficient amplification is possible represents an extremely important function of the radar receiver. The basic military requirement of radar, that of providing the greatest possible useful sensitivity, depends fundamentally on the efficient handling of the low-energy microwave received signal in the input of the radar receiver. The microwave character of the received signal and the extremely low amplitudes encountered contribute to the difficulties of radar input circuit design.

The techniques of microwave transmission available to the communications engineer have but recently been developed and are at this time still extremely limited in comparison to those methods commonly employed at the normal radio frequencies. Even short physical connections required between elements in the microwave region become "electrically long," a matter of several wavelengths in the usual case, and here the design problem becomes acute. Network element of inductance, capcitance, and resistance are not available in the form so efficiently employed at the lower frequencies. Waveguides and cavities at radar frequencies replace them, and the design of selective frequency networks in the microwave region becomes a matter of precise arrangement and control of complex mechanical forms.

Suitable means for vacuum tube amplification at frequencies above 1000 mc have not been available to date; this represents another extremely restricting situation for the radar receiver designer.

2.11 *Input Signal Characteristics*

The low amplitude of the signal at the input terminals of the radar receiver requires that this signal be efficiently utilized. The power of the received signal at this point under somewhat idealized free space assumptions is given by the following:

$$P_R = \frac{G^2 P A_\epsilon^2}{16\pi^2 D^4}$$

Where G = Power gain of common transmitting and receiving antenna
P = Transmitted power of radar system
$A\epsilon$ = Equivalent flat plate area of target (This represents an equivalent flat plate normal to the incident beam which reradiates all impinging energy)
D = Range to the target.

The two following sample computations are illustrative of the military radar system conditions:

1. Naval Vessel Search Radar System
   Frequency = 3000 mc
   Target range = 25 nautical miles
   Target-Destroyer (Effective flat plate area = 0.03 sq meter at 3000 mc)
   (This value has been determined from a study of target response with military radar systems)
   Power gain of Antenna = 30 db
   Transmitter Peak Power = 100 kw
   Received Peak Power = 13×10^{-14} watts
2. Airborne Search Radar System
   Frequency = 10,000 mc
   Target Range = 70 nautical miles
   Target-Destroyer (Effective flat plate area = 0.2 sq meters at 10,000 mc)
   Power Gain of Antenna = 30 db
   Transmitter Peak Power = 100 kw
   Received Peak Power = 11×10^{-14} watts

A reduction of the available received signal power, as computed above, is to be expected in practice due to multiple path effects and absorption and refraction effects over the propagation path.

2.12 *Input Circuit Noise Considerations*

While it is possible to conceive of providing sufficient gain within a radar receiver to meet any desired sensitivity requirement, this sensitivity cannot usefully be employed beyond certain limits as determined by the amplitude

of the noise disturbances at the input terminals of the receiver. Noise disturbances may be defined as the resultant unwanted interfering electrical energy at the point under consideration and includes contributions due to atmospheric disturbances, unwanted radiation from adjacent electrical equipment, microphonic disturbances, and noise due to vacuum tubes and thermal agitation. At microwave frequencies we are usually concerned only with the thermal agitation and tube noise contribution. Atmospheric disturbances at radar frequencies are negligible and microphonic and electrical interferences from adjacent electrical equipment can, by proper and sufficient engineering, be reduced to any desired level.

It has been shown[4,5] that the thermal noise (Johnson noise) voltage which appears at the input terminals of a radio or radar receiver is determined by the value of the resistance component of the generator impedance at this point. For maximum transfer of signal power the load termination is required to be equal to the internal impedance of the generator and for this condition the total thermal noise power delivered to the load is given by

$$P_N = KTB \text{ (watts)}$$

where:

K = Boltzman's constant = 1.38×10^{-23} Joule/degree abs.
T = Absolute temperature in degrees
B = Bandwidth under consideration in cycles per second; and the signal-to-noise ratio is given by

$$\frac{P_S}{P_N} = \frac{P_S}{KTB} \text{ (a numeric)}$$

where P_S = maximum available signal power.

If the signal generator referred to is followed by any 4-terminal network representative of a converter element, an amplifier, or a passive network, the effective signal-to-noise ratio at the output terminals of the network will be modified. To obtain a measure of this effect we may assign a figure of merit, F, to the network called the "noise figure" of the network and define this as the ratio of the available signal-to-noise ratio at the signal generator terminals to the available signal-to-noise ratio at the output terminal of the network.
This may be written as:

$$F = \frac{\frac{P_S}{P_N}}{\frac{P_{S_2}}{P_{N_2}}} = \frac{P_{N_2}}{KTBG} \text{ (a numeric)}$$

[4] "The Absolute Sensitivity of Radio Receivers," D. O. North, *R. C. A. Review*, Vol. VI, January 1942.
[5] "Noise Figures of Radio Receivers," H. T. Friis, *Proc. I. R. E.*, Vol. 32, No. 7, July 1944.

where:

$$G = \frac{P_{S_2}}{P_S}, \text{ by definition the "gain" of the network.}$$

or we may write:

$$P_{N_2} = FKTBG \text{ watts.}$$

It is common practice to express F in decibels given by the relation $10 \log_{10} F$.

For the case of two generalized networks in tandem following the signal generator and having the same effective bandwidth we may similarly write:

$$P_{n_{out}} = F_a G_a G_b KTB + (F_b - 1) G_b KTB$$

$$= \left(F_a + \frac{F_b - 1}{G_a}\right) G_a G_b KTB \text{ watts.}$$

where the subscripts refer to networks a and b.

The effective noise figure of such a system is given by:

$$F_{\text{system}} = \left(F_a + \frac{F_b - 1}{G_a}\right)$$

This expression indicates the importance of the gain of the first network in the over-all system noise performance.

As an illustration, a noise figure of 11 db and a loss of 6 db may be considered as acceptable performance for a typical silicon crystal converter operating at 3000 mc. If the following input circuit of the IF amplifier has an effective noise performance represented by a noise figure of 5db , the over-all system noise figure will be found to be 13 db. The reduction in system performance due to the noise contribution of the input stage of the IF amplifier here is approximately 2 db. If the system performance must be improved by increasing the power of radiation, the importance of this secondary noise contribution is apparent.

A comparison of the noise figures of a point-contact crystal converter element and the GL-2C40 Lighthouse vacuum tube used as an amplifier and as a converter element is given in Fig. 5. At frequencies below 1000 mc there is a definite advantage in employing a vacuum tube as a radio-frequency (RF) amplifier preceding the nonlinear element.

2.13 *1000* MC *Radio-Frequency Amplifier Design*

In the design of military radar systems for the 1000 mc operating range the GL-2C40 vacuum tube has been employed rather universally in converter circuits.[6] The essential design features of this special purpose triode

[6] "The Lighthouse Tube," E. D. McArthur and E. F. Peterson, *Proc. of National Electronics Conference*, Vol. I, 1944.

are illustrated in Fig. 6. The basic advantage of the GL-2C40 tube for use at high frequencies is found in its construction, whereby the tube elements are arranged to form an integral portion of the external circuit with a minimum of mechanical disturbance. At these frequencies external coupling circuits of the transmission line type are usually employed. This tube when operated at an anode potential of 250 volts has a mutual conductance of approximately 6000 micromhos and an amplification factor of 35. It has been customary to employ one or two stages of RF amplification associated

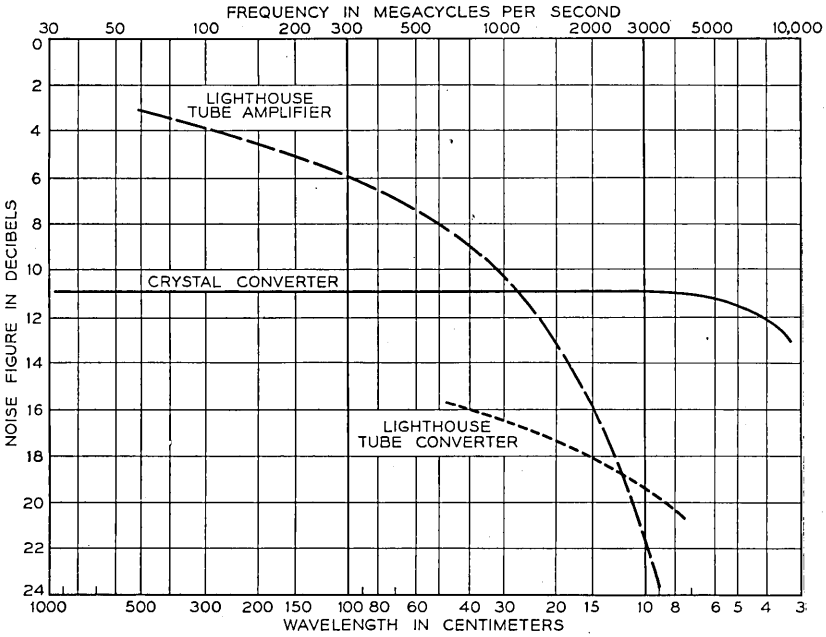

Fig. 5.—Comparison of noise figures for point-contact silicon crystal rectifier and GL2C40 vacuum tube.

with the nonlinear element and a beating oscillator using this same tube. The reduced performance of the GL-2C40 tube as a converter element as indicated in Fig. 5 is not of importance, if sufficient gain is provided prior to the actual conversion process, and the ability of this vacuum tube to operate at higher levels is a positive advantage.

The electrical circuit design techniques employed in this frequency region are based on the use of transmission line elements in place of the more or less orthodox lumped element configurations at the lower frequencies. The difficulties experienced in practical designs of radar converters of this type revolve about successfully terminating and satisfactorily isolating each stage so that confusing and inefficient interaction effects are minimized.

The simplified schematic of a typical radio-frequency amplifier which employs a GL-2C40 vacuum tube operating at approximately 1000 mc is given in Fig. 7, together with an outline of the mechanical arrangement of the tuning elements. This amplifier is of the tuned-grid, tuned-plate type

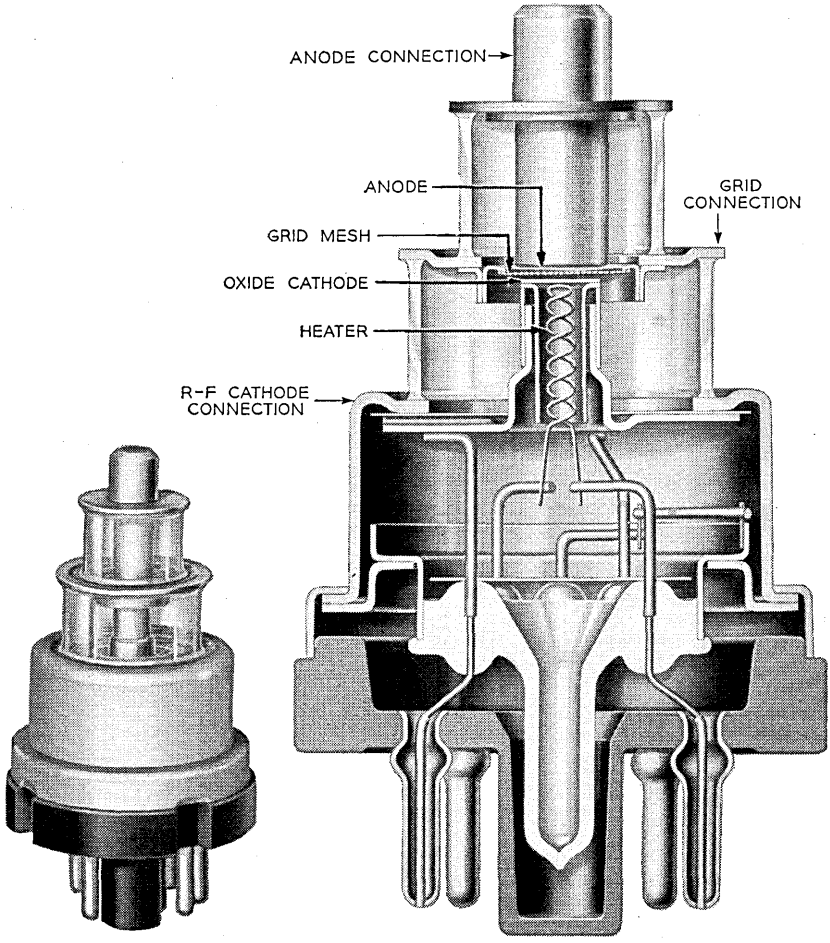

Fig. 6.—Constructional Features of the GL-2C40 (Lighthouse) vacuum tube.

of circuit where the input and output circuits consist of coaxial transmission line elements tuned by sliding plunger or ring elements, and is so constructed to include the GL-2C40 tube as an integral part of the tuning structure. The input coupling to the amplifier is achieved by means of a probe extend-

ing into the input or grid cavity and is proportioned for operating out of a 50-ohm impedance cable connection to the radar antenna system. The output coupling is obtained from a coupling loop located in the region between the grid and plate concentric sleeves. The gain of this RF amplifier design is 12 db when operating at a frequency of approximately 1000 mc and the noise figure of this component is 14 db.

2.14 *The Radar Converter*

The basic converter is illustrated in Fig. 8 and may be defined as a device which has two input pairs and one output pair of terminals and is charac-

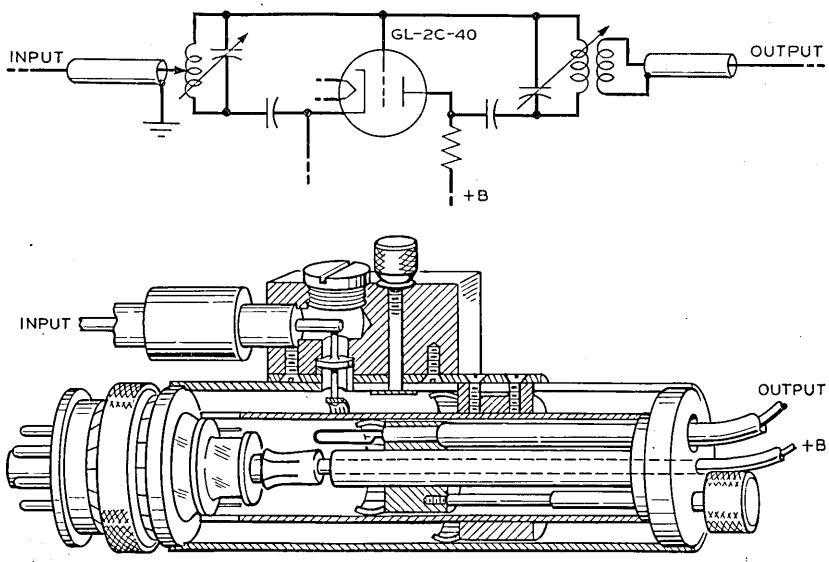

Fig. 7.—1000-mc Radio Frequency Amplifier. Simplified schematic diagram.

terized further by the property of delivering an output signal, which, in terms of amplitude of one of the input signals, is essentially linear but which has an output frequency related to the sum or difference of the two input frequencies. This frequency conversion is obtained by the use of an element which has a nonlinear voltage-current relationship and upon which is impressed the two input signals. The desired sum or difference frequency signal is then selected and utilized as the wanted signal output.

The basic configuration of the converter shown in Fig. 8 employs a nonlinear element with network coupling means to provide efficient transfer of signal power into and out of the component and a beating oscillator with its associated coupling network to supply the required additional input fre-

quency. One or more of the networks involved may, of course, be arranged alternatively in a parallel configuration if desired. The nonlinear element may be a vacuum tube with properly chosen operating conditions or a point-contact silicon crystal rectifier. The beating oscillator in the modern military radar converter employs special types of vacuum tubes such as the GL-2C40 type previously mentioned or the single-cavity velocity modulated types[7] at the higher radar frequencies.

A typical voltage-current characteristic of a point-contact silicon rectifier is shown in Fig. 9. This nonlinear characteristic may be expressed mathematically as a power series with coefficients whose amplitude decreases quite rapidly with the order of the associated term. If two sinusoidal voltages represented by frequency f_1 and f_2 are simultaneously impressed

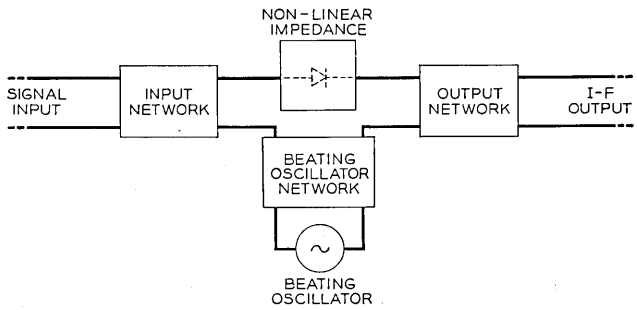

Fig. 8.—Basic configuration of a radar converter.

upon such a nonlinear element, the resultant current flowing in the output impedance will produce output signals of the form $nf_1 \pm mf_2$ where n and m are integers including zero. The effective amplitude of each of these modulation products is related to the magnitude of the power series coefficients. In the radar converter under consideration f_1 may represent the received signal frequency and f_2 represents the beat oscillator frequency. The difference terms of the above expression are of the greatest importance here because the desired output signal frequency has been chosen at a low value as compared with the input received radar signal. The selection of the wanted first-order difference term is accomplished by the frequency selectivity characteristics of the converter output coupling network and the following IF amplifier.

A major design problem encountered in the practical development of microwave radar converters is one concerning the design of the coupling networks. The previously referred to limitations of microwave network

[7] "Reflex Oscillators," J. R. Pierce and W. G. Shepherd, *Bell System Technical Journal*, Vol. XXVI, July 1947.

techniques and the difficulty in maintaining precise control of each element over the required band of frequencies are the fundamental problems of the radar converter designer. The network problem here is concerned with realizing the desired frequency conversion with a minimum of dissipation of the useful signal. This implies that coupling of the nonlinear element to the input and output terminals must be achieved in such a fashion that matched impedance conditions result for the signals in their respective frequency regions. Since the output signal has been shown to appear as a

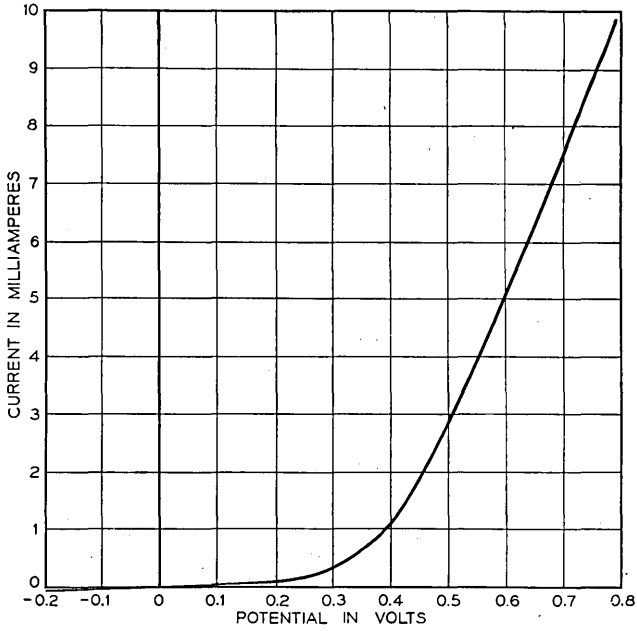

Fig. 9.—Typical voltage-current characteristic of a point-contact silicon crystal rectifier.

number of energy concentrations extending over a wide frequency range, it would appear that an efficient design of output coupling network would involve optimizing the impedance relationships over this wide-frequency band. Several factors tend to simplify this problem by restricting the output frequency band which must be considered in a practical radar converter design. First, the greatest amount of energy is found to be present in the lower order modulation products because of the rapid reduction in amplitude of the higher order terms in the equivalent expression for the nonlinear element. This results in a concentration of energy at the input, output, and beat oscillator frequencies and their respective second harmonic regions. Second, the ratio of f_1 to f_2 in a microwave radar converter is of necessity

essentially equal to one, this factor also contributing to a narrowing of the frequency regions of interest to those around the input, the beat oscillator, and the output values. The third factor, which is of assistance to the converter designer, is the effective separation of the input and output circuits by the loss of the nonlinear element. Where a vacuum tube is employed as the nonlinear element, the interaction of these circuits may be made quite negligible and, in the case of the crystal rectifier the inherent loss of this element, which may be of the order of 6 db and undesirable from a radar system performance standpoint, does simplify the converter network design.

It has been found in practice that it is sufficient to consider the impedance conditions at the internal terminals of the converter networks in the frequency regions which include $f_1, f_1 - f_2, f_1 + f_2$ and $2f_2 - f_1$.

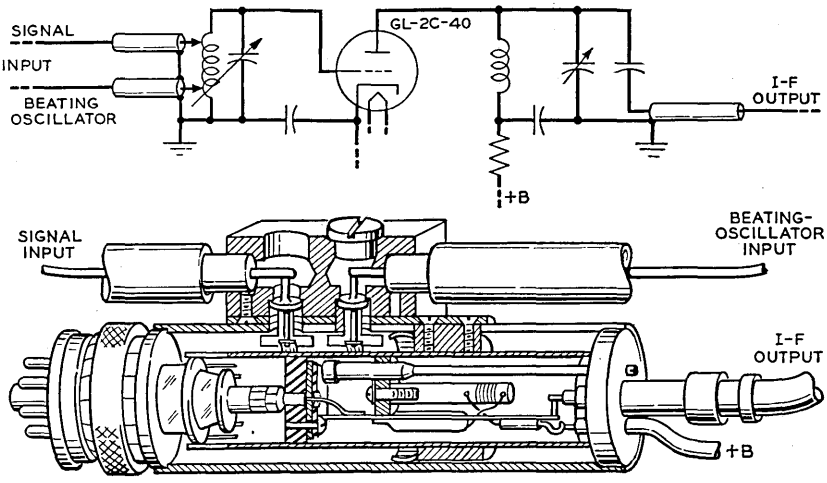

Fig. 10.—1000-mc Vacuum Tube Radar Converter. Simplified schematic diagram.

The matter of efficient transfer of power from the local beating oscillator to the nonlinear element is of secondary importance generally because of the relatively large amount of power available. This condition is advantageous allowing mismatch loss in this branch to effectively minimize the unwanted interaction effects with input and output circuits.

Figure 10 illustrates the schematic and certain constructional features of a vacuum-tube converter which has an operating frequency of approximately 1000 mc. The similarity of circuit and mechanical arrangement to that of the radio-frequency amplifier unit, shown in Fig. 7, is apparent. In the case of the GL-2C40 converter the two input frequencies are similarly probe coupled to the grid-cathode circuit, maintaining optimum impedance conditions for the signal input and locating the beat oscillator probe so as

to effect an impedance mismatch and thus reduce the interaction between this circuit and the input circuit. The output coupling network, in this case operating at 60 mc, consists of an inductive impedance tuned with a variable condenser. The output of this converter is fed into the following IF amplifier by means of a 75-ohm coaxial transmission line. The loss of this converter unit, defined as the ratio of the power of the wanted 60-mc output signal to the signal power impressed upon the input terminal, is

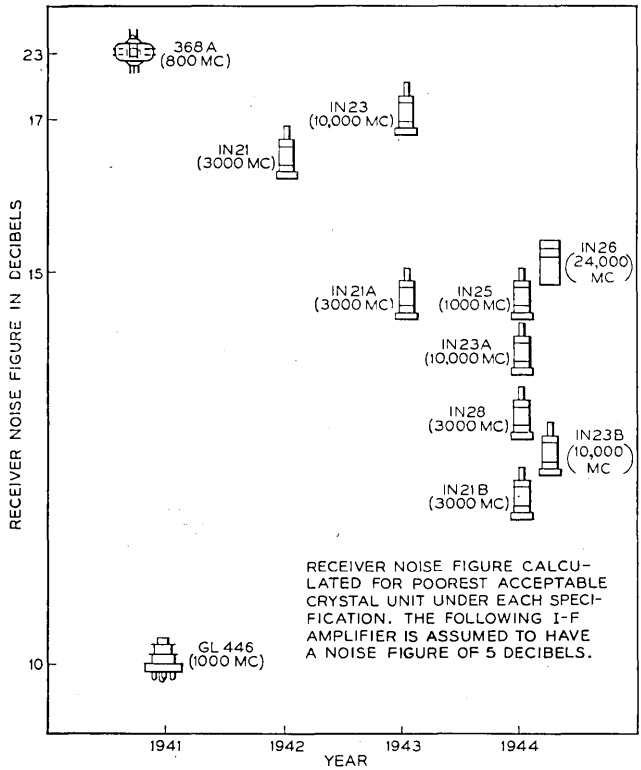

Fig. 11.—Chronological development of point-contact silicon crystal rectifiers and associated receiver noise performance.

approximately 6 db. The noise figure of a typical unit of this type is approximately 20 db, this value being of secondary importance since sufficient gain is provided in the associated radio-frequency amplifier.

At the higher radar frequencies the noise performance characteristics of silicon crystal-point contact rectifiers are considerably better than that of vacuum tubes available during the past war years. Figure 11 outlines the chronological developments of these units with respect to the receiver noise

performance. The performance of two types of vacuum tubes are included for comparison purposes. The development details of the silicon crystal unit have been discussed elsewhere.[8] This development, together with the corresponding magnetron and reflex oscillator studies, assumes a status of major importance in the progress of the development of military radar equipment during World War II, allowing the designers to extend the frequency of operation upward with increased system performance resulting.

It is sufficient to limit our attention to the frequency region 3000 mc and above in the consideration of the silicon crystal converter. It is apparent that the absence of suitable vacuum tube radio-frequency amplifiers in this region imposes a strict requirement on the efficiency of conversion of this component.

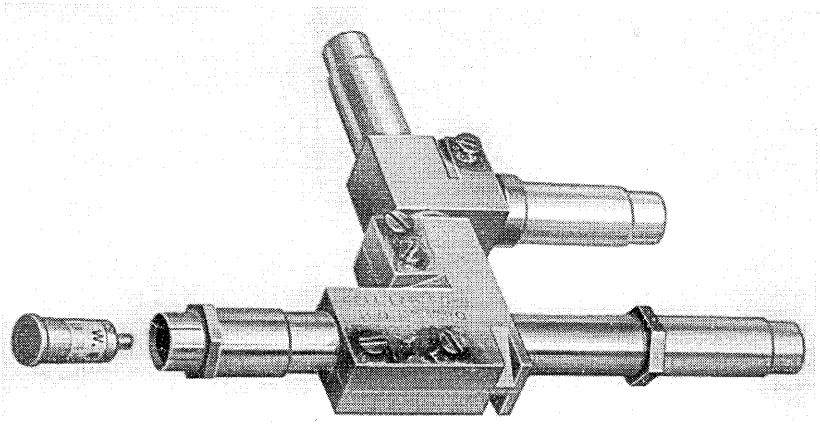

Fig. 12.—3000-mc Crystal Converter of an early design.

Historically, one of the first of the microwave converters of the silicon crystal type, operating at 3000 mc and which was employed in military radar equipment, is shown in Fig. 12 together with an illustration of the mechanical arrangement[9] in Fig. 13. In this early model the silicon crystal element was mounted in a cartridge type unit, a method which proved quite satisfactory and was followed for the remainder of the war years. The input tuning circuit of the converter here illustrated consists of a coaxial transmission line element having a length of approximately three-quarters of a wavelength and adjustable to enable fine control of tuning. The nonlinear ele-

[8] "Development of Silicon Crystal Rectifiers for Microwave Radar Receivers," J. H. Scaff and R. S. Ohl, *Bell System Technical Journal*, Vol. XXVI, January 1947.

[9] "Microwave Converters," C. F. Edwards, To be published in a forthcoming issue of *Proceedings I.R.E.*

ment is located at the high-impedance end of this transmission line, while the other end is essentially short-circuited at the input frequency by means of a small by-pass condenser element built into the IF output transmission line. The input line is coupled into this tuned circuit by means of a variable coupling probe and the local beat oscillator in turn is similarly coupled to the input line. The point of coupling of the beat frequency oscillator input is so arranged as to introduce an effective mismatch and thus provide adequate isolation of this and the input circuit. The output circuit of this converter includes the by-pass condenser previously referred to, together with the input transformer of the first IF amplifier stage. The average loss of a

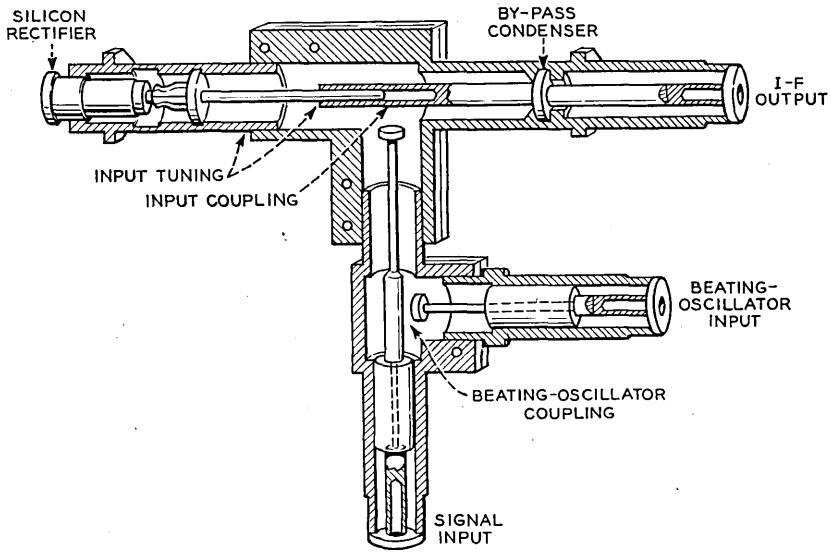

Fig. 13.—3000-mc Crystal Converter. Schematic diagram.

3000-mc crystal converter of this type was 6 db and a noise figure of 11 db was realized.

Another design of crystal converter which was developed during the early part of the war, and whose basic form was employed in many military radar equipments operating in the region of 10,000 mc, is shown in Fig. 14. Here the silicon crystal cartridge is positioned within the waveguide with its axis parallel to the E vector plane and at a point approximately one-quarter of a wavelength from the short circuiting piston which terminates this assembly. The IF output is obtained from the coaxial line mounting structure shown which offers a low impedance to the input frequency by virtue of its equivalence to a one-half wavelength element with a short circuit at the far end.

The dielectric supporting rings shown form an RF by-pass element minimizing the loss of input signal power in the IF output network. In this design the beating oscillator energy is introduced into the waveguide by mounting the reflex oscillator tubes adjacent to the waveguide in such a fashion that the output probe is inserted into the waveguide cavity at a point removed by an odd one-quarter of a wavelength from the face of the TR output iris. This assures reflection of the local oscillator energy which travels toward the TR tube directing it toward the crystal element. The degree of coupling of the reflex oscillator circuit is varied by adjustment of the distance that the probe is inserted within the waveguide. For airborne applications an additional oscillator tube is included for beacon reception. This basic form

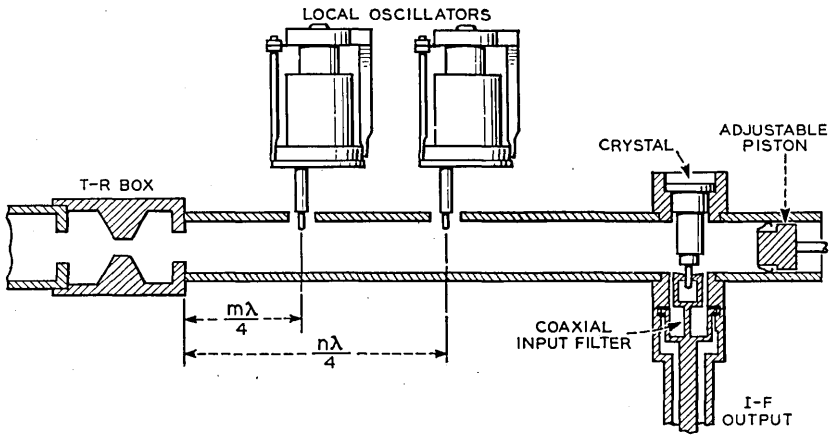

Fig. 14.—10,000-mc Crystal Converter. Schematic diagram.

of radar converter was employed in large numbers in the military airborne radar field during World War II.

A third type of crystal converter design which was developed in the latter period of the war is illustrated in Fig. 15. A basic difference in this structure is found in the use of a waveguide hybrid junction often referred to as a "magic tee." This junction has an electrical performance characteristic at microwaves similar to that of the hybrid coil common to low frequency communication circuits, i.e., a 4-pair terminal network with an internal configuration such that power applied to any one pair of terminals will appear equally at two other pairs of terminals, but will not be available at the remaining pair of terminals. Referring to Fig. 15, it should be noted that power applied to the input waveguide will appear equally in the output branches but is balanced out of the beat oscillator branch. In a similar fashion, the beat oscillator power will appear equally in the two output

branches but will not appear in the input waveguide. Certain impedance matching adjustments are obtained through the use of the matching rods positioned as shown.

The method of insertion of the crystal cartridge into the waveguide in this

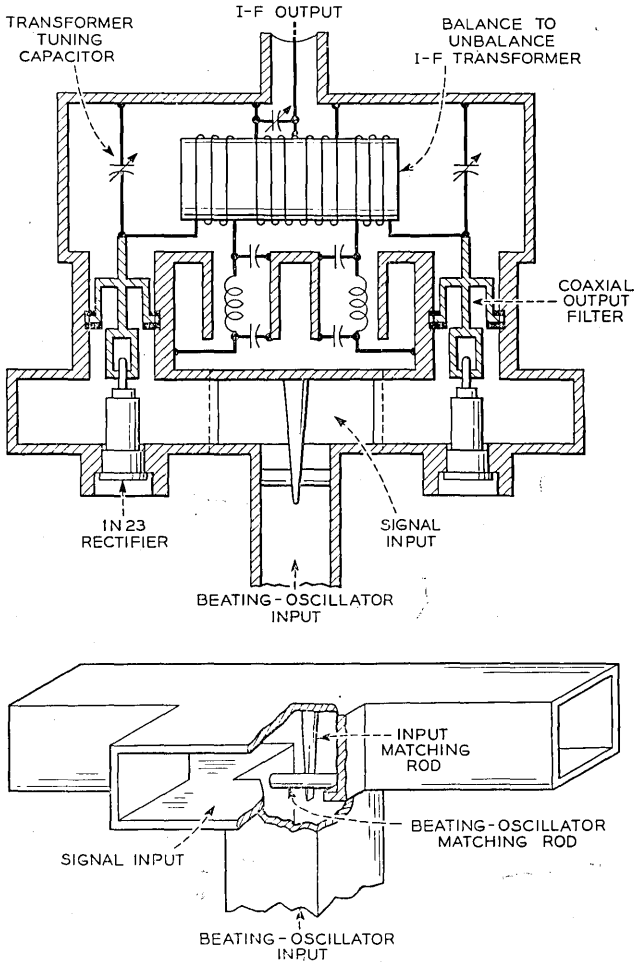

Fig. 15.—Balanced crystal converter employing wave-guide hybrid junction.

design follows the scheme employed in the converter just described. However, here two crystal elements are employed in a balanced form which necessitates a balanced-to-unbalanced impedance transformation of the IF output signal for transmission over a coaxial line to the input stage of the IF amplifier. The degree of balance obtainable here is necessarily a func-

tion of the similarity of the crystal elements as well as the other elements shown. In practice, no particular difficulty was experienced in maintenance of sufficient balance with the improved production control of crystals during the latter part of the war program.

The advantages of the balanced radar converter here described are two-fold. First, the signal power dissipation in the beating oscillator branch is reduced to a minimum and conversely the beating oscillator power fed back into the antenna and reradiated is reduced. Second, the noise sidebands, which are associated with the output frequency of the reflex oscillator, are reduced effectively in the IF output branch by the degree of balance available. This local oscillator noise sideband contribution is normally responsible for a definite degradation of the over-all radar receiver noise performance and hence, the use of a balanced converter will contribute to improved performance. An additional advantage of the balanced converter is the minimizing of signal branch impedance variation effects on the beating oscillator load impedance and, therefore, its frequency. The variation of the antenna impedance during the scanning cycle has in this design little effect on the tuning of the receiver.

2.15 *The Radar Receiver Beat Oscillator*

For microwave radar receiver purposes the selection of the local beat oscillator within the converter assembly has been essentially limited to two types of tubes, both of which were developed during the past war period. For radar systems operating at frequencies of 1000 mc and lower, the GL-2C40 lighthouse triode has served quite satisfactorily, while at frequencies above 1000 mc, the single-cavity reflex oscillator tube has been extensively employed. Both of these tube types have adequate power output and frequency stability characteristics to meet the normal radar system requirements.

Some of the desirable characteristics of a beat oscillator tube for use in military radar receivers can be listed as follows:

A. At least 20 milliwatts of useful output power is desirable. In the case of the silicon crystal rectifier element, the applied power is limited to approximately 1 mw; however, the availability of additional oscillator power enables the converter designer to effectively isolate the beat oscillator and signal branches by simple inpedance mismatch means.

B. The frequency stability of the ideal beat oscillator tube must be inherently good, or convenient means to automatically control this frequency must be provided. The maximum allowable radar receiver frequency variation due to all causes is of the order of 1 mc. In terms of the beating oscillator frequencies employed in the radar systems of the past war, this represents an allowable oscillator frequency variation

from all causes of from 0.1% to .01%. The possible influencing factors include temperature, atmospheric pressure, supply voltage, and load impedance variations with time, and mechanical shock and vibration.

C. It is extremely desirable that frequency control of the beat oscillator be available by remote electrical means. The use of automatic tuning control of a military radar receiver has proved a necessity during the past war and, as will be discussed in a later section, the rates of change of frequency encountered are found to be quite great. This requires essentially that an electrical control method of continuously adjusting the beat oscillator frequency be employed to obtain satisfactory receiver performance.

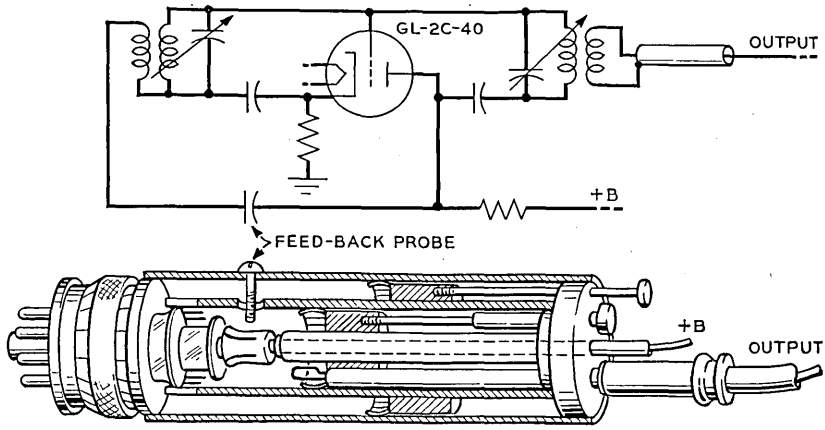

Fig. 16.—1000-mc Radar local beat oscillator employing GL-2C40 vacuum tube—schematic diagram.

D. It is desirable that the output of the beating oscillator tube be free from noise. In the usual radar system, if the output frequency of the beat oscillator is modulated with noise, a reduction in receiver performance will result. As previously discussed, the development of the balanced converter has provided the converter designer with some relief from this noise source and in this case this requirement assumes less importance.

A beat oscillator arrangement utilizing the GL-2C40 lighthouse tube, as developed for a military radar system operating in the 1000 mc region, is indicated in Figure 16. This assembly is quite similar mechanically to the RF and converter components employed in this frequency region and described previously. The positive feedback necessary to sustain oscillation is provided by means of a feedback coupling probe as shown. The oscillator output is available by means of a pick-up loop inserted into the

plate-grid cavity and thence to the output coaxial line. The frequency stability of this particular design has been quite satisfactory due to the considerable development effort expended on the mechanical design features of this assembly.

Another radar receiver beating oscillator which has been extensively employed in military equipment designs operating at 3000 mc and higher during the past war period is the reflex velocity-modulated oscillator. The 2K25 type, which is a typical single-cavity reflex oscillator for operation in the 10,000-mc region, is illustrated in Fig. 17. The general principle of operation is quite straightforward, but the complete theory of operation is exceedingly complex and has been described in detail elsewhere.[10] A beam of electrons of relatively uniform velocity and density is projected from a cathode surface toward a cavity space defined in part by two grids and then toward a repeller electrode beyond. The presence of the oscillatory potential between the two cavity grids acts to impart initial velocities to the electron stream in accordance with the cavity radio-frequency potentials existing at the time of crossing of this gap. Under certain operating conditions between these grids and the repeller electrode, which is maintained at a negative potential, "bunching" of electrons occur and upon the return of the electrons to the cavity region under the retarding influence of the repeller electrode, a certain amount of power may be extracted and utilized externally. As might be expected from this cycle of events, the optimum operating conditions necessary for reinforcement of oscillation within the cavity are related to the time required to return the electrons to the cavity with reference to the instantaneous oscillatory radio-frequency potential of the cavity. Thus, numerous modes of oscillation are found in this type of reflex velocity-modulated oscillator which are related to each other by integral numbers of periods of the oscillatory frequency and the transit time of the electrons. In the practical application of the reflex oscillator the number of useful modes are limited to perhaps two or three, the external power output available at the additional theoretical modes being reduced by dissipative conditions within the oscillatory system. The relation of repeller potential to the appearance of these modes is illustrated in Fig. 18 for the case of a 2K25-type oscillator. It should be observed here that the frequency at the maximum power output condition for each mode is the same, i.e. the frequency associated with the cavity dimensions for that series of modes. The cavity dimensions of the reflex oscillator tube are varied by the application of external mechanical pressure regulated by an adjustable tuning strut as shown in Fig. 17. The power for external use is obtained from a coupling loop located within the cavity region and transmitted through the base by means of a coaxial lead.

[10] Pierce and Shepherd, Loc. Cit.

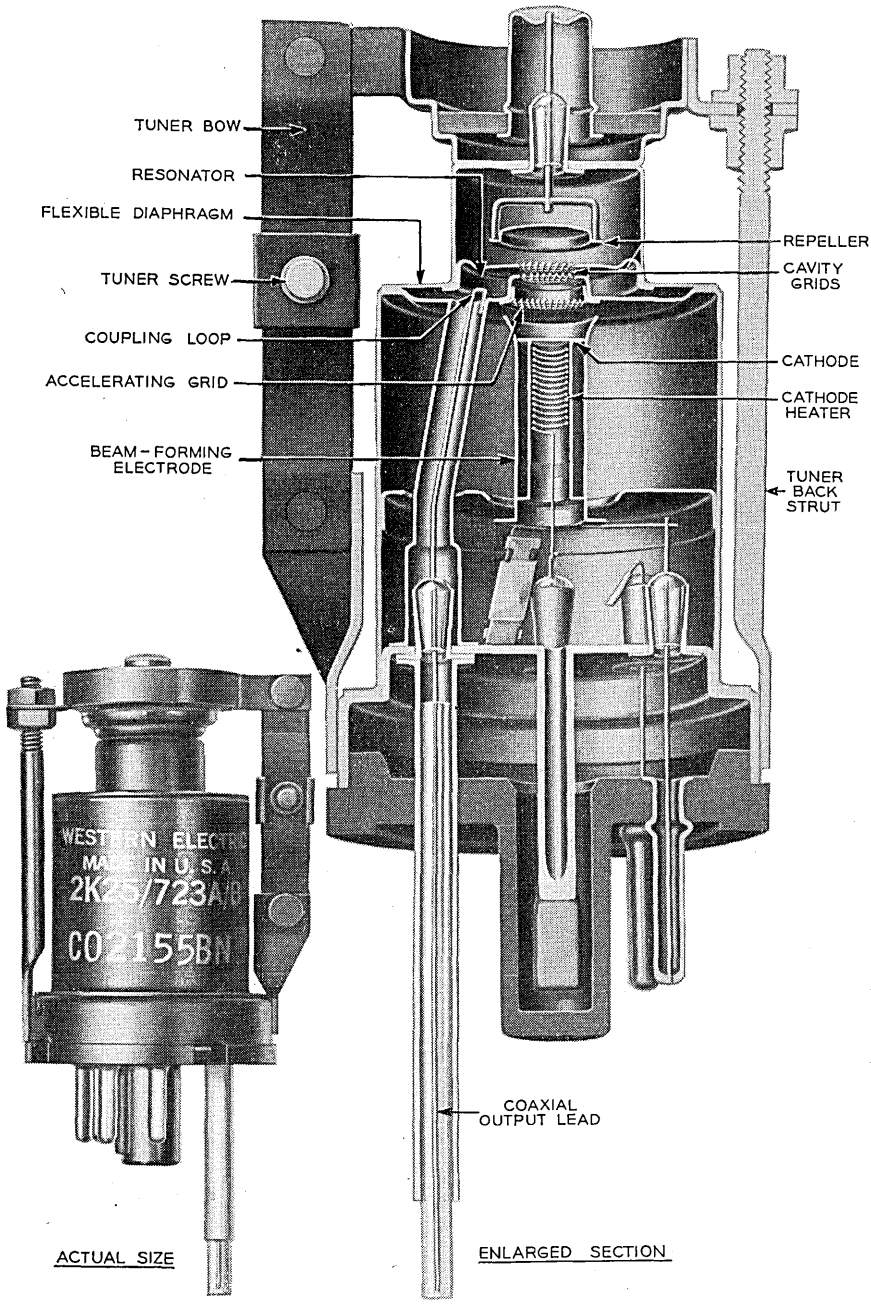

Fig. 17.—Constructional details of the type 2K25 single-cavity reflex oscillator for use at 10,000 mc.

The single-cavity velocity-modulated oscillator is admirably suited to electrical remote control of its oscillation frequency by means of the potential applied to the repeller element, thus lending itself to automatic frequency control in a simple manner. Figure 19 indicates the frequency and power output versus repeller voltage characteristic of a typical 2K25 10,000-mc reflex oscillator when operating at a normal mode previously shown in Fig. 18. It is customary to define the electronic tuning range of a reflex oscillator as that range of frequencies over which the power output exceeds

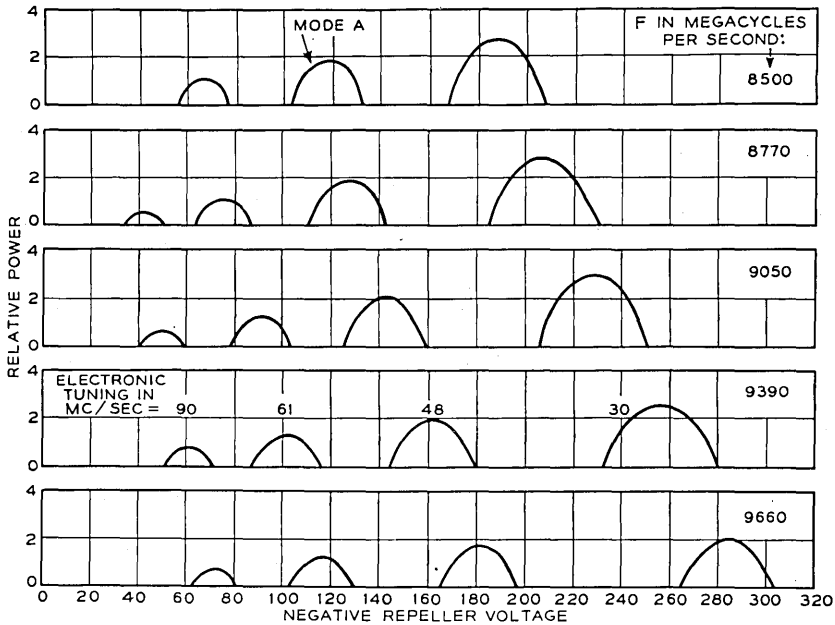

Fig. 18.—Typical output power modes vs. repeller voltage for a 2K25 type reflex oscillator.

50% of the maximum power output. The tube whose characteristic is illustrated in Fig. 19 would accordingly have an electronic tuning range of 53 mc.

2.16 *Typical Radar Input Circuit Designs*

An example of a radar receiver input circuit operating in the 1000-mc frequency range is shown in its final mechanical form in Fig. 20. This particular design was employed in several military ground radar systems including the Mark-20 Searchlight Control equipment of Fig. 1, and in modified form in several naval fire control systems. It consists of two stages of radio-frequency amplification, a converter stage, and a local beating

oscillator all of which employ the GL-2C40 lighthouse tube. This particular equipment example has been developed in the form of a sliding drawer to assure ease of maintenance but with no sacrifice in rigidity of mechanical assembly so necessary in this type of equipment. Further mechanical details of the cavity and tube structures of each component are shown in Fig. 21 and are generally similar to the examples previously described. These cavity structures are heavily silver-plated to assure good electrical and thermal conductivity. The problem of adequate conduction of heat from the GL-2C40 vacuum tube under the severe ambient temperatures

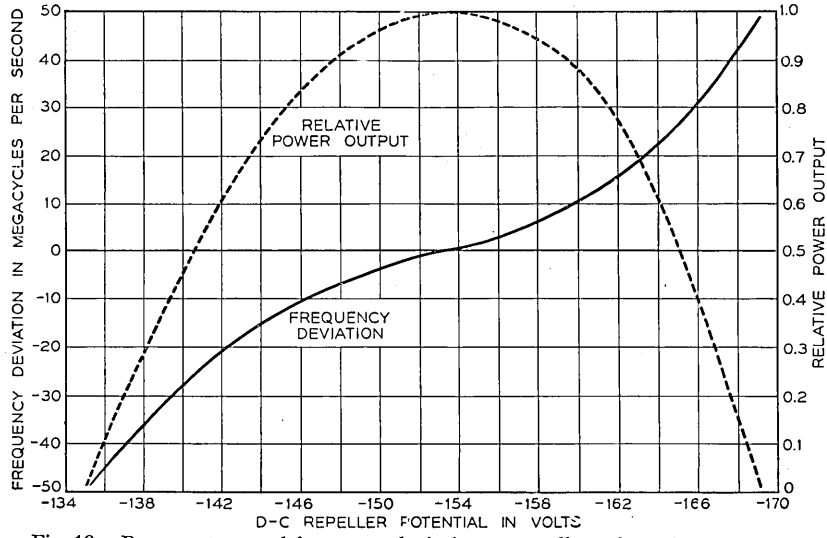

Fig. 19.—Power output and frequency deviation vs. repeller voltage for 2K25-type reflex oscillator.

encountered in military service is extremely important. Positive locking devices are provided for all adjustments in this mechanical design.

Figure 22 indicates the schematic diagram of this design. It may be observed that separation filters are employed extensively to assure negligible interaction effects between the various stages through the common power supply connections.

The over-all performance of this particular design of a radar receiver input circuit is as follows:

Input Frequency	1000 mc
Output Intermediate Frequency	60 mc
Over-all Band Width	5 mc
Over-all Gain	18 db
Over-all Noise Figure	14 db
Input Impedance	50 ohms
Output IF Impedance	75 ohms

The above performance is representative of the limits which all manufactured units are required to meet and also indicates the field performance which must be maintained for satisfactory military service. Under laboratory conditions and with a certain compromise of stability and ease of

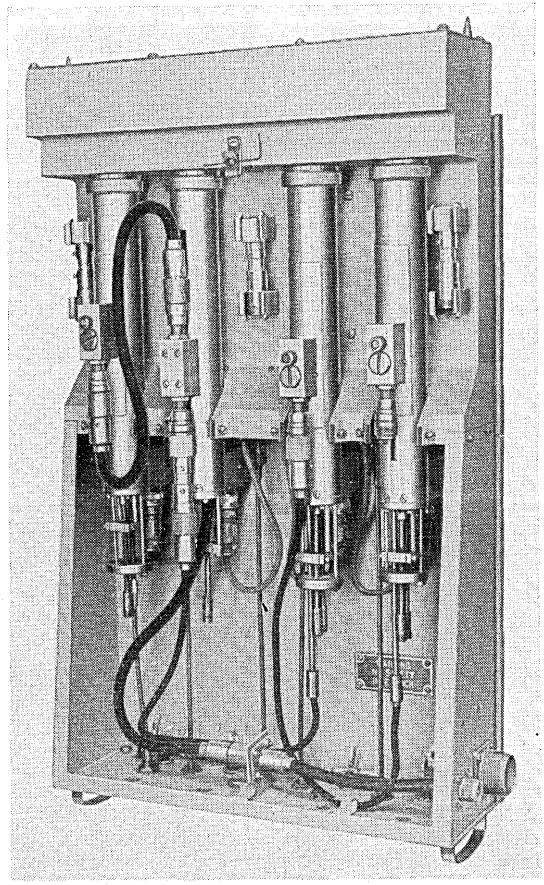

Fig. 20.—1000-mc Radar receiver input circuit design, including two stages of radio frequency amplification, converter, and beat oscillator.

adjustment, improved performance over the figures given here can be expected.

The design for manufacture of a converter assembly typical of airborne equipment methods is illustrated in Fig. 23. Here the equipment design reflects the fundamental requirement of radar equipment for aircraft—that of providing compact units of sufficient rigidity with a minimum of weight. This particular converter unit was employed in the AN/APS-4 Airborne

Search and Interception radar equipment shown in Fig. 3 and operates within the 10,000-mc frequency band. The automatic frequency control

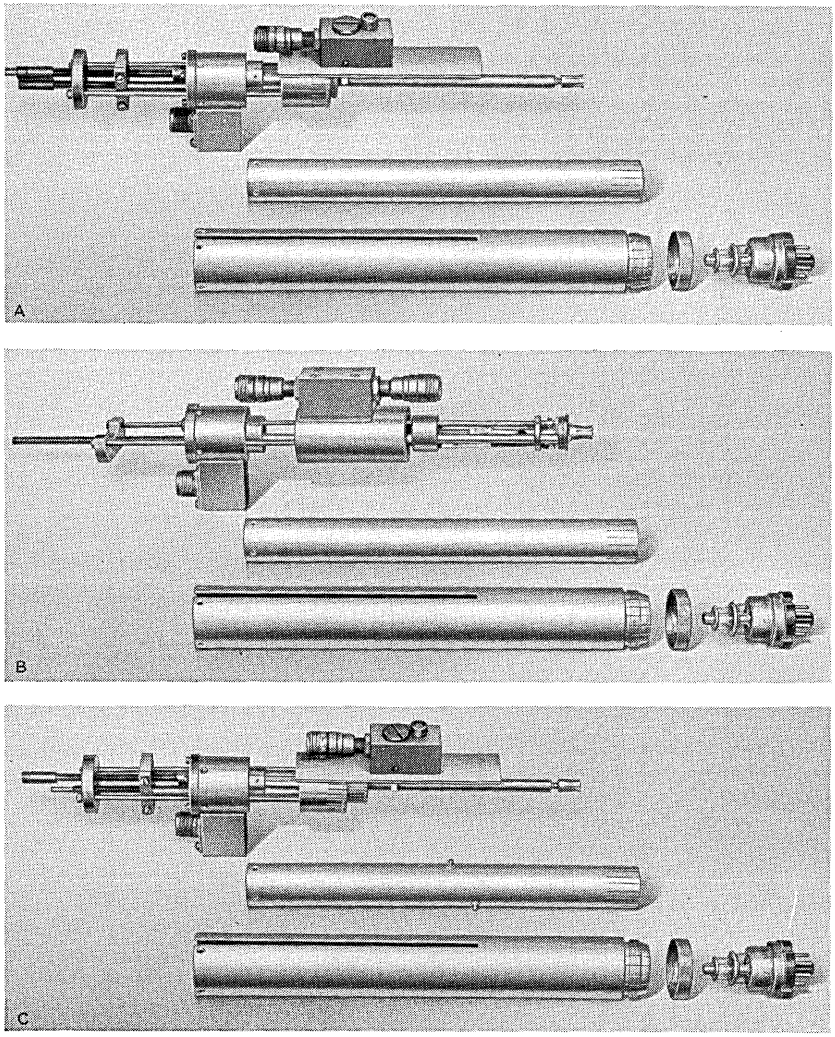

Fig. 21.—Mechanical details of cavity structures employed in 1000 mc radar receiver input circuit.

circuit and two *IF* preamplifier stages are also included here as an integral part of the converter assembly.

The schematic diagram of the converter portion of this assembly is given in Fig. 24. It should be observed that the basic arrangement of the crystal

converter is similar to a form described in a previous section. The signal in this example is introduced into the converter section of the waveguide through an iris following the TR tube. Two 2K25 reflex oscillator tubes are mounted upon this waveguide with their output probes extending into the guide proper. The crystal cartridge is located near the end of the waveguide with an adjustable piston terminating the guide. A waveguide to

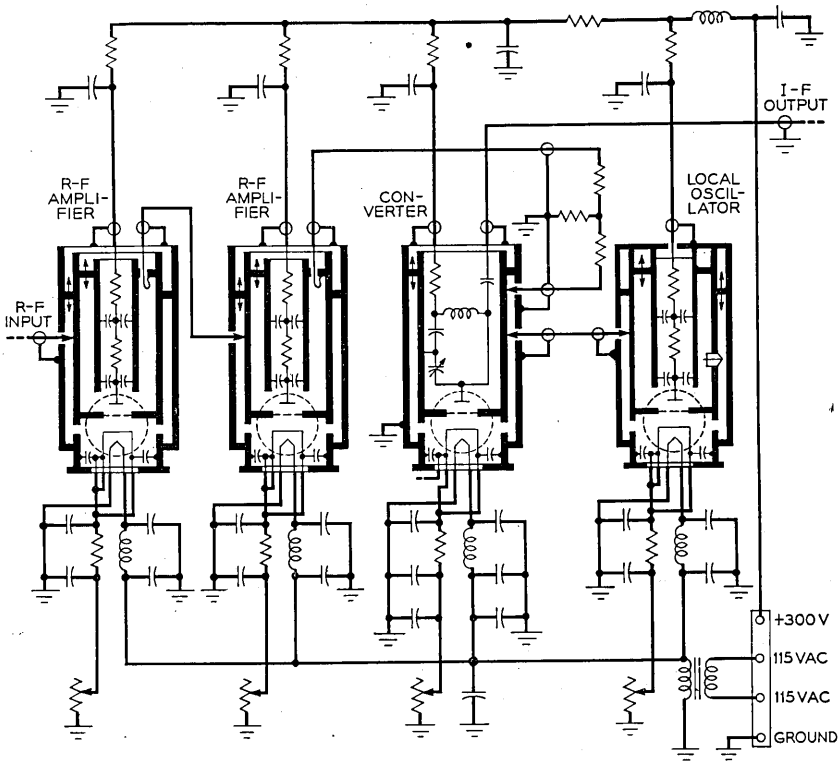

Fig. 22.—1000-mc Radar Receiver Input Circuit. Schematic diagram.

coaxial transforming section employs the crystal as an extension of its axial element with an adjustable capacitance element for tuning purposes.

It will be observed here that a shutter is included in this design, whereby the crystal element can be isolated from the signal input end of the waveguide. This is a most necessary device on all radar converters employing crystal converter elements to prevent accidental overload of the crystal. When the transmitter is not in operation and accordingly the TR tube "keep alive" is not energized, there is a possibility of subjecting the crystal element to signals of sufficient amplitude to destroy its characteristic. These over-

load signals may occur as the result of direct pick-up of an adjacent radar system or in certain cases atmospheric discharges. To prevent this a mechanical shutter is inserted into the converter which offers effective attenuation to any signal input. This shutter is withdrawn only if the proper TR "keep alive" voltage is available.

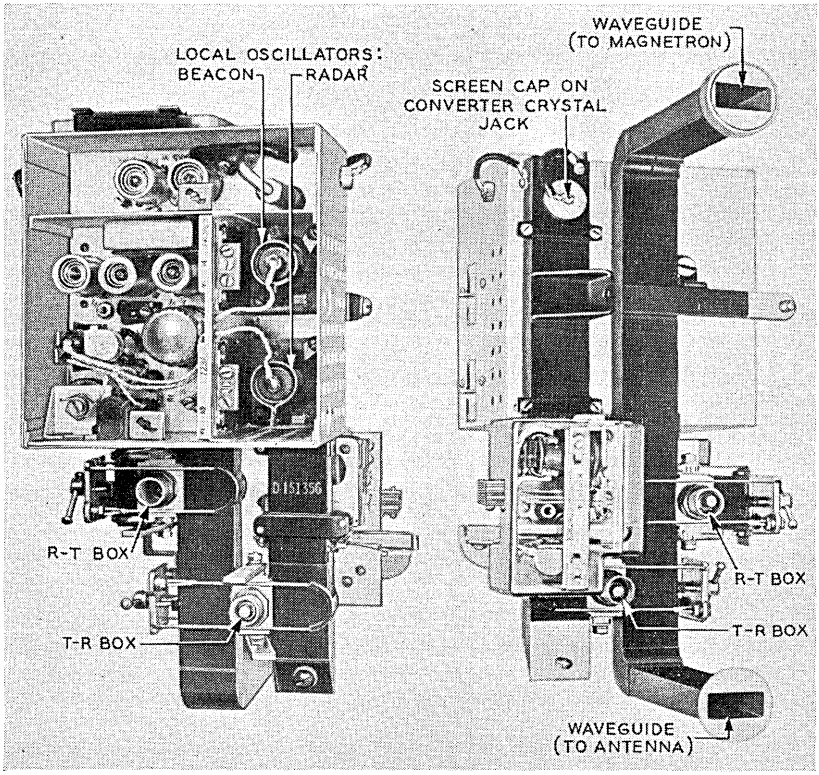

Fig. 23.—10,000-mc Converter and IF preamplifier assembly for AN/APS-4 airborne radar equipment.

The performance characteristics of this converter and IF preamplifier unit is as follows:

Radar Frequency	10,000 mc
IF Frequency	60 mc
Conversion Loss	6.5 db
Noise Figure of IF Preamplifier	4.5 db
Noise Figure of Converter	8.6 db
Noise Figure of Converter and Preamplifier	11.9 db
IF Band Width	4 mc

These values are representative of the performance under conditions of average crystals and average IF input tubes.

2.2 *The Radar Intermediate Frequency Amplifier*

The intermediate frequency (IF) amplifier component of the radar receiver has as its function the selection and amplification of the received signal following its conversion to the intermediate frequency. The further conversion of the IF signal to a video form suitable for use in the display device is usually included as an integral part of the IF amplifier and will, therefore, be considered here as an additional function of this component.

2.21 IF *Amplifier Requirements—Band Width*

The frequency-selectivity characteristic of the radar receiver is determined effectively by the IF amplifier, since the preceding converter and other microwave components offer little or no selectivity. The receiver

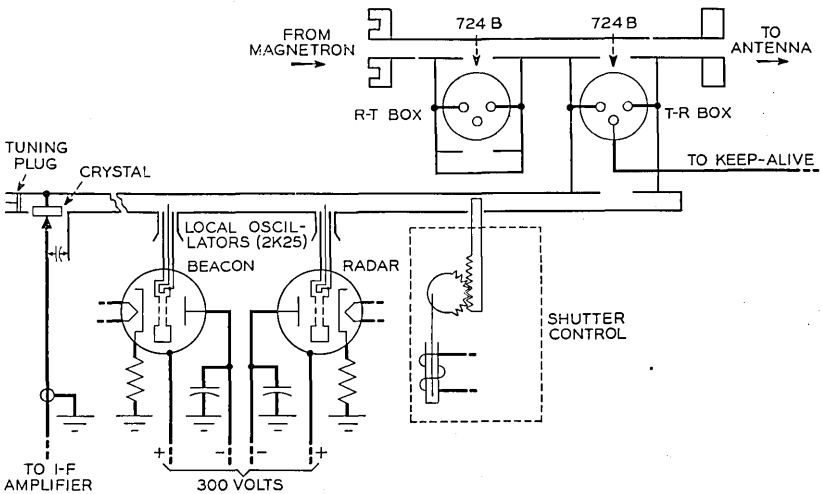

Fig. 24.—Schematic diagram of 10,000-mc AN/APS-4 converter unit.

band width required to adequately transmit the wanted signal, while restricting the noise contributions, is an extremely important factor in the radar system design and represents, therefore, a basic consideration in the design of the IF amplifier.

The receiver band width required to adequately transmit the basic received pulse information can be determined by a consideration of the frequency-energy characteristics of a radar pulse. The microwave pulse is created by the sudden application of a high-energy pulse to the magnetron microwave generator. It has been found sufficient to treat this output envelope as a simple rectangular pulse in band width computations. Figure 25 indicates the amplitude, time, and frequency relationships which exist for an idealized rectangular radar pulse envelope. It may be observed

that approximately 75% of the energy contained in the idealized original pulse will be available after transmission through a band-pass structure of band width dimension of $\frac{1}{\tau}$ cycles per second. A further doubling of the band width to $\frac{2}{\tau}$ cycles per second will increase the available energy by only about 15%. In the case of the practical radar-pulse envelope which usually is characterized by a trapezoidal form with finite rise and decay intervals, the energy contained at frequencies outside of a $\frac{1}{\tau}$ band is reduced somewhat over the idealized case illustrated in Fig. 25.

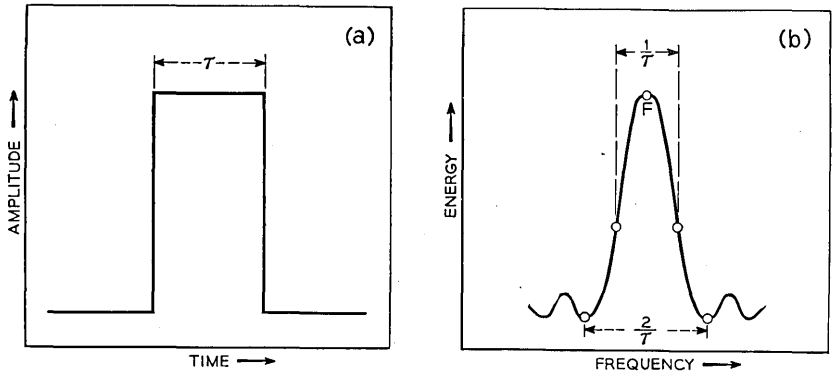

Fig. 25.—Amplitude-time and energy-frequency relationships for a rectangular radar pulse envelope.

The signal-to-noise ratio of the radar receiver is dependent on the over-all receiver band width as indicated in the previous section of this paper. It is extremely important then to restrict the IF band width as much as possible, consistent with adequate transmission of the signal itself. The final band width choice is that value where a further increase would result in a noise increase greater than the corresponding signal improvement and where a band width reduction would diminish the signal by a greater increment than the noise. The exact determination of the optimum radar receiver band width must be carried out using the final display device in making the signal-to-noise comparisons. If the radar system is to be employed for search purposes where echo presence is the primary measure of the performance of the equipment, the optimum over-all receiver band width has been found to be of the order of $\frac{1}{\tau}$ cycles per second resulting in an IF amplifier band width of $\frac{2}{\tau}$ cycles per second to adequately transmit the double-

sideband signal at this point. In the case of fire-control radar equipments, where precision range measurement is required, it is desirable to determine the range by reference to the leading or lagging edge of the radar received pulse. Here the optimum band width may be considerably greater than the value indicated above for a simple search system to assure a minimum rise time of the displayed pulse and an accordingly more precise determination of the position of the pulse. Additional factors which influence the radar receiver band width value in a particular system design involve the frequency stability of the microwave generator and the local beating oscillator, the sensitivity characteristics of the automatic frequency control system, the frequency stability characteristics of the IF amplifier itself, and finally the desire to permit ease of tuning by the radar operator.

The phase distortion introduced by the IF amplifier is of secondary interest in the case of radar systems. The faithful reproduction of all characteristics of the received radar pulse is usually not of extreme importance, since with few exceptions the criterion of presence is all important. The detailed form of the transmission characteristic is likewise not extremely critical, the usual "rounded" IF transmission characteristic, however, contributing somewhat to ease in tuning the radar receiver.

Gain Characteristics

A consideration of the converted input signal levels encountered and the video output level desired indicates the IF amplifier gain requirement. The input signal to the IF amplifier is determined by the type of converter employed and the presence or not of radio-frequency amplification preceding the IF section and the absolute noise power resulting. The video level at the second detector must be maintained at a sufficiently high level so that microphonic disturbances within the remaining video components are negligible and low enough to assure satisfactory detection without serious overload effects. Undesired feedback at the IF frequency also tends to limit the practical gain which can be introduced into the IF amplifier. In the military radar systems of the past war period the usual maximum gain associated with the IF amplifier was of the order of 110 db with a maximum detector output level of approximately 1 volt rms of input circuit noise. The extreme variation of the level of the desired radar signal makes necessary that provision for a large gain control variation be included in the IF amplifier design. This gain control often involves automatic, as well as manual, adjustment and commonly a gain variation range of the order of 80 db is required.

Another consideration which enters into the IF amplifier design and is associated with gain features, is the behavior of the amplifier in the presence of extremely large radar signals or enemy "jamming" signals. Optimum

protection against complete "blocking" of the IF amplifier under these conditions involves the use of extremely small-valued filter or by-pass elements which are associated with the grid and cathode circuits to present very short time constants and, accordingly, assure recovery of the amplifier in fractions of a microsecond after overloading by a large pulse signal. The gain control method is also chosen to minimize possible overloading by reducing the gain of the amplifier at a point as far forward in the radar receiver chain as possible.

Intermediate Midband Frequency

The choice of the intermediate frequency for a radar receiver is essentially a compromise between the need for reduction of unwanted external interference and noise, and the desire to realize maximum performance in terms of gain and noise figure.

The tendency to employ a high IF midband value arises from a consideration of the character of the certain local beating oscillator noise sidebands. As mentioned previously, the noise sideband output decreases as the frequency interval from the oscillator frequency is increased and it is apparent that a high value for the IF will be advantageous. In the case of balanced converters where the oscillator noise sidebands are reduced by the circuit balance, this factor assumes less importance. A moderately high IF is also advantageous in the elimination of the IF signal from the final detected video output which must be accomplished by the use of low-pass filters. The automatic frequency-control problem is somewhat simplified by the use of a high IF. The wider separation of the desired tuning point and the image response and the reduction of interfering TR pulse energy is a positive help in the performance of the automatic frequency-control circuits and will be discussed in detail in a later section.

There are also a number of factors which indicate that a low value of midband IF may be desirable. The noise figure of the input stage of the IF amplifier is generally better at a low frequency, though this improvement tends to be quite small for the band widths employed in the military radar system. A more important advantage of a low IF value is found in the improvement of the absolute frequency stability of the IF transmission characteristic under the influence of variations of tube and circuit capacitance.

Intermediate midband frequencies of 30 mc and 60 mc have been employed in the majority of military radar systems developed in the United States during World War II. In general, 30 mc has been employed quite extensively in naval and ground radar equipments for fire control where radar pulse widths of the order of one microsecond are used. For airborne radar equipments with the emphasis on compactness, weight, and the trend toward higher microwave transmission frequencies, 60 mc has proven to be an extremely popular intermediate frequency value.

The Second Detector

The final conversion of the IF signal to a video form is accomplished by simple detection. This process is usually associated with the IF amplifier because of the relative ease by which the video signal can be transmitted to the following display circuits, usually physically removed from the IF amplifier, as compared with the transmission problem which exists at the intermediate frequency.

Two types of second detector circuits which are commonly employed in radar receiver design are the linear diode rectifier and the plate circuit detector, both similar in form to those employed in prewar television practice. Several factors must be considered in the choice of the second detector operating characteristic. Linear detection of the signal is desirable from the standpoint of realizing the greatest possible visibility of weak radar signals in the presence of noise of comparable amplitude. In the case of lobing radar signals where bearing determinations are made by comparison of the return signal amplitude for two bearing conditions of the antenna radiation, the characteristic of the second detector enters to affect the sensitivity of azimuth response in two ways. The lobing sensitivity is increased by the use of a square law detector, however, the presence of a "jamming" signal of the CW type which may be located off axis can introduce a false bearing indication, which is not present when a purely linear detector is employed. In general, the linear detector has been employed in most radar systems developed during the past war period.

The detailed circuit design of the IF amplifier can be conveniently separated into three quite distinct parts. These include the input circuit design, the interstage arrangement, and the design of the second detector circuit.

2.22 IF *Amplifier Input Circuit Design*

The primary consideration in the IF amplifier input circuit design is the effect of this stage on the over-all receiver noise figure. As indicated previously, this over-all receiver noise figure is dependent on the performance characteristics of the first or input IF amplifier stage to a degree dependent on the loss of the converter stage preceding it. In the military radar field, employing microwave frequencies of 3000 mc and greater, the crystal converter is universally employed and the over-all noise performance is determined largely by the IF input stage. The use of high-gain pentodes in the IF amplifier assures that noise contributions from the following stages are negligible.

Figure 26 represents an equivalent input circuit of the IF amplifier convenient for discussion of the noise performance of this circuit. Here the noise contribution, exclusive of the signal source, is observed to be composed of two sources, one due to shot noise of the first IF stage referred to the grid

circuit and a second noise source related to active grid loading effects.[11]

The optimum IF amplifier input circuit design involves primarily the selection of impedance transformation means which results in the maximum over-all signal-to-noise performance for the radar receiver. It can be shown that this optimum value of impedance transformation is not that value which

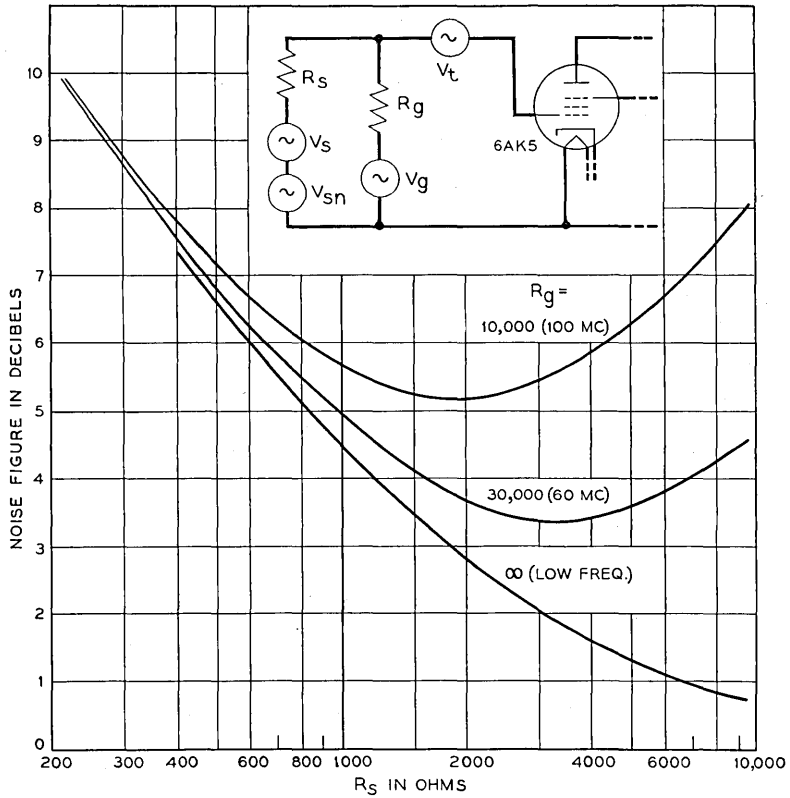

Fig. 26.—Simplified equivalent input circuit of an intermediate frequency amplifier and noise-figure vs signal source impedance.

maximizes the signal but rather is a condition where a definite signal mismatch obtains. This may be understood by an inspection of the characteristics of the two fictitious noise sources illustrated. The shot noise contribution of the vacuum tube employed in the input IF amplifier stage is here represented by the series noise generator V_T. Under conditions of shorted grid this is the only effective noise contribution, and this procedure offers a simple method for determination of the magnitude of this effect.

[11] "Considerations in the Design of a Radar IF Amplifier," Andrew L. Hopper and Stewart E. Miller, *Proc. I. R. E.*, November 1947.

The additional noise contribution under the condition where an impedance is placed in the grid circuit is shown by the noise generator V_G. This noise source is related to the active grid loading. The resistance R_G represents this effective loading which is due to transit time and tube lead inductance effects and, therefore, has a value which is associated with the frequency of operation and the particular design of tube employed. At very low frequencies, $R_G \rightarrow \infty$, the shot noise effects are entirely controlling, and the optimum IF amplifier input grid circuit condition for minimum noise figure is that condition where the impedance of the signal source approaches an infinite impedance. As the frequency of operation is increased, R_G assumes a finite decreasing value and the optimum signal source impedance is given by the relationship illustrated in Fig. 26. It should be noted that the frequency values associated with the above characteristic are indicative of the performance of the 6AK5 pentode, one of the most satisfactory of available tubes for this purpose. It should be observed that the input IF amplifier stage noise figure is independent of the impedance of the signal source providing that a perfect or lossless transformer can be employed to achieve the optinum impedance transformation indicated.

The realization of proper impedance transformation characteristic in the radar IF amplifier input circuit is basically a network problem. The input grid impedance which can be maintained over the desired band of frequencies is limited by the total capacitance present in the grid circuit. For narrow IF band widths, particularly at the lower frequencies, the realizable impedance at the grid may be in excess of the active grid loading value and here the noise performance indicated in Fig. 26 may be realized. However, for wide IF band widths at normal radar IF midband values the maximum grid circuit impedance which can be achieved under the limitation of the grid circuit capacitance will be less than the value associated with the active grid loading and the noise figure obtained will be somewhat higher than the optimum shown. This restrictive design condition is referred to as "band width limited." In modern military radar receivers this condition normally obtains.

To achieve the maximum input coupling network efficiency it is extremely desirable to minimize all parasitic capacitances under control of the designer and to employ the most effective network arrangement available. The double-tuned transformer and autotransformer networks are commonly employed for this purpose. Any loss in the impedance transforming network will result in further degradation of the noise performance, since this loss is effective in reducing the signal energy while having no effect on the tube noise level. The magnitude of the impedance transformation ratio required in a typical radar design case for optimum noise figure is approximately seven times, where a crystal converter of the type shown in Fig. 14

is employed, and the optimum grid impedance at 60 mc as shown in Fig. 26 is approximately 3000 ohms.

The vacuum tube employed in an input stage of an IF amplifier should have the following characteristics to achieve the optimum performance. The tube should be capable of providing sufficient gain to assure that the noise contribution of the following stages is negligible. The input conductance of the selected tube at the intermediate frequency should be as low as possible indicating generally that physical size should be small to assure small transit time effects and low lead inductance values. The noise output of the tube itself should be a minimum, this characteristic being somewhat controllable by proper emission characteristics. The characteristics of the most desirable of the vacuum tubes available to the radar receiver designer during the past war period for IF amplifier purposes is given in Table I.

TABLE I.—*Principal Characteristics of IF Amplifier Tubes*

Type	Heater Power Watts	Plate Current ma	Total Power Consumption Watts	Nominal Transconductance Micromhos	Interelectrode Capacitances Micromicrofarads		Band Merit B_0 mc
					Control Grid to Heater, Cathode, Screen Suppressor Grid	Plate to Heater, Cathode, Screen, Suppressor Grid	
6AC7	2.84	10	4.7	9000	11	5	89
6AG7	4.10	30	9.6	11000	13	7.5	85
6AG5	1.89	7.2	3.0	5100	6.5	1.8	95
717A	1.10	7.5	2.3	4000	4.9	3.8	73
6AK5	1.10	7.5	2.3	5000	3.9	2.8	117

The development of the 6AK5 pentode was the direct result of the necessity for improved radar IF amplifier performance, and details of this development and the performance of this tube have been described elsewhere.[12]

The noise present in a pentode is greater than in a triode, primarily due to the presence of additional grid structures. Because of this fact, a number of attempts have been made to employ triodes in the input stage of the IF amplifier. To prevent oscillation due to large positive feed-back present through the plate-to-grid interelectrode capacitance, neutralization methods have been employed. For moderate IF band widths at 60 mc such experimental designs have shown an improvement in noise figure of slightly more than 1 db over the pentode design; however, the criticalness of the neutralization scheme and the difficulties in extending the performance to wider IF band widths has not allowed this design to be adopted extensively to military radar equipment during the past war period.

[12] "Characteristics of Vacuum Tubes for Radar Intermediate Frequency Amplifiers," G. T. Ford, *Bell System Technical Journal*, Vol. XXV, July 1946.

2.23 *Interstage Circuit Design*

The design of the IF amplifier interstage circuit is basically concerned with achieving the greatest possible gain per stage while not compromising the frequency characteristic and stability, or complicating the structure to an extent where it will be difficult to realize the designed measure of performance under military operating conditions. The problem can be resolved into the choice of the vacuum tube and the selection of an interstage coupling network.

The gain of a pentode operated into a 2-terminal parallel resonant network which exhibits a maximum impedance R_o at resonance is given by $G_m R_o$ under the restriction $R_o << R_p$. If a band width ΔF is defined as that band of frequencies where the magnitude of the impedance Z of the network is equal to or greater than $\frac{R_o}{\sqrt{2}}$ it can be shown that

$$\Delta F = \frac{1}{2\pi R_0 C}.$$

The gain-band width product of an amplifier stage is a measure of performance of the stage and serves as a criterion for tube performance if a standard load impedance as above is adopted. Then the band merit B_o for this condition will be given by

$$B_0 = \Delta F G_m R_0 = \frac{1}{2\pi R_0 C}(G_m R_0) = \frac{G_m}{2\pi C}.$$

The band merit B_0 of a tube has the dimensions of frequency and may be interpreted as the frequency at which the voltage gain of the vacuum tube is at unity with a plate load impedance restricted solely by the sum of the plate and grid tube capacitances. The ideal IF amplifier vacuum tube will exhibit a high band merit figure, stable operating characteristics over the life of the tube, uniform characteristics during the production period, small size for compact amplifier use and for resulting mechanical rigidity, and finally low-power consumption, desirable from both the power supply standpoint and heat dissipation considerations. The actual types of vacuum tubes generally employed for radar IF amplifiers during the past military program in order of their availability were the 6AC7, 717A, and finally the 6AK5. The improvement in performance achieved through this succession of developments can be observed by reference to Table I and the band merit and power consumption figures for these tube types.

Figure 27 illustrates three types of interstage coupling networks which have been commonly employed in radar IF amplifiers for military purposes. The synchronous single-tuned network design has an advantage of simplicity of construction and permits relatively simple realignment procedures under

the limited resources of military field conditions. This type of interstage has been employed quite widely in radar equipments designed during World War II. To achieve the maximum gain per stage it is necessary to restrict the total shunt capacitance of the interstage circuit to the unavoidable elements due to tube and circuit arrangement. Additional capacitance contributions are avoided by the use of a variable inductance element adjustable through the use of movable magnetic cores to resonate the network to the desired midband IF value. The shunt resistance element is chosen to achieve the desired band width.

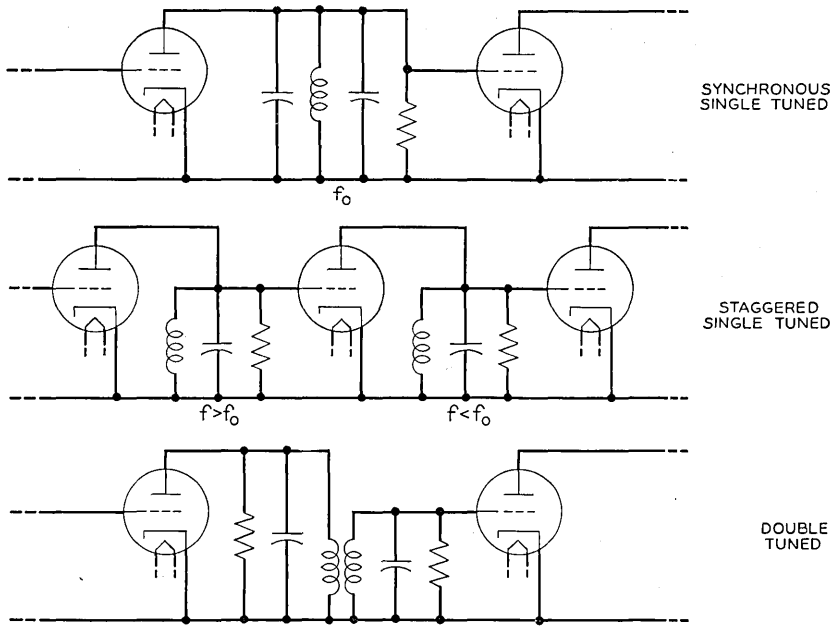

Fig. 27.—Typical IF Amplifier Interstage Circuits. Simplified schematics.

The band width required of each individual interstage circuit of a multistage amplifier of this type to meet an over-all band width requirement of B cycles is given by

$$B = \Delta F\sqrt{2^{1/N} - 1}$$

where ΔF represents the band width of the individual interstage network, defined as the band over which the response is within 3 db of the midband IF value, and N is the number of interstage circuits employed. As the individual interstage band width is increased to achieve the desired over-all value, the gain per stage is reduced and a greater number of stages is required

to meet the over-all gain requirement. The over-all gain of a multistage amplifier employing synchronous single-tuned interstage networks is given by

$$G_0 = \left(\frac{G_m\sqrt{2^{1/N} - 1}}{2\pi C_T B}\right)^N$$

where C_T represents the total interstage shunt capacitance and B is the over-all band width requirement. Table II presents the individual interstage band widths and the maximum over-all gain obtainable for multistage IF amplifiers having a 5 mc over-all band width requirement. Here the use of the 6AK5 pentode is assumed and the total interstage shunt capacitance is assumed to be 12 micromicrofarads. It should be observed that unavoidable misalignment of circuits, aging of tubes, and other such effects all tend to reduce the idealized computed performance under the practical military radar conditions and must be considered thoroughly in the design.

TABLE II.—*Interstage Band Width and Over-all Gain of Multistage IF Amplifiers*

No. of Amplifier Stages	Synchronous Single-Tuned Interstage		Double-Tuned Interstage	
	Interstage Band Width mc	Over-all Gain db	Interstage Band Width mc	Over-all Gain db
1	5	24	5.0	27
2	7.8	37	6.2	47
4	11.5	61	7.6	87
6	14.3	80	8.6	125
8	16.6	96	9.3	162
10	18.7	110	9.8	198

The double-tuned interstage network configuration shown in Fig. 27 is a somewhat more efficient circuit form than the single-tuned variety just discussed, and because of this improved performance has been employed to about the same extent as the synchronous single-tuned type during the past war. Its performance advantage lies in the basic fact that the transmission response curve for this structure has a flat-top characteristic resulting in a slower rate of over-all band width reduction as these circuits are cascaded. The ability to separate the output plate and the input grid circuit capacitances and the elimination of the plate-to-grid coupling capacitor with its additional parasitic capacitance to ground results in a greater gain-per-stage performance. In this structure the resonant frequency of both primary and secondary circuits corresponds to the midband IF and the conditions of equal Q of primary and secondary circuits and critical coupling are assumed. These conditions result in a smooth flat-topped response characteristic having optimum gain performance. The relationship between the individual inter-

stage band width and the over-all band width of a multistage amplifier employing double-tuned interstage circuits is given by

$$B = \Delta F \sqrt[4]{4(2^{1/N} - 1)}$$

which is illustrated in Table II together with the corresponding over-all gain of multistage IF amplifiers of this design.

The third type of interstage network arrangement illustrated in Fig. 27 represents a method employed to realize improved performance of the single-tuned interstage network type by resonating alternate interstages at frequencies above and below the desired midband IF value. This stagger-tuned interstage design permits greater gain per stage together with an increased over-all band width for each pair of amplifier stages over that obtained with the synchronous single-tuned design. In the case of IF amplifiers having six or more stages a variation of this stagger-tuned method can be employed where three successive interstages are considered as a design unit and the individual interstage resonances are adjusted below, above, and centered at the midband IF respectively. To afford a measure of the improved performance of a stagger-tuned IF amplifier we may consider the relative performance of a 6-stage IF amplifier of 5 mc over-all band width employing the 6AK5 vacuum tube. An individual interstage band width of 7.2 mc and an over-all gain of 116 db will result from the use of stagger-tuned interstage circuits while reference to Table II indicates the synchronous single-tuned design would have an over-all gain of only 80 db while the double-tuned design would result in an over-all gain of 125 db. The use of a triple stagger-tuned design would produce a 6-stage amplifier having approximately the same gain performance as the double-tuned example above.

The choice of the interstage network configuration to be employed in a radar IF amplifier must be made considering the circuit efficiency, the gain-frequency stability behavior, and with due regard for the ever-present problem of maintenance of performance under the field conditions of modern warfare. From a standpoint of circuit efficiency alone, it has been shown that the synchronous single-tuned interstage network is decidedly inferior to the more complex forms, but the obvious simplicity of construction of this type and the possibility of adjustment and realignment with simple methods available in the field is a strong recommendation for its adoption in military radar IF amplifiers. The double-tuned circuit has a considerable advantage in circuit performance over the case above, but some portion of this increased efficiency must be sacrificed since it is impractical to construct this network with adjustable elements. Here the normal variations in interstage capacitance with replacement of vacuum tubes or aging effects must not be allowed to reduce the over-all amplifier performance below the design limit. The solution to this problem must be achieved by design of each interstage circuit

to obtain a somewhat wider band under average tube conditions so that under subnormal but acceptable tube conditions the over-all performance of the amplifier is still within requirements. The use of stagger-tuned interstage designs will also result in increased performance over the basic synchronous single-tuned variety, but the maintenance of the over-all performance of a radar IF amplifier of this type involves relatively complex measurements not always possible under military conditions.

2.24 *Second Detector Design*

The final conversion of the IF signal to the video form, as required by the following radar display device, is accomplished by simple detection or rectification. For this purpose either a diode rectifier or a triode operating as plate circuit detector is usually employed. The second detector design follows the practices generally developed for television receivers prior to the war. The diode second detector method has the advantage of simplicity with no plate supply voltage being required, but the performance of such a detector is somewhat limited for the frequencies employed in radar systems. The linearity of rectification of a diode depends on maintaining a high load impedance relative to the internal impedance of the tube. The external load impedance is limited, by the presence of tube and parasitic circuit capacitance and the video band width required, to somewhat less than 1000 ohms for the typical radar case. The internal impedance of the usual available diode is of the order of several hundred ohms so that the linearity of detection suffers. The low value of the diode load resistance is also reflected in the termination of the last IF amplifier stage and affects the gain of this stage.

The plate circuit detector often employed consists of a triode operated near plate current cutoff. Here the detector load impedance is effectively isolated from the plate circuit of the last IF amplifier stage. The linearity that can be obtained from this type of second detector is essentially the same as with the usual diode detector.

The polarity of the detected video output signal may be chosen of either sign by proper circuit arrangement for convenience in the video amplifying and limiting circuits which follow. It is desirable to reduce the amplitude of the IF signal which appears at the output of the second detector to prevent overload and interference in the video amplifier following. This is accomplished commonly by the inclusion of a low-pass filter of simple form in the output circuit of the second detector.

2.25 *Typical Component Designs*

In the military radar system design it has been observed that a maximum video output signal of the order of one volt of noise is desirable as a design

objective resulting in an over-all gain requirement of the order of 110 db. If the radar system employs RF amplification, the entire IF amplification may be provided in one unit. However, in radar systems operating above 1000 mc it has proved advantageous to provide the total IF gain required in two separate amplifier sections. The IF preamplifier assembly is commonly designed to be mounted adjacent to the crystal converter located in the transmitter portion of the radar system and usually consists of two stages of IF amplification. The main IF amplifier is usually located at some distance from the preamplifier, commonly associated with the indicator components of the radar receiver. The main IF amplifier assembly includes the second detector circuit and occasionally one stage of video amplification is included.

The IF preamplifier location as described above is quire desirable, eliminating the need for a long transmission line connecting the IF output circuit of the crystal converter to the input stage of the IF amplifier. As has been discussed previously, the impedance transformation employed in the IF input stage is chosen to realize optimum signal-to-noise performance. The output impedance of the crystal converter is normally of the order of 400 ohms. To assure negligible impedance reflection losses in this circuit, any connecting cable employed would have to be designed to present a characteristic impedance of this order of magnitude which is inconvenient. The practical solution as employed in past military radar systems is obtained by locating the IF preamplifier in close proximity to the converter. The absence of long leads at this IF input stage is also advantageous in reducing the interference pickup into this low signal level point. After moderate amplification the output of the IF preamplifier is usually fed over a 75-ohm coaxial transmission line to the main IF amplifier.

Figure 28 illustrates the converter and IF preamplifier assembly as employed on the AN/APQ-13 and AN/APQ-7 airborne radar bombing equipments operating at 10,000 mc. The local oscillator and silicon crystal converter are arranged in a manner similar to a basic type previously described in this paper. The IF output of the crystal converter is introduced directly into the preamplifier assembly without exposure. This preamplifier is arranged to offer two stages of amplification employing the 717A pentode and using a double-tuned input, interstage, and output network. Figure 29 indicates the circuit arrangement. The gain of this IF preamplifier is 30 db and an IF band width of 6 mc is provided. The output transformer network is arranged to operate into a 75-ohm coaxial transmission line. It should be observed that provision is here included to disable the preamplifier by application of a positive pulse to the cathode circuit of the second amplifier tube. This feature reduces the gain of the IF preamplifier during the short interval coincident with the outgoing radar pulse, which assures that the TR tube

"spike" which precedes conduction will be attenuated and, therefore, less interfering with AFC operation. Further details of this effect will be discussed in a later section of this paper.

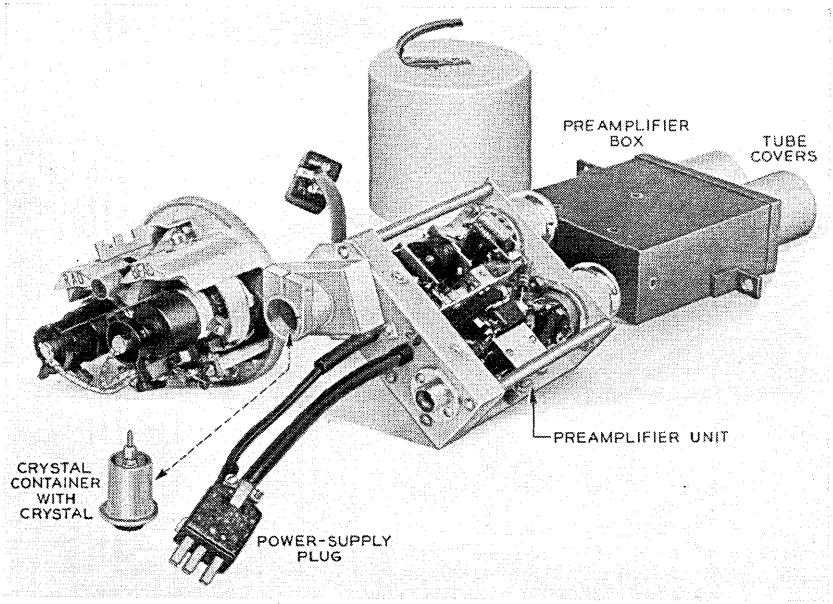

Fig. 28.—Converter and IF preamplifier assembly for AN/APQ-13 and AN/APQ-7 airborne radar bombing equipments.

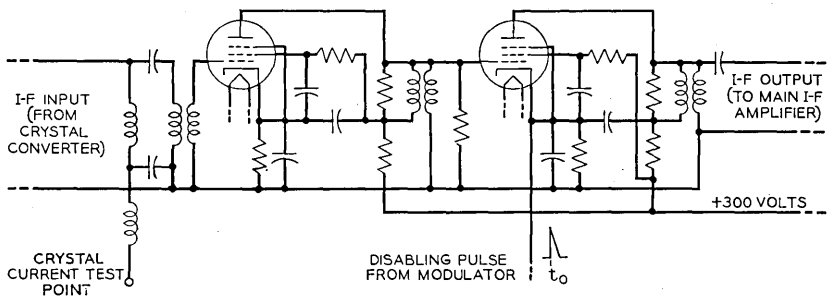

Fig. 29.—Simplified schematic diagram of IF preamplifier component of Figure 28.

Another example of equipment design of an airborne radar converter and preamplifier assembly has been illustrated previously in Fig. 23. In this design the 6AK5 tube is employed and single-tuned interstages and autotransformer input and output networks are employed; however, the general arrangement is quite similar to the design previously described.

The remainder of the IF amplifier gain required is of the order of 80 to

100 db which is usually provided in a main IF amplifier that can be located conveniently within the receiver indicator portion of the radar system. The main IF amplifier is commonly designed as a complete shielded unit, required by the high-gain concentration and desirable from the standpoint of allowing the same unit to be used in several radar systems. Three IF amplifiers are shown in Fig. 30 which well illustrates the technological development in this field during World War II. The first amplifier employing 6AC7 tubes was developed at the beginning of the war, has an over-all gain of 95 db with an approximate band width of 2 mc, and employs synchronous single-tuned

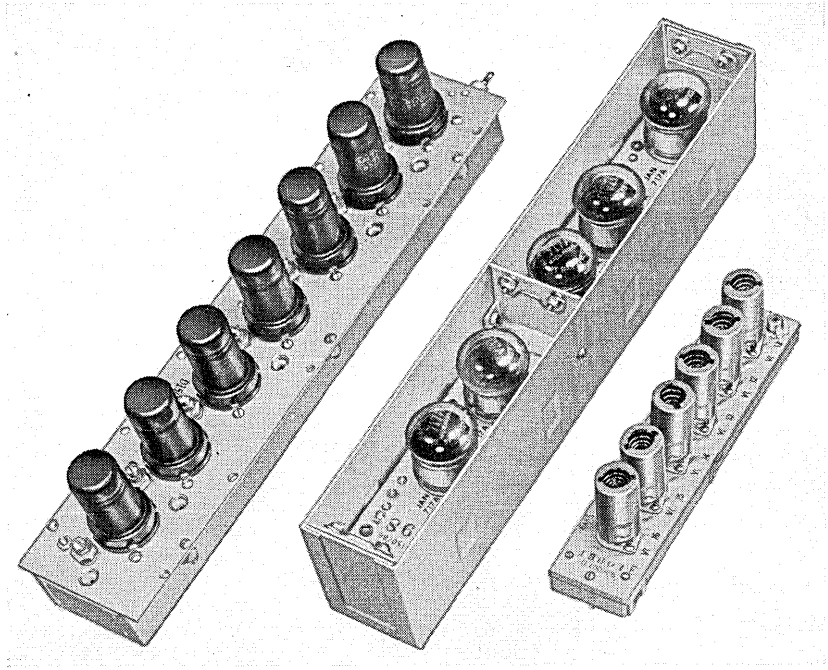

Fig. 30.—Typical IF amplifier equipment designs for military radar applications.

interstage networks. This design was employed extensively in early military radar equipments for land, sea, and air use. It has a total power consumption of 31 watts and weighs 2 pounds 4 ounces. The second amplifier illustrated was developed early in the war primarily for airborne search and interception radar systems and employs 717A pentodes with a double-tuned and single-tuned interstage combination of networks to produce a gain of 85 db with an over-all band width of 4 mc. The total power consumption is 11 watts and the weight here has been reduced to 1 pound 14 ounces. This design of IF amplifier with minor modifications was employed on the major-

ity of airborne bombing radar equipments produced by the Western Electric Company during World War II. The third IF amplifier design illustrated was developed somewhat later in the radar program for specific application to the AN/APS-4 light-weight airborne search and interception radar equipment. This amplifier employs 6AK5 tubes with synchronous single-tuned interstage coupling networks realizing an over-all gain of 100 db for a band width of 2 mc. The power consumption here is 14.5 watts and the weight has been reduced to 9 ounces. This amplifier design has been employed in a number of airborne radar equipments during the later period of the past war.

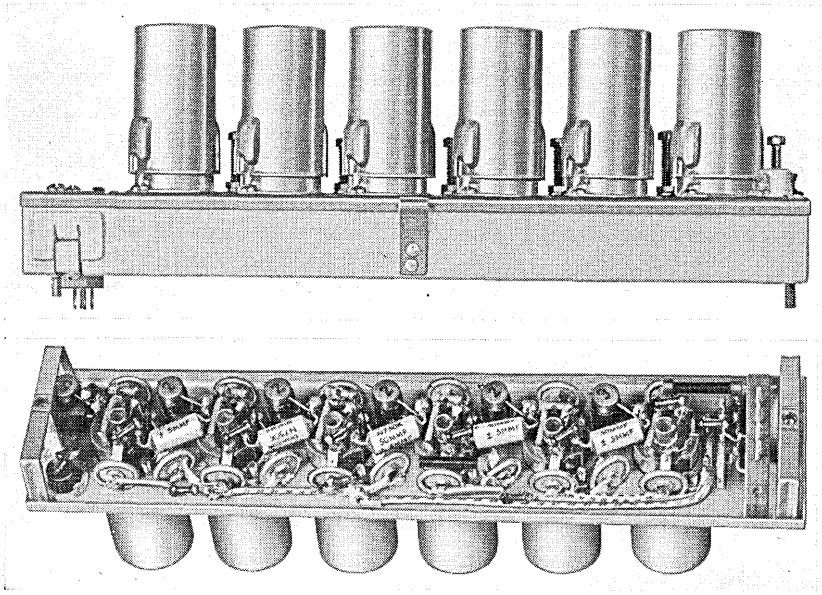

Fig. 31.—IF amplifier design as employed in AN/APS-4 airborne radar equipment.

Figure 31 illustrates further mechanical constructional details of the 6AK5 amplifier described above, and the schematic circuit arrangement is given in Fig. 32. Five stages of amplification and a second detector of a modified plate circuit type is included. A positive polarity video output is obtained from the cathode of the second detector and a single-section video low-pass filter attenuates the IF signal which appears at the detector output. A variable gain control voltage is applied to the plate circuits of the first three stages of the amplifier.

The mechanical arrangement of the components of this amplifier has been devised with a view to achieving optimum frequency and gain stability.

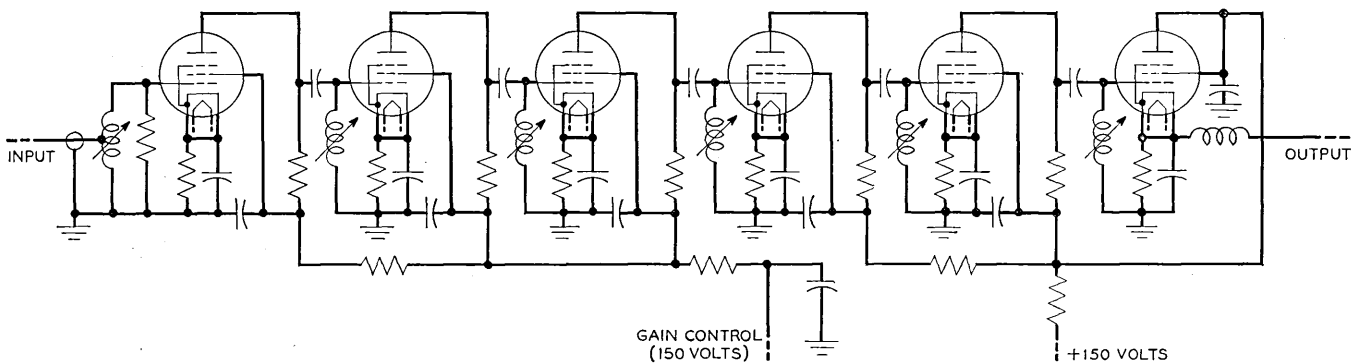

Fig. 32.—Simplified schematic diagram of 60-mc IF amplifier for AN/APS-4 radar.

This equipment design features short and rigid connections and the use of silvered-mica button-type by-pass elements which are mechanically anchored in slots cut into the chassis and soldered in place. The entire unit is arranged to plug into a multipin socket which supplies all power and receives the video signal output. The IF signal input is arranged for plug-in connection at the opposite end of the chassis.

The adjustable inductance elements shown are wound on forms having an approximate diameter of $\frac{1}{4}''$ and the small variation in inductance required to compensate for circuit variations is achieved by the use of tuning screws as illustrated. These coils are adjusted in manufacture by a comparison technique employing factory standards of the same form. The completed amplifier is aligned with mean capacitance tubes and all tuning screws locked and sealed. Sufficient design margin of gain has been included in this design to enable meeting the radar system gain requirements with a complete set of "low-limit" tubes.

2.3 *The Radar Video Amplifier*

The video amplifier of the radar receiver, which follows the IF amplifier and second detector, has as its function the final preparation of the received and detected signal for display. This process involves amplification of the signal in its now video form, introduction of additional coordinate signals and wave forms required for proper display, and often includes modification of the original amplitude characteristics of the signal itself to enhance the presentation. The radar video signal is quite similar in many respects to the television video signal and the circuit technology, therefore, parallels the television art in many respects. Two characteristics of the radar video signal result, however, in somewhat less stringent demands on the radar video amplifier design. The lowest frequency of concern in radar video practice is related to the repetition rate which rarely is found to be less than 250 pps., while it is customary to design television systems to adequately transmit signals of the order of 1 cps. The requirement of faithful reproduction of the radar pulse shape is usually of secondary importance; the quality of presence alone usually sufficing to meet the radar system design objective. In certain fire-control radar systems, however, the radar system band width must be adequate to reproduce the received pulse to an exactness of the order maintained in standard television practice. In general these somewhat reduced transmission requirements for radar purposes result in a desirable economy of circuit elements and power consumption.

2.31 *Gain-Frequency Considerations*

The limiting performance of a video amplifier can conveniently be evaluated by a consideration of the transmission problem at the extremities of the

video band of frequencies. At high frequencies the gain-frequency characteristic of a video amplifier stage employing pentodes as illustrated in Fig. 33 is given by

$$\frac{g_m R_L}{\sqrt{1 + f^2/f_H^2}}$$

where f_H represents the frequency at which the relative gain has been reduced 3 db over the value achieved at the video midband region. This cut-off frequency relationship is similar in form to that encountered in the radar IF

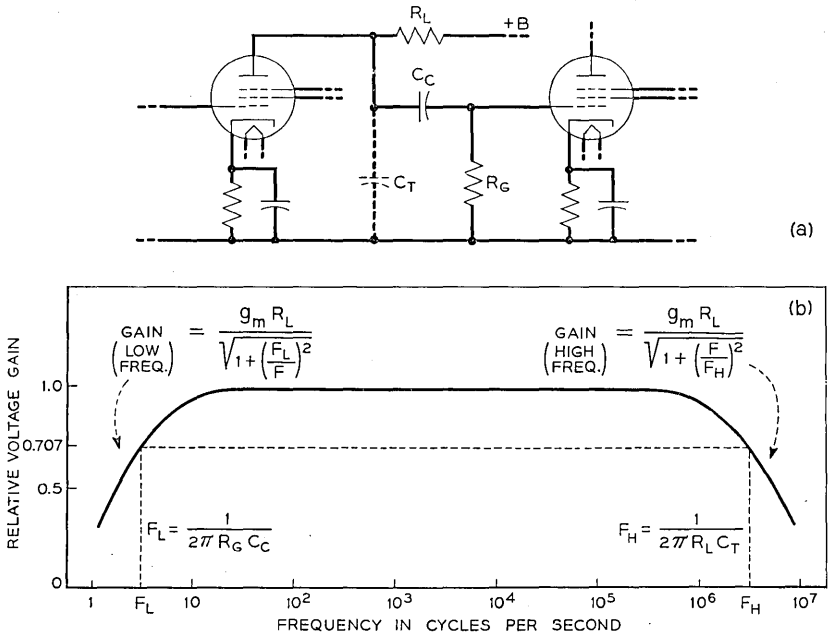

Fig. 33.—Radar video amplifier gain vs. frequency relationships.

amplifier design previously reviewed. In the video amplifier design the vacuum tube band merit B_o again determines the limiting performance of the amplifier, but since the associated video interstage circuit elements contribute considerably to the total circuit parasitic capacitance by reason of their large physical size, the effective band merit of a vacuum tube for video purposes must be considered in terms of the total tube and circuit capacitances. The additional consideration in vacuum tube choice for radar video amplifiers is one of load capacity, since the output signal voltage required for indicator use may range upward to several hundred volts.

In a somewhat analogous manner to the relationships discussed in the

design of IF amplifier interstage networks, the video amplifier performance at high frequencies can be improved by the use of more complex 2- and 4-terminal interstage networks. In military radar systems, however, the added performance realized is more than offset by the undesirability of the additional circuit elements required and the more complex maintenance problems that arise, so that usually only the simple resistance-coupled interstage design is encountered in radar systems.

At the low-frequency extreme of the video band the gain performance of the simple video amplifier is related to the product of the series interstage plate-grid coupling capacitance and the input resistance of the following grid circuit. The low-frequency cut-off of a video amplifier is again defined as the frequency where the gain has fallen 3 db over the value at midband frequencies and is given by $f_L = \frac{1}{2\pi R_G C_c}$. The highest value of R_G that can be employed is related to the grid current characteristics of the vacuum tube chosen. The use of a large value of C_c is undesirable for two reasons. First, the interstage shunt parasitic capacitance increases as a physically larger condenser is employed, which results in poorer high video frequency performance. Second, the use of large coupling capacitances is undesirable from the standpoint of increase in susceptibility to blocking or paralysis in the presence of large signals or enemy jamming. The low-frequency gain response can be improved by certain proportioning of the plate, screen, and cathode by-pass elements also resulting in somewhat less possibility of undesirable feedback through the common power supply impedance.

In certain military radar system designs, multistage negative feedback video amplifiers have been employed. Here considerably greater transmission band width may be realized with the simple interstage network design and an order of improvement in stability results. The feedback amplifier design in these cases usually involves common cathode feedback impedance between the first and third stages.

2.32 *Gain-Amplitude Considerations*

The use of nonlinear gain versus amplitude characteristics in a video amplifier is a condition peculiar to the radar system and represents a considerable departure from established television practice. The factors that indicate the desirability of this treatment of the signal involve the behavior of the amplifier under the extreme range of received radar and jamming signals encountered and the electro-optical characteristics of certain radar indicator cathode-ray tubes.

Definite amplitude limiting of the video radar signal is commonly included in military radar systems. By introducing amplitude limiting at an early part of the video amplifier, complete amplifier paralysis is avoided when

extremely large overloading signals are encountered. These signals may represent strong radar return echoes from objects in the vicinity of the radar antenna or may be due to enemy jamming signals. The ability of the radar receiver to recover in a short time following such serious overloading is an extremely important design consideration. In the case of jamming signals of a continuous-wave or long-pulse form, their effectiveness can be minimized by the inclusion of a high-pass network at the input of the video amplifier.

In the case of radar systems which employ intensity modulated displays of the B, C, and PPI forms the maximum useful brightness that can be attained is limited by "blooming," a phenomenon in which the cathode-ray tube spot on the fluorescent screen undergoes a sudden defocussing when the brightness is increased beyond a critical value. In addition, halation effects are quite pronounced in these long-persistence cascade layer screens and contribute to an undesired masking effect when large areas of extreme brightness are encountered. In these cases it is extremely important to limit the maximum amplitude of the signal that can be impressed upon the indicator. The usual radar video amplifier includes an amplitude limiting stage located early in the amplifier chain whose operating conditions are such as to be driven to plate current cut-off by signals which exceed a preselected amplitude.

The range of useful brightness of the cascade screen radar indicator is severely limited in comparison with the extreme amplitude range of the received radar signals. As has been discussed, the maximum useful brightness has been seen to be limited by halation and defocussing effects while the minimum brightness threshold is controlled by halation and ambient viewing conditions. These limitations of the viewing tube result in a criticalness of adjustment required of the radar operator to achieve the optimum performance of the radar system. In an effort to improve the general reproduction efficiency of the military radar system, several circuit forms have been devised whereby the amplitude of the indicator signal is related to the received radar signal in a nonlinear fashion. In certain instances two parallel amplifier paths have been provided where one path operates in a normal fashion until overload is reached when the second transmission path, designed to properly transmit the higher amplitude signals, becomes effective. In this manner two relatively linear amplification regions are provided with a step or amplitude limiting region interposed. Such a nonlinear circuit arrangement has been referred to as "duo-tone", indicative of the two reproduction regions employed. Another video nonlinear characteristic which was employed in a certain airborne radar bombing equipment developed toward the end of the war was of a logarithmic form realized by a two-path amplifier design. In general this nonlinear treatment of the radar signal amplitude has proven capable of reducing the critical adjust-

ment which has in the past been required of the radar indicator and in this respect has contributed some measure of improved performance under military operating conditions.

2.33 *D-c Restoration Methods*

It is pertinent to examine the exact form of the video signal encountered at the output of the video amplifier as it exists available for indicator use. The presence of series coupling condensers in the video amplifier has removed the d-c component from the signal as detected and, therefore, the average value of the signal is zero. In this form the amplitude of the positive and negative signal excursions are dependent on the form of the signal itself. If such a signal is impressed upon an indicator of the intensity modulated type the average brightness of the scene will remain constant, and the presence of several large amplitude signals will tend to drive any accompanying weak signals below the useful reproduction threshold and effectively fail to reproduce them. In the case of an A-type display where the video signal deflection modulates the beam, the no-signal base line will assume a position on the screen dependent on the video signal form. For these applications it is required that the d-c component be restored to the signal before display. In many other parts of the radar system d-c restoration is required to enable utilizing to the fullest extent the load capabilities of vacuum tubes under the conditions of varying duty cycles of the impressed wave forms. In sweep circuit design a considerable economy of power is achieved by operating the amplifier tubes at or near plate current cut-off for no-signal conditions. Through the medium of d-c restoration, the signal excursions are confined to positive regions only and then regardless of the duty cycle the signal range of amplitude impressed upon the tube is maintained within desired limits.

Figure 34 illustrates three circuit forms which are employed to "reinsert" the d-c component of an a-c video signal. The diode restorer commonly employed in radar systems is shown in Fig. 34a. The impressed input wave, assumed to have an average value of zero as shown, will cause the diode to conduct whenever the signal polarity is negative. During this diode conducting period the condenser C will be charged rapidly, the full effective negative peak signal voltage appearing across its terminals. During the following positive excursion of the signal this voltage difference will be applied effectively in series with the signal. The time constant RC is chosen large with respect to the period of the signal repetition rate and thus maintains this additive bias for the remainder of the signal cycle. Since the effective time constant during the diode conducting period is extremely small valued, limited only by the conductive internal resistance of the diode itself, an extremely small negative excursion time will suffice to

restore the grid circuit to reference zero potential. This particular d-c restorer circuit form is referred to as a positive restorer, indicative of the final polarity of the restored signal. A simple reversal of the diode elements will reverse the polarity of the restored signal.

Figure 34b illustrates the usual radar circuit form of a negative d-c restorer where the diode is eliminated, the normal vacuum tube grid circuit

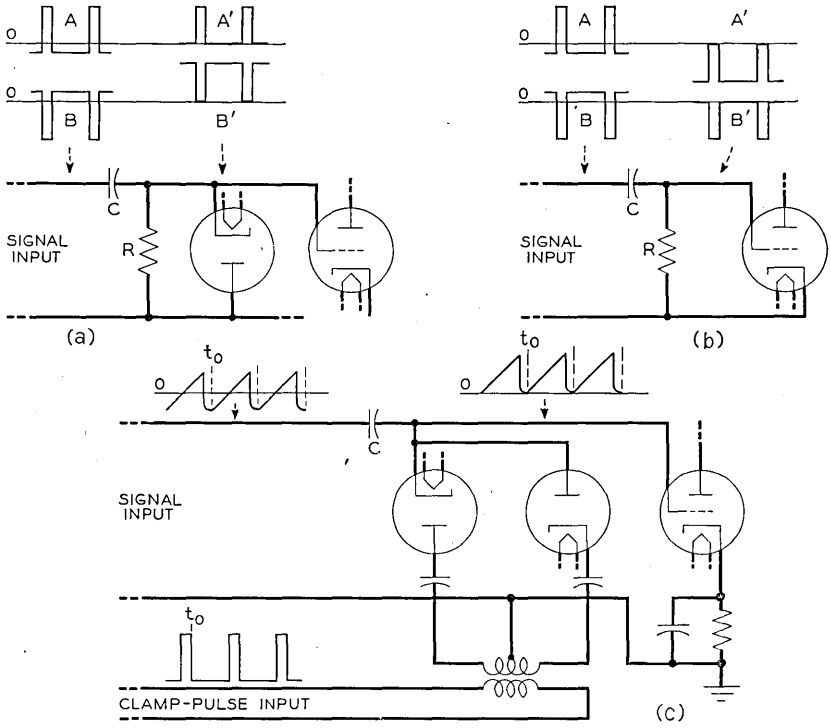

Fig. 34.—Typical D-c Restorer Circuit Forms. Simplified schematic diagrams.

serving here to fulfill this function. Here again an impressed signal form having an average value of zero is assumed, and a negative polarity restored signal is desired at the grid of the amplifier tube. During periods of positive excursions of the input signal the vacuum tube grid will conduct since it is normally operated at zero bias. The series condenser C is accordingly charged relative to the positive signal peak amplitude and this value of potential will be additively combined with the signal during negative excursions in a similar manner to the diode restorer action just described.

A third form of d-c restoration is known as a clamper or synchronized d-c restorer and is illustrated in Fig. 34c. Here a diode bridge circuit

is arranged to be normally nonconductive except during the application of a clamping pulse bias introduced as shown. During this clamping interval, the grid circuit point of the condenser is re-established to reference potential by the low impedance of the conducting diode circuit. At the time of decay of the clamping pulse wave forms the operation of this circuit follows the principles of the d-c restorer types just described. This circuit has been employed less extensively than the preceding simple d-c restorer methods because of the relatively more complex arrangement, but has an advantage in that the impressed signal may be clamped to a convenient reference potential at any particular repetitive point in the cycle.

2.34 *Typical Radar Receiver Video Amplifier Circuits*

The radar receiver video amplifier signal output is required to modulate the indicator by either position or intensity change. In the A type of display the video signal is usually impressed upon a pair of vertical deflection plates of an electrostatic type of cathode-ray tube to present the amplitude characteristics of the signal while the range to the target is displayed as the horizontal coordinate. The maximum video signal amplitude required here to deflect the beam satisfactorily is usually of the order of several hundreds of volts. In the case of B, C, and PPI forms of display the radar video signal is required to intensity modulate the cathode-ray tube. Here a maximum video signal amplitude of 50 volts is commonly required by the radar indicator.

In certain military radar system applications it is desirable to locate the indicator component at some distance from the main radar receiver and video amplifier assemblies. This requirement is commonly encountered in large naval vessel installations where the main radar components may be located below deck and the indicator mounted as a part of the gun pointing mechanism. In such cases video amplifier designs employing video transformer coupling between the output amplifier stage and a coaxial transmission line and between the line and the indicator circuit proper, have proven to be entirely successful.

The development of video pulse transformers for radar purposes represents a considerable advance in the art of communication transformer design. The greatly improved wide frequency band performance of these components is the result of the employment of improved magnetic core materials such as supermalloy having relative permeabilities upward of four times that available in the permalloy materials, improved techniques of coil winding distribution, and the use of additional network elements in the final configuration. Figure 35 illustrates the constructional features of such a video pulse output transformer which has a band width extending

from 100 cycles to 7 megacycles as employed in a naval fire-control radar equipment.

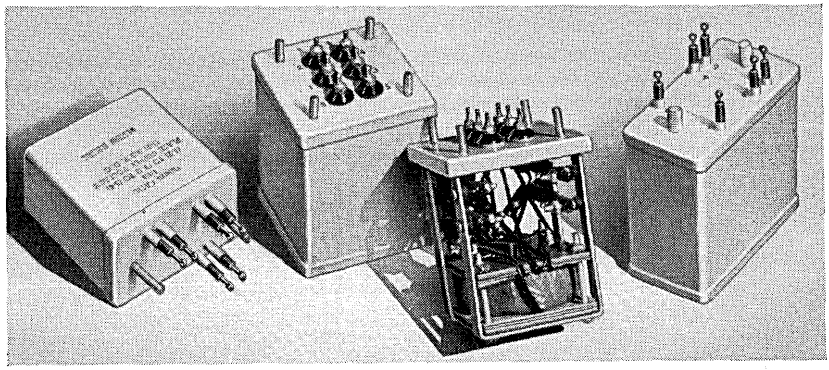

Fig. 35.—Typical designs of radar receiver video frequency transformers.

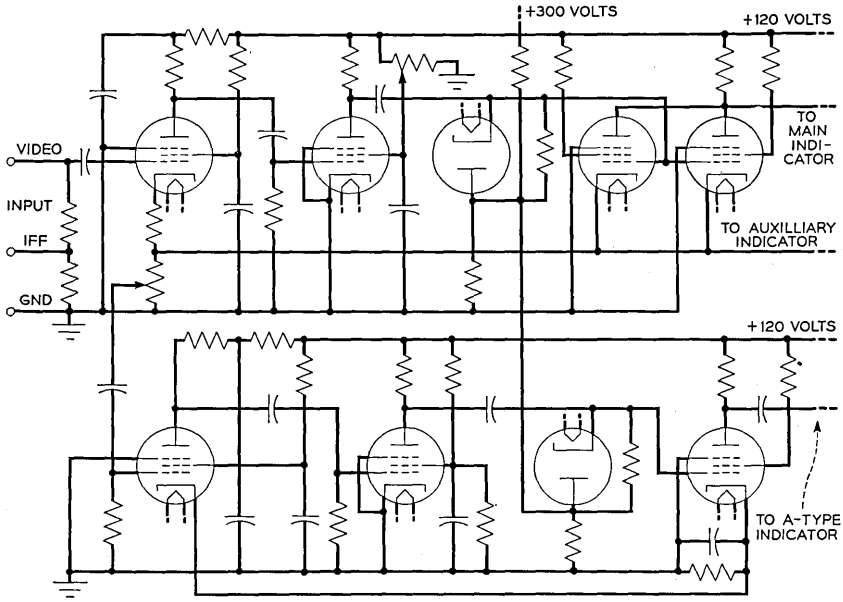

Fig. 36.—Simplified schematic diagram of video amplifiers as employed in AN/APQ-7 airborne radar equipment.

Figure 36 illustrates a video amplifier circuit arrangement as developed for the AN/APQ-7 radar bombing equipment during the latter period of the past war. This system employed two GPI type indicators, one of which was located at a remote station of the aircraft and included also an

A-type indicator which was employed for certain conveniences in operation and maintenance of the equipment. This circuit design includes a main video amplifier for the ground plan indication and a separate amplifier for the A-type display, both of which are of the negative feedback type. The limiting amplifier is included as the second stage with negative d-c restoration included in this grid circuit and diode d-c restoration at the grid of the last stage. To provide sufficient output signal level with the wide video band width required it was necessary to employ two 6AG7 tubes in parallel in the final output stage of the main video amplifier. The local indicator is fed from the plate circuit while the remote navigator's display is fed by means of a low impedance coaxial transmission line. The video gain control is essentially an adjustment of the video amplitude limiting level, the actual signal amplitude being previously adjusted by the IF amplifier gain control. The over-all gain of the main video amplifier is approximately 32 db with a band width of approximately 5 mc. The over-all gain of the A-type display amplifier circuit is approximately 43 db with a useful band width of approximately 6 mc.

2.4 *The Radar Indicator*

The radar indicator assumes a position of extreme importance in the components of the radar receiver. Here with a few specific exceptions all of the electrical information which has been obtained regarding the area under observation is finally correlated and converted into an optical display for use by the radar observer. In the discussion thus far, only the received radar microwave signal properly selected, amplified, and finally converted to the video form has been discussed in detail. The preparation of the additional coordinate and reference data necessary to properly present the complete scene is reviewed in the following sections. In this section the characteristics of the presentation will be reviewed from the standpoint of the requirements imposed by the various radar applications. The electro-optical characteristics of the display device are also discussed.

2.41 *Classification of Radar Display Types*

The number and types of display methods which have been developed for military radar systems during World War II are the result of the varied specific applications to which radar has been subjected. These types of displays are in general related directly to the functional classification of military radar systems previously discussed. It is of interest to consider at this time the various types of indicators which have become common in the radar field. Figure 37 illustrates the basic characteristics of the most important types of radar presentations.

Basically the three coordinates which determine the position of the target

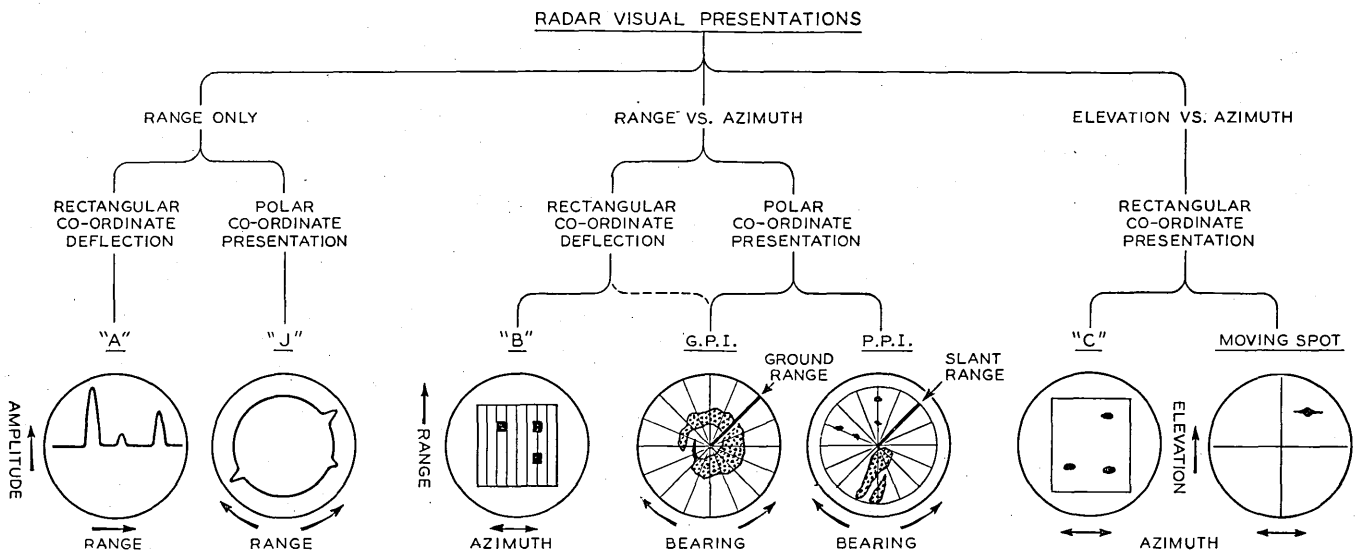

Fig. 37.—Typical military radar display types.

in space and which are determinable from a single radar observation location are the range to the target, azimuth angle with respect to a chosen direction axis, and elevation angle as measured from a convenient reference plane. The classification of radar displays shown in Fig. 37 results from the fact that the only available and convenient display device has the property of resolving only two such coordinates simultaneously. The radar display problem is then one of selecting the most important two coordinates for the specific radar application and choosing the presentation means accordingly. For example, if the radar system under consideration is to be employed on a surface naval vessel against similar naval vessel targets, it follows that elevation angle radar information is redundant and, therefore, type-A or B display patterns are quite satisfactory and are in fact the typical presentations which have been universally employed for surface target fire-control applications. The basic A-type indicator presents range-only data, but for fire-control purposes a modified form is often employed with lobe switching by which accurate training of the radar antenna is possible and bearing information is thus secondarily obtained.

For airborne radar search and bombing applications the presentation is concerned with targets, one coordinate of which is known by other than radar means. Since all targets of interest are in this case located on the ground plane, the relative location of which is determinable by reference to the altimeter and a gyroscopic artificial horizon within the aircraft, it is sufficient here to present all information as a 2-dimensional map. The presence of targets and to some extent their composition is observable as an intensity modulation of the field of view. For this type of application the PPI or its more exact successor the GPI form of presentation is extensively employed.

For military radar applications where fire-control information is desired pertaining to targets which are not confined to a definite plane all three determinable coordinates must be known and, therefore, presented to the radar observer. In certain instances this requirement has been fulfilled by the use of multiple displays each presenting the information regarding one or two coordinates and in cases where gun training is accomplished through separate operators for each coordinate axis, range, bearing, and elevation, this method has proven entirely satisfactory. During World War II the fast moving and highly maneuverable aircraft target has required a more direct and, therefore, faster system of gun pointing. In these cases, the operator has been provided with a display which electronically duplicates a sighting telescope and which merely requires the operator to position the gun (and associated radar antenna) until the target image is centered. To introduce a measure of range to the target the size or form of the target "spot" is often varied in accordance with the range data. For defense against low-level aircraft attacks this admittedly crude range information

has proven quite satisfactory. Similar presentation methods developed for airborne aircraft interception radar equipments have employed, in addition, separate instruments to notify the pilot or gunner at the time when the range to the target was proper for firing of the guns. Another variation in method of obtaining accurate range information simultaneous with the elevation and azimuth data is through the employment of automatic range tracking. In this case after identification and selection of the target has been made and the initial coincidence accomplished, the operator is then free to track in elevation and azimuth with the automatic tracking device continuing to furnish the changing range data to the gun.

Figure 37 indicates the fact that included in these display forms are variations which are a function of the deflection coordinates peculiar to the display device itself. The factors which determine this choice are related to the required form of the presentation from the standpoint of military use, the characteristics of the particular display device available and the mechanical form of the antenna scanning system.

It should be observed that a number of minor variations in the exact presentation is available to the radar system designer within the general classification indicated in Fig. 37. As mentioned previously, the A-type display may be modified to indicate azimuthal pointing errors. In this case, sometimes referred to as a K-type display, the radar system employs an antenna capable of producing two beams of radiation, available one at a time, with azimuthal bearings differing by the order of the beam width. Two signals, each of which is associated with one position of the radiated beam, are displayed in the basic A-type form with one slightly displaced in the range coordinate with respect to the other. By "steering" the antenna until the amplitude response of the desired target appears equal for each image, the target bearing is determined as the direction line bisecting the two antenna lobes.

It is often desirable to limit the display to a small area or to a small selected range interval to enable magnification of this particular portion of the scene. The accurate measurement of range for fire-control purposes can be accomplished on a conveniently small indicator screen by expanding only a selected small range interval of interest. The loss of information at other ranges under these conditions is unimportant. In certain airborne applications it is desirable to present large area information for navigational purposes, but at the time of starting the radar bombing attack the area of interest is limited to a narrow sector extending outward from the plane in the direction of the attack. Here a selected sector may be expanded with a probable increase in accuracy of individual target identification and final bombing accuracy.

In the "range only" classification of Fig. 37 the J-type of display has an

advantage of expansion of the range information by a factor of approximately three times for the same size screen. The A and J types are employed extensively in fire-control radar equipments.

In the range versus azimuth class of radar presentations the B scan historically preceded the other forms shown. Its application was found originally in airborne radar systems for interception purposes. It was commonly employed in conjunction with an auxiliary C-type indicator for target elevation determination. The B type of display suffers from a distortion due to the reproduction of polar coordinate information directly on a rectangular coordinate field. This particular form of distortion is not of major importance where only a few isolated aircraft targets are to be displayed, and in the case of guiding an aircraft to intercept the target the relative expansion of the azimuth scale at short ranges may be a slight advantage. When the B type of presentation is employed for navigation and observation of ground features this inherent field distortion becomes very objectionable when map comparisons of the radar image are required. The B type of display has also been employed extensively on narrow sector rapid scanning naval fire-control radar systems.

The plan position indicator (PPI) type of display was developed to overcome the objectionable distortion of the B-type display and to afford a method of presenting a 360° azimuthal pattern when rotating antenna structures were employed. This form of display essentially replaced the B-type display for aircraft search radar systems and has been since universally employed for ground and naval vessel search systems. Here the linear range trace on the screen is directed outward from the center of the tube, its radial position being synchronized with the instantaneous bearing of the scanning antenna. The map presentation is exact for ground and naval vessel radar locations and for low-flying aircraft radar systems the distortion is negligible, since the slant radar range to the target at low altitudes is essentially comparable to the range as measured on the ground plane. As the altitude of a radar equipped aircraft is increased, the map distortion of the simple form of PPI display also becomes quite objectionable and several modified forms of this display can be employed to improve the presentation. One of these involves delaying the time of start of the linear range sweep by a time interval corresponding to the propagation time of the radar pulse to the ground and return. In this manner a simple but desirable improvement in display is realized. As the military requirements during the later period of the past war became more exacting with the emphasis on high-altitude radar bombing, the remaining distortion of the delayed PPI presentation was found undesirable, and the necessity for accurate map display directly beneath the aircraft resulted in the development of the ground plan indicator (GPI). In this type of display the range trace is deflected as a

nonlinear function of time; its exact time function being dependent on the altitude of the aircraft. The altitude information is obtained from the aircraft altimeter and may be manually or automatically introduced into the radar receiver to produce the proper form of sweep function. These modified forms of PPI presentation were employed extensively in the large bombing through overcast radar program which attained a status of major importance toward the later portion of World War II.

The elevation versus azimuth classification of display forms is essentially restricted to fire-control and aircraft interception radar applications. As previously noted, the C-type display was developed early in the military radar program and has somewhat the same characteristics as the B scan in terms of the distortion which results in the display of polar coordinate data in a rectangular coordinate field without proper mathematical conversion. In the case of aircraft interception radar applications, this type of display is quite satisfactory and has been employed quite extensively for this purpose.

The moving spot (MS) form of radar display is usually associated with a radar system in which conical scanning or lobing is employed. Here the source of radiation of the antenna is arranged and rotated so as to provide a beam whose path describes a cone. If the target is located on the axis of this cone of radiation the signal response will be essentially constant for all instantaneous positions of the beam. If the target is positioned to one side of the cone's axis the received radar signal will be modulated at the frequency of the conical scanning process and the degree of modulation will be related to the angle between the conical axis and the bearing toward the target. This modulation information is utilized within the radar receiver to position an optical image on the face of the indicator screen in accordance with the direction of the target. In radar systems employing this form of indication the observer positions his radar antenna, and accordingly the associated weapon, to center the target image on the indicator. Mechanical or electronic cross hairs are employed as the reference axis. A measure of range to target information is often introduced into this form of display by assigning an arbitrary but distinctive size or shape to the target spot which can be varied in accordance with the range to the target being observed.

2.42 *The Cathode-Ray Tube*

The cathode-ray tube is without serious competition as the ideal radar indicator, primarily because of its unique high-frequency electro-optical response characteristic. Since the radar presentation requirements are not unlike those encountered in television practice, it is natural that the cathode-ray tube development for radar purposes should have progressed along simi-

lar lines originally established by prewar television. Two general types of cathode-ray tubes have been commonly employed in the military radar program, electrostatic and magnetic, these classifications being indicative of the deflection and focussing method employed.

Electrostatic Deflection Type

A typical form of electrostatic-type of cathode-ray tube suitable for radar indicator purposes is shown in Fig. 38. In this tube type the electrons emitted from an indirectly heated cathode surface are initially formed into a beam by passage through an aperture which serves as a beam density or ultimate brightness control element. Following this, the electrons proceed through another aperture which is maintained at a positive potential with respect to the cathode. This first anode together with the following second anode forms an electron lens system which focuses the beam on the fluores-

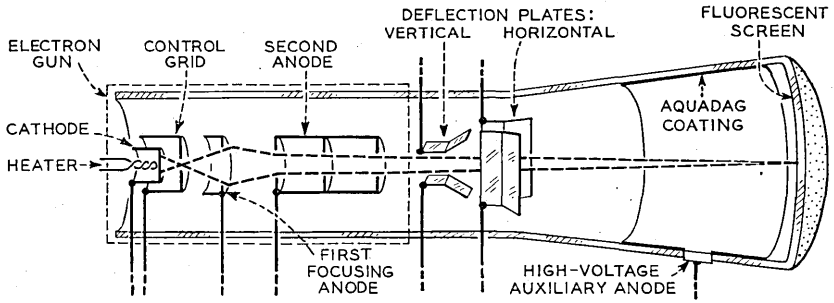

Fig. 38.—Schematic diagram of an electrostatic type cathode-ray tube.

cent screen surface. The relative potentials of these elements serve to enable focussing of the beam by electrical means. The deflection of the beam for scanning purposes is here accomplished by the introduction of an electric field formed by the application of potential across the deflection plates shown. Two pairs of plates enable separate horizontal and vertical deflection to be employed. The plates are formed as shown to enable obtaining the maximum deflection per unit of electrical potential applied without interference with the beam under large deflection conditions. The high-voltage auxiliary anode is provided in certain tube types to further accelerate the beam after deflection without an appreciable reduction of deflection sensitivity and results in an image of increased brightness.

To realize optimum performance of an electrostatic-type cathode-ray tube several precautions must be observed. Serious defocussing of the beam as it is deflected will result if the average potential of the pair of deflection, plates is allowed to vary substantially from the value present at the second anode. To minimize this effect, balanced sweep deflection amplifiers are

commonly employed in radar receivers employing electrostatic deflection, and the second anode is maintained at the average potential of these deflection plates. Astigmatism, the selective focussing in one direction on the screen at the expense of focus in the other, results from the mechanical limitations whereby the electric fields of the two pairs of deflection plates cannot be made effective at the same point within the tube. Some improvement can be realized in this respect by operating the pairs of deflecting plates at slightly different average potentials.

The limitation in deflection response at high frequencies is a function of the total deflection circuit capacitance. To eliminate the blocking condensers with their considerable parasitic capacitance to ground it is common radar indicator practice to operate the deflection plates directly from the

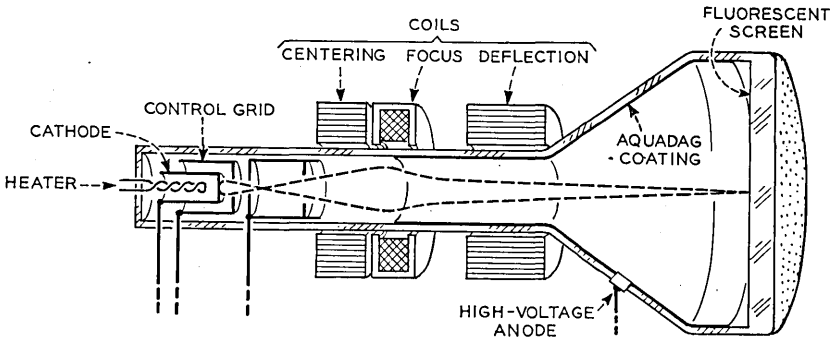

Fig. 39.—Schematic diagram of a magnetic type cathode-ray tube.

plates of the sweep amplifier tubes and then accordingly operate the cathode of the cathode-ray tube at a high negative potential.

Magnetic Deflection Type

A typical form of a magnetic-type cathode-ray tube is illustrated in Fig. 39. In this tube the electron gun structure comprises a heater, cathode, control grid, and second or screen grid which, together with the second anode, usually formed by an aquadag coating within the glass envelope and which is maintained at a high positive potential, roughly delineates the beam. The second grid in this case serves to shield the control grid from the high potential second anode and results in an improved control grid characteristic. The beam of electrons is focussed through the use of a magnetic field located as shown in Fig. 39, and produced by direct current flow through a coil or by a permanent magnet structure. The centering of the beam upon the screen under no deflection conditions is accomplished by the use of a distorting field commonly introduced as a part of the deflection coil and focussing assembly. The deflection of the beam for a rectangular coor-

dinate display system is here accomplished by magnetic deflection fields perpendicularly disposed and produced by a pair of deflection coils located at the junction of the neck and bulb as shown. In the polar form of display (PPI) usually only one deflection coil is employed for the production of the radial sweep, the angular deflection being produced by rotation of this coil about the neck of the cathode-ray tube in synchronism with the rotation of the antenna.

It is of interest to compare the relative characteristics of the electrostatic and the magnetic-type of cathode-ray tubes from the standpoint of their application to radar indicators. The electrostatic-type of cathode-ray tube has a distinct advantage of lighter total weight for the tube itself and the associated deflection circuits required, which in the case of airborne radar equipment design is an important factor in its favor. In general, it is desirable to present a large radar display field. For the larger diameter cathode-ray tubes the magnetic-type tube has an advantage of shorter over-all length which has proven an important equipment design factor for airborne radar equipment where the available operating space is severely limited. The magnetic-type cathode-ray tube requires weighty focussing and deflecting assemblies and large power supplies to furnish the heavy deflection current required, but because of the higher anode voltages which may be employed here, the screen brightness achieved is considerably greater than that available in the usual electrostatic type of cathode-ray tube. If the anode potential of an electrostatic type of cathode-ray tube is increased and hence the screen brightness, the deflection sensitivity is seriously impaired and a difficult deflection amplifier design results. From a deflection point of view, it is possible to achieve somewhat better performance in reproducing extremely high-speed sweeps by employing an electrostatic-type of indicator which has somewhat less serious parasitic elements which act to limit the high-frequency response. The final choice of type of cathode-ray tube for the radar indicator is dependent on the specific detailed considerations of the system in hand. No general and fast rules governing this decision are evident.

Characteristics of the Fluorescent Screen

The fluorescent screen of the cathode-ray tube upon which the final radar information is converted into the desired visual form consists of a deposit of certain materials which exhibits fluorescence when bombarded with a high-velocity electron stream. Phosphorescence, the continued emission of visible light after bombardment has ceased, is also a property of all of these screen materials. These screen materials, referred to as "phosphors", have characteristics dependent on their physical form as well as their chemical composition.

Two general types of phosphors have been commonly employed in military radar systems classified according to their phosphorescence characteristics. The medium persistence class of phosphors exhibit decay times of the order of milliseconds and are composed of a single layer of Willemite (zinc orthosilicate). This type of screen exhibits a green luminous response and is employed extensively in reproducing high-speed wave forms such as encountered in high-speed scanning systems, and for general A-type presentation purposes. The visible light output decays to the order of 1% of its initial value in approximately 50 milliseconds after electron excitation ceases. For photographic purposes other phosphor compositions of the same persistence class whose useful light output has a higher actinic value are commonly employed.

The long-persistence phosphors are composed of two layers of screen material which combination exhibits sustained phosphorescence, the visible light output decaying very slowly after cessation of bombardment. The double layer or cascade screen consists of an innermost layer subject to the direct influence of the electron stream which is composed of a silver activated zinc sulphide and a second layer adjacent to the glass envelope which consists of copper activated zinc cadmium sulphide. The first-named material fluoresces with an extremely brilliant blue light under bombardment and exhibits a rather rapid decay characteristic. The second layer is in turn excited by the blue radiation from the first layer and responds with a yellow visible emission which persists for a matter of several seconds after excitation ceases. The initial blue flash is appreciably absorbed by the second phosphor layer, but usually further optical attenuation is required to prevent eyestrain and degradation of night vision of the observer. This is commonly provided by the use of an amber optical filter placed over the screen face. The long-persistence characteristics available in this type of tube have proven invaluable in military radar systems which feature slow antenna scanning. In many of these systems the time between successive scans of the target may be of the order of a second or more and only through the use of the cascade-type long-persistence tube can the image be retained for this period of nonexcitation. Another property of the long persistence class of cathode-ray tube screens which is of advantage for radar purposes is an accumulative increase in brightness with successive scans of the target. Since the target image is usually repetitive as regards position on the screen, the image brightness will increase with successive scans while because of the random character of noise no such increase in noise image will result, and a small but evident signal-to-noise improvement obtains. The long-persistence type of screen characteristic is employed in the majority of military radar indicators of the B, C, and PPI-types.

Another general characteristic of the cathode-ray tube screen which influ-

ences the over-all system performance is the range of useful brightness available. The extreme variation in the radar response of targets in an area under observation has been discussed previously. The inability of the cathode-ray tube screen to convert this extreme range of electrical signals to a correspondingly large optical brightness range has been a restriction on the performance of military radar systems. Isolated measurements of the useful brightness range available in a cascade screen cathode-ray tube indi-

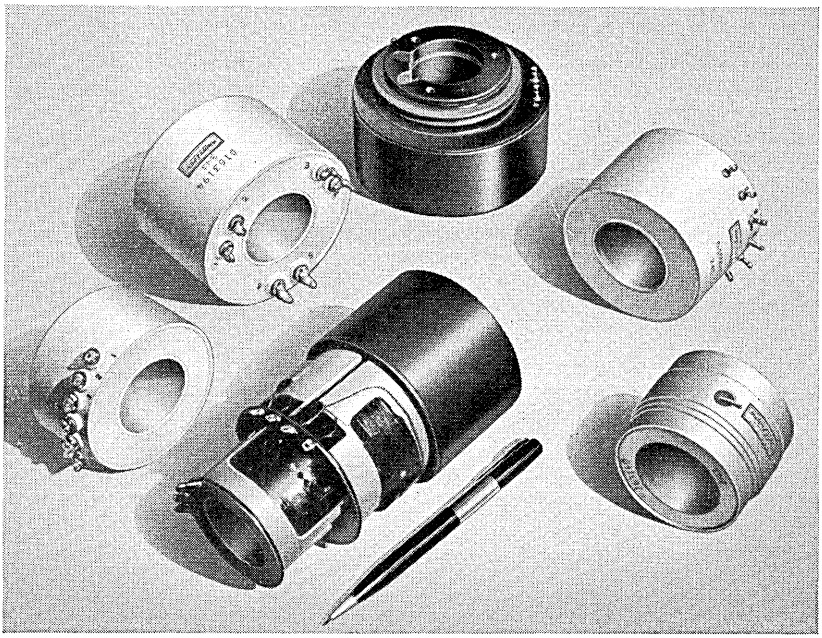

Fig. 40.—Typical magnetic focus and deflection coil designs as developed for military radar purposes.

cates that it is of the order of 10 to 1. The development of the logarithmic video amplifier and "duo-tone" is an attempt to improve this situation. In general this limited useful brightness range of the radar indicator results in a critical adjustment of the operating region of the indicator tube. In a practical military radar system operating under wartime conditions the inclusion of such a critical adjustment always effectively results in a reduction of performance from the optimum achieved in the laboratory.

2.43 *Typical Radar Indicator Component Designs*

Figure 40 illustrates a few typical component designs of magnetic deflection and focus coil structures developed for specific military radar applica-

tions during the past war. The deflection coils illustrated include both air and permalloy core structures as used in rectangular and polar types of displays. Where the radar system involves extremely short time interval sweep wave forms, the maximum inductance which can be employed in the deflection coil is limited by the power supply voltages available, and in these indicator designs the air-core type of deflecting coil is usually employed. Where the sweep wave form is relatively slower the permalloy core types have been extensively employed with an effective improvement in deflection sensitivity. For the PPI form of display a toroidal coil structure has been devised which contains two distributed windings connected in an opposing sense. The internal leakage flux of such a structure is essentially uniform and, therefore, satisfactory for magnetic cathode-ray deflection purposes. The usual PPI type coil structure is arranged to mount within a large ring ball bearing to enable rotation around the neck of the tube with provisions being included on the coil housing for slip rings to afford connection to the deflection coil proper.

With the increased emphasis on extremely accurate radar presentations, which developed during the later war years especially in connection with the radar bombing program, the design and manufacturing tolerances allowable in connection with the large scale production of these magnetic deflection coils were severely reduced. Figure 41 illustrates the constructional details of a deflection coil as employed in the AN/APQ-7 radar bombing equipment. The presentation in this instance is of the GPI type employing rectangular coordinate deflection and extremely fast sweep wave forms. This deflection coil structure employs accurately formed open air-core windings which are initially adjusted and cemented to concentric phenol plastic cylinder forms. This design features a vernier rotation adjustment of the horizontal and vertical pairs of coil assemblies to meet a manufacturing scanning requirement of $90° \pm 0.5°$.

Two examples of focussing and centering structures for magnetic-type cathode-ray tube radar indicators are included in Figure 40. The focus coil consists of a simple winding located axially about the neck of the tube with a shielding magnetic structure containing an annular air-gap which restricts the external field to a region including the cathode-ray tube electron beam. This structure is designed to produce a uniform magnetic field distribution in the complete area of the beam to avoid defocussing effects. In certain early-design airborne radar equipment applications where the equipment was subjected to extreme variations in ambient temperature over short periods of operation some difficulty in maintaining optimum focus was experienced. This defocussing, due to the change in coil resistance with ambient temperature and in part to dissipation in the winding proper, is minimized in the designs shown by the introduction of a varistor element

mounted in close proximity to the winding whose resistance temperature characteristic was chosen to compensate for similar characteristics of the winding proper. The beam centering structure included in the designs shown employs two pairs of coils arranged upon a closed magnetic core structure adjacent to the focus winding. The perpendicularly disposed magnetic fields are produced by direct current in the same fashion as discussed in connection with the deflection coil assembly.

Figure 42 illustrates the operation of a permanent magnet type of focussing and centering structure developed during the war and which was em-

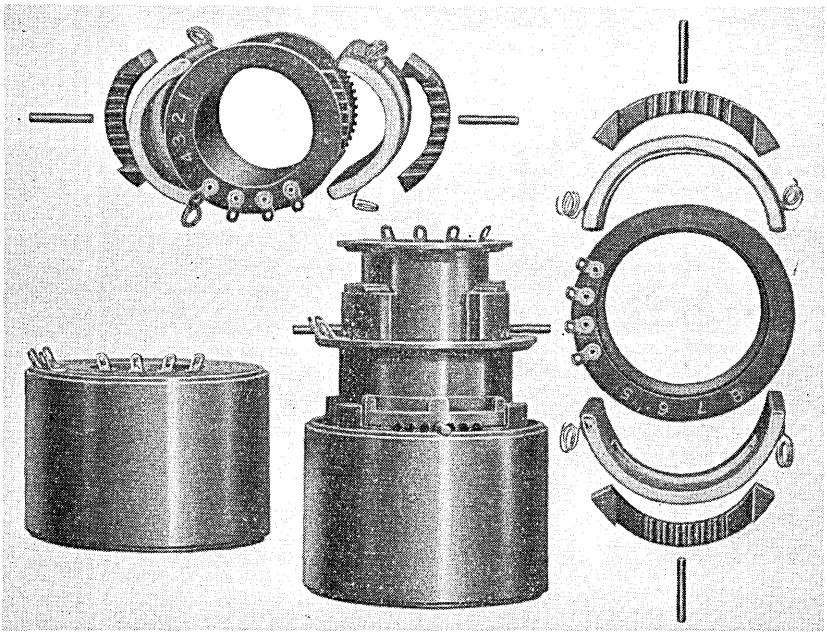

Fig. 41.—Constructional details—deflection coil design for AN/APQ-7 radar bombing equipment.

ployed extensively in airborne radar applications. Here a permanent ring magnet is equipped with a variable internal mechanical magnetic shunt whereby the focussing magnet field can be varied as shown. The centering of the beam is accomplished by means of a centering ring located as shown capable of being mechanically controlled along two perpendicular paths. Mechanical linkage arrangements provide location of the focus and centering adjustment controls on the indicator panel convenient to the operator. The permanent magnet type structure has the advantage of maintenance of proper focus and centering under conditions of extreme variations in ambient temperature. Similar permanent magnetic type structures have been em-

ployed to permanently deflect the beam for off-center displays such as the B-type and certain modified sector scanning PPI forms. Here the ampli-

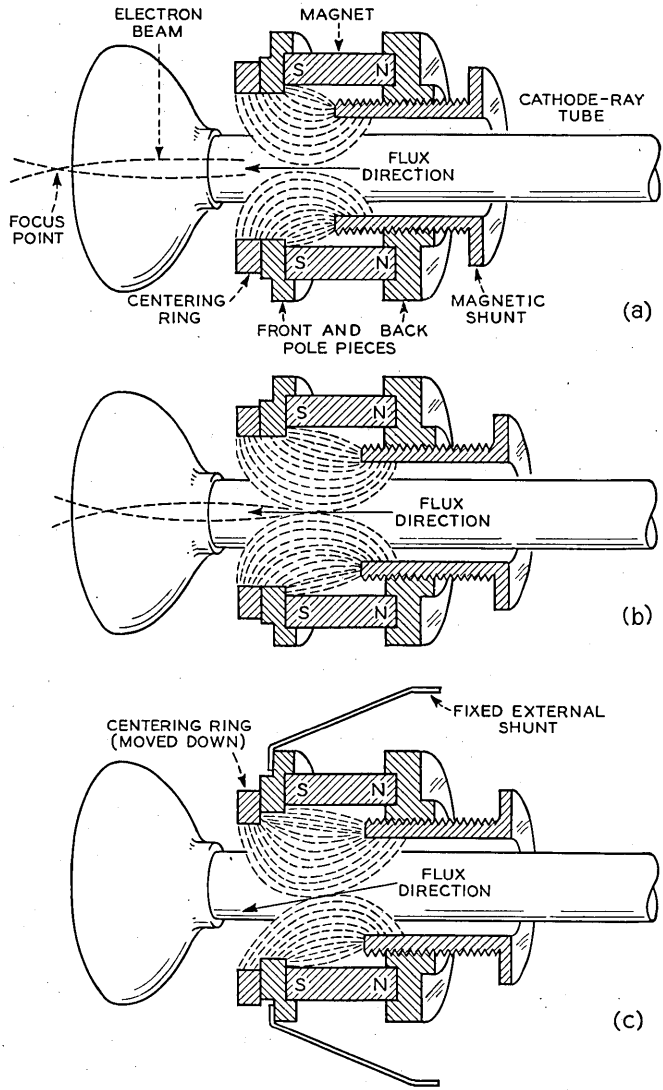

Fig. 42.—Operational diagram of permanent magnet type of focussing and centering structure for radar indicator.

tude of deflection required is approximately equal to the radius of the screen and this precludes the use of the usual beam centering structure located near the gun structure portion of the neck of the tube. To prevent physical

interference by the neck of the tube with the deflected beam such off-center display deflecting structures are mounted close to the junction of the neck and bulb of the cathode-ray tube.

As indicated previously the blue-flash characteristic of the excitation of the first layer of the cascade-type screen is usually reduced in intensity through the use of an optical filter placed between the screen of the cathode-ray tube and the observer. These optical screens are usually constructed of an amber-colored transparent plastic whose particular optical transmission characteristics are chosen in accordance with the particular phosphor and speed of scanning employed. It is common practice to engrave general range and direction reference lines on such screens, and in many cases variable edge lighting of these engraved screens is employed to enhance the display.

In certain applications of radar, namely, airborne reconnaissance and bombing operations, it is desirable to obtain a photographic record of the display to be used for training, briefing, or damage assessment purposes. It is customary in these cases to employ a stop-frame moving picture camera attached to the indicator and exposed periodically as desired. Figure 43 indicates the design of a radar indicator viewing attachment which was employed in connection with an airborne bombing radar equipment toward the end of the past war. In this design a partially silvered mirror is located at a 45° angle with respect to the axis of the cathode-ray tube. An illuminated image of an adjustable course marker located below the mirror is observed superimposed upon the radar presentation with negligible parallax distortion. A portion of the light of the radar image is also reflected from the surface of the partially silvered mirror, and together with the direct image of the course marker is available for photographic recording by the camera mounted as shown. Automatic exposure at any preselected time interval is provided, the exact exposure time being controlled by impulses derived from the azimuthal scanning mechanism of the radar antenna. The photographic recording of radar displays has become a matter of prime importance in the modern military operations and has added another consideration for the military radar indicator designer.

Figure 44 indicates an equipment arrangement of a PPI indicator as employed in the AN/APQ-13 radar bombing system. In this system the indicator is designed for convenient overhead mounting in the restricted radar operating space available in modern bombing aircraft. The deflection coil in this equipment is rotated about the neck of the 5″ diameter long-persistence cathode-ray tube by a geared selsyn motor energized from a similar selsyn unit mechanically linked to the rotating radar antenna. Permanent magnet focussing and centering is employed in this particular indicator. Figure 45 illustrates a somewhat similar packaging arrangement for

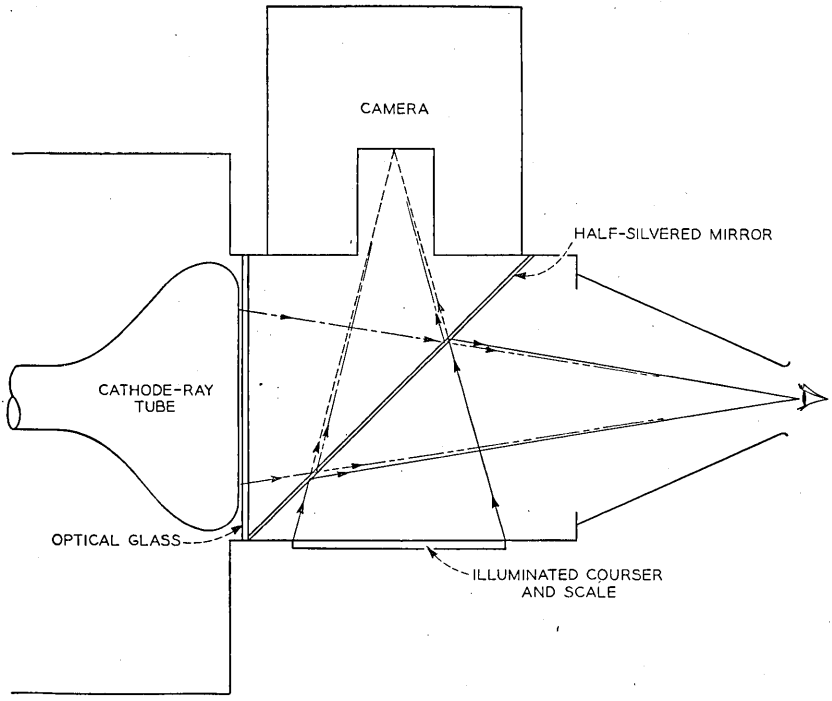

Fig. 43.—Mechanical arrangement of a radar indicator viewing and photographic attachment for AN/APQ-7 radar bombing equipment.

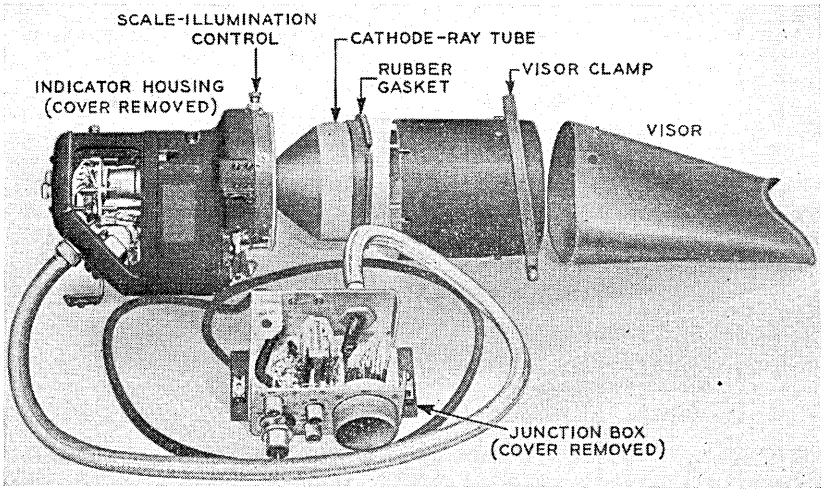

Fig. 44.—Indicator design for AN/APQ-13 radar bombing equipment.

an airborne radar low-altitude bombing equipment as employed extensively during the past war. Here the display employed is of the B variety utilizing a 5″ long-persistence cathode-ray tube. The focussing and centering magnetic fields here are produced by coils located as shown. The azimuth sweep voltage is obtained by means of a potentiometer mechanically geared to the sector scanning antenna. The permanent off axis deflection of the zero range line of the B display is here obtained by the use of a permanent magnet yoke mounted at the junction of the neck and bulb of the cathode-ray tube.

Figure 46 illustrates a typical form of an A-type indicator as developed for the SH Naval and Mark 16 mobile fire-control radar equipments. This unit includes provision for receiver tuning and video limiting adjustment convenient to the observer. The SH and Mark 16 radar systems employ

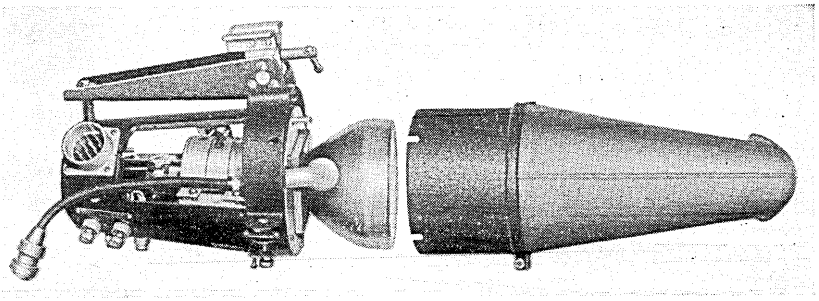

Fig. 45.—Mechanical design of AN/APQ-5 type B radar indicator.

both lobing of the antenna for precise azimuth bearing determination and also continuous rotation of the antenna for general search purposes. The indicator shown in Fig. 46 is employed when the lobing system is in operation and features a precision range sweep as well as the full range display. The equipment design here reflects the severe mechanical requirements which must be satisfied for electronic equipment which is to be employed on naval vessels or for trailer mobile ground service.

2.5 *The Radar Sweep Circuit*

2.51 *Function*

The sweep circuit components of a radar receiver are required to generate the specific voltage or current wave forms necessary to properly display the radar-received information in the desired form. These wave forms must also be actuated by or related to the various coordinate or computed types of data furnished to the radar receiver. The actual detailed configuration of the circuit employed for this purpose is dependent on the form of the input

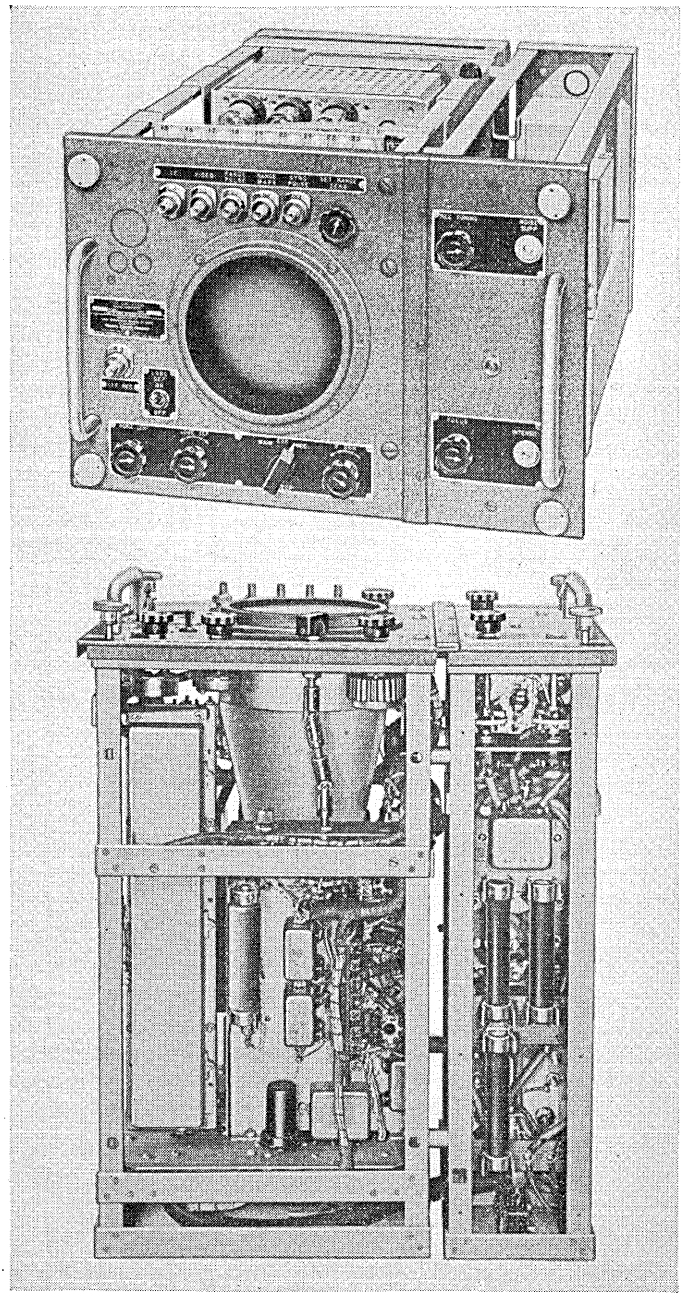

Fig. 46.—A-type indicator design for SH Naval radar equipment.

information available and upon the indicator deflection methods to be employed.

The sweep deflection problems may be separated into two quite distinct categories dependent on the speeds of operation involved. The slow-speed deflection systems originate with the required deflection of the beam of the indicator cathode-ray tube in accordance with the instantaneous position of the axis of propagation of the antenna structure. Since the antenna structures with which we are concerned at radar frequencies are of comparatively large dimensions, their motional velocities are extremely limited and accordingly the electrical information describing these slow mechanical changes contains only low-frequency components. The deflection problem associated with this information, in general, offers little difficulty to the radar receiver designer. Commonly employed methods of slow-speed sweep deflection include the use of potentiometers, selsyn generators or variable capacitors mechanically linked to the deflection axes of the antenna structure and associated circuits of relatively simple form whereby the electrical changes in the characteristics of these devices are more or less directly impressed upon the proper deflection axis of the indicator. In the case of the PPI form of display, it is quite common to synchronize the rotation of the deflection coil about the axis of the cathode-ray tube with the azimuth bearing of the antenna through the use of selsyn motors or servo mechanisms. In general, slow-speed sweep deflection problems are associated with bearing coordinate data only.

The determination of range to the target, on the other hand, requires high-speed scanning whereby the time interval encompassing the time of propagation and return of the radar pulse over the selected range interval must be completely displayed upon the indicator screen. The total time interval available to deflect the beam for range measurement purposes may extend from 2500 microseconds which represents a range measurement of approximately 240 miles down to perhaps 6 microseconds representing an expanded interval of approximately 1000 yards useful in certain fire-control applications. Here, with extremely small times available for deflection purposes, the radar receiver designer is faced with difficult circuit design problems where the usual negligible parasitic circuit elements now severely restrict the circuit performance. In the following discussion, therefore, emphasis will be placed upon the design factors involved in the development of high-speed radar sweep wave forms.

The radar sweep circuit can be considered as providing the following functions:

1. Generation of time wave forms.
2. Generation of display sweep wave forms.
3. Amplification of sweep wave forms.

2.52 *The Timing Wave Form Generator*

The generation of the timing wave forms consists of the preparation of specific voltage wave forms for use in the following sweep generator in accordance with timing information available at the radar receiver input. These timing data may consist of a pulse coincident or related to the outgoing radar microwave pulse serving as a reference for range display or, in the case of direction sweeps, may consist of signals related to the instantaneous position of the antenna.

The basic wave forms employed in this connection consist of rectangular pulses where the duration of the pulse may be controlled to serve as a measure of time, extremely short-duration pulses useful as time markers, and various combinations of these. In general, these wave forms are characterized by their nonsinusoidal form. The generation of these nonsinusoidal wave forms is accomplished by a number of specialized electronic circuits, which though apparently quite complex can be resolved generally into a combination of relatively simple basic circuit forms.

The Multivibrator

The "trigger" or multivibrator circuit was developed nearly thirty years ago and provides the fundamental circuits for the sweep circuit designer. Figure 47a illustrates a simple historical form of a trigger circuit which is of the Eccles-Jordan type. The essential current-voltage relationship which characterizes this circuit and all circuits employed for this purpose is a negative resistance characteristic which exists over a limited portion of the operating range of the device. In the case of the electronic circuit shown in Fig. 47a this negative-resistance characteristic is bounded by two stable limiting conditions. Referring to the trigger circuit of Fig. 47a, the chronological order of operation can be described as follows: Assume V_1 is conducting a somewhat larger current than V_2 so that the potential at the plate of V_1 is lower than the corresponding point at V_2 due to the voltage drop across the plate resistor R_1. This condition further implies that the grid potential of V_2 as determined by the connection from the plate of V_1 through the coupling resistor R_3 is lower than that at the grid of V_1. Similarly the grid potential of V_1 is at a higher positive potential, due to its connection with the plate of V_2. The action is cumulative and results in stablizing the circuit under the condition where the plate current of V_2 is entirely cut off and the voltage drop across V_1 is less than the grid bias voltage E_c.

If now a voltage is impressed across the input terminals of either a positive or negative form, the circuit will be driven away from this stable equilibrium condition as follows. Assume now that a large positive pulse be applied to the circuit shown. The tube V_1 which is operating in a conducting con-

dition will not be affected but the grid of V_2 will be raised in potential by the amplitude of the enabling pulse. The plate current flow in V_2 under this influence will reduce the plate potential of V_2 and accordingly will tend to decrease the positive bias of V_1. The accompanying plate current reduction of V_1 will increase its plate potential and this will result in increasing the grid potential of V_2 through the coupling resistance R_3. Again the cumulative effect will be to abruptly cut off the plate current of V_1 and operate V_2. Thus an abrupt switching of this electronic circuit results when a single enabling pulse is impressed upon it. The wave form across one of the plate

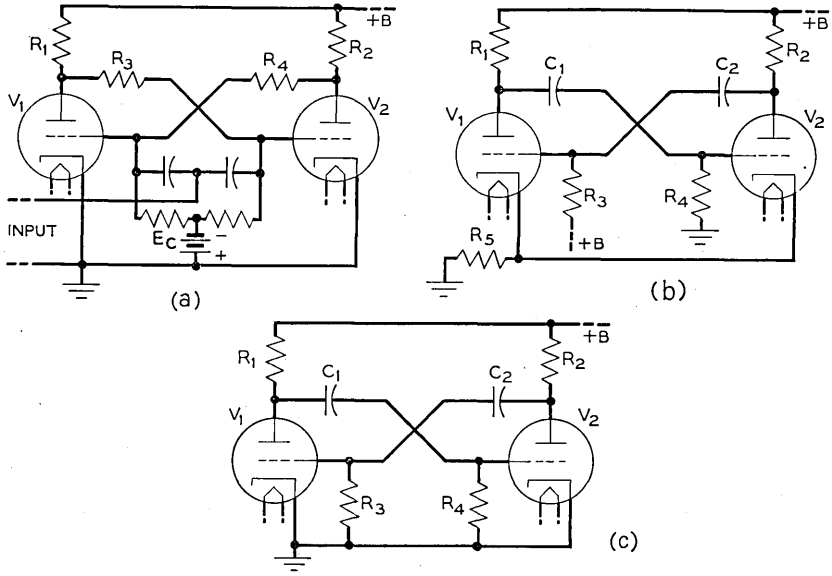

Fig. 47.—Basic Multivibrator Circuit Forms.

resistances is of a rectangular form whose duration is determined by the time interval which exists between the two applied excitation pulses.

A basic modification of the fundamental trigger circuit which has been found most useful in radar sweep circuit is given in Fig. 47b. Here the original circuit form has been modified so as to permit a complete cycle of operation upon excitation by a single actuating pulse. The duration of the cycle is here internally controlled by the arrangement and value of the circuit elements. This form of multivibrator is characterized by having one stable equilibrium condition and is known as a "one shot" type.

The chronological order of operation of this circuit type may be considered as follows: V_1 is normally conducting heavily because of the large positive grid potential impressed upon it by the plate supply battery and the connec-

tion through R_3. The plate current of V_1 flowing through the common cathode resistor R_5 results in a large effective bias applied to V_2 which continues to maintain V_2 in a cut-off condition. If a negative pulse of relatively short duration is impressed upon the grid of V_1 this tube will be driven toward cut-off with an attendant increase in the plate potential of V_1. This positive increase in voltage will be impressed upon the grid of V_2 causing V_2 to conduct plate current. The resulting decrease in the potential at the plate of V_2 further decreases the grid potential of V_1 through the coupling condenser C_2. This action progresses until V_1 is driven beyond plate current cut-off and V_2 is conducting. This condition remains as long as the discharge of the condenser C_2 through R_3 will maintain the grid of V_1 at a net negative potential. When the condenser C_2 has discharged sufficiently to allow the grid of V_1 to increase above the cut-off value, V_1 will again conduct and the resultant action will reduce and eventually cut off the plate current of V_2. The duration of the cycle of operation is here shown to be dependent on the time constant of the circuit R_3 C_2 and may accordingly be controlled as desired by proper selection of these elements. The return of the grid of V_1 to a very high positive voltage point in the circuit has a definite advantage which may be considered as follows: A variation of the grid voltage of V_1 required to cut off the plate current will influence the time duration of the cycle of operation. Here the time rate of change of the grid voltage has been made extremely large by the choice of the return to the high-voltage supply. Thus, an order of magnitude increase in the duration stability of the circuit is achieved.

A further modification of the trigger circuit furnishes the third general type of multivibrator employed in the radar receiver field. This circuit form, called the "free-running" type, has the property of presenting two unstable limiting conditions and accordingly will produce sustained oscillations of a nonsinusoidal form. Figure 47c illustrates this circuit arrangement. The essential circuit change over that given in Fig. 47b, is seen to be the elimination of the stable equilibrium condition of V_1 by the absence of a positive potential on the grid of V_1.

In the free-running type of multivibrator shown, the duration of operation of a particular tube is related to the time of discharge of the coupling condenser and the grid resistance associated with the tube. If a different time constant is chosen for each tube circuit, an unsymmetrical wave form, i.e.—a pulse-to-no-pulse interval ratio other than one, can be produced. In general, the free-running multivibrator is seldom used in this basic form because of the limited repetition-rate stability of this circuit. It is customary, however, to trigger this free-running type of multivibrator with short-duration pulses having a slightly higher repetition-rate than that determined by the multivibrator circuit constants. In this manner the repetition-rate may be

externally controlled as desired. It is also possible to synchronize this particular form of circuit at a submultiple of the externally available trigger repetition frequency.

Pentodes and other now available multi-element vacuum tubes, where the multivibrator interstage coupling involves additional control elements, are commonly employed in the modern radar receiver. Wave forms other than the basic rectangular pulse forms appearing at the plate terminals of the multivibrator circuit are available at various other points in the circuit and are often employed in specific applications.

One other basic form of pulse producing electronic circuits is known as the "blocking-oscillator" type: two typical examples of which are illustrated in Fig. 48. Here the positive feedback of energy required to produce the multivibrator characteristic is realized through the use of a single vacuum

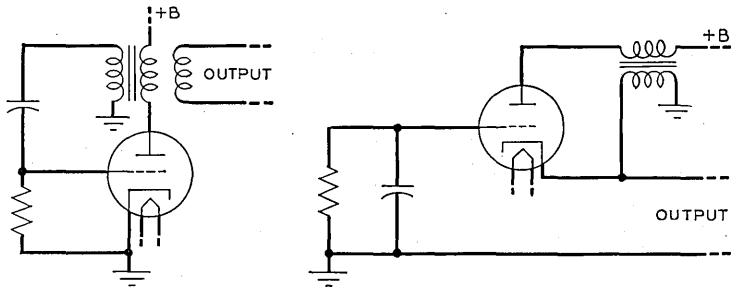

Fig. 48.—Typical Blocking-Oscillator Circuit Forms.

tube and a transformer feedback circuit. This form may be described as an oscillatory vacuum tube circuit where the grid circuit is so arranged to be driven negative after one or more cycles of operation. This results in an intermittent oscillation and the production of nonsinusoidal wave forms similar to those produced by the general multivibrator circuits previously described. The basic advantage of the blocking oscillator circuit form is one of economy of vacuum tubes and attendant power supply reduction.

Typical Timing Wave Circuits

The practical military equipment requirements of World War II with the emphasis on compactness and low-power consumption has resulted in the development of a myriad of specialized circuits which reflect the ingenuity of the electronic circuit designer and the basic flexibility of the modern vacuum tube. In general, however, these circuit developments are quite similar operationally to the basic forms here described.

Figure 49 illustrates a typical circuit arrangement of the sweep timing portion of a PPI indicator as employed in a naval search radar equipment.

In this particular radar system the transmitting magnetron is pulsed from a free-running modulator and, therefore, the controlling timing reference pulse for sweep purposes must be obtained from the modulator circuit. In many other military radar systems it has proven desirable to time both the transmitter modulator and the receiver sweep circuits from a common controllable repetition frequency source. As shown in Fig. 49, a positive synchronizing pulse as obtained from the transmitting modulator is delivered to the radar receiver for range timing reference and here applied to the "clipper" portion of the timing circuit. It was considered here desirable to clip or limit the timing pulse to gain freedom from timing instability, due to possible amplitude variations and to eliminate any possible negative excursions of the timing pulse which might cause faulty operation of the following multivibrator circuit. The multivibrator shown is a modified form of the "one-

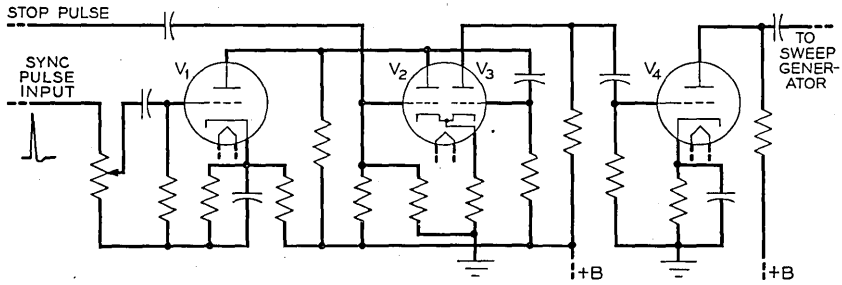

Fig. 49.—Radar Sweep Timing Circuit. Simplified schematic diagram.

shot" type described previously. The grid of V_3 is normally maintained at a positive potential through its connection to the positive plate supply source and accordingly V_2 is normally cut off.

Upon application of the positive synchronization pulse to V_1 and the resultant lowering of the plate potential of V_1 the grid of V_3 is driven below cut-off decreasing the voltage drop across the common cathode resistance and causing V_2 to conduct. This condition will be maintained until the coupling condenser has discharged sufficiently to permit V_3 to again conduct. In the circuit here described, however, this controlling time constant has been selected to be somewhat larger than the total period of the sweep rate and the termination of the sweep timing pulse is accomplished by an external stop pulse applied as shown. This stop pulse is developed in the following sweep amplifier circuits not here shown and is controlled directly by the deflection current. Details of this stop-pulse timing and generation is given in a later section.

The output of this timing circuit shown here then is observed to consist of a rectangular pulse whose leading edge is related to the time of the out-

going radar pulse and whose duration has been controlled by the limits of deflection desired on the radar indicator tube. This form of sweep circuit is known as a "start-stop" type and has proven extremely satisfactory as employed in a number of military radar equipments designed during the past war period.

2.53 *The Sweep Wave Form Generator*

The sweep wave form generator is required to generate the specific voltage or current time functions required to properly deflect the electron beam of the cathode-ray display device. The timing of the interval of this sweep wave form is provided by the timing or synchronizing circuits just described.

In general, it has been required that the range sweep wave form amplitude be essentially a linear function of time over the range interval under observation. During the latter portion of the war, certain airborne applications of radar did require that a specific nonlinear wave form be employed, but the commonly employed displays (A, B, C, and PPI) are usually operated with linear range deflection sweep circuits.

The basic method of obtaining a sweep voltage wave form which increases with time is illustrated in Fig. 50a. In this circuit V_1 is normally operating at little or no bias and, therefore, due to the large voltage drop across the plate resistor R, the plate potential of V_1 is considerably lower than the plate supply voltage B. If a negative rectangular pulse is applied to the grid of V_1 the tube will be abruptly driven to cut-off and, due to the current flow through the condenser C, the plate potential will rise exponentially as indicated to eventually assume the value of the supply voltage B. At the time of end of the negative driving pulse, V_1 will again conduct and the potential at the plate of V_1 will be abruptly reduced as shown.

There are several methods employed in radar sweep circuits to improve the linearity versus time of the fundamental exponential sweep wave form. The first of these takes advantage of the fact that the initial rise of the exponential wave form in the limit is a linear function of time. By using only a small portion of the wave form shown and supplying later amplification to produce the desired deflection, a simple improvement results. This form of linear sweep generation represents the original and by far the most common of the types employed in military radar systems during the past war.

Figure 50b illustrates a method of improving the linearity of the sweep wave form whereby the exponential wave form generated by the basic condenser charging operation is modified through the use of feedback. As shown here the asymptotic value of the exponential charging voltage has been increased by a factor of $(\mu + 1)$ and the effective time constant of the charging circuit has likewise been increased by the same factor. The use of an amplifier in the feedback circuit having an effective gain of 50 would

result in an improvement in linearity comparable with the circuit of Fig. 50a, where the plate supply voltage was increased by the same factor.

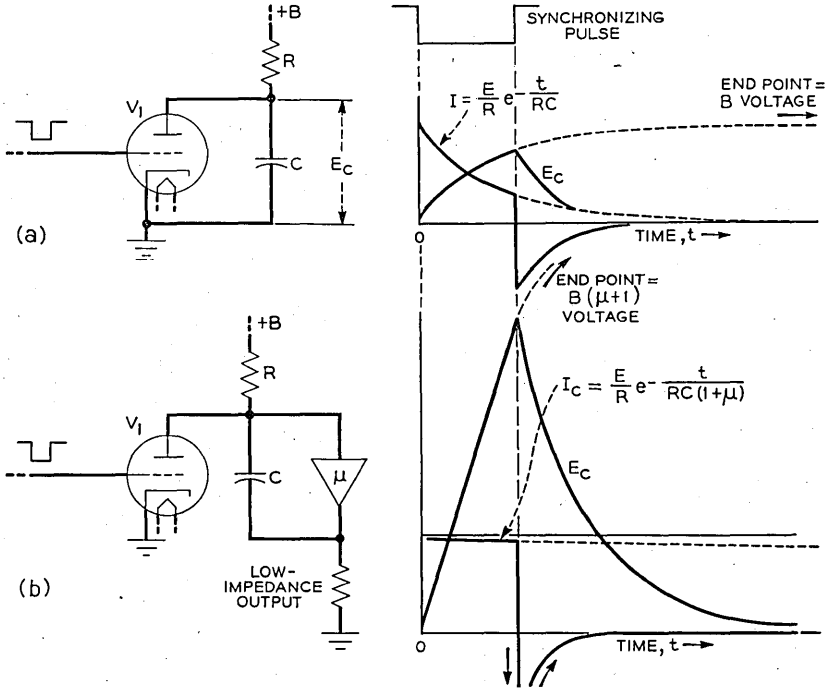

Fig. 50.—Radar sweep generation circuits—basic form and modified by negative feedback to improve linearity.

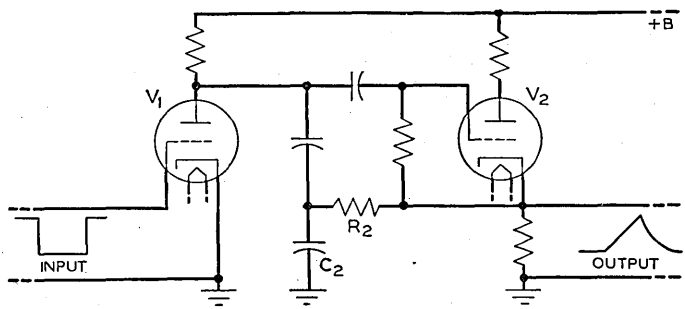

Fig. 51.—Circuit employed to improve linearity of sweep wave form by integration method.

A further method of improving the linearity of the generated sweep wave form is illustrated in Fig. 51 where an additional correction voltage is superimposed on the exponential sweep wave form. This correction voltage is

derived by integration of the sweep wave form as impressed upon the elements R_2, C_2 and the voltage appearing across C_2 is effectively superimposed upon the output wave form. As employed on an airborne bombing radar equipment, a circuit similar to that shown in Fig. 51, was employed where a residual nonlinearity of less than 0.5% was achieved and maintained under severe military operating conditions.

In certain instances it is desirable to generate a sweep wave form which has a specific nonlinear time characteristic. An illustration of one such case as applied to airborne radar is given in Fig. 52. Here the airborne radar display was required to present a nondistorted ground plan which in

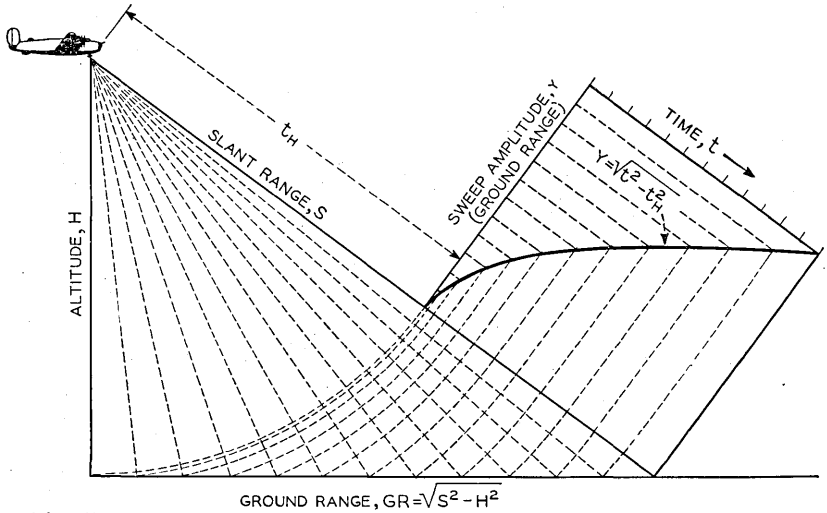

Fig. 52.—Development of hyperbolic sweep wave form for true ground plan radar presentation.

turn required that the range sweep wave form be of a hyperbolic form. The start of the display sweep must be delayed in time corresponding to the time of propagation and return of the radar pulse between the aircraft and the ground. This delay may be produced by the use of a multivibrator of a convenient form, actuated by a pulse coincident with the outgoing radar pulse, and where the duration of the multivibrator pulse is controlled either manually or automatically by reference to the aircraft's altimeter.

The hyperbolic sweep wave form illustrated may be approximated mathematically as the sum of a linear and a series of exponential terms. In this particular application, it was found sufficient to consider a linear and two additional exponential terms only to satisfy these specific requirements. Figure 53 indicates the method employed to generate this specific wave form. As indicated, the desired theoretical hyperbolic sweep function has

an infinite starting slope which cannot be provided with the practical limitations of frequency band width and power available so that here the actual delay used was chosen as 0.9 H, resulting in evident but acceptable distortion in the display in the area directly beneath the aircraft. Figure 53b indicates the fundamental circuit method of generating this wave form. The linear term is generated across the capacitance C_0 and the series current flowing through the additional elements R_1, C_1 and R_2, C_2 supplies the two

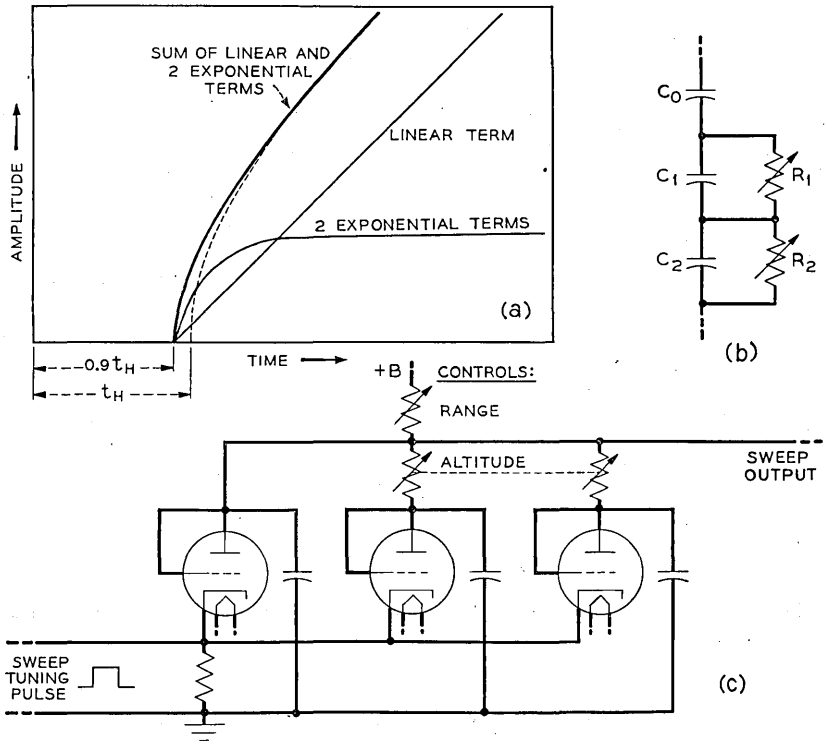

Fig. 53.—Hyperbolic sweep wave form generation—simplified schematic diagram.

additional exponential voltage wave forms. The resistances R_1 and R_2 are required to be variable, their value being determined by the altitude of the aircraft. The practical form of the circuit employed is outlined in Fig. 53c, which includes the additional resistor required to enable modifying the rate of rise of the sweep wave form in accordance with the selected interval of ranges to be displayed.

2.54 *The Sweep Amplifier*

The remaining portion of the radar sweep circuit is concerned with the amplification of the properly timed and generated sweep wave forms to

assure adequate deflection voltage or current for display purposes. The sweep amplifier for range deflection purposes is essentially a specialized form of video amplifier which must be capable of wide band transmission to adequately reproduce the short time sweep wave forms and whose output characteristics are such as to properly supply the high voltage or current signals as required by the radar display system. Two general sweep amplifier design problems are presented for the two basic radar indicator types. The

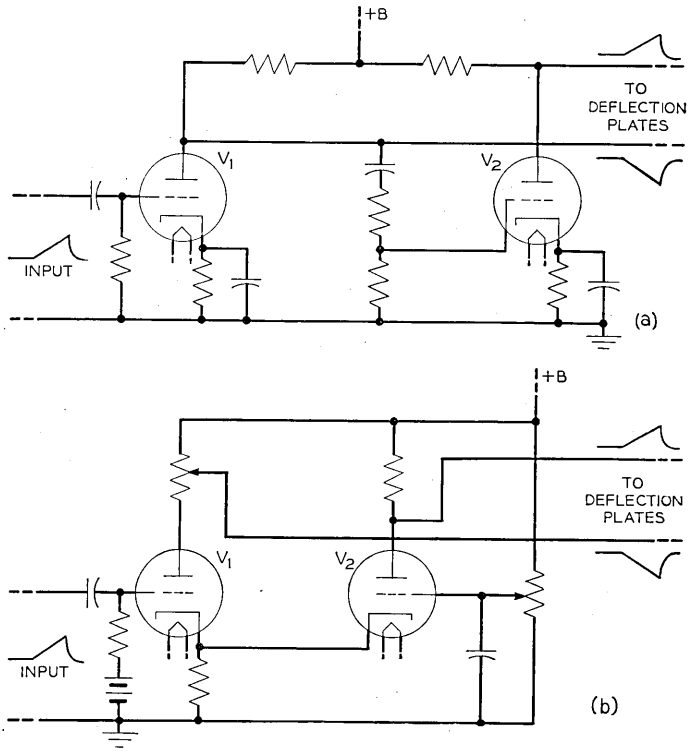

Fig. 54.—Range sweep amplifier circuit schematics for electrostatic-type radar displays.

electrostatic type cathode-ray tube generally requires a balanced to ground deflection signal of moderately high amplitude while the magnetic type cathode-ray tube requires a large deflection current for its operation.

Figure 51a illustrates a simplified schematic of a range sweep deflection amplifier to be employed with an electrostatic type-A radar display. Here the previously generated sweep wave form is impressed upon the grid of V_1 and after amplification a portion of the signal of opposite polarity and of amplitude comparable with the input signal at the grid of V_1 is applied to the grid of V_2. The plate circuit of each tube is connected directly to the deflection plate of the electrostatic cathode-ray tube. In this instance,

the average potential of the horizontal plates of the indicator is maintained at a value determined by the d-c plate potentials and, as indicated previously, this same potential should be applied to the second anode of the cathode-ray tube to avoid defocussing effects. Another variation of a phase inverter amplifier which is commonly employed in radar sweep circuits is illustrated schematically in Fig. 54b. In this instance, a common cathode impedance is employed to accomplish similar excitation of the balanced output tubes. If one grid is excited the plate current flow of this

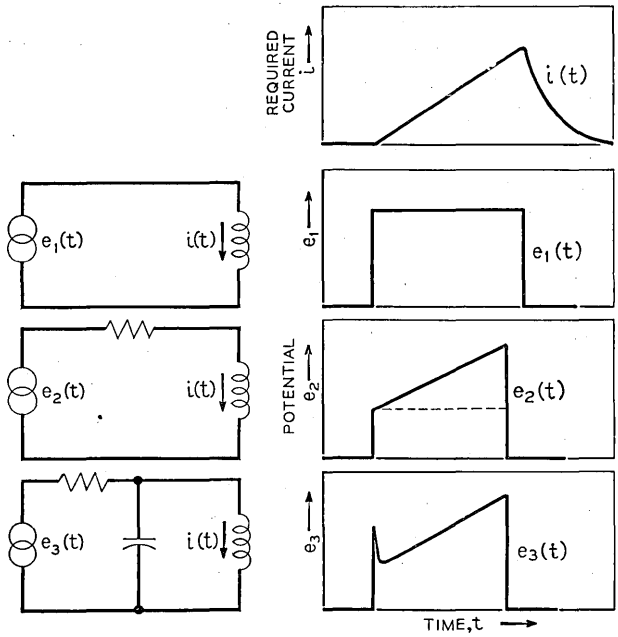

Fig. 55.—Voltage-current-time relationships for magnetic deflection structures.

tube through the cathode resistance serves to excite the second tube and a balanced output sweep signal voltage will result. The values of the plate resistors in this form of circuit are of unequal values and must be adjusted to produce the desired balanced output. The additional control illustrated in the grid circuit of V_2 may be employed to serve as a d-c positioning control.

The sweep amplifier design considerations involved for the magnetic deflection type of cathode-ray tube radar indicator are somewhat more involved, due primarily to the character of the amplifier load impedance. In the case of magnetic deflection the final flux density, and accordingly the sweep current through the deflection coil, is required to be proportional to

the deflection time function desired. If a linear deflection function is assumed, as shown in Fig. 55, producing a linear sweep, the necessary form of the applied voltage wave will vary depending on the inductance, the resistance and the parasitic capacitance of the coil circuit. These conditions are illustrated in Fig. 55. It is entirely possible to generate sweep voltage functions of the forms indicated here for application to a linear amplifier and deflection coil circuits and in fact such an approach was employed in early military radar designs of World War II. It has, however, proven more convenient to employ negative feedback amplifiers whereby the deflection coil current output is maintained proportional to the applied voltage at the input of the sweep amplifier. In this manner, a sweep generator voltage wave form can be employed which has the characteristics desired of the final deflection.

A simplified schematic of a feedback sweep amplifier to be employed in connection with a magnetic deflection radar indicator is shown in Fig. 56. In this example the impressed sweep wave form voltage having the essential characteristics of the desired deflection time function is impressed upon the grid of V_1. This sweep form is amplified and the deflection coil current of the output stage which flows through the 80-ohm cathode resistance common to the first and third stages produces a voltage drop proportional to this current which is effectively applied between the cathode and grid of the first stage thus completing the negative feedback loop. If sufficient forward gain and adequate feedback is provided, the deflection coil current can be made to assume the essential characteristics of the original impressed voltage sweep wave form. It should be observed that the grid of the third stage is biased negatively beyond plate current cut-off to insure that the deflection coil current has an initial value of zero before the start of the sweep. If this condition is not observed, the zero range point on the indicator will be a function of the d-c current of the output stage and in the case of a PPI form of display, the zero range region will assume the characteristics of an open circle and map distortion at the short ranges will result. In this amplifier circuit, application of the sweep signal to the grid of V_3 will not result in deflection current flow until the tube is driven above cut-off. During this time the feedback is not effective and the over-all gain of the amplifier is at its maximum value. Due to the inductive characteristics of the amplifier load impedance, the initial rise in current will be delayed slightly with respect to the applied voltage and accordingly a further delay of the feedback voltage is introduced by the use of a time constant in the common feedback network. The result is a delaying of the applied feedback voltage with a corresponding period of maximum gain of the amplifier which tends to produce a sharp increase in deflection coil current at the time of the

start of the sweep. After this short interval of time, the feedback becomes effective and the output current and input voltage correspondence obtains.

It is essential in this type of circuit that the feedback be determined entirely by the deflection coil current if optimum operation is to be obtained. It should be observed that this condition requires that the screen current which also normally flows through the feedback impedance does not con-

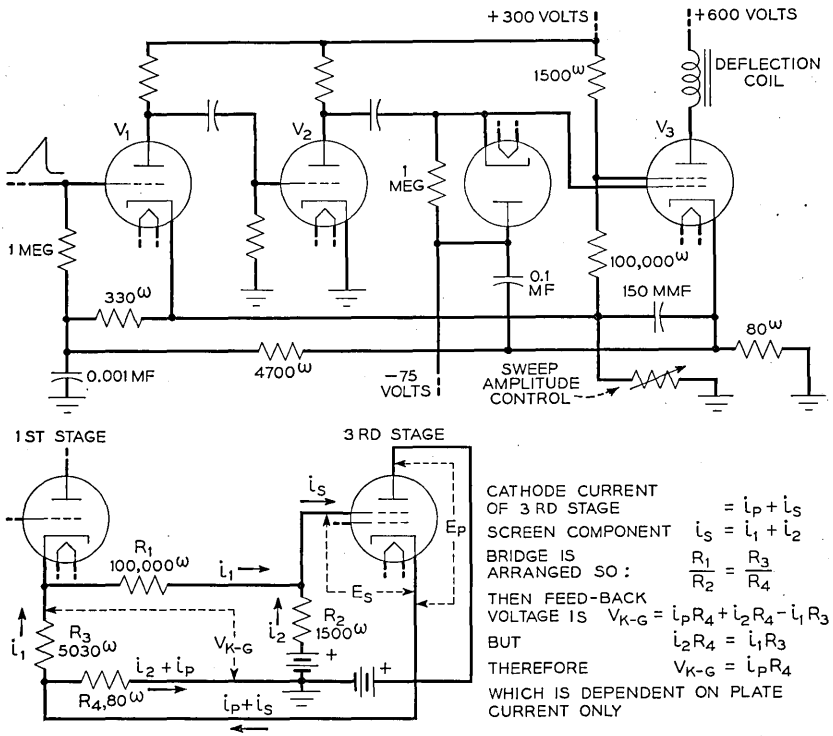

Fig. 56.—Radar range sweep amplifier employing negative feedback and screen grid bridge circuit—simplified schematic.

tribute to the net feedback. Figure 56 illustrates the bridge circuit which has been devised to accomplish this. A voltage from the screen of the third stage is directly applied to the cathode of the first stage, this voltage being equal in magnitude and of opposite polarity to that which appears across the feedback impedance due to the third stage screen current flow. This bridge circuit operation is independent of the absolute screen voltage value.

To insure identical starting potential conditions regardless of the duration of the range sweeps in use, d-c restoration is employed in the grid circuit of the last stage. The action here is similar to the operation described previously in connection with video amplifier design. The delay inherent in

the magnetic deflection circuits must be carefully considered in the overall radar receiver design, if the display is required to reproduce short-range information. In such cases, it is customary to insert delay networks in the video channel introducing a delay to the received signal equal to that present in the indicator deflection system, or to "pre-pulse" the deflection circuits prior to the time of the outgoing radar pulse.

It is desirable from a power consumption and display appearance standpoint to limit the range deflection of the radar indicator only to that amplitude required to adequately fulfull the display requirements. A method commonly employed is indicated in Fig. 57. Here a measure of the current flow through the deflection coil, and accordingly the amplitude of the deflection of the cathode-ray tube beam upon the screen, is obtained from the feedback voltage of the sweep amplifier. This voltage is impressed upon a

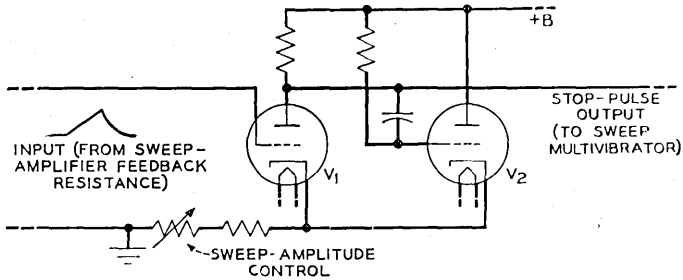

Fig. 57.—Range sweep stop pulser circuit for limiting sweep deflection.

"sweep-stop" pulser which upon rising to a preselected value corresponding to the desired sweep amplitude is caused to trigger this circuit. The output pulse of this circuit is then employed to operate the sweep limiter portion of the sweep timing multivibrator previously described, thus terminating the sweep timing pulse proper.

2.6 *Circuits for Radar Range and Bearing Measurement*

In this review of radar receiver design principles only the presentation of the received radar signal in a form convenient to the observer has been considered. To fully utilize the complete radar information available, determination of the complete coordinates is necessary with an exactness which is determined by the specific use of the data and by the capabilities of the radar system itself. This section will be devoted to a review of the methods employed to generate electronic markers necessary for the determination of range and azimuth and elevation angles. These markers include both the fixed variety, whereby the approximate coordinates of a radar target can be determined by inspection, and steerable markers by

which means precise coordinate data necessary for most military applications are determinable. As indicated previously, the optical filters commonly employed over the screen of the radar indicator often serve as a medium for display of range, azimuth or elevation coordinate markings: however, these methods are seldom completely satisfactory in military fire-control radar systems because of errors introduced by the ever-present size or position variations in the electronic display field. Their use has been strictly limited to search or reconnaisance radar systems.

2.61 *Electronic Bearing Marker Circuits*

The bearing marker methods reviewed here are applicable generally to both azimuth and elevation angle determination. A method of azimuth or elevation bearing determination which can be associated with a lobing antenna system and an A-type indicator has been mentioned previously. This method remains an extremely precise system which has the desirable advantage of simplicity. During the latter part of the war, automatic tracking was applied to this method where the actual comparison of the lobes of the selected target signals was carried out electronically and the resultant antenna steering information utilized as the final bearing data. In a strict sense, however, only an indication of error in antenna training is observable to the operator on the radar equipment proper. The exact bearing data must be obtained from a measurement of the position of the antenna itself.

In the case of the continuous scanning systems employing B, C, or PPI presentations, it is common practice to provide a steerable electronic marker which can be superimposed upon the display field and by which means relatively exact azimuth and elevation angles can be determined by target and marker coincidence. This electronic marker method has the advantage that it is subject to the same size and position display field distortion influences as the received pulse signal, thus eliminating this source of error.

A circuit arrangement which has been employed in connection with a naval vessel radar search system to brighten a selected and variable range trace of the PPI indicator to serve as an electronic azimuth marker is given in Fig. 58. In this example the rotating antenna structure is equipped with a small permanent magnet pole piece whose cyclic excursions past a sealed magnetic reed relay cause a pair of contacts to close indicating coincidence. The relay structure is likewise mounted on a ring which can be rotated with respect to the scanning axis of the antenna. The relative bearing of a target is thus determinable by a knowledge of the angular position of the relay capsule with respect to the lubber line of the vessel. The circuit of Fig. 58 produces one brightened range trace for each revolution of the antenna upon closure of the bearing marker relay contacts and is ar-

ranged to be unaffected by any subsequent chatter or false switch closures. The pedestal generator which includes vacuum tubes V_1 and V_2 which are normally operated below plate current cutoff produces upon closure of the bearing marker switch contact a rectangular negative pulse having a duration of 10,000 microseconds. This pulse operation is independent of additional chatter effects following the initial contact closure. The following single-cycle bearing mark multivibrator is normally held inoperative by the bias voltage developed on the cathode of V_3. The grid of V_3 is continuously excited with the range sweep start pulses of an amplitude insufficient to actuate this multivibrator circuit. The presence of the 10,000-microsecond pedestal is sufficient, however, to allow the following range sweep

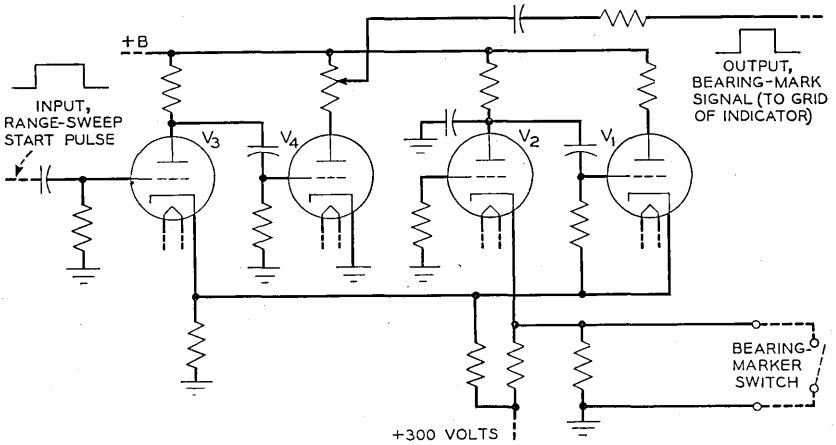

Fig. 58.—Electronic azimuth bearing marker circuit—simplified schematic.

start pulse to operate the multivibrator. The output of this circuit is then a 550-microsecond pulse which represents a time slightly longer than the maximum range to be displayed (60,000 yards) but shorter than the period of the sweep repetition rate. This positive 550-microsecond pulse is applied to the modulating grid of the PPI indicator tube through an adjustable trace brightness control element.

Another convenient azimuth display method which has been extensively employed in naval and airborne radar systems involves the use of "true North" presentations. Here the PPI azimuth indication is presented in terms of a compass reference, the actual instantaneous position of the radial trace on the screen representing the compass direction of the antenna beam. In the indicator previously illustrated in Fig. 44 the compass information is introduced by means of a differential synchro inserted in the antenna-indicator synchronizing connections whose angular displacement is

portional to the instantaneous heading of the aircraft. In the SL radar indicator shown in Fig. 61 the compass information is introduced by means of a mechanical differential rotation of the indicator deflection coil proportional to the angular position of the compass repeater mechanism.

2.62 *Range Marker Circuits—Fixed Range Markers*

A simplified schematic diagram of a convenient fixed range mark generator circuit which has been extensively employed on airborne radar search systems is given in Fig. 59. Here the radar system requires 1- and 5-statute mile fixed range markers. The sweep start multivibrator pulse is applied to the grid of V_1 as shown. In the absence of a signal, this tube

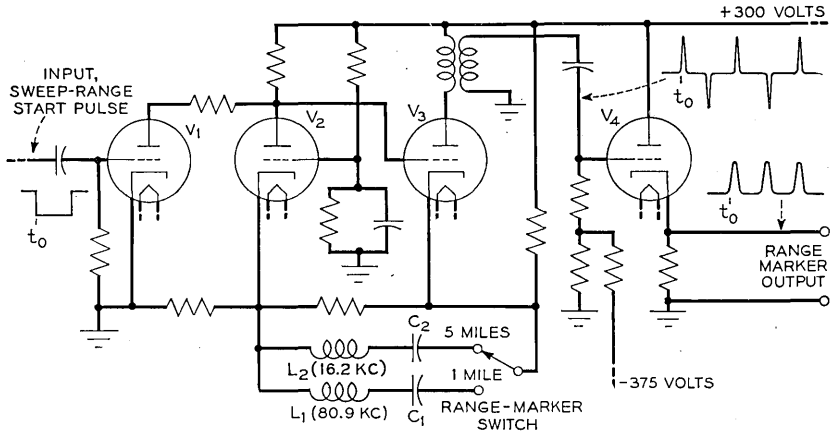

Fig. 59.—Fixed range marker circuit—simplified schematic.

operates at effectively zero bias, and because of the large plate current flow reduces the effective plate potential of V_2 and the grid potential of V_3 to a low value. Since the cathode of V_3 is subject to a large positive potential, this tube is cut off and the oscillatory circuit shown is inoperative. Upon application of the negative start pulse, V_1 is cut off for the duration of this pulse and the attendant rise in the V_3 grid potential permits the oscillator circuit to function. The series resonant elements L_1 C_1 and L_2 C_2 determine the frequency of oscillation by providing a high value of positive feedback at series resonant frequency. The output of V_3 which consists of approximately sinusoidal pulses is differentiated by means of the air-core transformer The differentiated pulses are then applied to a cathode follower or stage biased to cut off where the output is limited to the desired fixed range mark pulses for indicator display. By careful choice of elements and equipment arrangement, this simple circuit form has

produced an entirely satisfactory range marker signal for radar search systems.

Variable Range Marker Circuits

Variable range marker circuits are employed where more precise range information is required for missile control applications of radar. Here the observer may position the electronic range mark to obtain coincidence with the selected target, and from an associated calibration of this positioning control, determine the range coordinate. For search or reconnaissance purposes it is often desirable to determine range with somewhat more accuracy than is afforded by the display of fixed markers, and for this purpose,

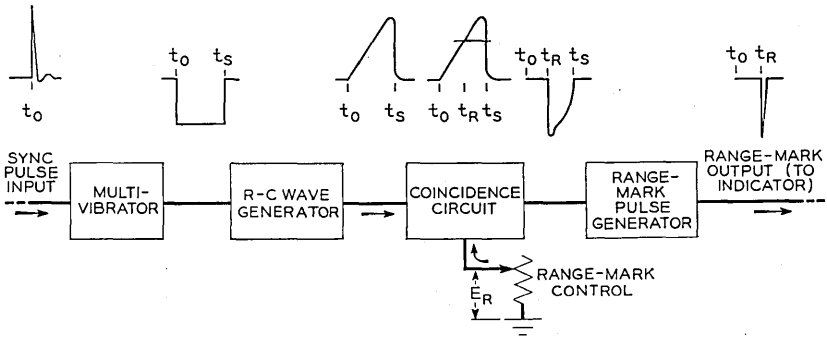

Fig. 60.—Variable range marker circuit of moderate precision—simplified schematic.

several designs of moderate precision variable range marker circuits have been developed and employed during the past war period.

Figure 60 illustrates the circuit operation of a variable range mark generator of moderate precision. This circuit operation depends on a pulse obtained from the transmitting modulator to serve as the zero time or range reference. This is applied to a single-cycle multivibrator which produces a rectangular pulse whose leading edge is coincident with the time of the synchronizing pulse and whose duration is somewhat greater than the maximum range measurement required. A saw-toothed voltage wave form is generated in the following RC wave generator by means similar to the sweep wave form generation described in a previous section of this paper. The coincidence circuit which follows consists of a vacuum tube biased below cut-off whose exact cut-off bias is determined by the range mark potentiometer setting. This coincidence circuit is thus inoperative until the saw-toothed input signal has reached the value of the cut-off voltage, at which time this circuit functions and produces a sharp decrease in its plate potential. The effective time delay which is here produced with respect

to the time of the synchronizing pulse is observed to be a function of the rate of change of the saw-toothed wave form and the setting of the range control potentiometer which may be calibrated directly in units of range to the target. The following range mark generator differentiates this coincidence circuit output wave form and furnishes the desired amplification. Zero range calibration is here provided by employing a sample of the zero time reference pulse and introducing this voltage into the range control circuit.

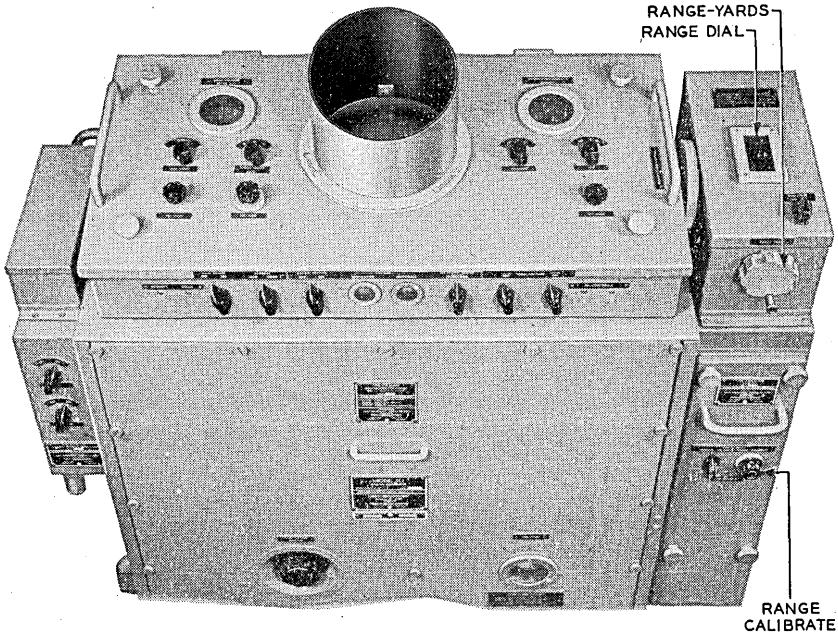

Fig. 61.—Transmitter-receiver-indicator assembly as designed for SL-Naval Search Radar equipment.

Figure 61 illustrates the transmitter-indicator assembly of the SL naval vessel search radar system. This system employs a PPI display with available range sweeps of 5, 25 and 60 nautical miles. The assembly shown to the right of the main unit contains a variable range marker circuit of the type just described. This range mark is positioned by means of the control located toward the top of this unit and its calibration is observable through a window located on the top panel. Here a maximum measuring range interval of 40,000 yards is available. In this application, the RC elements of the wave generator are enclosed within an oven and maintained at a constant temperature by thermostatic means. The accuracy achieved in this example, without recourse to calibration means involving targets at known

range, is ± 200 yards at the maximum range with an accuracy of ± 100 yards for targets within 5 nautical miles.

For more precise determination of range than is afforded in the circuit just described, two methods have been extensively employed. The first method involves the production of a known time delay by actual measurement of the time of propagation of an acoustical wave through a liquid medium. Here the physical length of path is varied to produce the variable delay. The second method involves the phase shifting of a known precise sinusoidal frequency standard which bears a fixed phase relationship to the time of the outgoing radar pulse.

The "liquid delay tank" variable range unit over-all operation may be observed by reference to Fig. 62. The zero time range reference is obtained in the form of a pulse coincident with the outgoing radar pulse. This pulse actuates the one-cycle multivibrator shown to produce a sharp high-ampli-

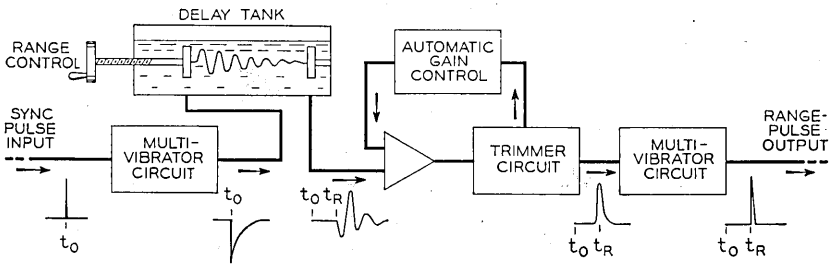

Fig. 62.—Liquid delay tank type of precision variable range unit—block diagram of operation.

tude output pulse, here relatively independent of amplitude and form characteristics of the synchronizing pulse and which is applied directly to the delay tank. This delay tank consists of a suitable container filled with a mixture of iron-free ethylene glycol and water so composed as to produce a zero temperature-velocity coefficient at 135°F, at which temperature the liquid is maintained by thermostatically controlled electrical heaters. In this temperature region the temperature-velocity characteristic is such as to produce a decrease of velocity of 0.1% for a temperature variation of 14°F. Located at one end of this tank is a quartz crystal, approximately $\frac{7}{8}''$ square and 0.040″ in thickness, mounted securely on a brass plate which serves as one electrode and which is immersed in the liquid. A similar crystal element is attached to a lead-screw carriage and located so that the face of this crystal is parallel to the fixed crystal. The distance between the crystal faces can be varied by rotation of the lead screw. The sharp voltage wave applied to the transmitting crystal causes it to oscillate in a damped vibration at its natural frequency for longitudinal waves which in this case

is of the order of 1.4 megacycles. The mounting plate and surrounding liquid serves to highly dampen this oscillation. A short vibrational wave train is projected through the liquid toward the receiving crystal. The amplitude of this disturbance is only slightly attenuated by viscous dissipation for the maximum path length here employed. The large area of the crystal relative to the wave length results in a highly directive radiation and is reflected in a parallelism requirement for the crystal faces of the order of .01″. The voltage developed across the receiving crystal upon application of this delayed acoustical wave consists of a main response followed by minor disturbances due to re-reflections between the crystals.

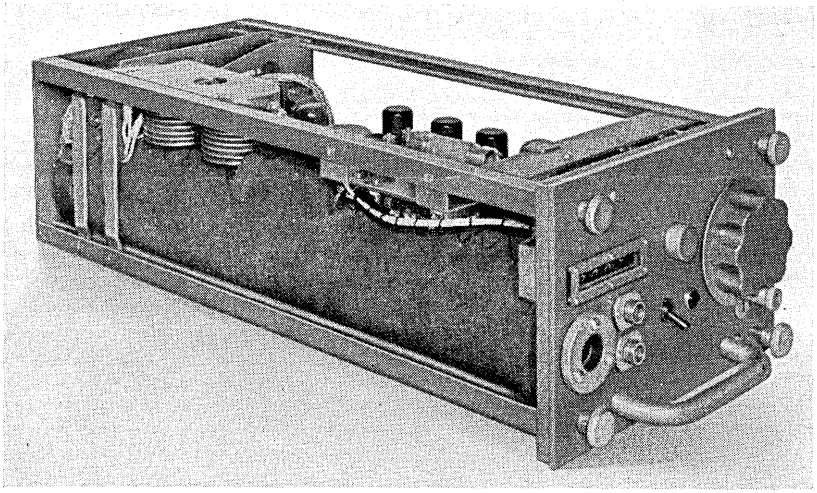

Fig. 63.—Liquid delay tank type of precision variable range unit.

The following amplifier shown in Fig. 62 is required to increase the .005-volt received signal to approximately 20 volts. This gain supplied is controllable by means of an automatic gain control circuit so as to provide a relatively constant amplitude of the first response signal. The following trimmer circuit consists of a pentode operating below cutoff such that a signal of at least 20 volts is required for plate current flow. Since the AGC circuit operates to adjust the gain of the amplifier to this condition, only the first and highest response peak is transmitted to the final range pulse multivibrator circuit where a sharp narrow rectangular pulse is produced to be employed in the following indicator circuit.

Figure 63 is a photograph of the liquid-tank type of variable range unit as developed and manufactured early in the past war and employed extensively in naval fire-control radar systems. This unit includes provision for a

maximum range measurement of 40,000 yards with an accuracy of ± 40 yards at this range under normal field operating conditions.

The use of the liquid range unit is practically restricted to ground and naval vessel application because of its weight and the problems of handling these critical liquids. Another variable range unit development was initiated to meet the same accuracy requirements as above, but to be more suitable for aircraft and other extreme ambient applications. The phase-shifting type of variable range unit whose operation is illustrated in Fig. 64 was the result of this effort.

The input start-stop single-cycle multivibrator circuit produces a rectangular pulse output wave form whose leading edge is coincident with the time of the outgoing radar pulse and whose duration encompasses the maximum range time to be measured, in this example 270 microseconds.

The timing wave generator and associated phase shifting circuit is shown schematically in Fig. 65. The resonant frequency of the oscillatory circuit is 81.955 kc which period represents an equivalent radar range interval of 2000 yards. An initial d-c current of approximately 10 ma is present in the $L_1\,C_1$ circuit in the absence of input start signals. Upon application of the negatively poled rectangular start-stop pulse V_1 and V_2 are abruptly driven to cutoff and the energy associated with the magnetic field of L_1 produces local current flow and oscillation at a frequency determined by $L_1\,C_1$. The initial circuit conditions here are the same as the zero voltage condition for each cycle of a sustained oscillation and the behavior of the oscillatory system is the same as for the case of sustained oscillation. The absolute average potential of the oscillation is maintained constant regardless of the magnitude of the duty cycle. Positive feedback of the timing wave is included in the V_3 cathode connection in such a manner that uniform amplitude of the timing period throughout the active period results. The purpose of the remaining circuits shown in Fig. 65 consisting of V_3, V_4 and V_5 is to produce four output timing wave voltages whose relative phases differ by 90°. These voltages are to be later combined in such a manner that continuous phase shift of the output timing wave results. Two quadrature voltages are here produced by the use of LR and CR networks so proportioned that $\omega L_2 = \dfrac{1}{\omega C_2} = R_2$ at 81.955 kc. The desired four timing wave outputs are produced by the use of the phase inverter stages V_4 and V_5.

The method here employed to combine four quadrature voltages to enable continuous relative phase shift of the resultant output is illustrated in Fig. 66. This phase shifter capacitor consists of four quadrant shaped stator sectors which are equal in area and shape and which are mounted parallel to a ring stator as shown. A carefully shaped eccentric dielectric vane rotor

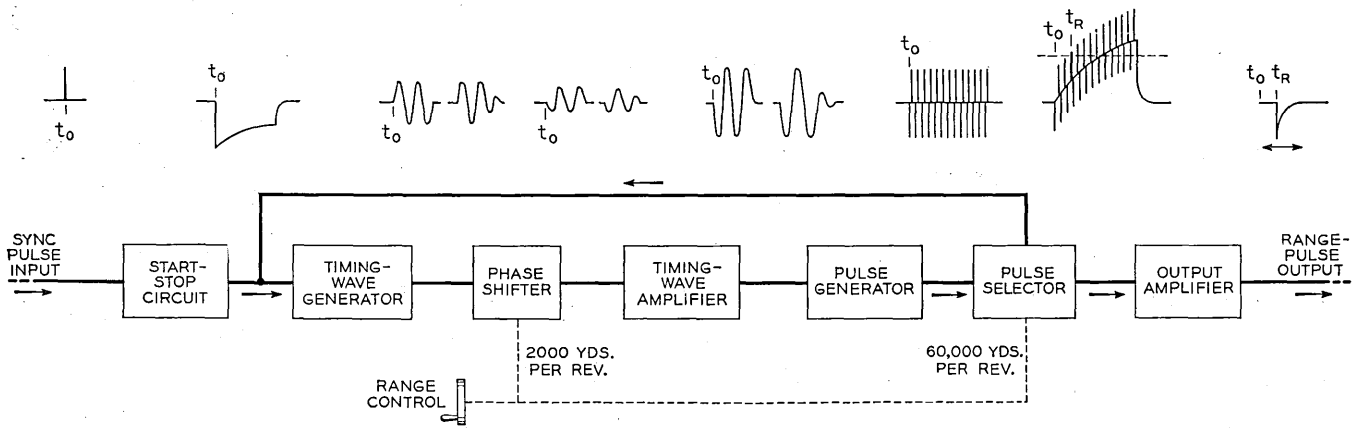

Fig. 64.—Phase shifter type of precision variable range unit—block diagram of operation.

is provided whose rotation between the stator elements affects each quadrant stator capacitance in a like manner. As illustrated the resultant output voltage which appears from the ring stator to ground has a phase shift relative to any applied wave which varies linearly with angular displacement of the condenser shaft.

The function of the following amplifier shown in Fig. 64 is to provide a high-impedance termination for the phase-shifting condenser, and to provide increased amplitude of the timing wave. The pulse generator which follows limits or clips the applied timing wave, and differentiates the re-

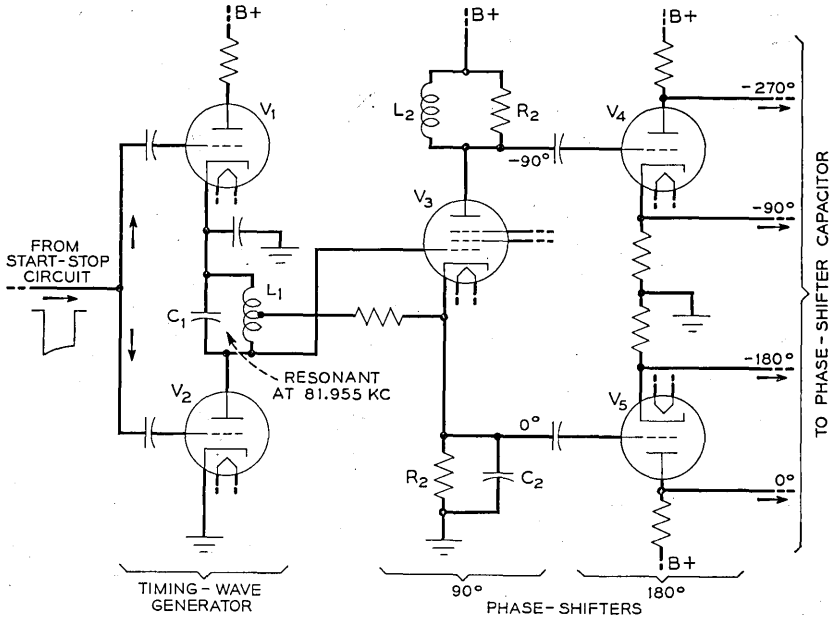

Fig. 65.—Timing wave generator circuit of phase shifter type range unit.

sultant wave form. The output here consists of trains of alternate positive and negative timing pulses.

The pulse selector component shown in Fig. 64 enables obtaining delay intervals greater than 12.2 microseconds the value associated with 360° phase shift of the timing wave. An increasing exponential saw-toothed wave form is generated starting at zero time reference by an RC circuit having a time constant of the order of 800 microseconds. The timing pulses are applied additively with this exponential to the grid of a vacuum tube operating below cutoff, its exact value of bias being determined by the setting of a potentiometer control. At the time that the grid signal amplitude exceeds this critical cut-off bias value, this tube conducts abruptly as

shown and an output pulse is produced whose position on a time scale is determined by the additive phase shift of the timing wave and the setting of the pulse selector potentiometer. By mechanically gearing the potentiometer and phase-shifting condenser, the final rotation of the control shaft will result in an output pulse whose delay will increase uniformly and correspond to 2000 yards per revolution of the control. Further amplification is furnished in the output amplifier shown.

Figure 67 illustrates the final equipment features of a phase-shifting type of variable range unit as developed for naval vessel radar system application. It will be observed that this unit is mechanically interchangeable with the liquid range unit shown in Fig. 63.

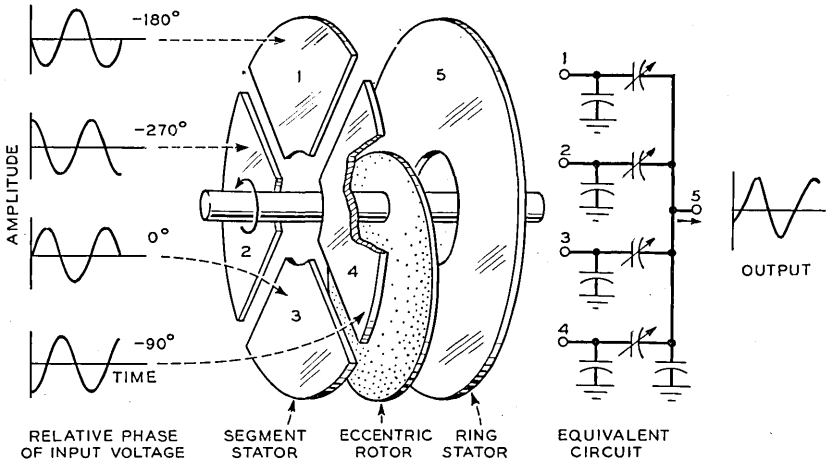

Fig. 66.—Schematic outline of operation of phase shifter condenser.

In this model, the parallel resonant timing wave oscillatory circuit is maintained at a constant temperature by employing an electrically heated oven. Measurements made on this design indicate that the range shift error to be expected for a "warm-up" period of 6 minutes was .03% or 15 yards at 45,000 yards range. After 6 minutes time, thermal equilibrium is reached and the total range error will be less than 20 yards at 45,000 yards range. The unit here illustrated has been universally employed in the majority of naval vessel fire-control radar systems of the past war and these basic circuit principles have served for range measurement in other applications including precision radar bombing.

2.7 *Automatic Frequency Control and Automatic Gain Control*

2.71 *Automatic Frequency Control*

The automatic frequency control (AFC) of the local beating oscillator to

assure correct tuning of the radar receiver has become an extremely important feature of the military radar system and the successful solution of

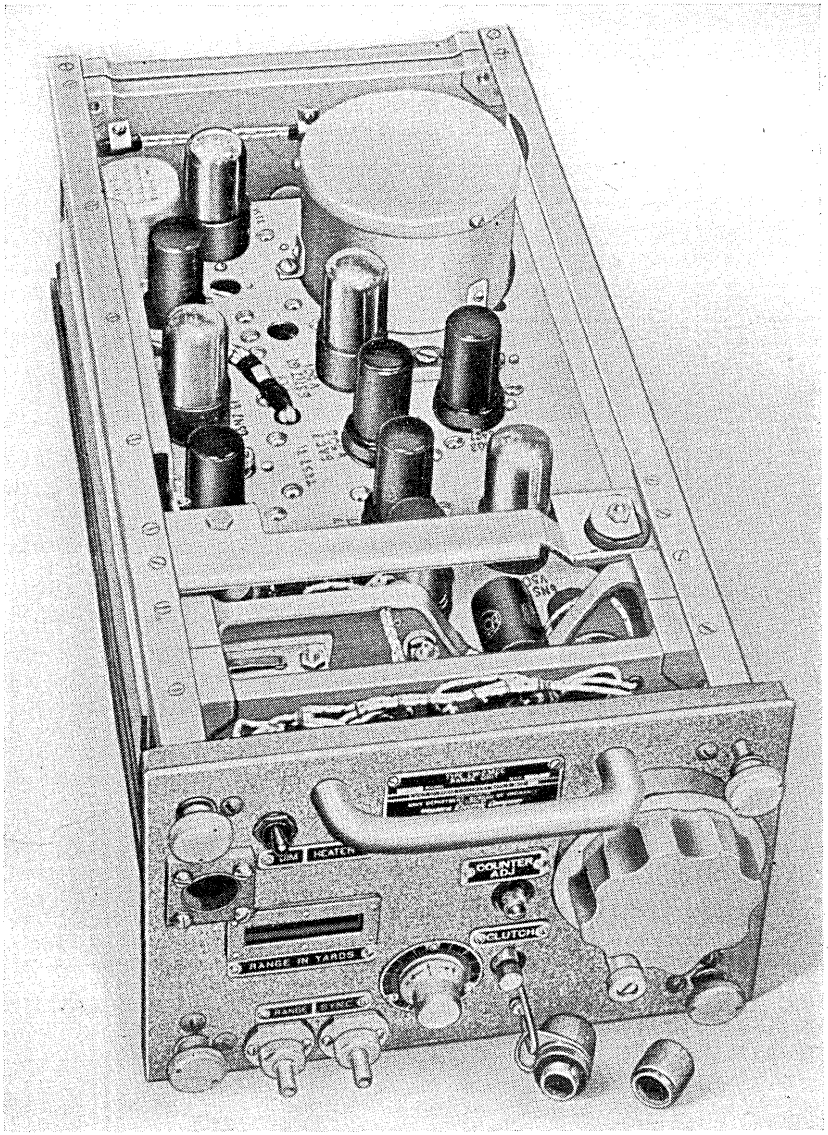

Fig. 67.—Precision variable range unit of the continuous phase shifter type.

this problem has contributed greatly to the practical success of radar during World War II, by assuring consistent optimum system performance under

severe military field conditions. In the case of the usual radio-communication system, some knowledge of character and extent of the information which is being transmitted is available to the receiving location which may serve to evaluate the receiver operating performance, but in the case of the military radar system such reference data is not always available. The usual military operating conditions for radar systems are extremely severe which, in general, tends to degrade the performance. Mistuning of the radar receiver and the attendant reduction of the performance of the system must be immediately evident to the operator even under conditions where no radar signal returns are present.

During the first years of the past war, this tuning problem was recognized and the initial attempts at solution involved the inclusion of receiver tuning indicators to serve as an indication of adjustment. As the radar systems became more complex and with the trend toward the use of higher transmission frequencies the necessity for completely automatic continuous tuning adjustment of the receiver became increasingly evident and the present types of automatic frequency control devices were developed. It has been determined that in the specific case of airborne radar bombing equipment operating at 10,000 mc that the automatic frequency control of the receiver tuning is an absolute necessity, since the radar operator cannot under the normal military operating conditions maintain the system performance in this regard to a small fraction of the optimum.

Functions and Requirements

The basic reference for a radar automatic frequency control system must be the transmitter frequency since it is required that the receiver be properly tuned under the condition where no radar return signals are available. Either the frequency of the transmitter magnetron or the local beating oscillator frequency may be adjusted from an electrical error signal whose characteristics are related to the tuning point. Magnetrons whose frequency was conveniently controllable by remote electrical means were not then available so that the later method has been universally applied in military radar systems developed during the past war period.

It is pertinent to review the nature and extent of the frequency instability of a radar system to derive the requirements to be imposed upon an AFC device. The sources of frequency instability are associated with the transmitter as well as the receiver elements of a radar system. The magnetron frequency is determined in part by the physical dimensions of its oscillatory cavity structure, and as would be expected, ambient temperature and pressure conditions exert a decided influence. For example, a typical thermal coefficient of frequency for a magnetron may be as high as 200 kilocycles per degree Centigrade which over the range of ambient temperatures

to be considered important for military equipment may result in a frequency shift of 20 mc from the time the equipment is turned on until thermal equilibrium is established. The magnetron frequency is extremely sensitive to its terminating load impedance. This termination in a radar equipment is composed of the antenna, the interconnecting RF transmission line, and the duplexing devices. The typical radar antenna system employs rotating joints or connecting devices to enable transfer of RF power to the antenna proper while it is mechanically operated over its scanning cycle. These connections cannot be made to present an entirely uniform impedance over their entire mechanical operating range and thus introduce variable impedance irregularities to the magnetron generator. The frequency of these impedance variations may range from a fraction of a cycle per second to perhaps 60 cps. The input impedance of the antenna proper is dependent on the extent and character of nearby obstructions in the radiation path. The characteristics and form of the radome employed to protect the antenna contribute to the variable impedance characteristics of the antenna and thus influence the magnetron frequency. An additional instability in magnetron operation which is introduced through power supply variations within the modulator and transmitter portion of the system must also be considered in the detailed design of the AFC system.

The receiver itself is responsible for a major contribution to the frequency instability characteristics of the radar system. The local beat oscillator frequency is critically dependent on the physical dimensions of its oscillatory structure and on the supply voltages. The effects of temperature and atmospheric pressure on the frequency of a reflex oscillator of the types previously described is considerable. For example, a thermal coefficient of 0.25 mc per degree Centigrade, typical of the 10,000-mc tubes, will produce a total excursion of perhaps 25 mc over the range of ambients experienced in military equipment. In the case of supply voltage variations, a 5-mc frequency shift will result for a 1% change in anode and repeller potential for a typical 10,000-mc reflex oscillator. Another source of receiver frequency instability is associated with the shift of the IF amplifier frequency selectivity characteristic with tube aging and operating conditions.

If the operating requirements for an AFC system are now reviewed from a consideration of these factors, it will be observed that for a radar system operating at the higher frequencies a total effective frequency change of perhaps as much as 50 mc may be encountered whose rate of change, in general, will be relatively slow and may be classified generally as effects due to "warm up". In addition fast variations of frequency will be present whose rates of frequency change may extend from 1 mc per second per second to 1000 mc per second per second. At the lower radar frequencies

these frequency variations will be somewhat lower with an attendant reduction of the range of operation required of the AFC circuit.

AFC Circuit Design Considerations

To obtain a measure of the basic frequency reference for AFC purposes the direct approach is evident. A sufficiently attenuated sample of the outgoing radar pulse may be obtained from the transmitter and after sepa-

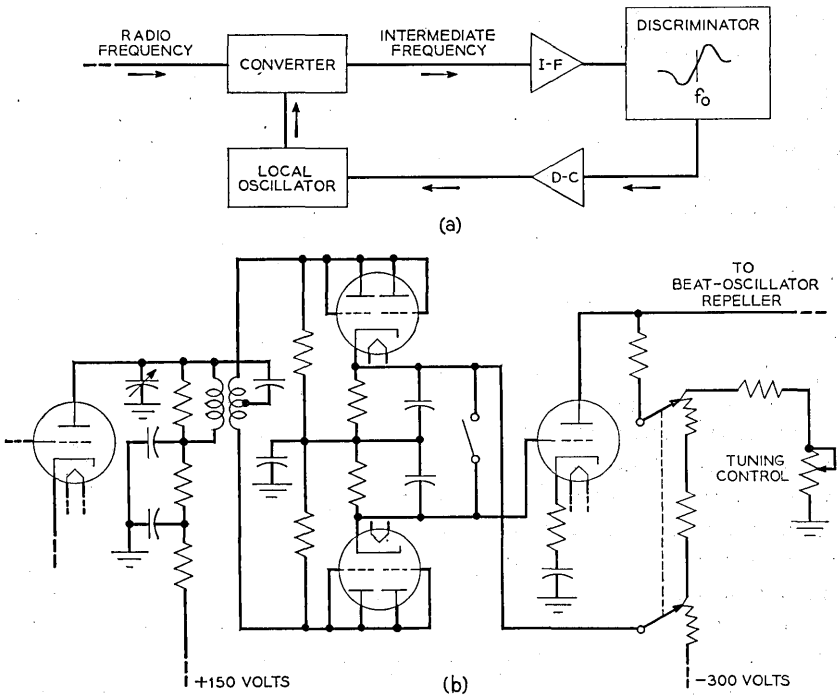

Fig. 68.—Radar AFC system—block diagram and circuit arrangement.

rate conversion but, under the influence of the regular receiver beat oscillator, may be employed as a true sample of the outgoing signal as it exists with the normal receiver IF channel. The separate AFC converter method has been employed in some military radar equipment but has the disadvantage that additional conversion components are required. A second method is more economical of equipment and has been extensively employed during the past war period, but this later type of AFC circuit has limitations which are imposed on it by the character of the IF signal as normally available in a radar receiver. Figure 68a illustrated the essential elements of such an AFC system for a radar receiver. It will be here observed that a

sample of the IF signal after normal conversion and some amplification is applied to a frequency sensitive discriminator circuit and the resulting error signal is employed to readjust the beat oscillator frequency. The outgoing radar pulse is normally attenuated effectively by the TR circuit, and thus the remaining signal available for AFC purposes is due to inherent leakage of the TR elements. As previously indicated, the frequency spectrum of the output "spike" of the TR device extends over a wide frequency range, due primarily to the small finite delay in the breakdown of the TR tube. The energy frequency distribution characteristic of this spike is to a large degree independent of the magnetron frequency and, therefore, must be considered as an undesirable masking signal and accordingly reduced to a noninterfering level. As previously indicated this is usually accomplished by disabling one or more of the IF amplifier input stages for a short time interval coincident with the outgoing radar pulse.

With a signal available which is related to the frequency of the outgoing pulse, the remainder of the AFC design is concerned with the utilization of this information to accomplish the automatic tuning of the radar receiver. To determine the frequency gain characteristic of the discriminator circuit it is pertinent to examine the frequency repeller potential relationship of the local beat oscillator. This relationship for a 2K25-type reflex oscillator operating at 10,000 mc shown in Fig. 19 is approximately 2 mc/volt and is representative of the tubes of this type. This quantity provides an indication of the "loop gain" required for a satisfactory AFC circuit.

Typical AFC Circuit Designs

Figure 68b illustrates the essential elements of a radar AFC discriminator and amplifier circuit. This consists of an input circuit which is required to furnish the means for frequency measurement, rectifier elements to convert this frequency deviation information to a proportional voltage error signal, followed by an amplifier to increase the amplitude of this signal to the required level to adequately control the frequency of the local beat oscillator.

The operation of the discriminator input circuit may be observed by reference to the vector diagram of Fig. 69a. The input circuit, essentially a double-tuned transformer having a low value of mutual inductance, serves to couple the AFC rectifier to the preceding IF amplifier tube. The resonance frequency of both primary and secondary circuits is maintained at the desired midband IF tuning point, in this example, 60 mc. The output of the balanced secondary winding of this input network is applied to a balanced rectifier shown in the vector diagram as E_1 and E_1'. In addition a portion of the IF signal voltage which appears across the primary winding is also applied to each element of the balanced rectifier. At resonance, the primary and secondary voltages assume a quadrature relationship as indi-

cated. The vector relationships for frequencies above and below this resonance, as shown, result in an amplitude change across the rectifier circuit. Figure 69b illustrates a typical rectified voltage versus frequency characteristic of such an array. The location of the actual crossover zero voltage point is determined only by the resonance of the secondary circuit over the limited range under consideration here. The primary resonance contributes essentially only to the symmetry of the voltage output versus frequency characteristic. The introduction of the time constant elements in the detector output circuit integrates the pulse output and are chosen with due regard

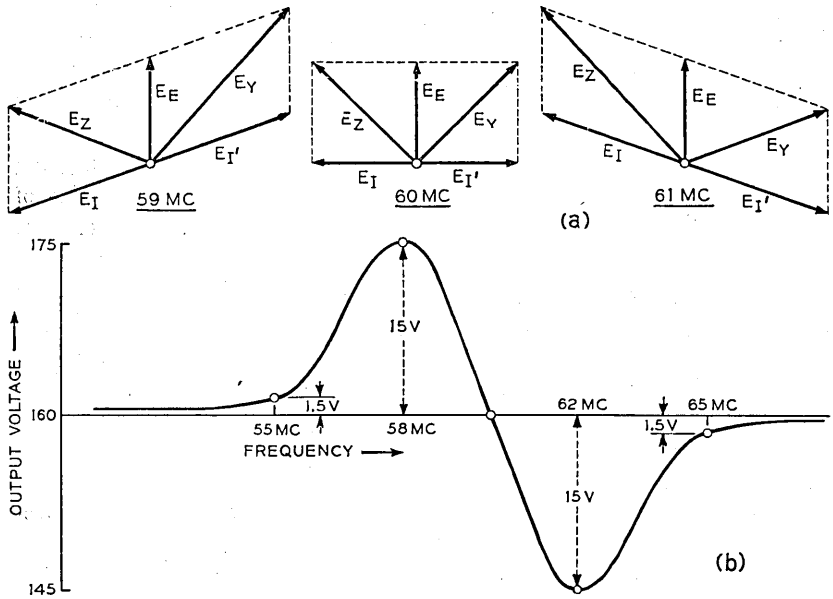

Fig. 69.—Operation of the AFC circuit—vector relationships in input circuit and output voltage vs. frequency characteristic.

to the maximum frequency rate of change which this circuit must control. The d-c amplifier shown is normally biased to operate at maximum gain consistent with stability, to produce the maximum sensitivity to frequency change and to accordingly achieve the least threshold deviation from the ideal tuning condition. Provision for disabling the AFC circuit is included to enable initial manual adjustment of the beat oscillator repeller potential. With the circuit shown here, failure of the AFC circuit proper will result in the return of the repeller potential to that value originally selected by initial tuning and further manual control may be used.

It is often convenient to describe the effectiveness of an AFC circuit in terms of its "pull in" range and its "hold in" characteristics. "Pull in"

will be defined as the ability of the AFC circuit to restore proper tuning conditions with sudden application of the signal. The "hold in" characteristic of the AFC system will be defined as the ability of the circuit to maintain proper tuning conditions as slow changes occur in the frequency of the control signal. In the AN/APS-4 airborne radar equipment previously referred to, which employs an AFC circuit similar to the form here described, the "pull in" range is approximately ± 5 mc from the 60-mc midband value and the "hold in" range includes the entire tuning range of the reflex oscillator employed which is of the order of ± 40 mc. This example will maintain the tuning within 0.5 mc of the desired tuning point over the range of conditions encountered in wartime aircraft applications.

In some applications use has been made of a frequency scanning process whereby the AFC output voltage, in the absence of a suitable controlling signal within the IF band, is caused to vary periodically in a saw-tooth fashion thus causing the local beat oscillator frequency to vary, sweeping across the complete tuning range of the receiver. When the desired signal frequency is produced the AFC then functions in the normal manner. This form of circuit was employed in certain radar equipments developed during the early part of the war and a somewhat similar oscillatory AFC circuit has been employed in connection with later developed thermally tuned reflex oscillators and reported elsewhere.[13]

An automatic frequency control unit designed in connection with the AN/APQ-7 radar bombing equipment which operates at 10,000 mc is illustrated in Fig. 70 and Fig. 71. The basic operation of this equipment example is similar to the d-c amplifier type previously described but includes certain modifications important for this particular application. In this circuit the plate potential of the first IF stage of the AFC unit is obtained as a positive pulse from the transmitting modulator thus enabling the AFC circuit only during the short interval of time encompassing the outgoing radar pulse. This arrangement assures that no detuning of the receiver will result from spurious or nearby signals after the radar pulse has been transmitted. The rectifier elements here consist of triodes operating near plate current cut-off which results in improved linearity of detection. The d-c amplifier portion of this AFC circuit is arranged somewhat differently from the example previously discussed, including in this case balancing controls to account for tube and circuit variations. At the condition of resonance, in this case 60 mc, the voltages applied to each grid of the amplifier are equal and the net repeller potential is determined entirely by the manual control value. The overall output range of voltage for this circuit is ± 20 volts, which in this application represents a ± 40-mc frequency change for the associated

[13] "Considerations in the Design of Centimeter-Wave Radar Receivers", Stewart E. Miller, *Proc. I. R. E.*, Vol. 35, No. 4, April, 1947.

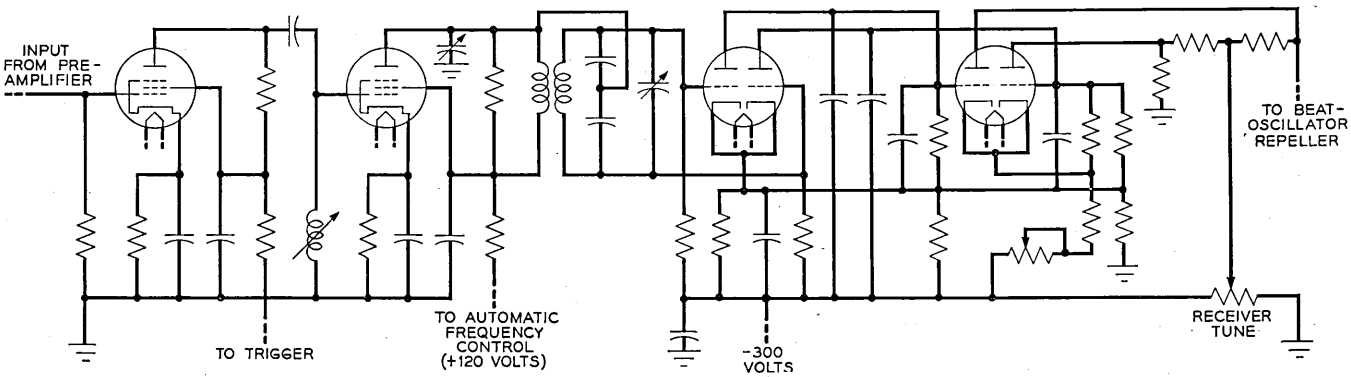

Fig. 70.—AFC circuit schematic for AN/APQ-7 radar system.

reflex oscillator. Variations in the amplitude of the controlling signal are of less importance by virtue of the biasing action of this d-c amplifier circuit. The performance of this design includes maintenance of the tuning point of this receiver to within ± 0.25 mc of the center of the IF band which in this case is 60 mc.

2.72 *Automatic Gain Control*

Automatic gain control (AGC) of a selected radar signal is often required in military radar systems employed for fire control or aircraft interception purposes. In the case of the common search radar system, AGC is seldom required. The radar receiver AGC function is quite similar to that required of this circuit in the usual radio communication system, i.e., automatic am-

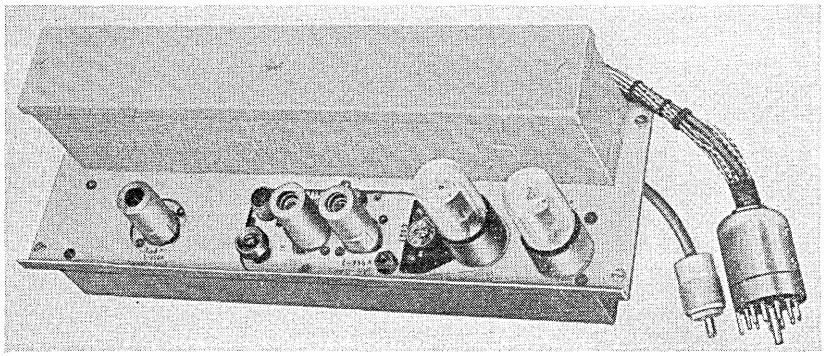

Fig. 71.—AFC component design as employed in AN/APQ-7 airborne radar system.

plitude stabilization of the desired signal. For the radar receiver case, however, the desired signal must be selected on a time interval basis.

In the usual type of automatic tracking radar system, the target is selected by manual alignment of a range and/or bearing "gate". This gating process is essentially a modulation process by which the complete received radar pulse signals are modulated with a rectangular pulse synchronized with the outgoing radar pulse. The modulating pulse or gate has a finite amplitude only over the time interval under observation. In this manner all received information, except that occurring during the selected time interval, is effectively rejected and the automatic gain control circuit operation is entirely defined by the data present during this time interval.

The remainder of the automatic gain control circuit is concerned with the measurement of the amplitude of the selected signal, usually by a peak voltage measurement, the averaging of this measurement over a convenient time interval, and the production of a suitable gain control voltage to be impressed upon the radar receiver IF or video amplifier circuit. The detailed

AGC circuit design is dependent to a major extent upon the dynamic characteristics of the associated automatic tracking device. The subject of automatic tracking design principles cannot be reviewed here and accordingly more detailed AGC design consideration must also await inclusion in such a future report.

2.8 *Radar Receiver Power Supplies*

The remaining components of the radar receiver to be here reviewed consist of the power supplies necessary to produce the various d-c potentials as required for the operation of the electronic components of the receiver. The principal design problems associated with these components arise from the relatively poor stability characteristics of the prime sources of power available at the military scene and the rather severe output voltage requirements to adequately serve the precision nature of radar reception, display, and measurement. The supply voltages necessary for a military radar receiver range from low bias potentials upward to 5000 volts for cathode-ray tubes and TR application with both polarities often required.

2.81 *Primary Power Sources*

The characteristics of the primary source of power available for the military radar system are dependent on the area of use of the equipment. In the case of mobile ground radar installations, the gasoline engine driven generator represents the typical primary power source. In the case of large mobile radar systems it is customary to employ 115-volt—60-cycle primary power, while in certain more portable designs 115-volt—400-cycle primary power has proven satisfactory. The frequency and output voltage of a gasoline engine driven alternator cannot be maintained within the narrow limits desired by the radar receiver and here the major burden of precise voltage regulation must be carried by the electronic regulated power supply within the radar receiver.

For naval vessel radar installations 115–230-volt—60-cycle primary power is commonly available on the larger vessels. For PT and similar smaller craft, certain radar installations have been employed operating from 24–48 volts direct current with motor generator sets supplying 60-cycle or 400-cycle power for the radar system. In the case of undersea craft, the storage battery is employed as a primary source of power and motor generator sets are employed to obtain 115 volts, 60 cycles in most instances.

The primary source of power for aircraft radar purposes is either a low voltage (27 volts) d-c generator driven by the aircraft engine or an alternator similarly driven. If d-c power is available, an additional motor generator set may be employed to furnish the 115-volt—400 to 800-cycle power for the radar equipment use. Voltage regulators of the carbon pile compres-

sion or electronic types are usually employed here, resulting in a nominal ± 3% voltage stabilization. The extreme variable electrical loads imposed upon the aircraft power system by electrically operated gun turrets and other combat equipment result in increased emphasis being placed on adequate regulation capabilities of the radar receiver power supplies. In addition, the ever-present requirement of minimum weight for aircraft equipment results in motor generator designs employing a minimum of magnetic material and usually results in a variation in output voltage wave shape with load. This factor must also be considered in the detailed design of the aircraft radar receiver power supplies.

During the initial airborne radar development program, the power frequencies in common use were 400 cps and 800 cps. The British use of direct coupled aircraft engine driven alternators produced variable frequency output voltages ranging from 1200–2400 cps dependent on the engine speed. In connection with the electronic warfare standardization program for equipment to be used jointly by our allies, the aircraft radar system was required to operate over the entire range of power frequencies extending from 400 cps to 2400 cps. All of the airborne radar equipment developed during the later half of World War II was designed to meet these variable power frequency requirements.

2.82 *Low Voltage Power Supplies*

The electronic regulated power supply has been universally employed to furnish the stable low voltages as required by the radar receiver. Here the output voltages required extend from 50 volts to 600 volts with maximum direct current required extending upward to 500 ma.

The basic electrical circuit arrangement of such a power supply is shown in Fig. 72. In this circuit, the regulating element consists of a variable series impedance, furnished in the form of a vacuum tube and resistance combination, whose magnitude may be controlled electrically from an error signal associated with the output voltage of the power supply and a reference voltage. The control circuit consists of a bridge network which includes a constant voltage gas-discharge tube as one element. A d-c amplifier is connected across the output terminals of this bridge circuit and serves to amplify the error signal for use in the regulating element. If the output voltage of the power supply varies from the desired value for any cause, the error signal appears at the output terminals of the bridge circuit, due to the effective unbalance of this circuit at all voltage levels except the reference value. The error signal after sufficient amplification is impressed upon the grid of the series regulating tube with a polarity such that a corrective impedance variation results. The degree of regulation obtainable is a function of the loop gain provided and the absolute stability of the output voltage

is determined primarily by the constancy of the reference voltage derived by the use of the gas-discharge tube. By incorporating wide frequency band characteristics to the loop gain elements, the maximum rate of change of regulation can be extended, and this circuit becomes very effective in reducing the fundamental and harmonics of the primary supply voltage. The effective impedance of a radar receiver power supply of this type is of the order of one ohm, a factor of extreme importance in reducing the unwanted interaction between the various receiver components by coupling due to this common impedance. Other variations in circuit arrangement for regulated power supplies are occasionally employed, the most common of which involves the use of a vacuum tube as a shunt regulating element as contrasted with the series arrangement shown here. In certain low-current

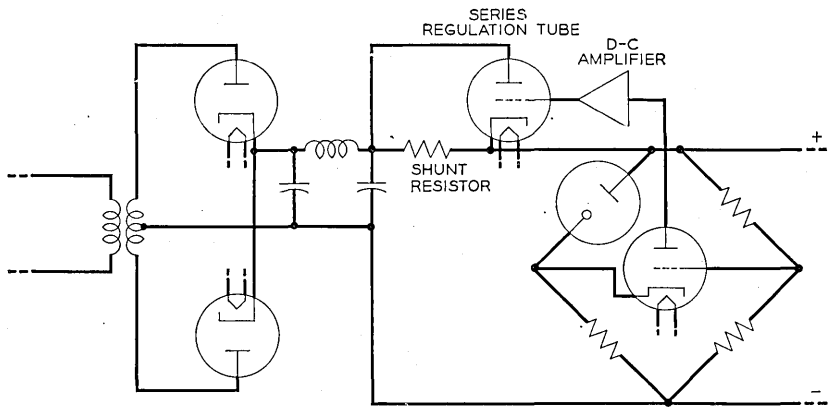

Fig. 72.—Simplified circuit schematic of low-voltage power supply—Series regulation type.

applications the use of gas-discharge tubes of constant voltage characteristics are occasionally employed in a shunt circuit configuration.

Figure 73 illustrates the equipment arrangement of a radar receiver power supply as employed for an airborne radar bombing system. In this example is included one non-regulated and three regulated rectifier power supplies with output voltages of +600, +300, +120 and −300 volts available for the radar receiver. The forced ventilation feature shown here is required to prevent extreme temperature rise of the components under high altitude conditions in the presence of considerable heat dissipation by the rectifier and series regulating circuits. Each power supply is designed as a separable subchassis within the over-all enclosure to provide for ease in manufacture and testing of the unit. The weight of this complete unit as installed in a military aircraft is approximately 50 pounds.

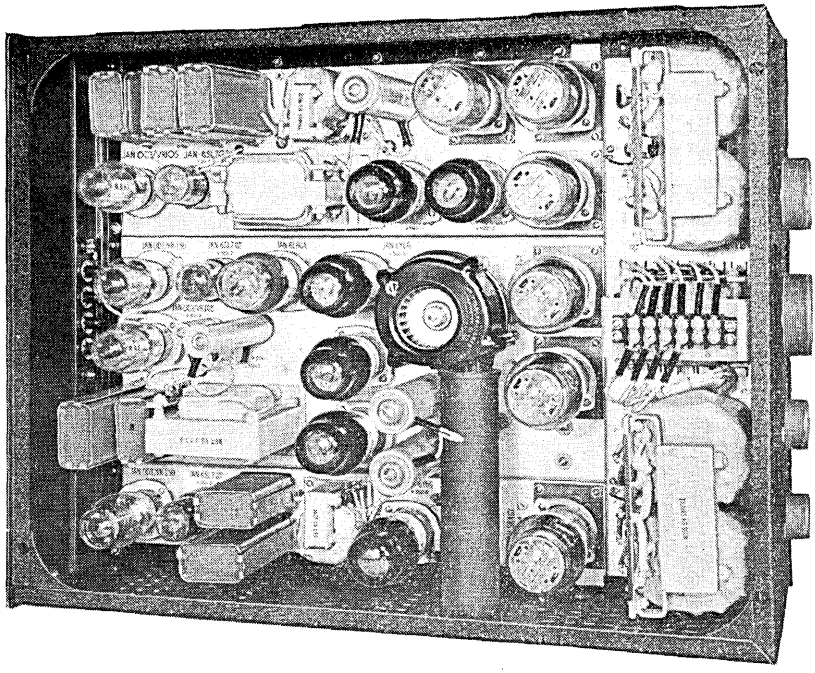

Fig. 73.—Low-voltage power supply for AN/APQ-7 airborne radar system—Mechanical features.

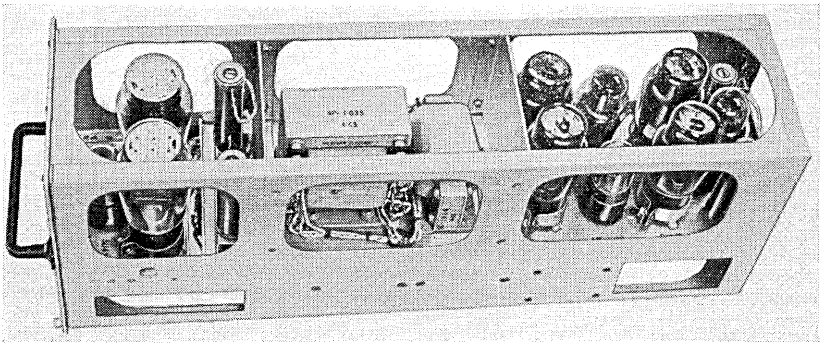

Fig. 74.—Low-voltage power supply for AN/APQ-5 low altitude radar bombing equipment.

Figure 74 indicates the mechanical design features of a typical airborne radar receiver power supply of the series regulated type as employed in the AN/APQ-5 radar bombing equipment. This example illustrates the emphasis which is placed on compactness and lightweight construction of airborne radar components.

To obtain the maximum dependable performance from the various power transformers and coils employed in the radar receiver power supplies under the severe military field conditions, a considerable development program was carried on throughout the past war. At the beginning of this program the only available method of insuring adequate transformer winding insulation under extreme humidity conditions involved the sealing of the structure in a metal container. For aircraft service, where weight is of prime concern, this added weight could not be tolerated so that here an open type of structure was extensively employed, with the protection to the winding being furnished in the form of several coats of varnish followed by an enamel overcoat. With the increased emphasis on high-altitude operation of military aircraft and the rapid temperature and pressure changes involved, a development program was instituted to improve the open-type transformer sealing process. The result of this program has produced the Flexseal process whereby the service life of this type of power transformer has been increased as much as ten times that obtained with the varnish process formerly employed. This process involves a multiple-dip varnish coating method where the varnish is thickened by the addition of talc, a very fine low-gravity wettable inert filler. This process results in the formation of a relatively thick plastic shell which completely surrounds the transformer structure. One of the features of this process is found in its simplicity, whereby no special equipment was required to carry out the procedure, an important factor during a wartime production program. Figure 75 illustrates a number of typical open-type power transformers which were employed on various military radar projects, all of which incorporate the Flexseal treatment for improved service life.

2.83 *High Voltage Power Supplies*

The high voltage, as required for radar receiver cathode-ray tube indicator purposes, varies from 2000 volts to 5000 volts, and for the TR tube keep-alive potentials of the order of 1000 volts must be provided. In these cases, however, the d-c current requirements are quite small and generally no regulation means are required for stabilization of the voltage, the stability of the primary source of power usually being sufficient.

The design problems encountered in this type of power supply are concerned primarily with the requirements of reliability of operation under severe military operating conditions, and further require that only circuit elements having well-defined factors of safety be employed in such applications.

Figure 76 illustrates a number of typical high-voltage transformer designs which have been employed in military radar systems during the past war period. Both air insulated and oil immersed types of structures are shown.

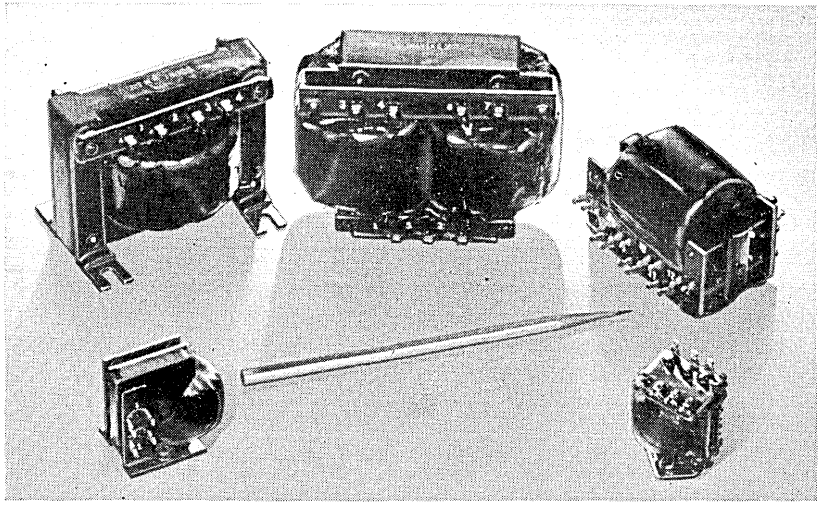

Fig. 75.—Flexseal treated open-core type power transformers as developed for airborne radar application.

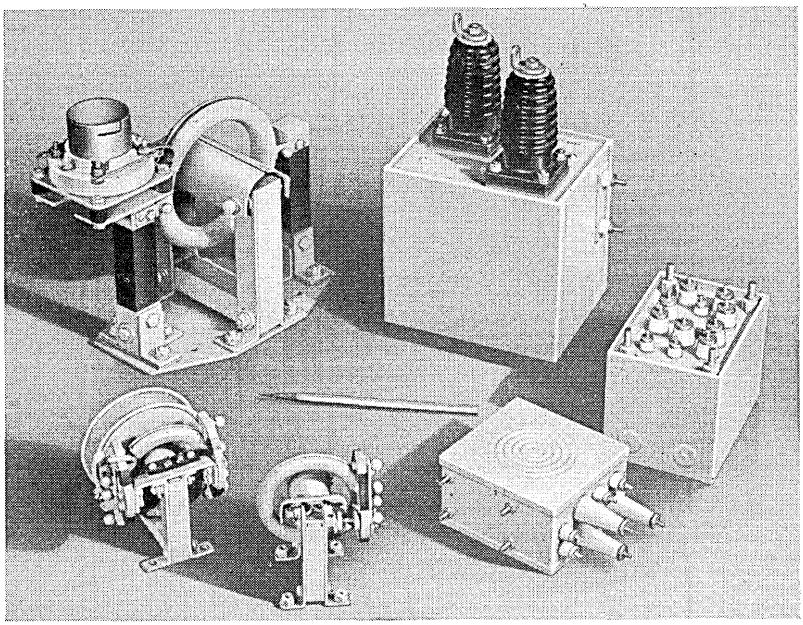

Fig. 76.—Power transformer designs for high voltage radar power supply application—Air-insulated and oil-filled types are included.

The use of air insulation in a high-voltage transformer results in a relatively low coupling coefficient between primary and secondary windings and

accordingly restricts the range of power frequencies over which satisfactory regulation and operation can be expected. With the emphasis on power supply frequencies extending from 400 cps to 2400 cps for aircraft purposes, this air insulated type of structure was abandoned in favor of oil immersed types. The primary disadvantage of the oil immersed type of transformer is the increased weight of the unit.

A high-voltage power supply design as produced for airborne radar system application is shown in Fig. 77. In this example +4900 volts is supplied for cathode-ray tube indicator purposes and −1000 volts is available for the TR tube keep-alive circuit. This unit employs an air insulated type of

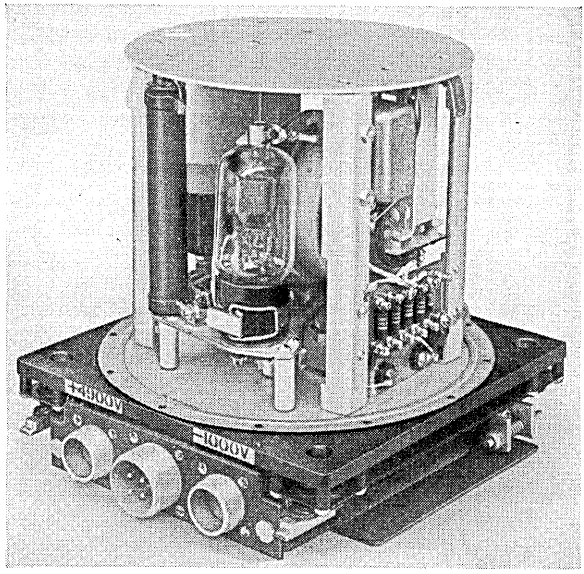

Fig. 77.—High-voltage power supply for airborne radar receiver application—pressurized type.

high-voltage transformer and by the use of a hermetically sealed enclosure operated at sea-level atmospheric pressure, satisfactory performance at high altitudes is realized.

Conclusion

The complete technical story of radar is of a magnitude comparable to a detailed report of the military campaigns of this past global war. During this period, the Bell Telephone Laboratories developed for manufacture more than 70 specialized radar systems for the Armed Services. It has been possible here only to review the major technical considerations which in-

fluence design of a military radar receiver and to present a few radar circuit and equipment illustrations of the specialized technology that has resulted. It is a tribute to the ingenuity and industry of the workers in the radar field that this technology, developed under extremely accelerated and difficult conditions, will have a permanent value in future communication systems design.

The material used in this paper represents the concrete contributions of countless individual workers within and without the Bell Telephone Laboratories. The equipment products illustrated are the product of concentrated effort on the part of the staff of the Western Electric Company who produced these specialized and complex radar systems in quantities and within schedules necessary for the successful prosecution of the war. It is regrettable that it is an impossible task to assign individual credit for these specific military radar contributions.

High-Vacuum Oxide-Cathode Pulse Modulator Tubes

By C. E. FAY

Introduction

IN PRACTICALLY all pulsed oscillators such as those used in radar, some means must be provided to apply the pulse voltage to the oscillator circuit. In many early radars, a high-vacuum modulator was used for this purpose. The pulse was generated at low power level and then amplified by means of one or more stages employing high vacuum tubes. The final stage was required to block, or cut off the d-c supply voltage with no pulse applied, and to permit as much as possible of the d-c voltage to appear on the oscillator during the pulse. Since most radar oscillators operate at pulse voltages of from 5 to 20 kv and require currents of several amperes during the pulse, the requirements of the modulator tubes are quite severe. Standard transmitting[1] tubes were used at first, the higher power tubes having the necessary voltage rating and having in general a fair amount of cathode emission. Tubes were operated in parallel to provide the required amount of current. Practically all of these tubes were of the thoriated tungsten filament type. For example an early army radar, the SCR268,[2] employed 8 tubes in parallel having a total filament power of 1040 watts to provide a pulse current of about 10 amperes. The use of such equipment in portable or airborne service would be obviously impractical because of the large power consumption, bulk, and weight. In an attempt to provide tubes more suited to this type of service, those described in this paper were developed.

Tube Requirements

The function of the high-vacuum modulator tube essentially is to act as a switch to turn the pulse on and off at the transmitter in response to a control signal. The best device for this purpose will be the one which requires the least signal power for control and which allows the transfer of power with the least loss, from the transmitter power source to the oscillator.

If the oscillator must be supplied with a pulse of voltage E_p and current I_p,* or power E_pI_p, then the voltage which must be supplied by the transmitter power supply will be $E_b = E_p + e_p$, Fig. 1, if e_p represents the voltage

* It is assumed here that the pulse is rectangular in shape. This is usually the desired shape and is fairly well approximated in most cases.

drop in the modulator tubes necessary to allow current I_p to pass. The plate efficiency of the modulator is then simply $\frac{E_p}{E_b}$ and the power dissipated in the modulator tube plate is $I_p e_p$ during a pulse. The average power dissipated in the plate is then $I_p e_p$ multiplied by pulse length and by pulse frequency. The heat storage capability of the plate is ordinarily great enough that the average power is all that needs consideration.

The conditions imposed on the modulator tube are somewhat analogous to those of a class C amplifier at low frequency. The main difference is that the angle of operation is very small, and there is usually no appreciable backswing of plate voltage since the load is essentially a resistance. Typical

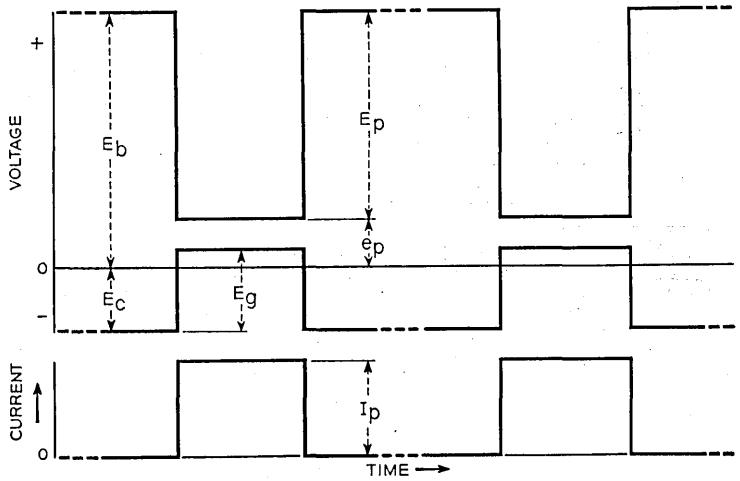

Fig. 1—Current and voltage relations in a pulse modulator tube.

modulator circuits are shown in Fig. 2. It is sometimes found desirable to employ a shunt inductance across the oscillator in the interest of a sharp cutoff of the pulse on the oscillator, particularly where capacitances to ground of various circuit components are appreciable. This results in an additional current demand on the modulator tube since the current through the inductance must also be supplied. The oscillator is often coupled to the modulator circuit by means of a transformer in order that desirable impedances are realized in each circuit.

Design Considerations

It was apparent on first consideration of the high-vacuum modulator problem that use of oxide coated cathodes would be of enormous advantage

in keeping power requirements down. Heretofore the use of oxide cathodes in high voltage power tubes had been found very difficult, particularly where filamentary cathodes were employed. Any spark or momentary discharge in operation usually resulted in the burning out of the relatively fragile filaments. This result was caused mainly by the fact that a considerable amount of energy was of necessity available from the power supply equipment. However, in pulse service it is possible to limit the amount of energy available so that a momentary tube breakdown will not result in damage to a reasonably rugged equipotential cathode. Also, in the interest

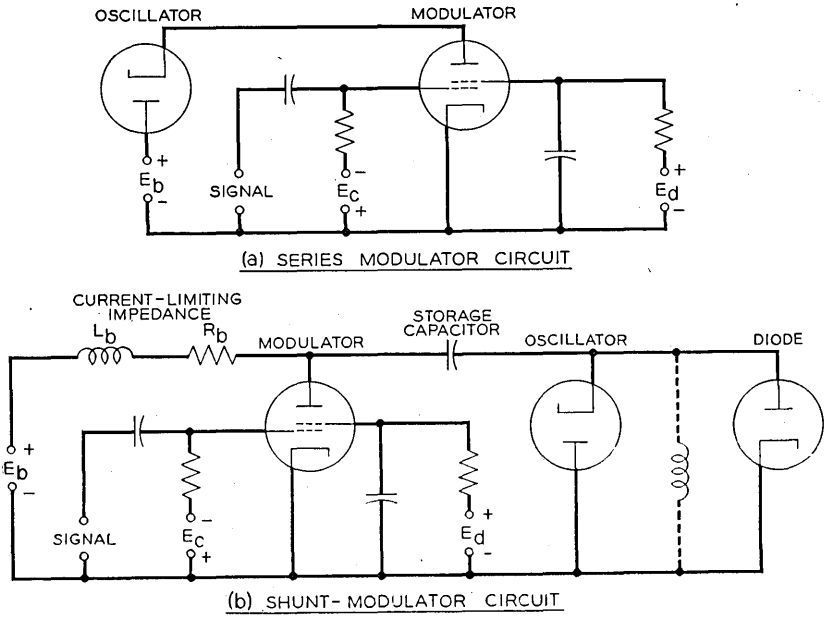

Fig. 2—Typical pulse modulator circuits.

of conserving control power it is desirable to build high perveance tubes which require very close control-grid to cathode spacings. This is much more easily accomplished with rigid cathode structures rather than filamentary cathodes, especially for service conditions under which extreme shock and vibration may be encountered.

Conservation of drive power requires that the modulator tube have high power-gain. This is most easily provided in the tetrode which provides a high over-all amplification factor with reasonable drive characteristics. Lining up the control-grid and screen-grid wires is of course advantageous in the interest of minimizing screen dissipation and getting the largest possible portion of the cathode current to the plate. The control-grid to

plate capacitance is of little importance as long as it does not store much energy, there being little chance for oscillation in such a circuit. While it is desirable to operate with as low a minimum plate voltage as possible, it is of little additional advantage to bring the plate voltage below the screen voltage if the screen voltage is about 1000 volts and the supply voltage 15 kv. It was therefore thought permissible to increase plate to screen spacing beyond the optimum for best characteristics in the interest of high voltage and screen dissipation ratings.

The insulation in the tube between plate and other electrodes must be capable of withstanding the full supply voltage plus a comfortable margin. This dictates that if internal insulators are used they must have long path and that the bulb must have sufficient length to prevent flash-over externally.

The 701A Vacuum Tube

At the time of this development a tube was very urgently needed for a Navy radar application.[3] Since speed was of prime importance it was decided to take parts of a standard oxide-cathode beam-power tetrode, Western Electric 350A, and mount them in a structure capable of withstanding the required voltage; 12 kv in this case. Accordingly a cruciform structure was designed in which four sets of 350A electrodes were mounted on ceramic members attached to a molded glass dish-stem as shown in Figure 3. The four cathodes have a total coated area of approximately 14 square centimeters. A molybdenum plate of cruciform section mounted from a lead-in at the top of the bulb was used. This construction eliminated internal insulators between plate and grids other than the bulb. The control-grid of the 350A is normally gold plated to inhibit primary emission. This feature was retained in the 701A and the screen-grid also gold plated. The plate to screen-grid spacing was increased over that normally used in the 350A in order to allow somewhat better cooling of the grids and to allow greater clearance for high voltage reasons. This made the characteristics depart from good "beam tube" performance but at the high voltage condition of operation this was of little consequence. Characteristic curves of the 701A indicating performance under both high voltage and low voltage conditions are shown in Fig. 4. Since no experience was available at the time of this development to indicate what currents could safely be drawn from the cathodes under pulse conditions, the matter of rating these tubes was mainly guesswork since time was not available to await the outcome of life tests under various conditions. The ratings put on the 701A are as shown in Table I.

For the immediate application in hand, which required 12 ampere pulses at about 10 kv, it was decided to specify two 701A tubes operating in paral-

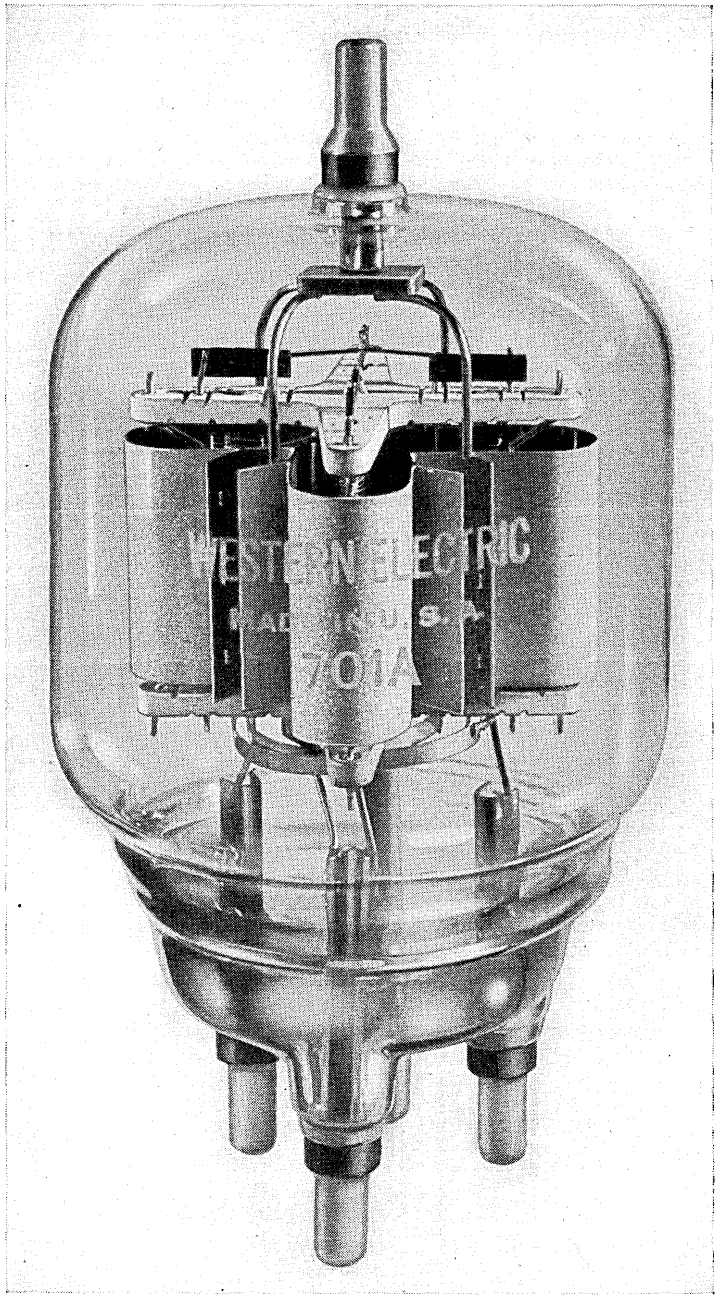

Fig. 3—The 701A vacuum tube.

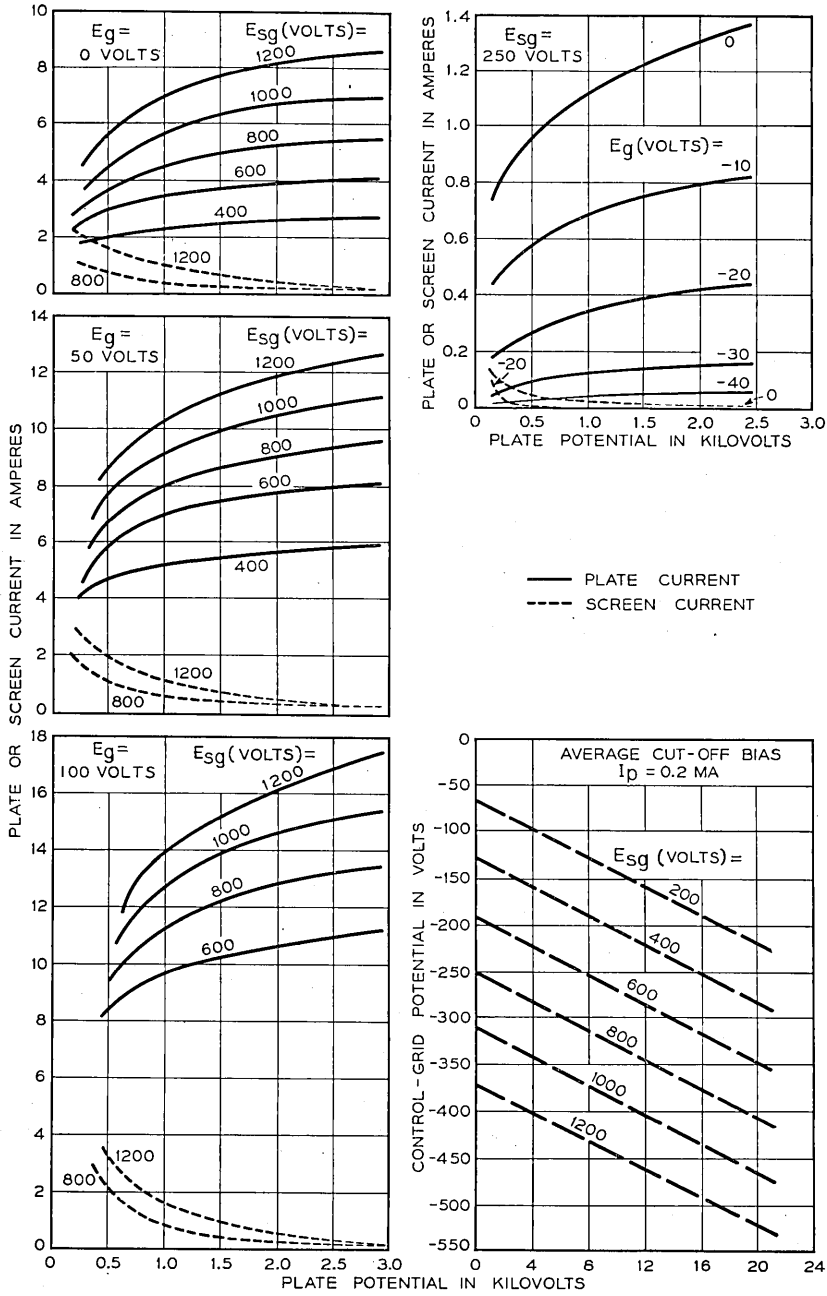

Fig. 4—Characteristics of the 701A vacuum tube.

lel. The pulse in this case was trapezoidal having a base width of about 4μ seconds and a top width of about 1.75 μ seconds; repetition rate was 1600 per second. When the tubes were operated under these conditions there was customarily some sparking within the tube in the first few minutes and then it apparently "aged in," and operated satisfactorily. At the rated heater voltage, the cathodes operated at about 800°C (brightness). This temperature would normally provide a cathode life of more than 1000 hours. Life tests in the laboratory indicated satisfactory performance for about 2000 hours. Reports from the Navy were difficult to obtain but those which were obtained indicated similar results. End of life was caused by both loss of cathode emission and by primary grid emission. Mechanically the tube proved to be reasonably rugged for normal service. However, shocks sustained in shipment of tubes caused mechanical misalignment in

TABLE I
TABLE OF RATINGS OF OXIDE-CATHODE PULSE MODULATOR TUBES

Tube	Heater Voltage	Heater Current	Peak Plate Voltage	Peak Screen Voltage	Peak Plate Current	Plate Dissipation	Screen Dissipation	Max. Duty Cycle for Peak Plate Current	Capacitances		
									C_{in}	C_{out}	C_{gp}
	Volts	*Amperes*	*KV*	*KV*	*Amperes*	*Watts*	*Watts*		*mmf*		
701A	8	7.5	12.5	1.2	10	100	15	0.005	56	11.5	3.2
715A	27	2.15	14	1.2	10	60	8	0.002	35	7	1.2
715B	26	2.10	15	1.25	15	60	8	0.001	35	7	1.2
5D21	26	2.10	20	1.25	15	60	8	0.001	35	7	1.2
426XQ	8	7.5	25	1.5	20	150	15	0.001	46	7.5	0.6

some cases, indicating a need for a more rugged structure for use in the armed services.

THE 715A TUBE

The advent of airborne radar made the development of high power lightweight transmitters an urgent requirement. In this case long life was somewhat subordinate to lightweight and small dimensions. Ruggedness was also a requirement. The electronic properties of the 701A tube were well suited for airborne radar but the large bulk was an extreme disadvantage. Work was begun on a tube using the same cathodes as the 701A but having a simpler and more rugged mechanical structure. Out of this evolved the 715A tube. In this tube the cathodes were placed side by side and enveloped by a single control-grid, screen-grid and plate. In order to provide the necessary ruggedness and to keep the grids cool, heavier grid wires were used and they were wound on very heavy supports of high heat-

conductivity material. Both grids were gold plated as in the 701A. All electrodes were mounted between two specially shaped ceramic insulators which provided a relatively long path between plate and grids. This structure is shown in Fig. 5. Heat radiating fins were attached to the ends

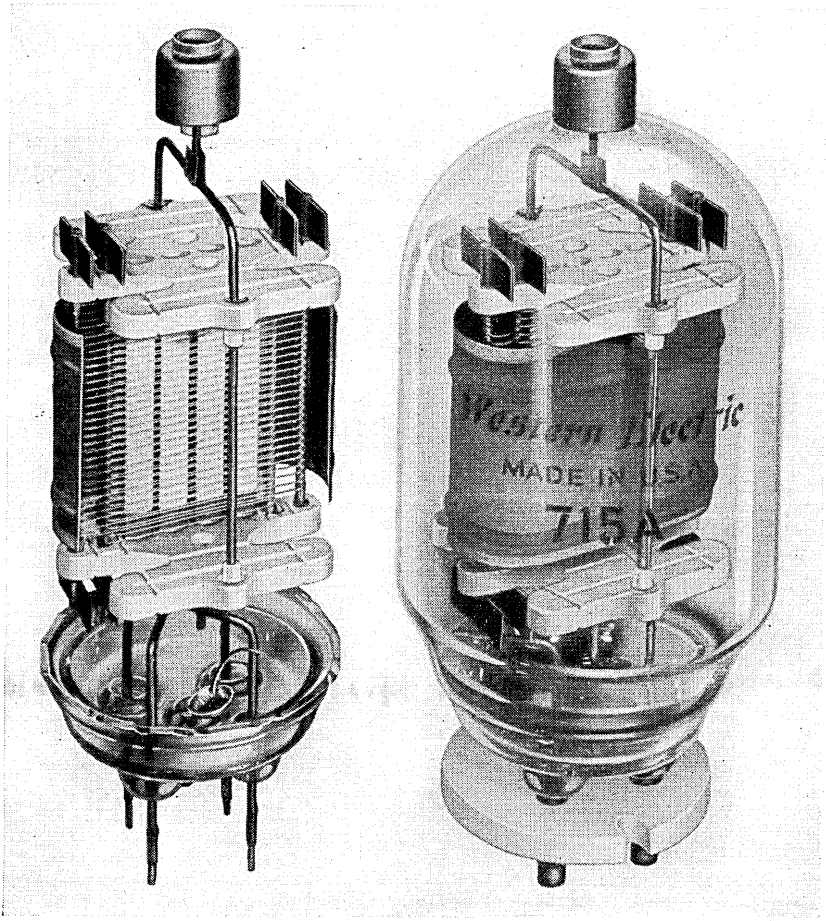

Fig. 5—The 715A vacuum tube.

of the control-grid and screen-grid supports. The plate is molybdenum with zirconium coating on its outside surface. This coating was employed to increase the thermal emissivity of the plate in the interest of a low operating temperature. It also serves to absorb some gas. The cathode, heater and grid terminals of the tube were brought out in the moulded-glass 4-Pin

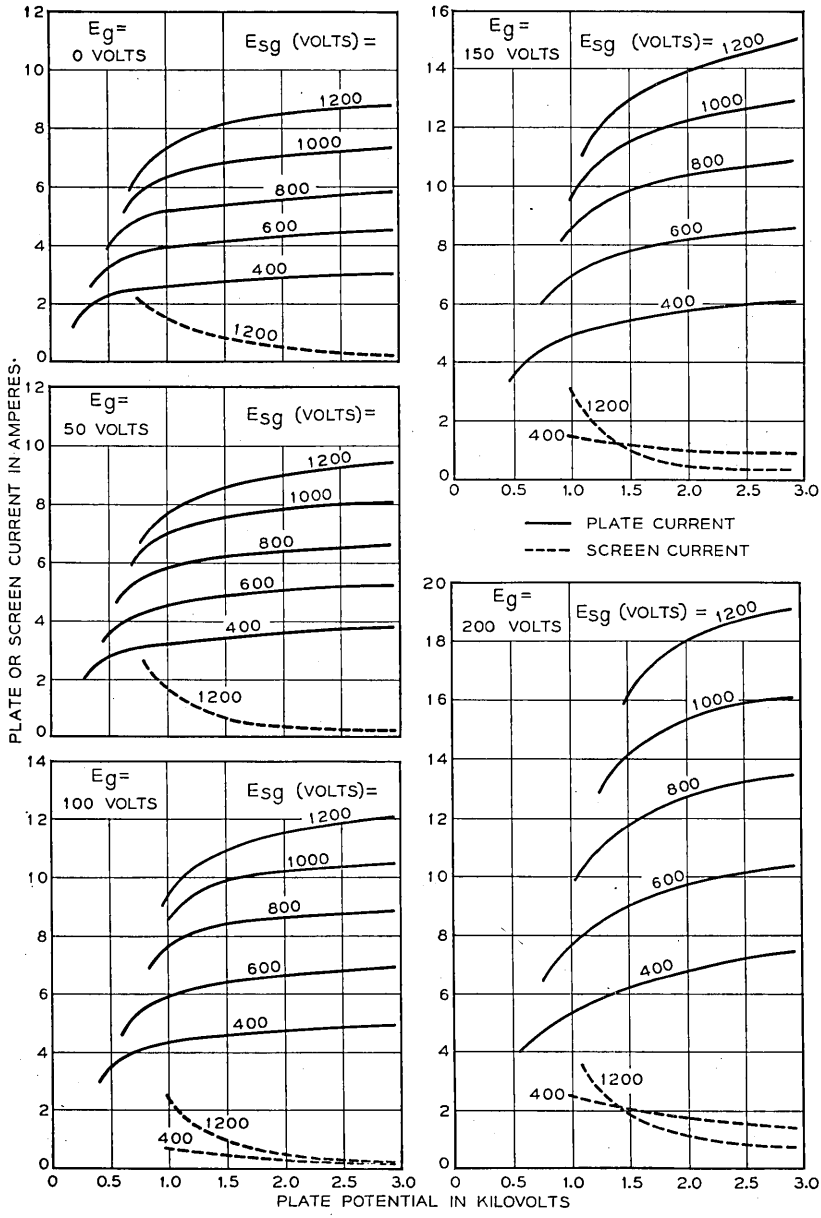

Fig. 6—Characteristics of the 715A vacuum tube.

base, and the plate terminal out the top of the bulb. This provided a very rigid structure which could stand extreme shock and vibration condi-

tions. Although this structure sacrificed something in electronic performance over the 701A it still was quite satisfactory as a pulse modulator.

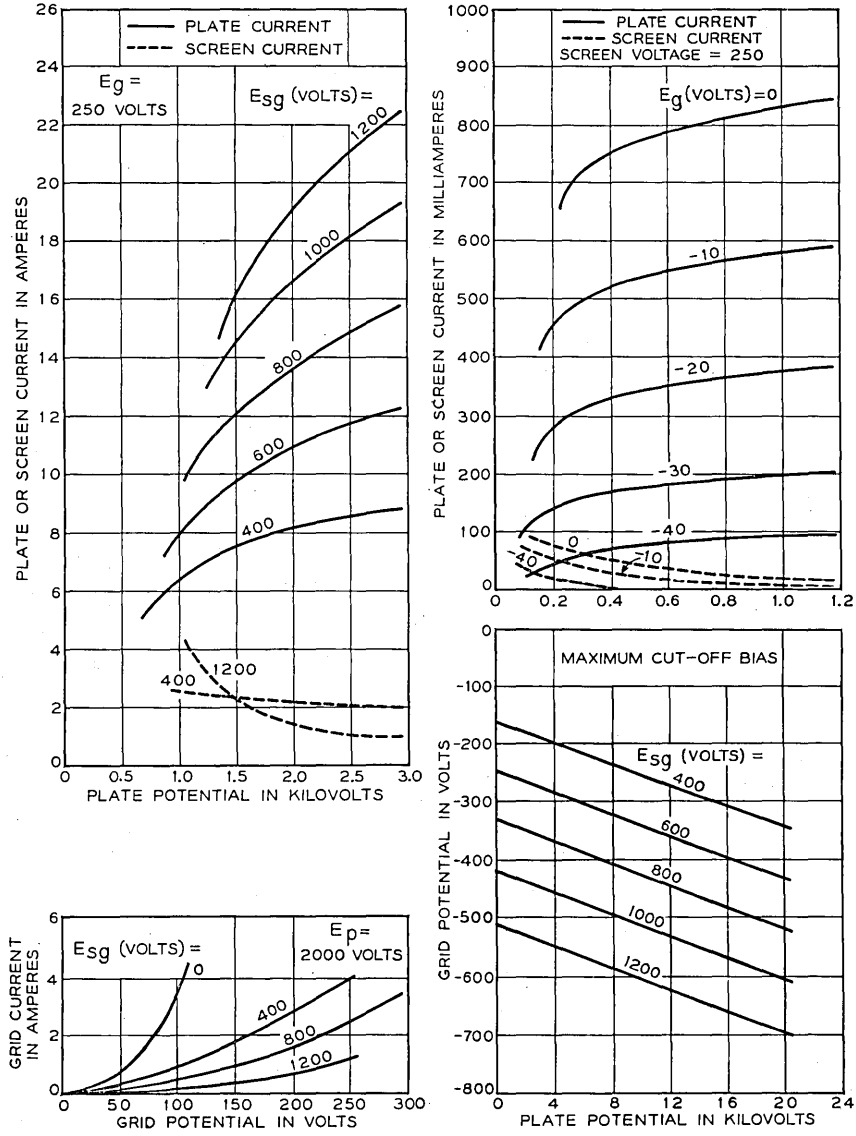

FIG. 6 (Continued)

The characteristics of the 715A tube applicable to both high voltage and low voltage operation are shown in Fig. 6. It was found that in spite of

the internal ceramic insulators, satisfactory operation could be obtained at voltages as high as 15 kv. Since the 715A was designed primarily for airborne applications it was found desirable to design the heater to operate directly from the aircraft's storage battery which was a 24 volt battery.

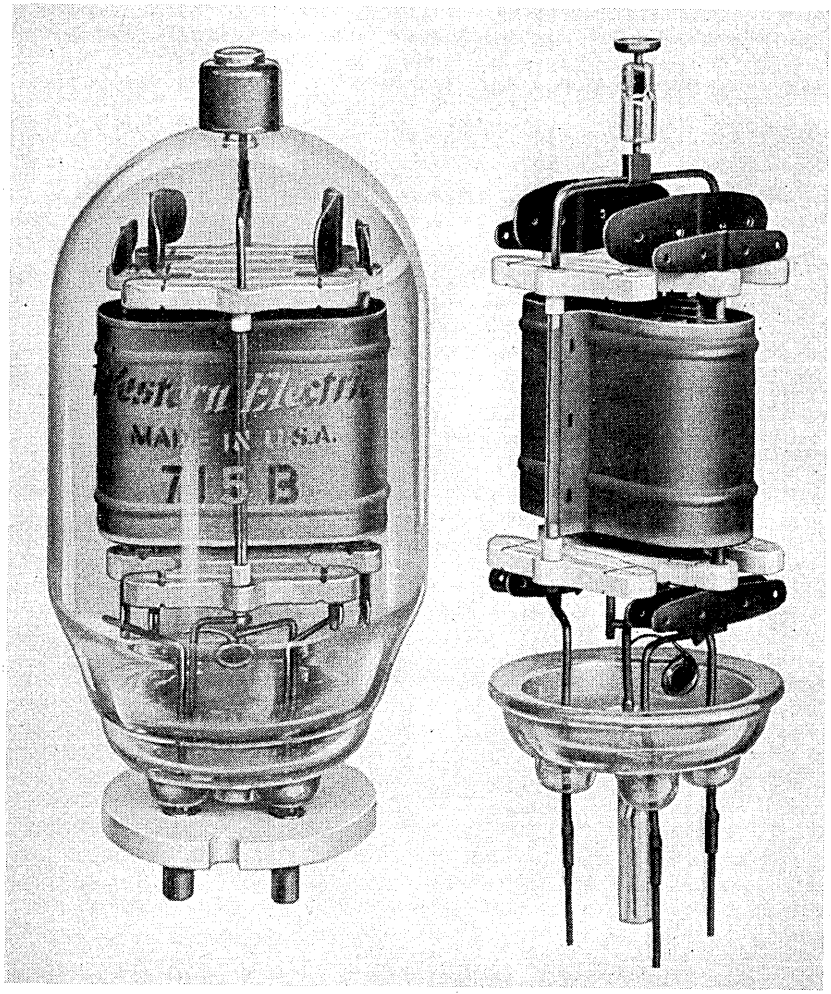

Fig. 7—The 715B vacuum tube.

It was also desirable that the equipment be operable when the charging generator was not running, at which point the voltage might be as low as 22 volts, and also when the generator was charging and the voltage as high as 28.5 volts. This required a compromise in the design of the heater which

resulted in operation of the cathode at somewhat higher than normal temperature under rated conditions. The ratings of the 715A tube are given in Table I.

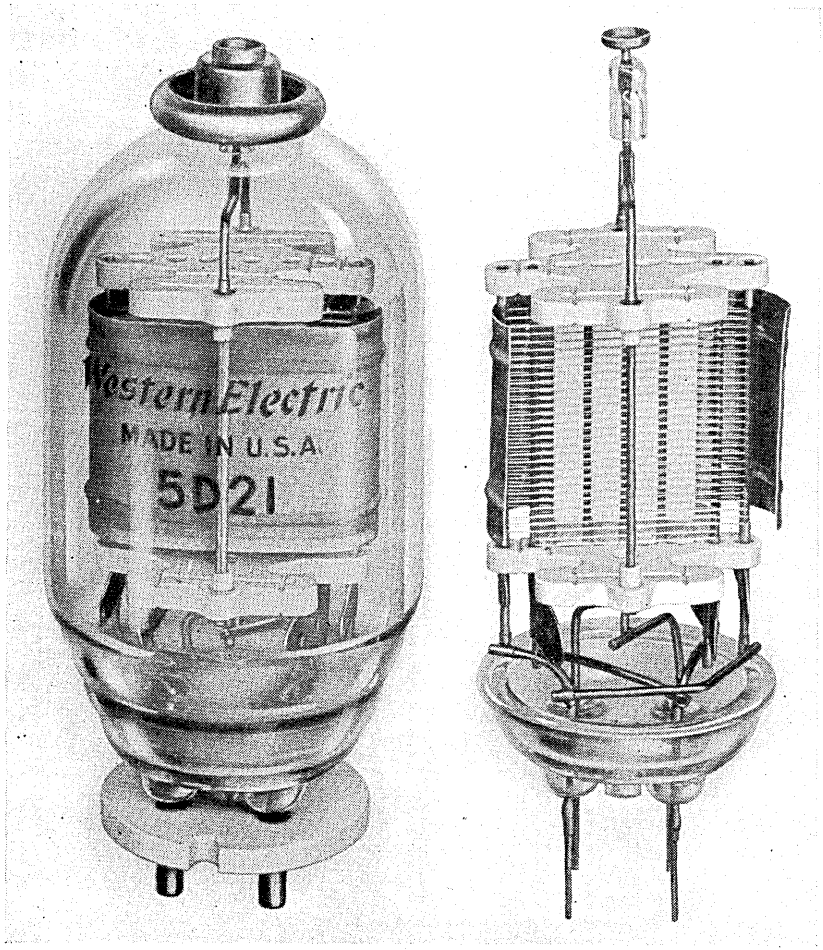

Fig. 8—The 5D21 vacuum tube.

The 715B Tube

Some applications developed which required a peak pulse current slightly greater and of longer duration than that for which the 715A was rated. Meanwhile more experience with the 715A and improvements in processing techniques indicated that a higher peak current rating was justifiable providing the grid temperatures were not increased.

The 715B tube is essentially the same structure as the 715A except that larger radiating fins are attached to the ends of the grid support wires. Figure 7 shows the structure of the 715B tube. The characteristics were identical but the ratings were changed, as indicated in Table I. The life obtained in laboratory life tests under rated conditions averaged between 500 and 1000 hours. Failure was usually caused by grid emission or loss of cathode emission.

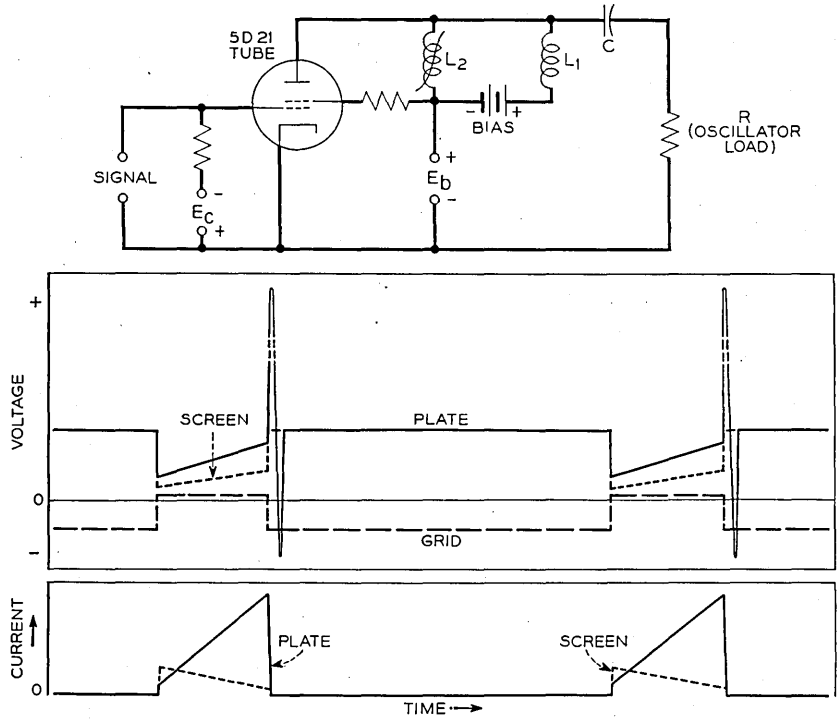

Fig. 9—Non-linear coil modulator circuit with illustration of the current and voltage relations in the 5D21 vacuum tube.

The 5D21 Tube

In response to the demand for further improvement of this structure in its ability to withstand higher voltage, the 5D21 tube was developed, Fig. 8. It is of the same family as the 715A and 715B. It was found that higher voltages could be used if the grid cooling radiators were removed from the top end of the tube. The cooling of the grid was maintained by providing copper wire connections from the bottom ends of the grid support wires to the base seals. This and the use of a specially designed plate terminal cap enabled the voltage rating to be raised to 20 KV.

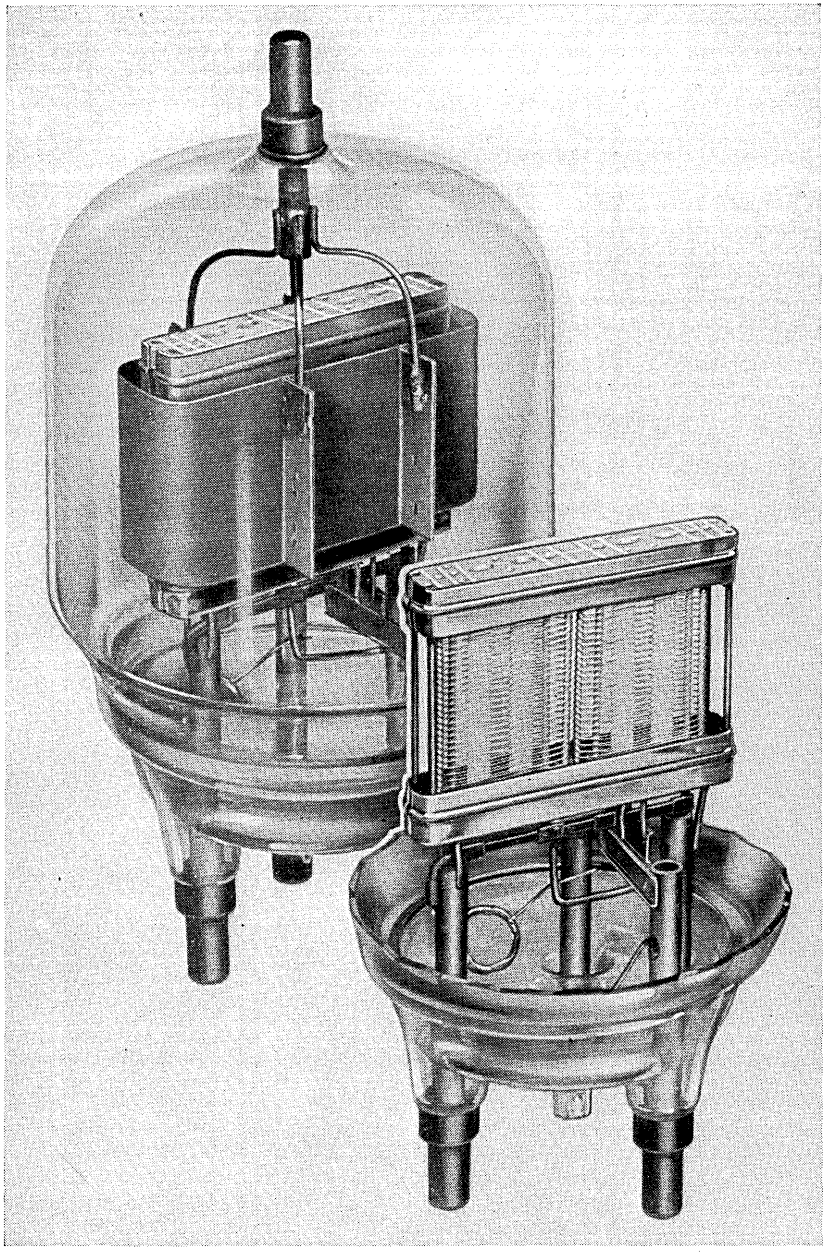

Fig. 10—The experimental 426XQ vacuum tube.

The 5D21 tube also found application as the control tube in non-linear coil type modulators.[4] Here the function of the tube was to permit passage

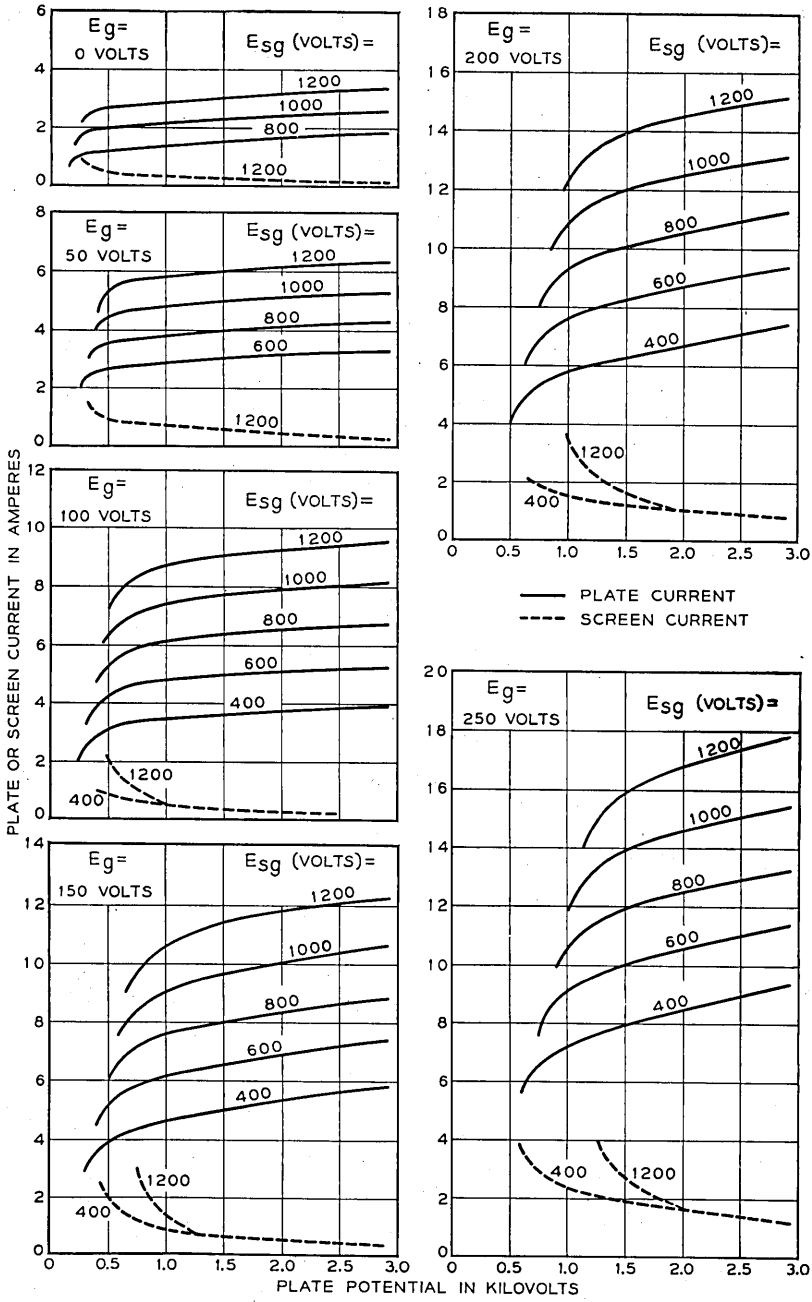

Fig. 11—Characteristics of the 426XQ vacuum tube.

of a moderately high current through an inductance and then suddenly to cut off the current and withstand the resulting voltage which built up across the circuit. A schematic of this type of circuit is shown in Fig. 9. In this circuit the tube is required to pass about two amperes peak plate current which builds up over a period of about 150 microseconds. The d-c. voltage under these conditions is about 1000 to 4000 volts and the screen voltage may be obtained from the same source through series resistance. The grid is driven only slightly positive. Screen-grid dissipation is one of the limiting factors in this type operation. Primary emission from the screen

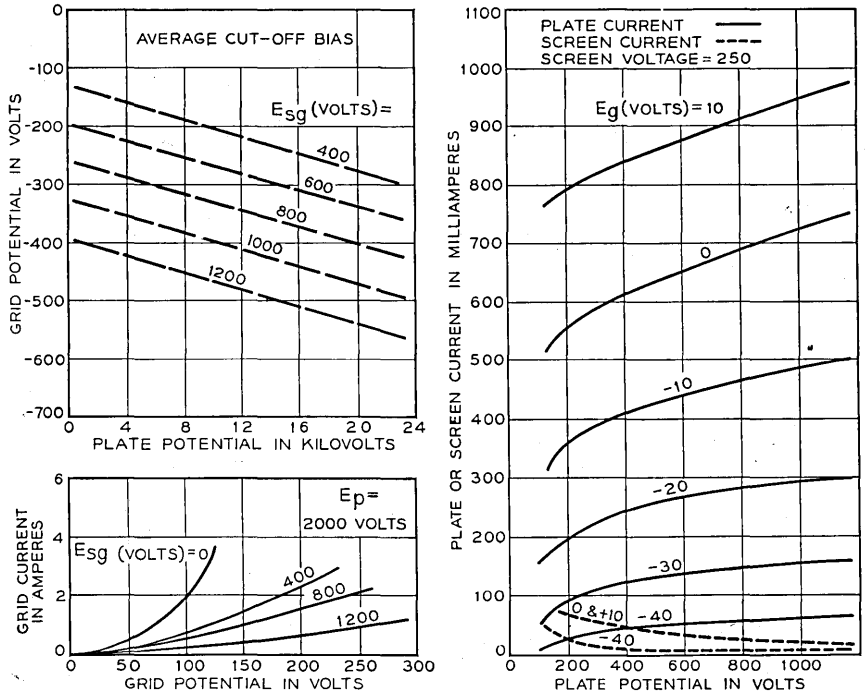

FIG. 11 (Continued)

grid, being present when the plate rises to its very high potential, tends to discharge the circuit prematurely, the energy wasted appearing as heat at the plate.

THE 426XQ TUBE

Since there was considerable demand for tubes capable of operating at voltages as high as 25 KV, a tube was developed to operate at this voltage. The limit of the 5D21–715B type structure seemed to have been reached at about 20 KV. It was also desirable to increase the current rating of the

tube since in a laboratory test equipment a pulse power of 1.5 to 2 megawatts was needed. The laboratory number 426XQ tube shown in Fig. 10 was the result. Four of these tubes in parallel were capable of providing pulses of about 1.75 megawatts. In the 426XQ tube, the bulb used on the 701A was employed and the plate supported entirely from its terminal in this bulb. The same four cathodes were used, but were spaced farther apart than in the 715-type tube. Two separate control-grids and two screen-grids were used, each pair encompassing two cathodes. This allowed a reduction of dissipation per grid compared to the 715-type, otherwise similar techniques were employed. The characteristics are shown in Fig. 11.

The tentative ratings applied to the 426XQ are given in Table I. The allowable peak plate current was increased for this tube because the technique of processing had improved so that a higher level of cathode activity was consistently realized. Also the greater spacing between cathodes and use of two sets of grids resulted in better grid cooling. The tube was not used in any radar equipment, because by the time it was available the trend in radar equipment was toward small, compact apparatus in which spark gap and transmission line modulators[5] found considerable application. The 426XQ proved very satisfactory in laboratory test equipment. One set of these tubes operated for somewhat more than 2000 hours.

The Chief Problems

The difficulties experienced with this series of oxide-cathode pulse modulator tubes can be divided into three general classifications, namely: sparking, cathode emission, and grid emission.

The sparking in these tubes can roughly be divided into two types, which may be called inter-electrode sparking and cathode sparking. Inter-electrode sparking is a discharge between two electrodes of the tube caused by the momentary breakdown of the insulation between them or by a gas discharge. If the breakdown of insulation is caused by light deposited films, the resultant discharge usually causes removal of the film and cures the trouble automatically, provided no other damage is done to the tube. Gas discharges from isolated pockets may be initiated by the high fields or by bombardment by stray electrons. If these pockets are not numerous they are usually dissipated after a few minutes of tube operation such that further sparking is very intermittent and probably not of sufficient intensity to interfere with operation. The gas so released is ordinarily taken up by the getter in the tube so that operation is not subsequently impaired.

Cathode sparking may be caused by positive ion bombardment of the cathode or by poor adherence of cathode material when subject to electro-

static fields. This type of sparking usually does not clear up and when it becomes serious the tube must be replaced.[6] It can be aggravated by sparking in the oscillator part of the radar system. There is some evidence to indicate that very high rates of rise of the pulse current drawn from the cathode may tend to produce cathode sparking. At rates of rise in excess of about 50 amperes per microsecond per square centimeter of cathode area a tendency for increased sparking has been noticed.

Cathode emission, here as in any other tube, is governed by cathode temperature and other considerations such as quantity and kind of gas in the tube, the core material, coating material, and techniques of processing. No attempt will be made to consider these factors in this paper as they are sufficiently complex that no very clear cut dissertation can be given. Standard core materials and coatings were employed with good results. It was found that the double carbonates (Ba, Sr) were less subject to sparking than the triple carbonates (Ba, Sr, Ca). The cleanliness and previous treatment of the other parts of the tube seemed to be the major factor in determining the level of emission obtained.

Primary grid emission, or thermionic emission from the control-grid and screen-grid, was one of the most difficult problems in the development and production of these tubes. Many trials were made using different materials and coatings on the grids, but from all considerations gold was found to be the most satisfactory. The grids in all the tubes described here are gold plated or gold clad molybdenum. It is not considered that the use of molybdenum for the core material is necessary, it being used here mainly because it seemed to be the most economical material that had sufficient stiffness to maintain grid alignment. Materials that tend to alloy with gold easily are not suitable as it was found that gold alloys were not as good as pure gold on the grid surface. The limitation involved in the use of gold is that the temperature of the grid must be kept low enough that evaporation of gold is not serious. This temperature limit is probably about 700°C. If gold is evaporated, the grid soon loses its coating and primary emission builds up rapidly. Also, the cathode emission seems to be poisoned by the gold vapor.[7]

ACKNOWLEDGMENT

The author wishes particularly to acknowledge the contributions of his immediate associates, Messrs. H. L. Downing, J. W. West, and J. E. Wolfe in the development of this series of tubes. Many others also made important contributions. We are also indebted to the M.I.T. Radiation Laboratory for data from life tests which they conducted on many of these tubes.

REFERENCES

1. R. Colton, Radar in the U. S. Army, *Proc. I.R.E.*, Vol. 33, pp. 740–750, November 1945.
2. The SCR-268 Radar, Editorial, *Electronics*, Vol. 18, pp. 100–109, Sept. 1945.
3. W. C. Tinus and W. H. C. Higgins, Early Fire-Control Radar for Naval Vessels, *Bell Sys. Tech. Jour.*, Vol. 25, pp. 1–47, Jan. 1946.
4. E. Peterson, Coil Pulsers for Radar, *Bell Sys. Tech. Jour.*, Vol. 15, pp. 603–615, Oct., 1946.
5. F. S. Goucher, J. R. Haynes, W. A. Depp, and E. J. Ryder, Spark Gap Switches for Radar, *Bell Sys. Tech. Jour.*, Vol. 15, pp. 563–602, October 1946.
6. E. A. Coomes, The Pulsed Properties of Oxide Cathodes, *Jour. Applied Phys.*. Vol. 17, pp. 647–654, August 1946.
7. J. Rothstein, The Poisoning of Oxide Cathodes by Gold, (Abstract) *Phys. Rev.* Vol. 69, 1st/15th June 1946, p. 693.

Polyrod Antennas

By G. E. MUELLER and W. A. TYRRELL

The polyrod, a new form of microwave endfire antenna, is described. This consists of a properly shaped dielectric rod protruding from a metal waveguide. For applications requiring moderate gain, it possesses desirable electrical and mechanical properties. It is useful as a unit antenna in broadside arrays on account of its low crosstalk into adjacent polyrods. This paper describes work done from 1941 to 1944 at the Bell Telephone Laboratories, Holmdel, N. J. Important individual contributions are acknowledged in some of the footnotes. A report of this development has been withheld from earlier publication for reasons of military security.

1. Introduction

A UNIFORM rod (or "wire") of dielectric material without metallic boundaries is a well-known type of single conductor transmission line. In this kind of waveguide, a portion of the energy travels along in the space outside the rod. At discontinuities, including those caused by proximity to other objects, radiation takes place. For this reason, the dielectric waveguide has not become generally useful as a transmission medium, this need having been satisfied by the hollow metal pipe. The tendency toward radiation inherent in the dielectric guide is turned to advantage, however, in a new form of radio antenna. Here the objective is to encourage radiation from all parts of the dielectric rod. In progressing along the rod, therefore, power is gradually transferred from within the dielectric to the space outside. At a point where the transfer has been effectively completed, the rod can be terminated abruptly. By proper design, this radiating structure is an endfire antenna. Since it has been most often fabricated from polystyrene, it has become known as the polyrod antenna. It is especially useful for microwaves.

We must now review and examine certain features of dielectric rod transmission and of endfire antenna theory, for their bearing on polyrod design and performance.

2. Dielectric Wire Transmission[1]

A dielectric rod can be energized with an infinite variety of transmission modes. These are in general hybrid waves[2] possessing transverse and longitudinal components of both E and H. We shall here be concerned only

[1] Hondros and Debye, *Ann. der Phys.*, Vol. 32, pp. 465–476; J. R. Carson, S. P. Mead and S. A. Schelkunoff, *B.S.T.J.*, Vol. 15, pp. 310–333, 1936; G. C. Southworth, *B.S.T.J.*, Vol. 15, pp. 284–309, 1936; S. A. Schelkunoff, "Electromagnetic Waves," pp. 425–428, D. Van Nostrand, New York, 1943.

[2] Except in the case of circular symmetry. Cf. Schelkunoff, *loc. cit.*, pp. 154, 425.

with the lowest mode,[3] that which is the counterpart of the dominant wave[4] in a metal pipe. If a dielectric-filled metal guide is excited at the dominant mode, and if the metal shield is abruptly terminated, the wave energy will continue on in the unsheathed dielectric rod and will be confined almost exclusively to the lowest hybrid mode. This is, indeed, the most common way of exciting the dielectric wire.

The extent to which the power is concentrated within the dielectric is a function of the rod diameter and dielectric constant. This is shown[5] in Fig. 1. If the curves for the two different dielectric constants are replotted against the effective diameter, $\frac{D\sqrt{\epsilon}}{\lambda}$, they become more nearly

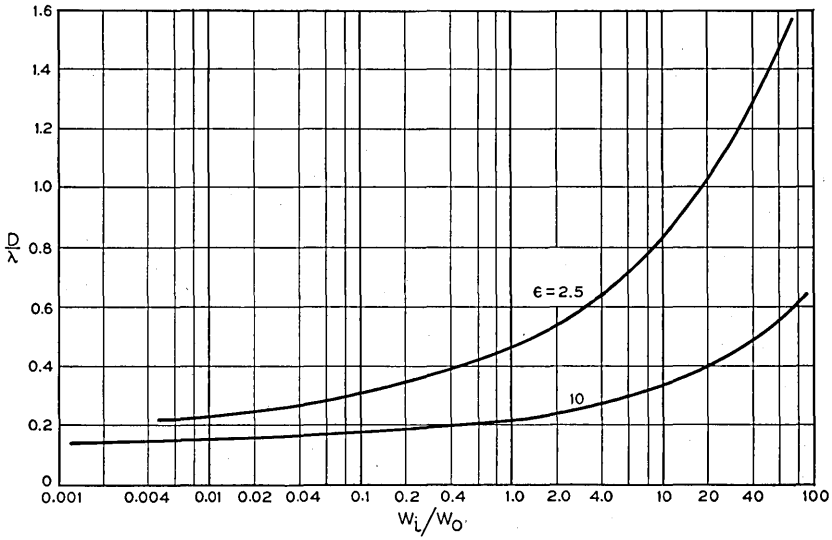

Fig. 1—Ratio of power inside W_i to power outside W_o for a cylindrical dielectric wire.

coincident. A universal curve cannot be given, however, because the field-retaining effect of a dielectric-air interface increases with increasing dielectric constant.

The phase velocity within the rod is also a function of the diameter and dielectric constant, as shown[5] by Fig. 2. When $\frac{D}{\lambda}$ is very small compared with unity, the rod exerts negligible guiding action, and the transmission is close to that in free space. For rods of large diameter, the power is con-

[3] Unlike all other modes in a dielectric wire and all modes in a conducting pipe, the lowest dielectric wire mode theoretically has its cutoff at zero frequency. Cf. Schelkunoff, *loc. cit.*, p. 428.

[4] That is, the TE_{11} mode in circular pipe or the TE_{10} mode in rectangular pipe.

[5] Figs. 1 and 2 are based on calculations by Dr. Marion C. Gray.

fined almost entirely within the rod, and the phase velocity approaches that in an unbounded medium of the same dielectric constant. By choosing intermediate values of $\frac{D}{\lambda}$, $\frac{v}{c}$ can be varied between these limits.

3. Endfire Antennas

We consider a linear array of isotropic radiators, infinite in number but so closely spaced as to occupy a finite length. We assume that the radiators are uniformly excited from a feed line, a transmission line parallel to the array phasing the various elements according to phase velocity on the line. The radiation pattern is given by[6]

$$r = \left| \frac{\sin \pi(\rho \cos \theta - \beta)}{\pi(\rho \cos \theta - \beta)} \right| \tag{1}$$

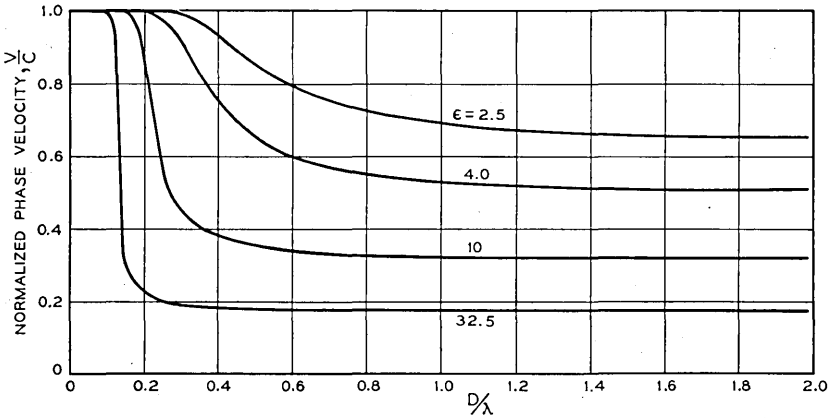

Fig. 2—Normalized phase velocity for a cylindrical dielectric wire.

where r = relative field strength
θ = angle with respect to the array axis
ρ = length of array in free space wavelengths
$2\pi\beta$ = phase shift in radians in the feed line from one end of array to the other end.

The pattern is symmetrical about the array axis.

Plotted from (1), Fig. 3 shows the pattern of a six wavelength radiator, $\rho = 6$, for selected values of β. When $\beta = \rho$ (= 6 in this case), phase velocity along the feed line is equal to free space velocity, and the resulting pattern is endfire. With $\beta = \rho + 0.5$ (= 6.5) the pattern remains endfire and the major lobe becomes sharper. For $\beta < \rho$ and $\beta > \rho + 0.5$ (as shown by $\beta = 5.0, 5.5, 7.0$) the pattern deteriorates into a forward conical beam.

[6] R. M. Foster, *B. S. T. J.*, Vol. 5, p. 307, 1926.

The gain of a uniformly excited endfire antenna[7] with $\beta = \rho$ is 4ρ. For $\beta \neq \rho$, the gain can be written

$$g = 4A\rho. \tag{2}$$

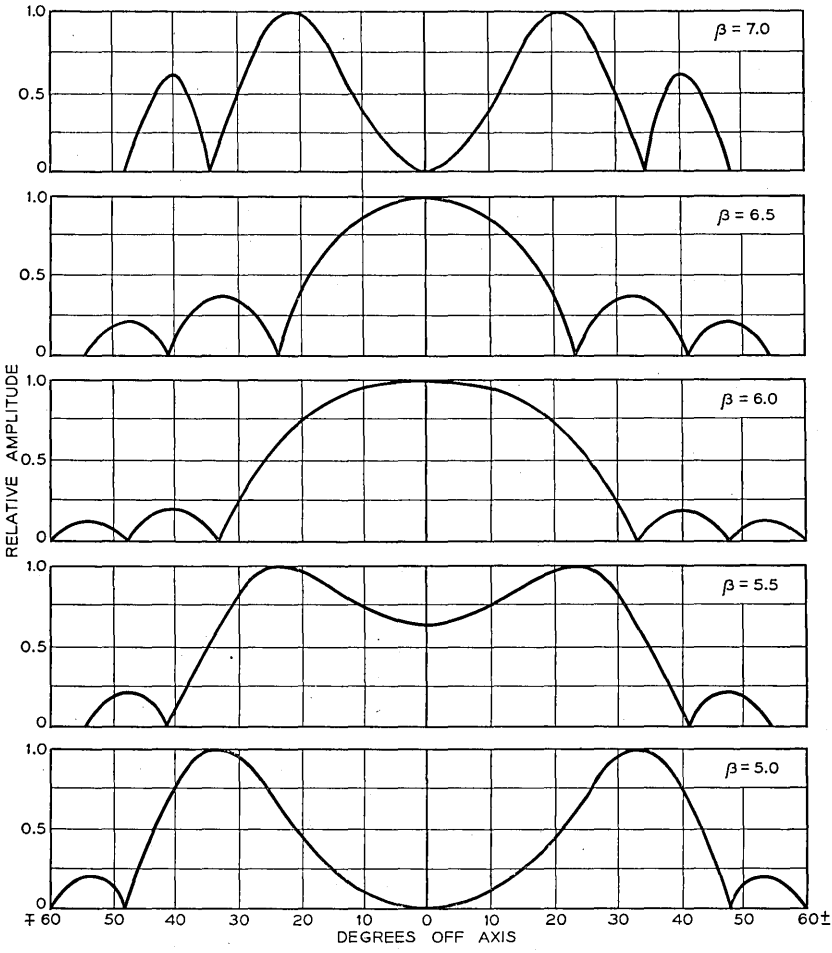

Fig. 3—Directional patterns of a six wavelength ($\rho = 6$) continuous array.

The factor A is given graphically in Fig. 4 as a function of $2\pi(\beta - \rho)$, the phase lag.[8] The highest gain occurs for a phase lag of approximately π radians relative to free space transmission, that is, for $\beta = \rho + 0.5$, in conformity with the patterns of Fig. 3. For a short radiator, A is about 2; with increasing antenna length, A approaches 1.8.

[7] Schelkunoff, *loc. cit.* p. 347.
[8] Fig. 4 and equation (5) were supplied by Dr. H. T. Friis.

The width of the major lobe is given by

$$\text{Beam Width} = \frac{B}{\sqrt{\rho}}. \tag{3}$$

The constant B depends on $\beta - \rho$ and on the manner in which beam width is defined. For width in degrees between half power points, and with $\beta - \rho = 0.5$ for maximum gain, B is computed from (1) to be about 60.

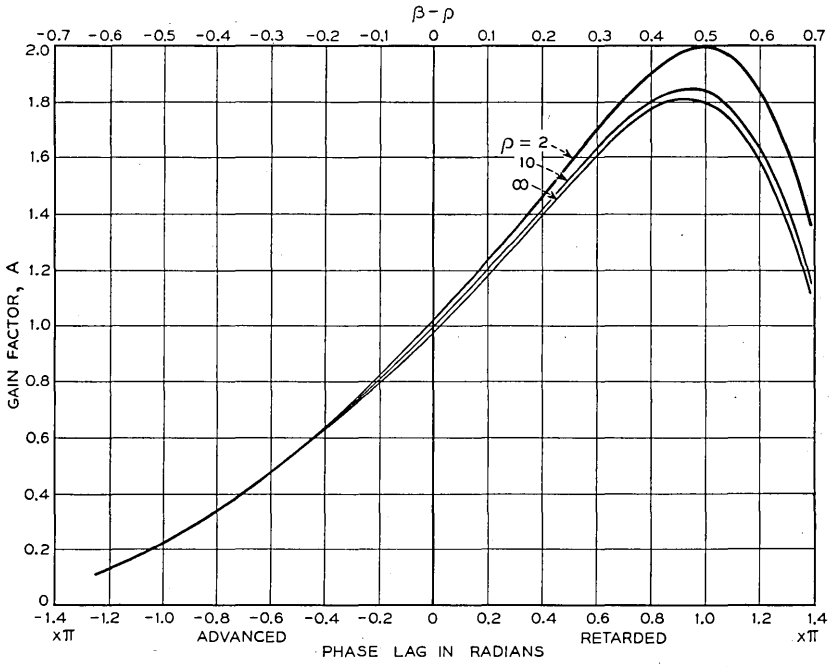

Fig. 4—Gain factor A as a function of phase lag in endfire arrays.

If a sinusoidal variation in excitation voltage along the radiator is superposed on the constant amplitude assumed for (1), we get

$$r = \left| a \frac{\sin \pi(\rho \cos \theta - \beta)}{\pi(\rho \cos \theta - \beta)} + (1 - a) \frac{\cos \pi(\rho \cos \theta - \beta)}{1 - 4(\rho \cos \theta - \beta)^2} \right| \tag{4}$$

where a is defined in Fig. 5. This figure gives patterns of a six wavelength radiator according to (4) for various values of a. Here β is fixed at 6.5 for maximum gain. Tapering symmetrically away from the center decreases the minor lobes. The gain is also decreased, but to a lesser extent.

Exponential tapering comes about from heat losses and radiation losses in the feed line. With attenuation α per wavelength, (1) becomes[8]

$$r = \sqrt{\frac{2\cosh \alpha\rho - 2\cos 2\pi(\cos\theta - \beta)}{\alpha^2\rho^2 + 4\pi^2(\rho\cos\theta - \beta)^2}} \tag{5}$$

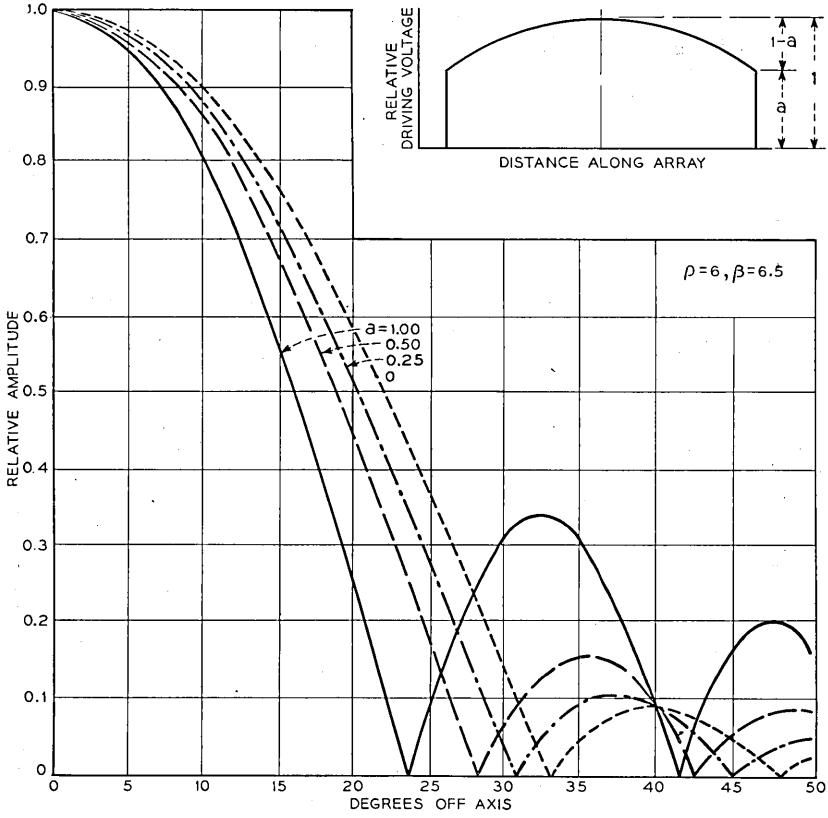

Fig. 5—Effect of sinusoidal tapering of power upon directional characteristic of a six wavelength continuous array.

Feed line attenuation increases slightly the minor lobe amplitudes and fills in the nulls. Exponential tapering caused by radiation can be reduced or eliminated if the coupling of the radiating elements to the feed line is gradually increased along the line.

4. The Polyrod Antenna

It has been found experimentally that a suitably proportioned dielectric rod can act as an efficient endfire radiator. A complete understanding of

[8] Loc. cit.

its operation involves the solution of Maxwell's equations subject to the boundary conditions appropriate to the configuration. An analysis of this sort is not available because of its mathematical complexity. However, a satisfactory explanation of polyrod operation, especially for engineering purposes, can be obtained by establishing analogies with array theory, coupled with existing knowledge about transmission in uniform dielectric wires. In this treatment by analogy, we remain essentially ignorant of the local fields in the vicinity of the dielectric, the role played by the discontinuities at both ends of the antenna, and other detailed features. We do have, however, a working theory which predicts closely the features of the radiation as observed at a distance. Under these circumstances, insistence upon a rigorous field solution has not so far appeared necessary.

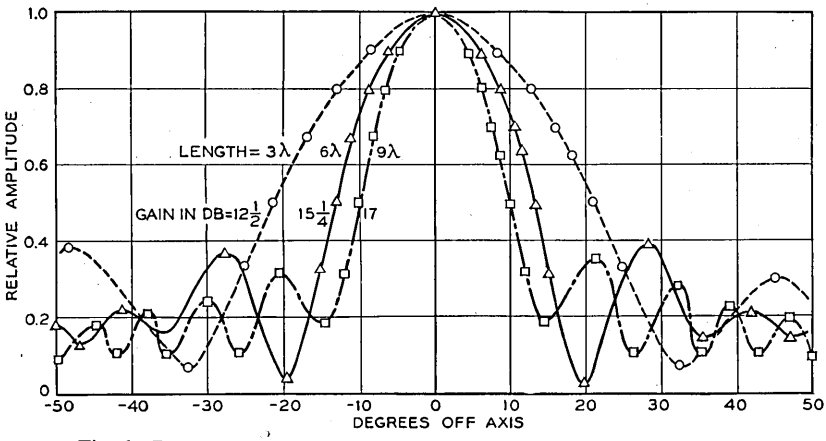

Fig. 6—Data on polyrods of uniform rectangular cross-section $\frac{1}{3}\lambda$ by $\frac{1}{2}\lambda$.

Experimental data have been obtained at frequencies in the vicinity of 3000 megacycles except for Fig. 9, representing work at 9000 megacycles. For the sake of generality, these results are presented in dimensions of λ, the free space wavelength. In all cases, polyrods have been energized from a dielectric filled metal guide whose conducting sheath is abruptly terminated, the dielectric continuing on as the radiator.

The earliest form of polyrod[9] was a polystyrene rod of uniform rectangular cross-section, about $\frac{1}{3}\lambda$ by $\frac{1}{2}\lambda$. Figure 6 shows the gains and directional patterns measured for such rods in three different lengths. In a plane normal to the axis, the radiation is approximately isotropic. The observed gains are proportional to length. They are greater than 4ρ by a factor of

[9] The earliest work on polyrods was done in 1941 by Dr. G. C. Southworth. Cf. his *U. S. Patent* 2,206,923 issued in 1940.

about 1.4. Phase velocity in these rods was not measured and is not available from theory. Referring to Fig. 4, however, we must assume at least 0.4π radians of phase retardation to explain the increased gain. When the pattern for the 6λ rod is compared with the sharpest pattern ($\beta = 6.5$) in Fig. 3, the observed characteristic is sharper than expected even with a phase retardation of π. The amplitudes of minor lobes are in good agreement. Attenuation, as revealed by the amplitudes at minima in the patterns, is apparently appreciable but not serious.

The principal defect of the uniform polyrod is the strong minor lobes. This is remedied by tapering the amplitude of radiation symmetrically about the midpoint, as suggested in Fig. 5. To obtain such tapering let us start at the waveguide end with a relatively thick rod. From Fig. 1, this tends to retain a larger fraction of the power and should therefore not radiate so strongly. Let us decrease the cross-section gradually in progressing along the rod, thus increasing the power radiated. Upon reaching a point near the center, we find the power in the rod already considerably diminished by the radiation which has already taken place. Beyond this point, gradually decreasing radiation is automatically secured with a uniform cross-section as a result of previous radiation.

This line of reasoning, calling for a polyrod tapered down in cross-section only in the first half of its length, is verified experimentally. Since detailed field analysis is not available for the polyrod, the most favorable proportions have been found empirically. Three examples will be described.

Figure 7 shows a 6λ rectangular polyrod linearly tapered for a little more than half its length from a base $\frac{1}{2}\lambda$ square to a rectangular section $\frac{1}{4}\lambda$ by $\frac{1}{2}\lambda$. the remainder being uniform. The tapering is confined to the magnetic plane. Measured phase velocity and directional pattern are included in Fig. 7. By reference to Fig. 5, the observed minor lobe amplitudes correspond to a value of a somewhat less than 0.5. The gain, considerably improved over the uniform rod, implies from (2) a value of 1.86 for A in remarkable agreement with Fig. 4.

Figure 8 shows data on a 6λ cylindrical polyrod linearly tapered for about half its length from a diameter of 0.5λ to 0.3λ with the remainder uniform. The pattern is very similar to that of the preceding example; the gain is slightly reduced, and $A = 1.66$. From Fig. 1, $\epsilon = 2.5$, about half the power is internal for $\frac{D}{\lambda} = 0.5$, while less than one-tenth is internal for 0.3. Agreement between Figs. 2 and 8 for phase velocity is fairly good.

Figure 9 gives information[10] about an 8.65λ radiator which resembles the

[10] Supplied by Mr. C. B. H. Feldman.

conical-cylindrical design of Fig. 8, but which is longer and is tapered for slightly less than half its length. The minor lobes (solid curve) are all lower than 0.125, a marked improvement over Fig. 8. From the measured gain, A is 1.82.

Regardless of whether the cross-section is square, rectangular, or round, radiation is nearly isotropic about the axis of the polyrod. For the patterns

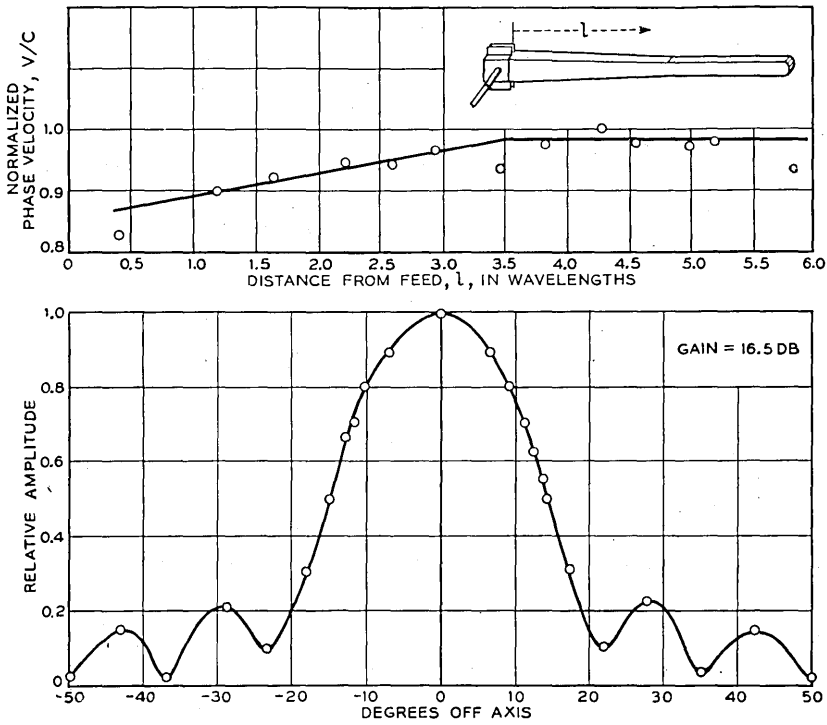

Fig. 7—Data on a 6λ tapered rectangular polyrod.

in Fig. 6–9, beam widths in degrees between half-power points correspond to values of B in (3) between about 50 and 60.

The characteristics of polyrods can thus be correlated with array theory for isotropic radiators continuously distributed along an axis. There are, to be sure, minor discrepancies which might become more serious in a different range of polyrod proportions. For the lengths and cross-sections tested, however, equations (1) to (5) describe polyrod performance very satisfactorily for engineering purposes.

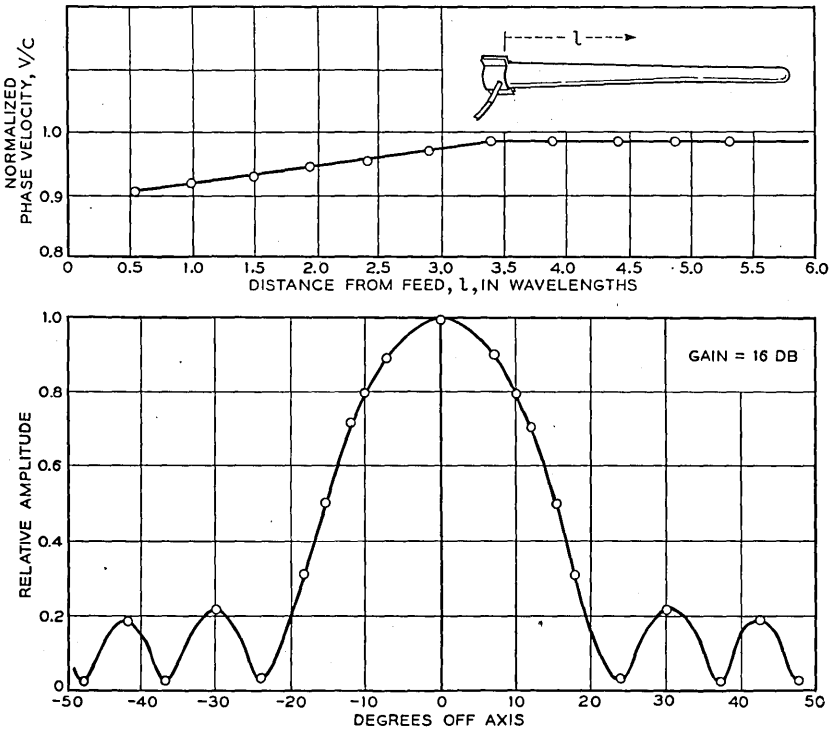

Fig. 8—Data on a 6λ tapered cylindrical polyrod.

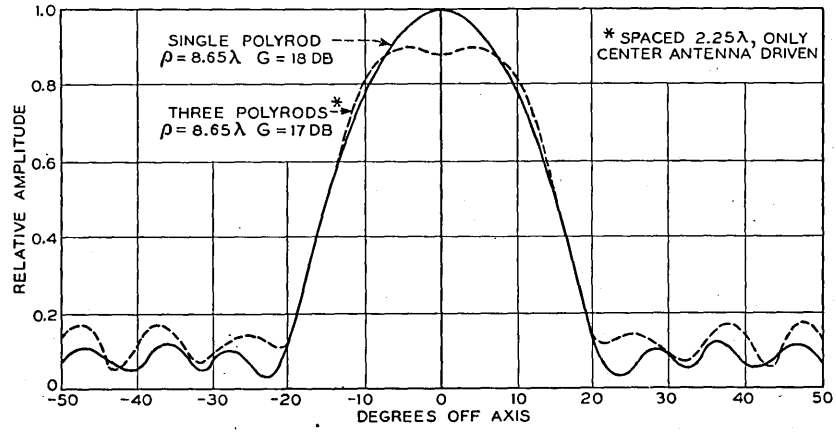

Fig. 9—Data on an 8.65λ tapered cylindrical polyrod, including effect of adjacent similar polyrods.

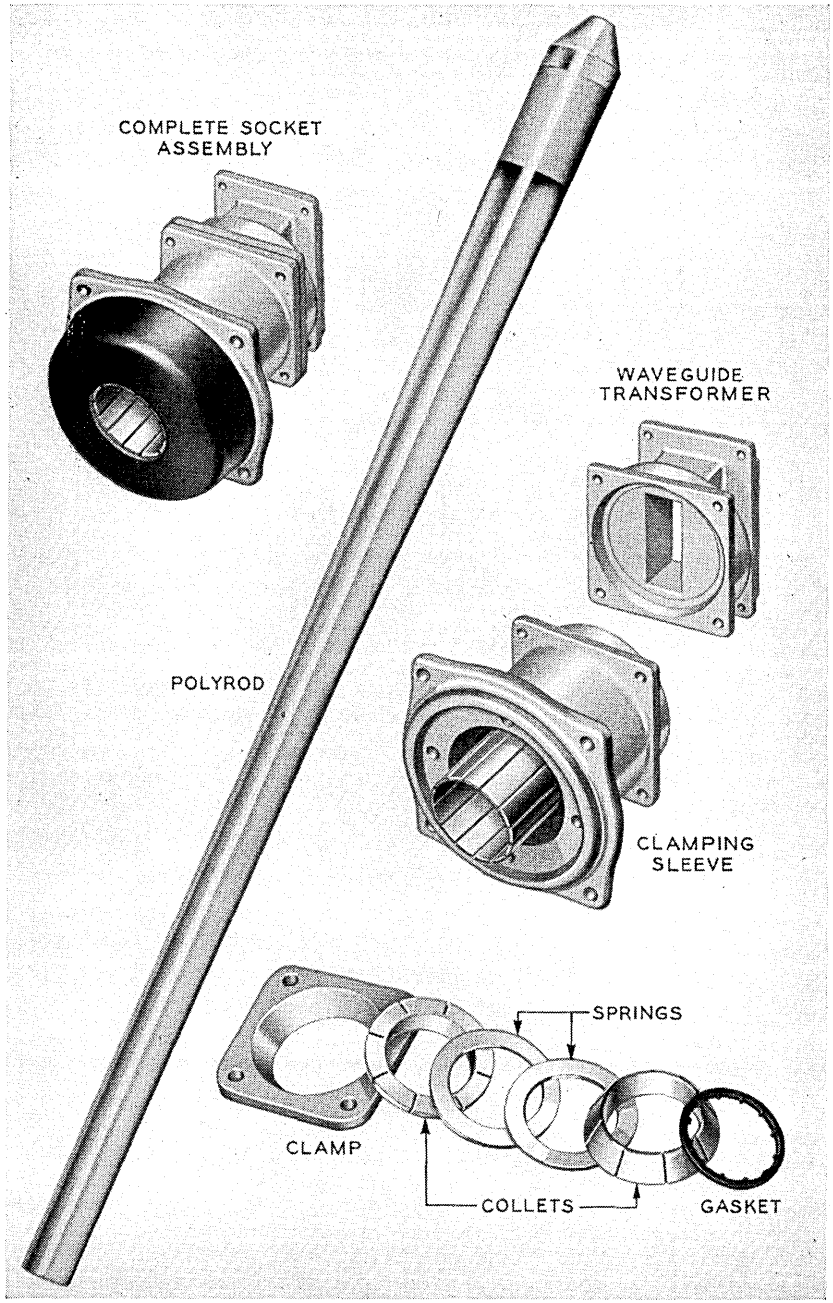

Fig. 10—Polyrod and waveguide feed details.

5. Construction and Operational Details

Figure 10 shows a production model of a polyrod for 3000 megacycles, with means for matching it to a rectangular waveguide.[11] A two-iris transformer is used with a resulting width of 4% between the 1 *db* standing wave points. The clamping illustrated is designed to maintain a firm grip on the rod despite tendencies of the polystyrene to cold flow.

Another type of coupling is indicated in Fig. 11. Here the polyrod is still fed from a waveguide but this is in turn transformed to a coaxial line. The composite can thus be regarded as a coaxial to polyrod coupling. The coaxial line taps at point *b* onto the short-circuited antenna *a-b-c* at a point

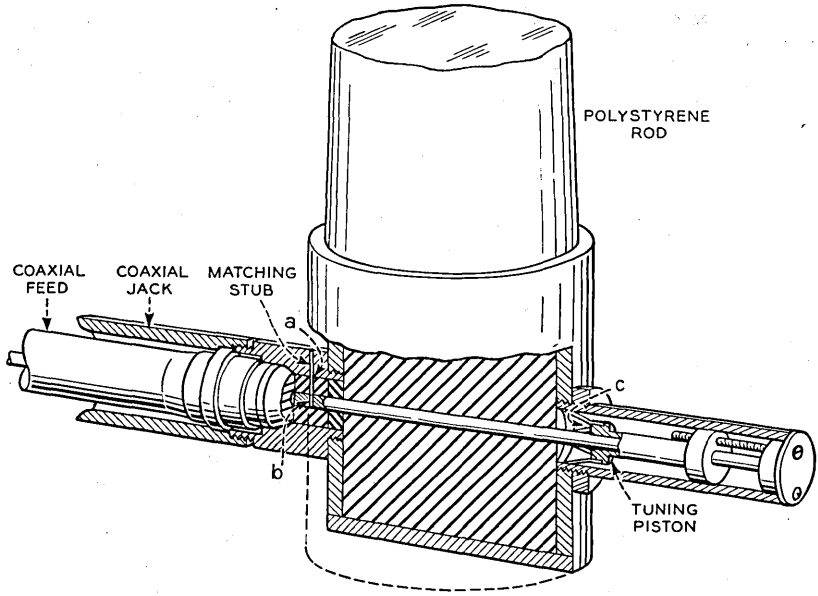

Fig. 11—Coaxial feed for polyrod.

chosen to match the characteristic impedance of the coaxial line. The back end of the waveguide is short circuited by a metal cap a quarter wavelength behind the transverse wire antenna. A movable coaxial plunger provides tuning. This arrangement has a bandwidth of 1% to the 1 *db* standing wave points.

The frequency response of a polyrod is inherently broad. The directive pattern varies slowly with both phase velocity and amplitude distribution along the axis. As shown in Figs. 1 and 2, these quantities are slowly varying functions of λ over a considerable range of polyrod proportions. At

[11] Developed by Mr. D. H. Ring.

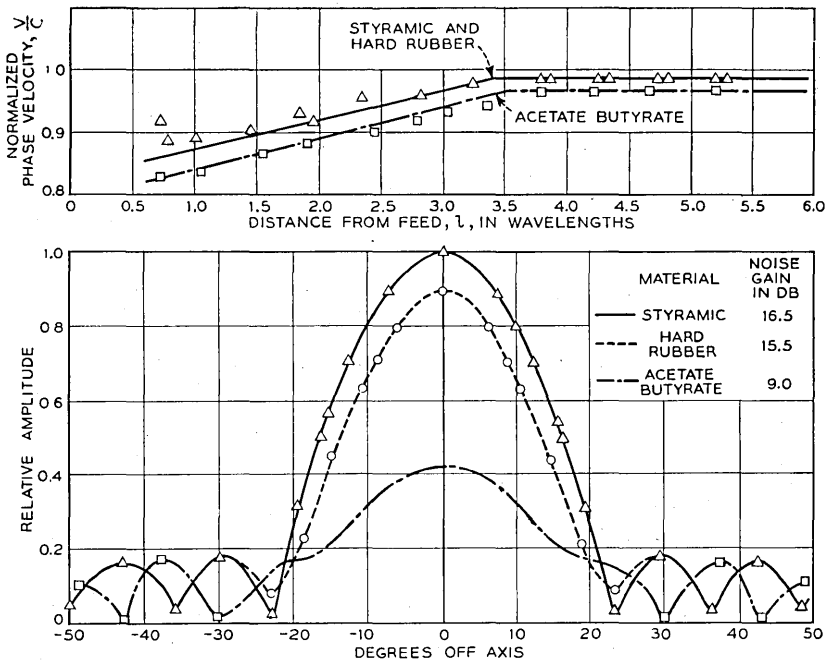

Fig. 12—Effect of dielectric loss on polyrod performance.

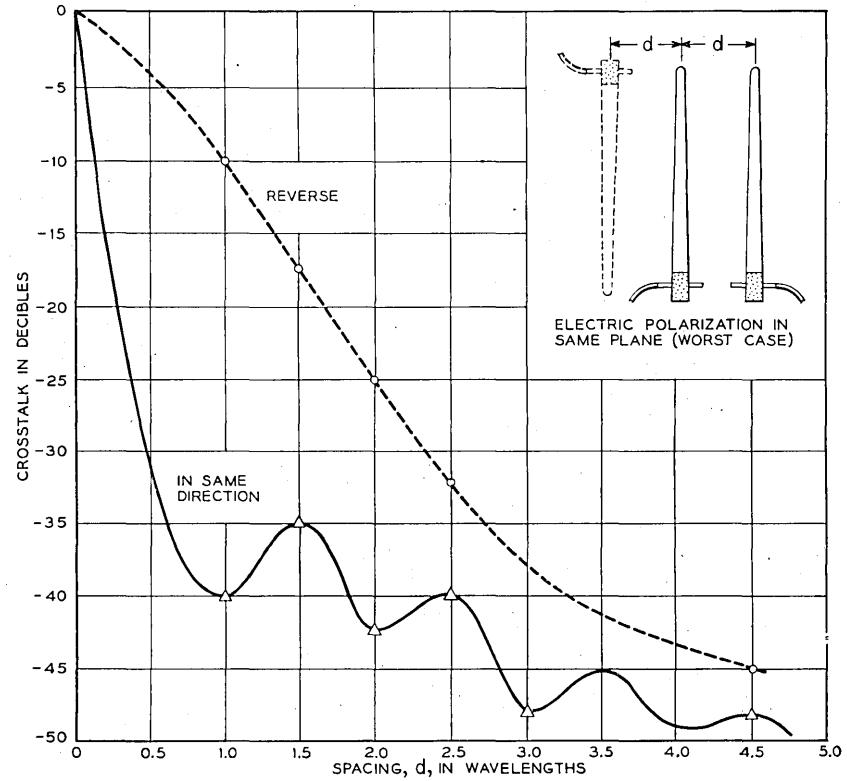

Fig. 13—Crosstalk between polyrods.

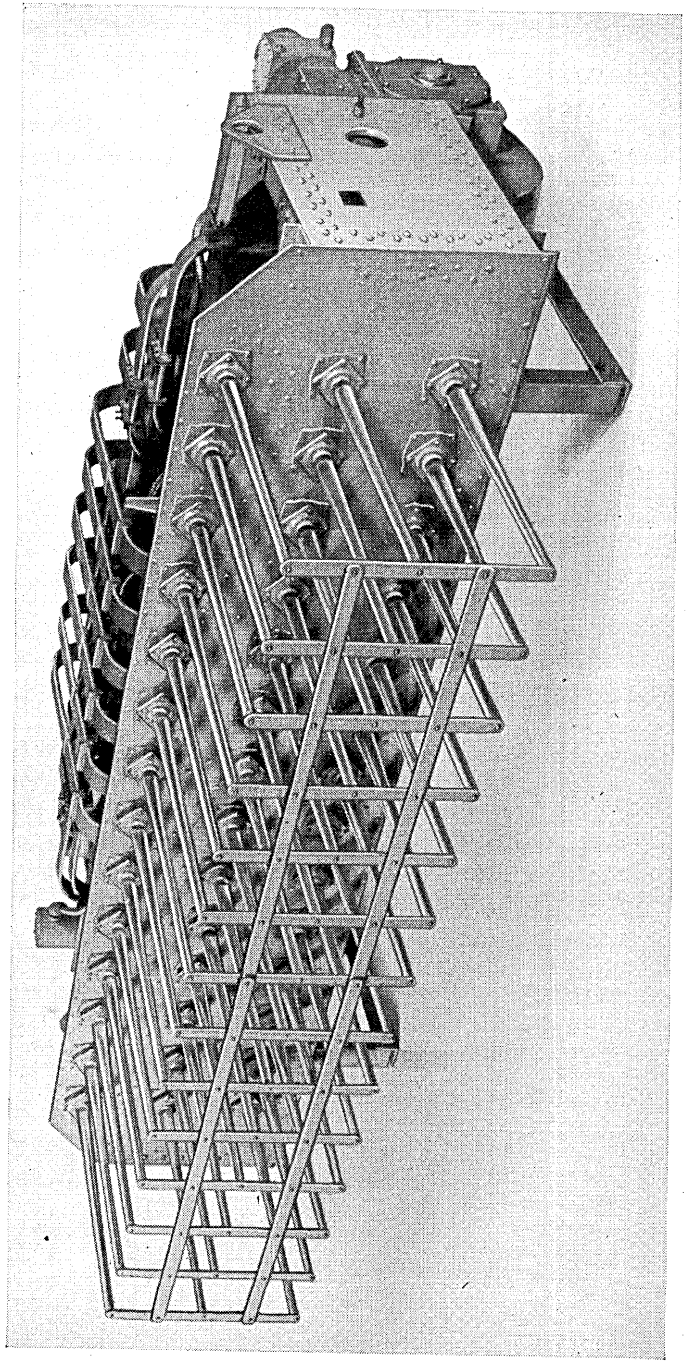

Fig. 14—Broadside array of polyrods.

present, the usable bandwidth is therefore limited primarily by the frequency response of the coupling arrangements from polyrod to waveguide or coaxial line.

We have been exclusively concerned so far with plane polarized radiation. A circularly symmetrical polyrod such as in Fig. 8 can be used equally well to radiate circularly polarized waves. To do this, the polyrod is fed from a waveguide in which circulary polarized dominant waves are generated by means of a 90° phase shift section.[12]

The effect of dielectric loss upon polyrod performance is shown in Fig. 12, to be compared with Fig. 7. The power factors are: Styramic, 0.0005; hard rubber, 0.003; acetate butyrate, 0.020; polystyrene, 0.0002. Materials having power factors less than 0.001 are satisfactory for polyrod antennas.

Figure 13 shows the crosstalk between adjacent polyrods, that is, the power received in one radiator when the other is energized. For polyrods pointing in the same direction, separations greater than a wavelength insure low mutual coupling. This makes the polyrod attractive as the element in broadside arrays. Proximity to other undriven polyrods affects the gain and directional pattern to a greater extent, as shown in Fig. 9.

More generally, the performance of a polyrod is affected by proximity to any metallic or dielectric objects. The gain and pattern must be determined empirically for each new configuration. It has been found that a metal rod can be placed parallel to a polyrod without seriously affecting its behavior so long as a separation of a wavelength or more is maintained. Sheets of dielectric material can be brought even closer without adverse effect so long as large surfaces are not in direct contact with the polyrod. These and other experiences suggest that the polyrod is relatively unaffected by nearby objects.

Tests have been made of the effect of fresh and salt water in the form of a spray or solid stream playing on a polyrod. Provided that puddles do not form on the surface, as can happen with rectangular polyrods, the effect is a decrease of 1 to 2 *db* in gain under the worst conditions.

In conclusion, for microwave applications involving moderate gains of 15 to 20 *db*, the polyrod assumes a convenient physical form and displays high electrical efficiency. It is less subject to disturbance by nearby objects than might be expected. It is especially useful as an element in broadside arrays. As an example of such arrays, Fig. 14 shows a 42 rod steerable beam antenna used in an important type of Navy fire control radar.

[12] For a discussion of this subject, cf. A. G. Fox, "An Adjustable Waveguide Phase Changer," to be published in *Proc. I. R. E.*

Targets for Microwave Radar Navigation

By SLOAN D. ROBERTSON

The effective echoing areas of certain radar targets can be calculated by the methods of geometrical optics. Other more complicated structures have been investigated experimentally. This paper considers a number of targets of practical interest with particular emphasis on trihedral and biconical corner reflectors. The possibility is indicated of using especially designed targets of high efficiency as aids to radar navigation.

Introduction

IT NOW seems likely that radar, developed during the war, will find increasing application as a navigational aid for aircraft and surface vessels. In fact there are good reasons for expecting that peace-time radar can be made even more efficient than its war-time prototype.

There are two ways of improving radar performance. One may concentrate on the radar set proper with the object of increasing either the power of the transmitter or the sensitivity of the receiver. Or, one may take steps to improve the echoing efficiency of the targets. The latter was, of course, not possible during the war since most of the targets of interest were controlled by the enemy. It is a purpose of the present paper to consider the design of various targets of high echoing efficiency and wide angular response which may be placed at strategic points as aids to radar navigation. The ideal reflector to serve as a "beacon" or "buoy" for guiding radar-equipped aircraft or ships would present a highly effective area to incident radiation over a full 360° in azimuth, and would also be operative over a fairly broad vertical angle. The value of a particular target for navigational purposes may therefore be considered in terms of two factors: effective area, and angular response.

The echo received by a radar from a particular target can be calculated by the formula:[1]

$$W_R = W_T \frac{A_R^2 A_{eff}^2}{\lambda^4 d^4} \tag{1}$$

where W_R = echo power available at the terminals of the radar antenna.
W_T = power launched by radar.
A_R = effective area of radar antenna assuming that the same antenna is used both for transmission and reception.

[1] This equation follows directly from Equation (1) of a paper by H. T. Friis, "A Note on a Simple Transmission Formula," *Proc. I.R.E.*, Vol. 34, pp. 254–256, May 1946. The radar transmission formula is obtained by applying Friis' formula twice; first to the transmission from the radar to the target, then to the transmission from the target to the radar.

A_{eff} = effective area of target.[2]
λ = wavelength.
d = distance between radar and target.

The above formula applies to the case where free-space propagation prevails; that is, where multiple path or anomalous transmission effects are absent.

It is apparent from the formula that, at a given wavelength and range, the received echo power can be increased by increasing the transmitted power, the size of the antenna, or the effective area of the target. The present paper will consider only the latter.

In some cases the effective area of a target can be calculated from simple geometrical optics. For the more complicated structures it is always possible to measure the effective area by comparing the signal reflected by the object in question to the signal reflected from a simple target of known effective area.

Flat Plates

The simplest target for which the effective area can be calculated is a flat metal plate oriented so as to be perpendicular to the incident radiation. It can be demonstrated that a flat plate with all linear dimensions large in proportion to the wavelength of the incident radiation has an effective area which is substantially equal to its geometrical area. Diffraction effects at the edges of such a plate are small in comparison with the energy reflected from the central portion of the plate.

Flat plates, however, have the serious disadvantage that, in order to create strong echoes, they must be maintained accurately perpendicular to the incident rays. At other angles of incidence the echoes fall off rapidly. For this reason flat plates are of limited value as targets for use in navigation.

Dihedral Corner Reflectors

A dihedral corner reflector consists of two perpendicular, plane conducting surfaces which are usually arranged so that they intersect along a common line. Figure 1 shows a typical dihedral reflector. The dihedral reflector has the important property that a ray which enters the corner will experience a reflection from each of the surfaces and will return in the direction from which it came, provided of course that the entering ray lies in a plane which is perpendicular to the line of intersection of the planes which form the

[2] The term "effective area" as used in this paper refers to the equivalent flat plate area of a target. The echoing effectiveness of a target may alternatively be expressed in terms of the cross section of an equivalent isotropic reflector as described by Schneider, "Radar," *Proc. I.R.E.*, Vol. 34, p. 529, August 1946. The alternative unit is called the "scattering cross section" and is frequently denoted by the symbol σ, although Schneider uses S. The two quantities are related by the equation $\sigma = 4\pi A^2_{eff}/\lambda^2$. Both units are useful. For most of the targets considered in the present paper, A_{eff} does not vary with λ and is therefore preferable.

corner. The latter restriction constitutes the principal objection to the practical use of dihedrals. The path of a typical ray is shown in Fig. 1.

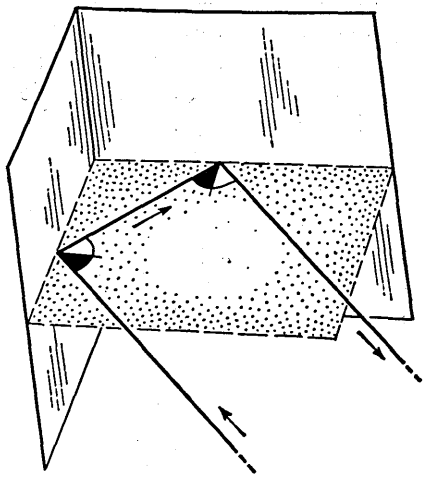

Fig. 1—Dihedral corner reflector.

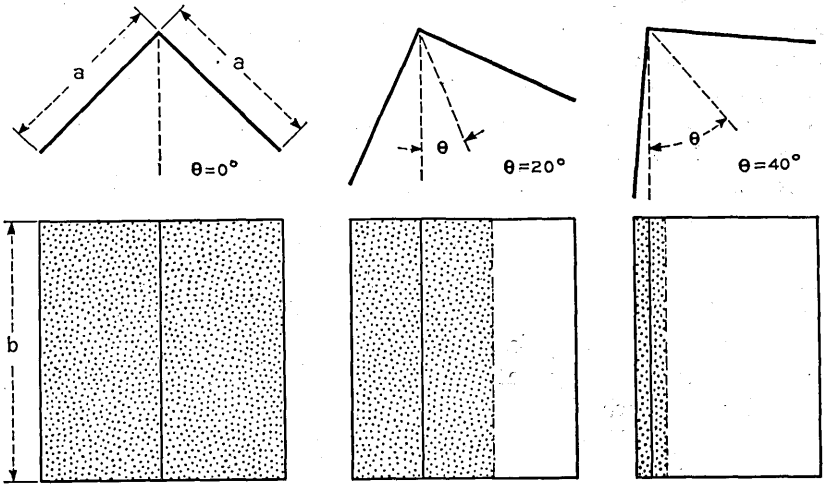

Fig. 2—Variation of effective area of a dihedral with aspect angle.

The effective area of a dihedral reflector depends upon both the size of the reflector and the orientation of the reflector with respect to the incident rays. Figure 2 shows how the effective area varies as the dihedral is rotated about the line of intersection of the two planes. The effective areas for the different orientations are shown by the shaded regions in the lower part of the

figure. For a reflector having the dimensions shown in the figure the effective area for different angles of incidence θ can be calculated by the formula.

$$A_{eff} = 2\ a\ b \sin (45° - \theta)$$

where θ is always considered positive and less than 45°.

Figure 3 shows the polarization of the reflected ray for differently polarized incident rays. For our purpose, the incident rays may be assumed to enter the left side of the reflector shown in the figure and the reflected rays may be assumed to emerge from the right. It is apparent that if the incident ray is polarized either parallel or perpendicular to the line of intersection of the two surfaces the reflected ray will be polarized in the same plane as the incident ray. If the incident ray is polarized at an angle of 45° to the line of intersection, the reflected ray will be polarized perpendicularly to the incident ray. In the latter case the signal received back at the radar will not ordinarily be accepted by the same antenna which launched the incident radiation.

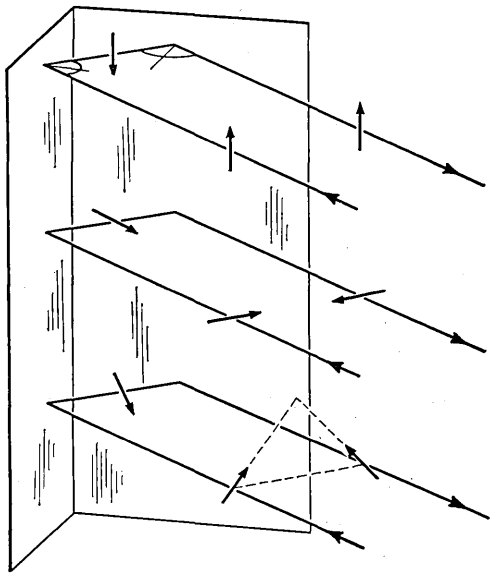

Fig. 3—Polarization effect in a dihedral reflector.

Trihedral Corner Reflector

Assume that three reflecting surfaces AOB, AOC, and BOC are placed so as to form the right-angled corner illustrated in Fig. 4. In general, electromagnetic waves, upon striking an interior surface of the device, will undergo a reflection from each of the three planes and return in a direction parallel to

and with the same polarization as the incident ray. The path of a typical ray is shown by line 1, 2, 3, the particular ray chosen having entered the reflector along a line perpendicular to the plane of the paper. Points 1 and 3 represent the initial and final points of reflection, respectively, whereas point 2 represents the intermediate reflection point.

Two important conclusions can be drawn from a careful inspection of the path 1, 2, 3; namely, the projections of points 1 and 3 are diametrically opposite on a circle drawn about point O as a center, and points 1 and 3 appear to be images of point 2; i.e., the ingoing ray at 1 appears to be directed toward

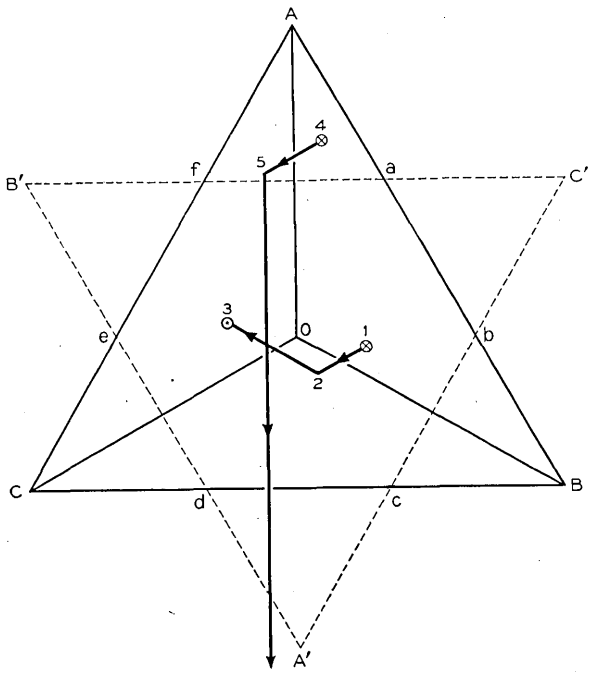

Fig. 4—Trihedral corner reflector showing the paths of typical rays.

the image of point 2 in plane AOB, and the outcoming ray at 3 appears to come from the image of point 2 in plane AOC.

Not all rays falling upon a corner reflector of finite dimensions will be reflected in the direction of the source. For example, a ray striking point 4 in Fig. 4 may be reflected successively at points 4 and 5, but if the plane BOC is not sufficiently extended it will not undergo the necessary third reflection required to return the ray in the incident direction.

The portion of the projected cross-section of a corner reflector which is able to return incident radiation to the source is called the "effective area." It is, of course, a function of the aspect, that is to say, the angle at which the

reflector is being viewed, as well as the geometrical configuration of the reflector. For some of the simpler configurations the effective area can be readily determined by the following procedure.

Project the aperture of the reflector through the apex O to form the image (A′ B′ C′ of Fig. 4); then project the aperture and its image upon a plane perpendicular to the incident rays. The area common to the projections of the aperture and its image is equal to the effective area. The effective area of the triangular reflector of Fig. 4 is, therefore, represented by the hexagon a b c d e f. Only those rays, perpendicular to the plane of the paper, which

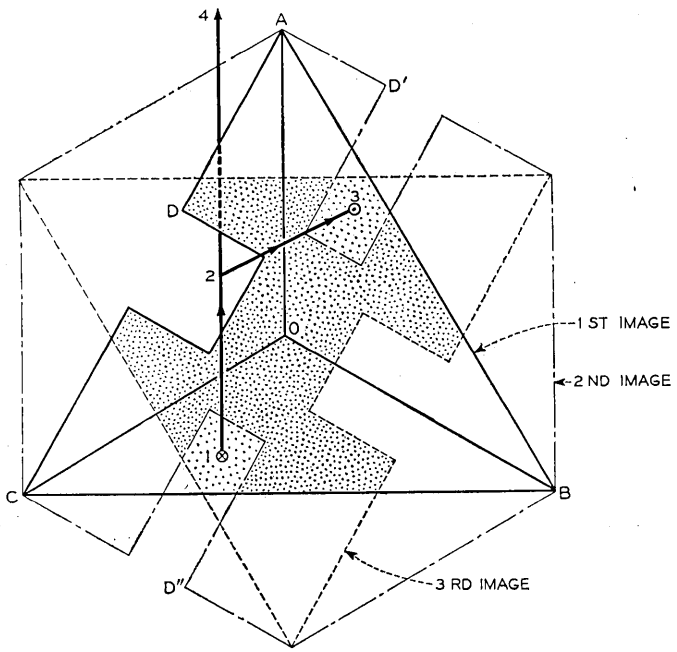

Fig. 5—Determination of effective area of trihedral corner reflector.

fall inside the hexagon will be returned. Exactly the same procedure is used in determining the effective area for other aspect angles.

The above rule must, however, be applied with caution. Situations arise in which rays falling upon the area determined by this method do not return to the source. Figure 5 shows a reflector in which this difficulty is encountered. This reflector differs from the previous reflector in that it has a notch cut in one of the reflecting surfaces. The projection of the aperture upon the plane of the paper is indicated by the solid line; that of its image by the dotted line. According to the rule of the preceding paragraph, one would expect the effective area to be defined by the total shaded area of the figure.

Such, however, is not the case. It was stated earlier that the ingoing rays appear to be directed toward the images of the intermediate reflecting points. This requires that the images of the intermediate reflecting points fall inside of the effective area. In Fig. 5, the images of the notch fall inside of what would otherwise be the effective area. Since the notch is incapable of serving as an intermediate reflector, the more lightly shaded areas are excluded from the effective area. In the absence of the notch, a ray entering at 1 would be reflected at 2 and emerge at 3. In the presence of the notch, however, it passes through plane AOC and escapes in the direction of 4.

Therefore, in order to determine the effective area of a corner reflector of arbitrary shape and aspect, one must take account of three loci of points defined by the aperture as follows:

1) The aperture itself

2) The locus of points determined by taking the direct mirror image of each point of the aperture with respect to each of the two surfaces of the trihedral not containing the point. For example, point D of Fig. 5 will have the images D′ and D″ with reference to planes AOB and BOC, respectively. The complete locus of points determined in this way is represented by the dot-dash line of Fig. 5.

3) Locus of points on aperture after each has been assumed to have been projected through the vertex. This image is pictured by the dotted lines of Fig. 5.

These three images of the aperture can, for simplicity, be referred to as the first, second, and third images, respectively. The effective area is the area common to the projections of the first, second, and third images of the aperture upon a plane passing through the apex of the reflector and perpendicular to the incident rays. For a given aperture and aspect, a corner reflector can theoretically be replaced by a flat plate located at the apex. The size and shape of the flat plate will vary with the aspect as well as with the configuration of the aperture. The above procedure has been of considerable aid in studying reflectors having apertures of arbitrary shape.

Although the graphical analysis just given is sufficient to enable one to compute the effective area of a reflector for any aspect angle, it is frequently more conveneint to determine the complete response pattern of a reflector experimentally. Most of the experimental results reported in this paper were obtained with a 1.25 centimeter radar arranged as shown in Fig. 6. Echo levels were measured on the screen of a type-A indicator using a calibrated intermediate frequency attenuator to restore the signal to an arbitrary reference level. It is believed that the levels measured in this way are accurate to within $\pm \frac{1}{2}$ decibel. The coordinate system used in recording and presenting the data is given in Fig. 7. The reflector was mounted on a turntable which could be rotated about horizontal and vertical axes.

Curves for the response patterns of a corner reflector of triangular aperture are shown in Fig. 8. These curves were obtained with a reflector constructed of silver-painted plywood whose aperture was in the form of a 24-inch equilateral triangle. It had been previously determined that, with suitable paints, reflectors of this construction behaved exactly as though they were made of sheet metal.

Depending upon its angle of arrival, a ray may be reflected by a corner reflector in one of four ways. If the angle is too oblique, the ray may not be returned in the direction of the source at all. If the incoming ray is

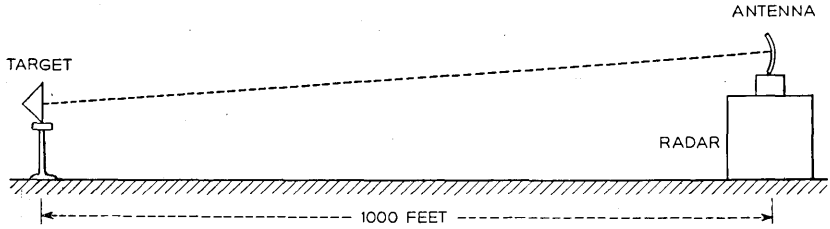

Fig. 6—Arrangement of apparatus for measuring effective areas of targets.

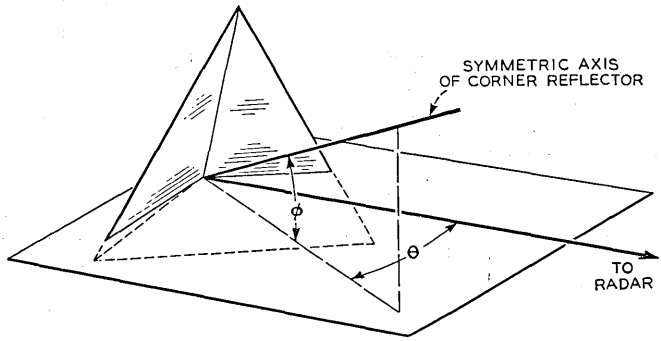

Fig. 7—Coordinate system used in presenting data.

exactly perpendicular to one of the three reflecting planes, it will be returned to its source after only one reflection. Should the ray arrive in a direction exactly parallel to one of the three planes, it will again be returned in the direction of its source but in this case it is reflected twice as in a dihedral. This particular mode of reflection is illustrated by the sharp peaks at the extremities of the curves in Fig. 8. For all remaining angles of approach the ray will be returned after three reflections in the manner already described. The central regions of the curves represent this type of reflection which is of principal interest in practice.

The effective area of the triangular trihedral reflector along the symmetric axis ($\theta = 0, \phi = 0$) can be computed from the geometry of Fig. 4.

$$A_{eff} = 0.289\,\ell^2 \tag{3}$$

where ℓ is the length of one side of the aperture such as CB. The effective area at other aspect angles can be computed by relating the echo level at the aspect in question with that along the symmetric axis.

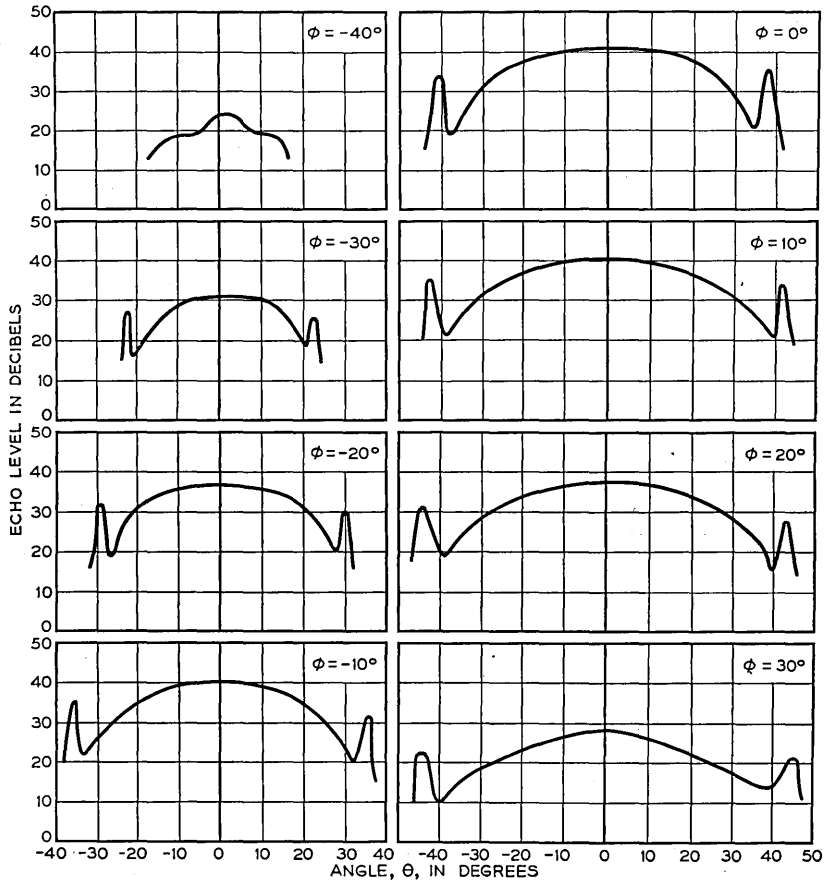

Fig. 8—Echo-response patterns of a triangular trihedral reflector.

It should be pointed out that the effective area for trihedral reflections is independent of wavelength where the reflector is large enough so that geometrical optics prevail. If the wavelength is increased, however, the sharp dihedral peaks at the edges of the pattern will be broader.

In the case of the triangular corner reflector the response levels for aspect angles of 30°, as measured from the symmetric axis, are down by 10 decibels. For many applications a flatter response pattern is desirable.

The present investigation led to the discovery that the response pattern of a corner reflector can be modified by a suitable alteration of the geometrical configuration of the aperture. There is even the suggestion that the response can, to a certain degree, be made to conform to a somewhat arbitrary pattern within a region extending to approximately 30° from the principal axis. The procedure for accomplishing this has, so far, been one of trial and error since the difficulties of a general mathematical solution appear to be

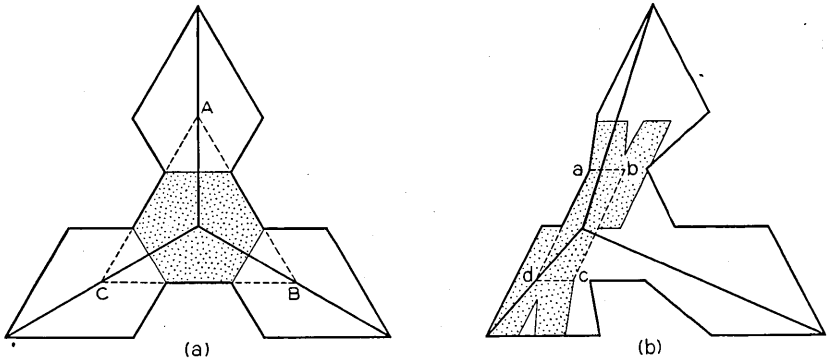

Fig. 9—Compensated corner reflector.

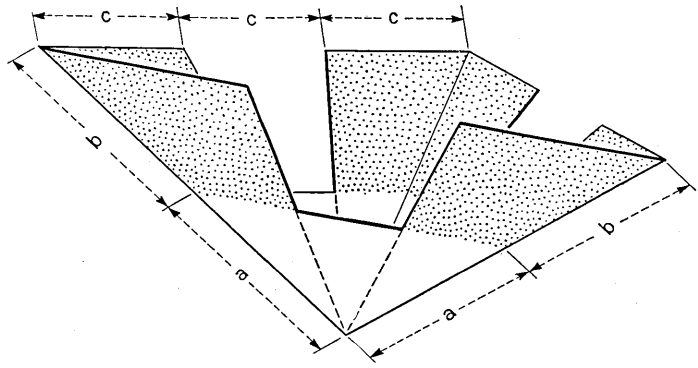

Fig. 10—Dimensions of face of compensated reflector.

insurmountable, at least in a practical sense. For practical purposes, however, it is comparatively easy to conduct a few graphical experiments in order to design a reflector having the desired response pattern.

Figures 9a and 9b show two views of a modified corner reflector which was designed to have a relatively flat response characteristic out to angles of 30° from the central axis. Each of the three sides of the reflector, instead of being triangular as formerly, has the contour shown in Fig. 10. The shaded regions of Fig. 10 represent the surface which has been added.

In Fig. 9a, one is assumed to be looking into the reflector along the symmetric axis. The effective area is represented by the shaded hexagon. Evidently, the effective area of the modified reflector is identical to the effective area of the original triangular reflector A B C. Therefore, for this particular aspect, the effective area has not been changed by the addition of the material at the corners.

Figure 9b is a view of the reflector at $\theta = 30°, \phi = 0°$. Again, the shaded region represents the effective area, and the parallelogram abcd is the effective area of the reflector before modification. The modification has evidently introduced a substantial gain in effective area for this aspect. A graphical comparison of the effective areas of Figs. 9a and 9b shows them to be of comparable magnitude.

With the dimensions defined as in Fig. 10, a corner reflector was constructed with a= b= 17″. The response curves of this reflector are plotted in Fig. 11, along with the curves of the ordinary triangular reflector. A substantial improvement in response is exhibited by the compensated reflector. In the region extending out to 30° from the axis, the response level varies by no more than a couple of decibels. The response appears to rise slightly in the vicinity of 20°. This could, perhaps, be reduced by a more appropriate shaping of the sides of the reflector.

The variation of the response curve with the ratio $\frac{b}{a}$ has been studied briefly. It appears that a value of $\frac{b}{a} = 1$ is about right, for the 30° contour to equal the axial response. If $\frac{b}{a} < 1$, the reflector will only be partially corrected; if $\frac{b}{a} > 1$, it will be overly corrected. In the uncorrected reflector with triangular aperture, $\frac{b}{a} = 0$.

If $b/a = \infty$, that is, if $a = 0$, one would expect to obtain a response curve having a minimum value on the axis and rising to a maximum on either side. A reflector having these properties is illustrated in Figs. 12a and 12b. Again Fig. 12a is the axial aspect, whereas Fig. 12b is the 30° aspect. In the former, the effective area should be zero; in the latter, it has the value represented by the shaded portion. A reflector of this kind, in which b = 34″ and a = 0, was constructed and tested. The experimental results are shown in Fig. 13. The minimum is, perhaps, not as low in value as expected because of residual reflections from the support upon which the reflector was mounted. As expected, however, the curve passes from a minimum on the axis to maxima on either side.

The above examples serve to illustrate some of the results which can be realized with trihedral reflectors. We have seen that the response characteristic can be controlled by appropriate modifications of the geometrical configuration of the aperture.

Experiments were performed in order to determine the reduction in echo caused by errors in the internal angles at the corner.

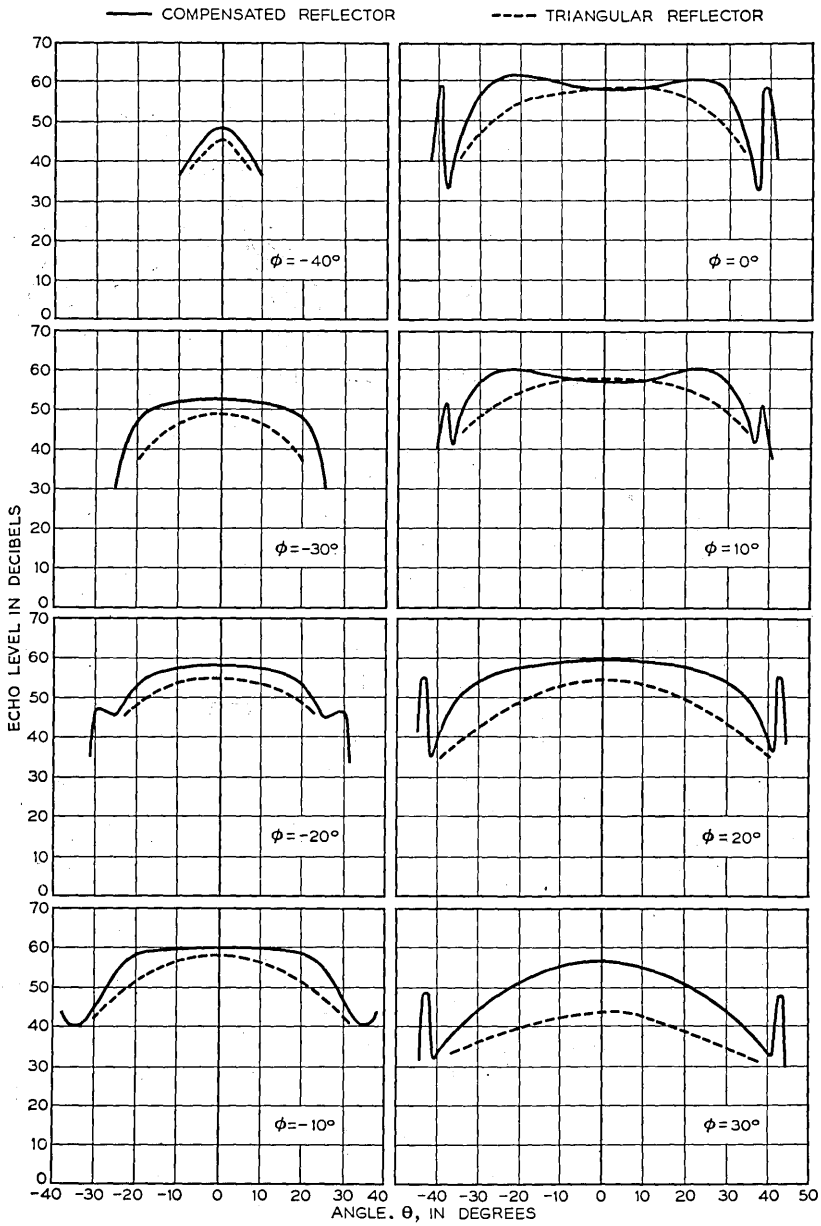

Fig. 11—Response of compensated reflector compared with that of triangular reflector.

In the first set of experiments only one of the internal angles was altered from its nominal value of 90°. Figure 14 shows the apparatus used in the

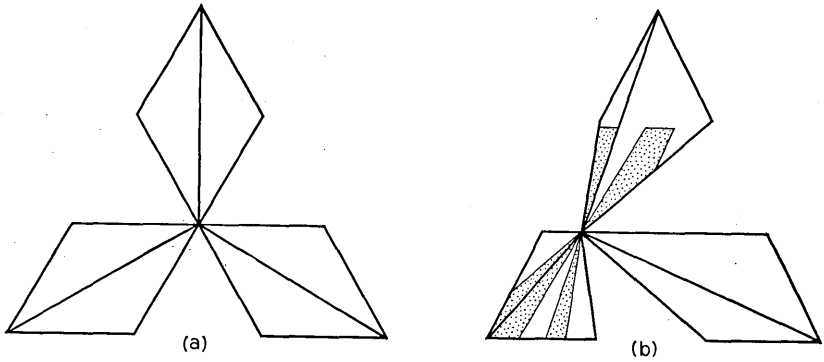

Fig. 12—Modified reflector having minimum response on axis.

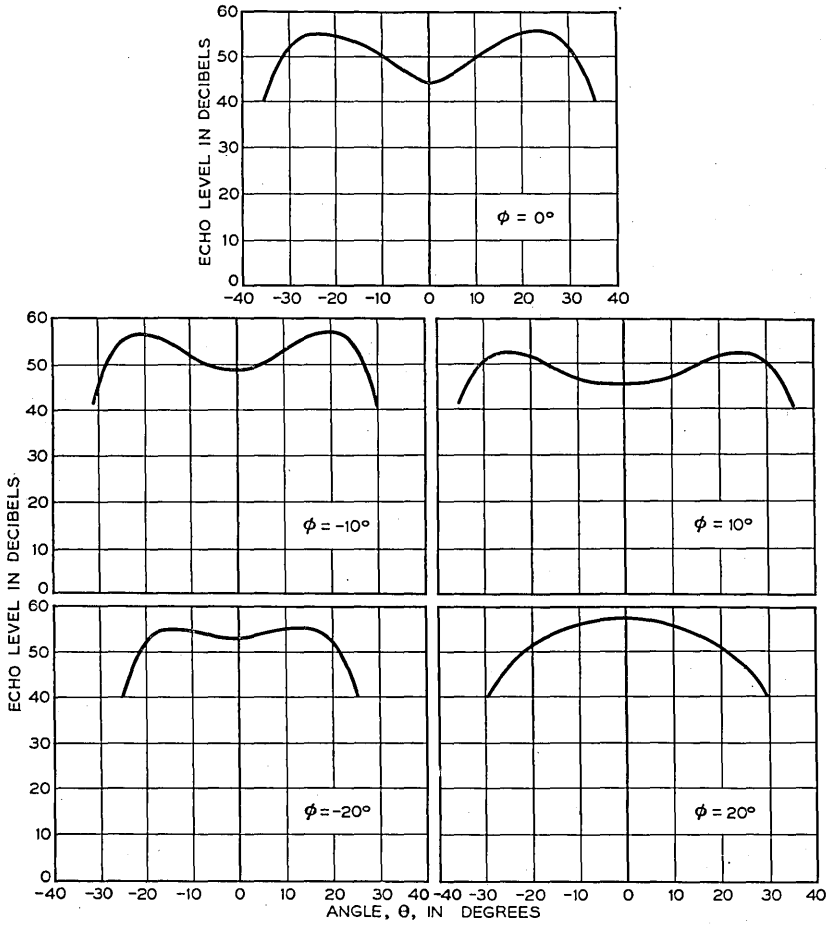

Fig. 13—Response patterns of reflector of Fig. 12.

experiment. The 24-inch reflector was constructed of silver-painted plywood and hinged along the intersection of the two upper surfaces so that the angle α could be varied at will. A series of response patterns were taken for various values of α. These are shown in the lower part of Fig. 14. It will be observed that one effect of changing α is to lower the echo level. This appears, however, to be accompanied by a somewhat flatter response curve. The radar used in this experiment had a wavelength of 1.25 centimeters.

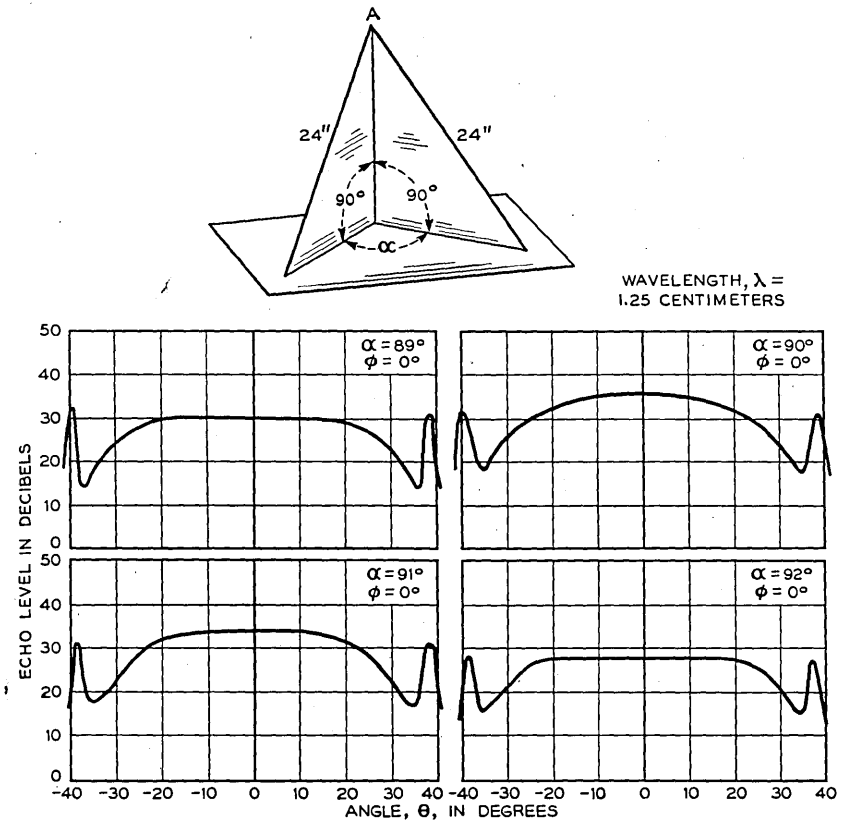

Fig. 14—Effect of an error in one of the corner angles of a trihedral upon its performance.

A second series of experiments was conducted in which all three internal angles were varied simultaneously. The curves shown in the upper half of Fig. 15 show the axial echo level for various sizes of reflector as a function of the internal angles α. It will be noted that for the 24-inch reflector an angular error of $\frac{1}{2}$ degree results in an echo-level reduction of two decibels, while the same angular error in the $9\frac{3}{8}$ inch reflector produces only a negligible reduction. The lower part of the figure shows some response patterns

taken with a 24-inch triangular reflector for several values of α. A wavelength of 1.25 centimeters was used in obtaining both sets of curves. Later, similar measurements were made at a wavelength of 3.2 centimeters. It was found that the loss of signal is a function of the linear error of the aperture in wavelengths rather than the angular error in degrees. Thus a given angular error in a $9\frac{3}{8}$-inch reflector at a wavelength of 1.25 centimeters will produce the same loss in signal as the same angular error in a 24-inch reflector operating at a wavelength of 3.2 centimeters.

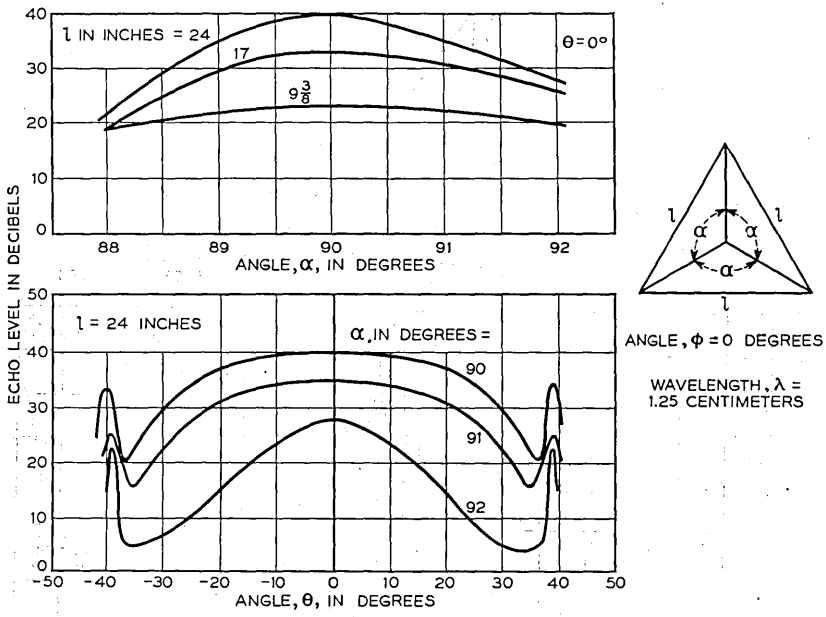

Fig. 15—Effect of an error in all three corner angles upon the performance of a trihedral.

Spheres and Cylinders

Formulas for the effective areas of spheres and cylinders which have dimensions large in comparison with a wavelength have been supplied by J. F. Carlson and S. A. Goudsmit of the Radiation Laboratory.[3] The effective area of a sphere of radius R is given by

$$A = \frac{R\lambda}{2} \tag{4}$$

where λ is the wavelength.

For a cylinder of radius R and height L, both large with respect to a wavelength, the effective area for rays perpendicular to the axis of the cylinder is

$$A = L\sqrt{\frac{R\lambda}{2}} \tag{5}$$

[3]Unpublished Report

It will be of interest to compare the sphere and the cylinder with corner reflectors and flat plates. The response pattern of a sphere is ideal in that it is uniform in all directions. Unfortunately its effective area is small in comparison with that of corner reflectors or flat plates having the same cross-sectional area. The cylinder has a symmetrical response pattern in the plane

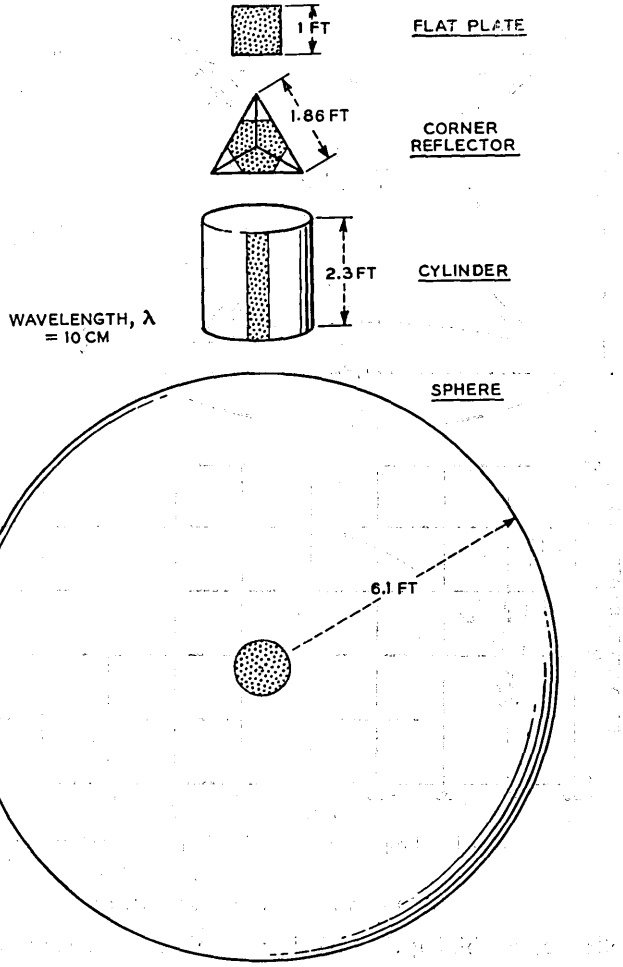

Fig. 16—A comparison of several representative targets having equal effective areas.

perpendicular to the axis but is very sharp in the plane of the axis. The effective area of a cylinder is intermediate between that of a corner reflector and a sphere. Figure 16 is a scale view of a flat plate, a corner reflector, a cylinder, and a sphere all having an effective area of one square foot at a wavelength of 10 centimeters. For shorter wavelengths the flat plate and

the corner reflector would remain the same size, whereas the cylinder and the sphere would have to be larger in order to maintain the same effective areas. At a wavelength of 1 centimeter the sphere would have to have a radius of about 60 feet.

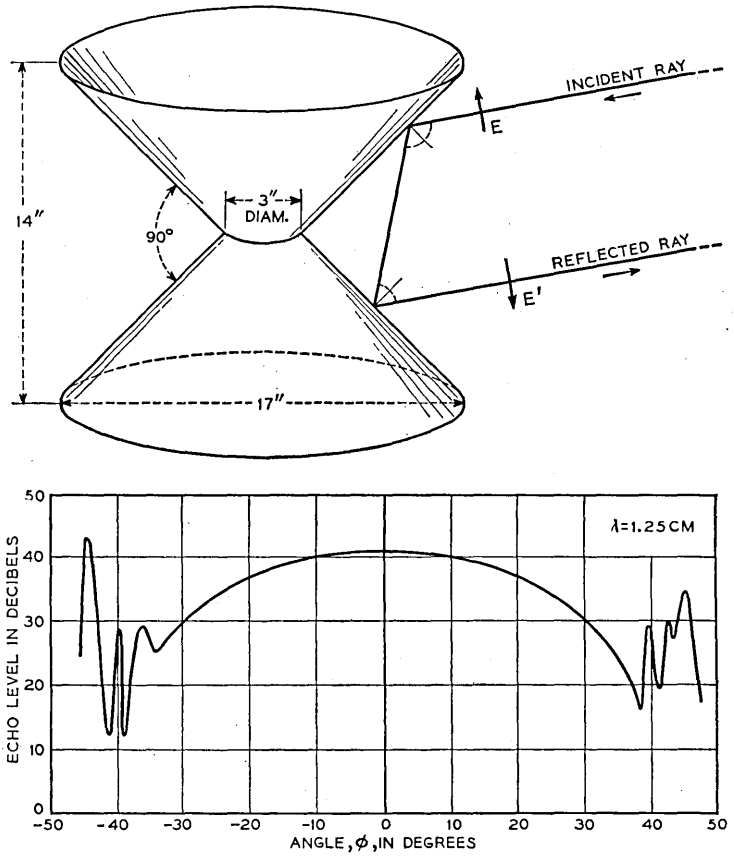

Fig. 17—Properties of the biconical corner reflector.

Biconical Corner Reflector

A reflector, combining the 360° horizontal response characteristic of the cylinder with a vertical response like that of the corner reflector, was evolved and is illustrated in Fig. 17. As shown here, the device consists of two conical surfaces placed in juxtaposition such that the generatrices of one cone intersect those of the other at right angles. The operation of the reflector is somewhat like that of a dihedral corner reflector in that a ray, upon striking one of the cones, is reflected to the other and then returns in the direction of

the source. The "Biconical" reflector may perhaps be likened to a cylinder which automatically orients itself so that the impinging rays are always perpendicular to the axis.

A biconical reflector was constructed of sheet metal having the dimensions indicated in Fig. 17. The vertical response pattern was measured and is plotted in the lower portion of the figure. Because of the circular symmetry of the reflector, the vertical response curve shown will be equally valid for all angles of azimuth. At $\phi = 0°$ the reflector exhibited an effective area of 0.16 square feet. The measurements were made at a wavelength of 1.25 centimeters.

In the above experiment the incident radiation was polarized in the plane of the axis of the cones. In another test with the polarization perpendicular to the axis the received echo was reduced by four decibels. This effect is not as yet entirely explained. It probably results from a depolarizing effect similar to that encountered in the dihedral corner reflector, complicated however by the curvature of the cones.

Only a limited amount of data is available for predicting the effective area of a biconical reflector over a wide range of sizes and wavelengths. The available data indicate that to a rough approximation and for a given polarization the effective area varies directly as the square root of the wavelength and as the three-halves power of the diameter of the cones, assuming that the height of the reflector is approximately equal to the diameter.

Tables of Phase Associated with a Semi-Infinite Unit Slope of Attenuation

By D. E. THOMAS

This paper presents tables of the phase associated with a semi-infinite unit slope of attenuation. The phase is given in degrees to .001 degree with an accuracy of ± .001 degree and in radians to .00001 radian with an accuracy of ± .000015 radian. The method of constructing the tables and a brief analysis of the errors are given. An appendix, which gives a detailed explanation with specific examples of the use of the tables in determining the phase associated with a given attenuation characteristic or the reactance associated with a given resistance characteristic by means of the straight line approximation method given in Bode's "Network Analysis and Feedback Amplifier Design," is included for the benefit of those who are not already acquainted with this method. The Appendix also presents an example of a non-minimum phase network[1] in which the minimum phase determined from the attenuation characteristic fails to predict the true phase of the network.

THE method described by Bode[2] for the determination of the phase associated with a given attenuation characteristic or the reactance associated with a given resistance characteristic has proved to be an extremely useful laboratory and design tool. In this method the attenuation (or real) characteristic, plotted versus the log of frequency, is approximated by a series of straight lines. The phase (or imaginary component) is then determined by summing up the individual contributions of each elementary straight line segment to the total phase (or imaginary component).

The most elementary straight line characteristic which can be used to construct a given straight line approximation is that in which the attenuation plotted against the log of frequency is constant on one side of a prescribed frequency, f_0, and has a constant slope thereafter. Such a characteristic has been called by Bode a "semi-infinite constant slope" characteristic.[3] A semi-infinite unit slope of attenuation or one in which the attenuation changes 6 *db* per octave, or 20 *db* per decade is shown in Fig. 1. The phase associated with this attenuation characteristic is plotted in Fig. 2.[4] The independent variable was chosen as f/f_0 for values of f less than f_0 and f_0/f for values of f greater than f_0 to keep it finite for all values of f and in order to show the phase plotted exactly as it is given in the tables to follow. The phase associated with a semi-infinite constant slope of

[1] For a complete discussion of *minimum phase* see Hendrik W. Bode, "Network Analysis and Feedback Amplifier Design," D. Van Nostrand Company, Inc., New York, N. Y., 1945.

[2] Ibid: Chap. XV, page 344.

[3] Ibid: Chap. XIV, page 316.

[4] Ibid: Chap. XIV page 317.

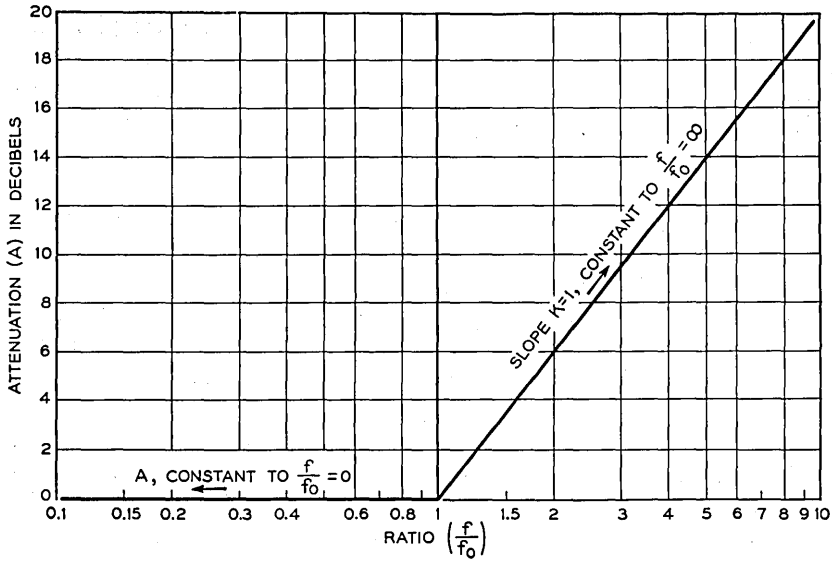

Fig. 1—Semi-infinite unit slope of attenuation.

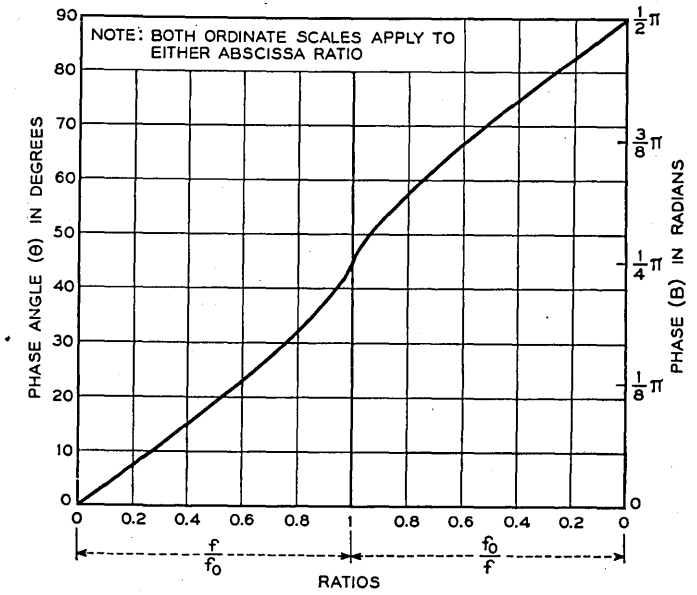

Fig. 2—Phase associated with semi-infinite unit slope of attenuation of Fig. 1.

attenuation of the same character as the semi-infinite unit slope of attenuation of Fig. 1 but of slope k, is k times the phase given in Fig. 2.

Bode points out,[5] however, that the building up of the complete imaginary characteristic from a single primitive curve, namely a semi-infinite real slope, suffers from the disadvantage that the phase contributions of the individual slopes may be rather large positive and negative quantities, even though the net phase shift is fairly small. In order to avoid this disadvantage, Bode recommends that the individual finite line segments which constitute the straight line approximation to the real characteristic be regarded as the elementary characteristics used in the summation of the total phase. He then gives a series of charts, plotted as a function of f/f_0, of the phase associated with a finite line segment having a 1 *db* change in attenuation and with a ratio of the geometric mean frequency (f_0) of the two terminal frequencies of the finite line segment to the lower terminal frequency as a parameter (ratio designated a).

However, problems have arisen where, even with the finite line segment phase charts, the phase contributions of the various elements were sufficiently large and nearly equal positive and negative quantities that difficulties in interpolation between the curves for the various values of a, given on the charts, resulted in a sufficient lack of precision that the quantity being sought was lost.

Because of the usefulness of the method in question, and with its application to a wider variety of problems, means of increasing its over-all precision and simplification of computation have constantly been sought. It had occurred to several engineers independently that a table of phase versus frequency for a semi-infinite unit slope of attenuation would prove extremely useful. The phase in radians at frequency f_c, associated with a semi-infinite unit slope of attenuation commencing at frequency f_0, is given by Bode as[6]

$$B(x_c) = \frac{2}{\pi}\left(x_c + \frac{x_c^3}{9} + \frac{x_c^5}{25} + \cdots\right) \tag{1}$$

where:

$$x_c = \frac{f_c}{f_0} = \frac{\omega_c}{\omega_0}, x_c < 1.$$

The computation time required to determine the phase at a given frequency by summation of the above series is such, that the work required to get the phase at a sufficient number of points and to a sufficient number of significant figures to prepare an adequate table proved to be sufficient to discourage this procedure.

[5] Ibid: Chap. XV page 338.
[6] Ibid: Chap. XV, page 343.

The derivative of (1) above, however, proves to be quite simple and easy to evaluate. It is given by Bode as:

$$\frac{dB}{dx_c} = \frac{1}{\pi x_c} \log \left| \frac{1 + x_c}{1 - x_c} \right| \tag{2}$$

$$= \frac{2}{\pi}\left(1 + \frac{x_c^2}{3} + \frac{x_c^4}{5} + \cdots\right), x_c < 1. \tag{2a}$$

It therefore seemed that since the phase had already been computed by the Mathematical Research Group of the Bell Telephone Laboratories, Inc., at a

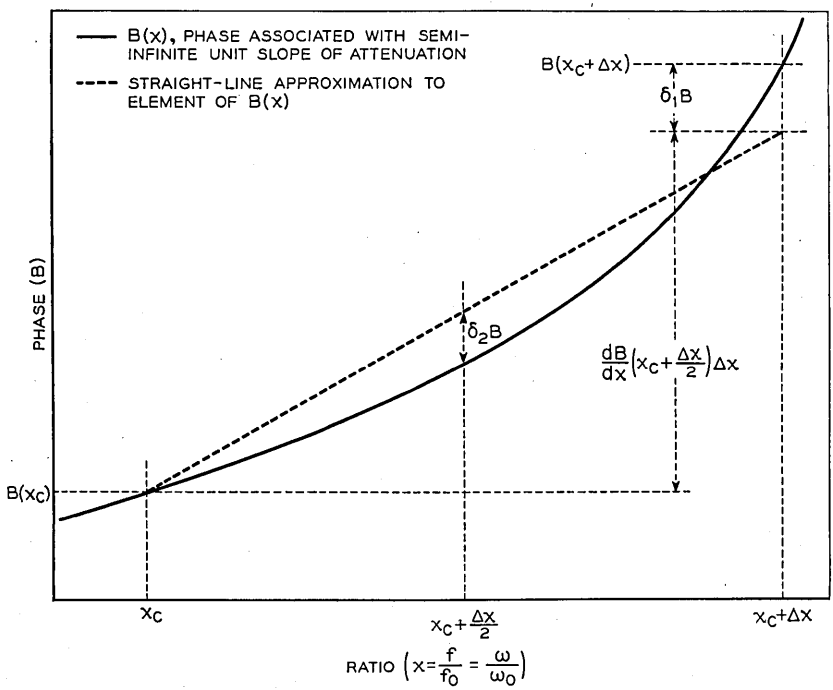

Fig. 3—Element of Fig. 2 for $f/f_0 < 1$ expanded qualitatively.

considerable number of points, using the infinite series expansion of (1) above the function in the regions between known values of phase could be constructed by assuming the intervening curve of phase as a function of $x = \frac{f}{f_0}$ to be a series of straight lines having the slope given by (2) above over intervals Δx of x made sufficiently small that the resultant straight line approximation would approach the true phase curve to the desired degree of accuracy for the table contemplated.

In order to evaluate the errors involved in such a procedure let us refer to Fig. 3 where a segment of the desired phase function to be constructed is qualitatively represented on a large scale. It is assumed that the phase at x_c, $B(x_c)$, is known and that it is desired to determine the error $\delta_1 B$ in phase computed for $x_c + \Delta x$ when it is assumed that the phase curve is a straight line from $B(x_c)$ at x_c, to $x_c + \Delta x$ having a slope, $\frac{dB}{dx}\left(x_c + \frac{\Delta x}{2}\right)$, the slope of the true phase curve at $x = x_c + \frac{\Delta x}{2}$.

Then:

$$\delta_1 B = B(x_c + \Delta x) - B(x_c) - \frac{dB}{dx}\left(x_c + \frac{\Delta x}{2}\right)\Delta x \tag{3}$$

where:

$$B(x_c) = \frac{2}{\pi}\left[x_c + \frac{x_c^3}{9} + \frac{x_c^5}{25} + \cdots\right]$$

$$B(x_c + \Delta x) = \frac{2}{\pi}\left[(x_c + \Delta x) + \tfrac{1}{9}(x_c^3 + 3x_c^2\Delta x + 3x_c\Delta x^2 + \Delta x^3)\right.$$
$$\left. + \tfrac{1}{25}(x_c^5 + 5x_c^4\Delta x + 10x_c^3\Delta x^2 + 10x_c^2\Delta x^3 + 5x_c\Delta x^4 + \Delta x^5) + \cdots\right]$$

$$B(x_c + \Delta x) - B(x_c) = \frac{2}{\pi}\left[\Delta x + \frac{x_c^2\Delta x}{3} + \frac{x_c\Delta x^2}{3}\right.$$
$$\left. + \frac{\Delta x^3}{9} + \frac{x_c^4\Delta x}{5} + \frac{2x_c^3\Delta x^2}{5} + \frac{2x_c^2\Delta x^3}{5} + \frac{x_c\Delta x^4}{5} + \frac{\Delta x^5}{25} + \cdots\right]$$
$$= \frac{2}{\pi}\left[\Delta x \sum_{n=1}^{n=\infty}\frac{x_c^{2n-2}}{2n-1} + \Delta x^2\sum_{n=1}^{n=\infty}\frac{nx_c^{2n-1}}{2n+1}\right.$$
$$\left. + \Delta x^3\sum_{n=1}^{n=\infty}\frac{n(2n-1)x_c^{2n-2}}{3(2n+1)} + \cdots\right]$$

$$\frac{dB}{dx}\left(x_c + \frac{\Delta x}{2}\right)\Delta x = \frac{2}{\pi}\Delta x\left(1 + \frac{1}{3}\left[x_c^2 + 2x_c\left(\frac{\Delta x}{2}\right) + \left(\frac{\Delta x}{2}\right)^2\right]\right.$$
$$\left. + \frac{1}{5}\left[x_c^4 + 4x_c^3\left(\frac{\Delta x}{2}\right) + 6x_c^2\left(\frac{\Delta x}{2}\right)^2 + 4x_c\left(\frac{\Delta x}{2}\right)^3 + \left(\frac{\Delta x}{2}\right)^4\right] + \cdots\right)$$
$$= \frac{2}{\pi}\left[\Delta x + \frac{x_c^2\Delta x}{3} + \frac{x_c\Delta x^2}{3} + \frac{\Delta x^3}{12} + \frac{x_c^4\Delta x}{5} + \frac{2x_c^3\Delta x^2}{5}\right.$$
$$\left. + \frac{3x_c^2\Delta x^3}{10} + \frac{x_c\Delta x^4}{10} + \frac{\Delta x^5}{80} + \cdots\right]$$
$$= \frac{2}{\pi}\left[\Delta x\sum_{n=1}^{n=\infty}\frac{x_c^{2n-2}}{2n-1} + \Delta x^2\sum_{n=1}^{n=\infty}\frac{nx_c^{2n-1}}{2n+1}\right.$$
$$\left. + \Delta x^3\sum_{n=1}^{n=\infty}\frac{n(2n-1)x_c^{2n-2}}{4(2n+1)} + \cdots\right].$$

Since Δx will be small compared to unity and since an error function is being computed it is permissible to take only the 1st term of the difference between the true phase and the computed phase, i.e. the Δx^3 term, and drop all higher order terms of Δx.
Then:

$$\delta_1 B \doteq \frac{2}{\pi}\left[\Delta x^3 \sum_{n=1}^{n=\infty} \frac{n(2n-1)x_c^{2n-2}}{3(2n+1)} - \Delta x^3 \sum_{n=1}^{n=\infty} \frac{n(2n-1)x_c^{2n-2}}{4(2n+1)}\right] = \frac{\Delta x^3}{6\pi} \sum_{n=1}^{n=\infty} \frac{n(2n-1)x_c^{2n-2}}{2n+1}. \tag{4}$$

The equation (4) above for $\delta_1 B$ gives only the error for a single increment Δx of $x = f/f_0$. If the phase is known at $x = x_a$ and $x = x_b$ and it is desired to determine the phase at points between $x = x_a$ and $x = x_b$ then since $\delta_1 B$ always has the same sign the errors due to successive increments of x will be cumulative and the total error at $x = x_b$ will be n times the average of the $\delta_1 B$ errors of each increment of Δx between x_a and x_b where n is the total number of equi-increments of x taken between x_a and x_b. However, since the individual $\delta_1 B$ errors decrease as the cube of Δx, the individual errors will decrease as the cube of the number of increments taken between the two frequencies at which the phase is known, whereas the cumulative $\delta_1 B$ error will increase only in proportion to the first power of n. Therefore, the net result will be a vanishing of the cumulative error inversely as the square of the number of frequency increments taken to approximate the curve in the interval in question. It therefore follows that the accuracy of the proposed method of building up the function, in so far as the phase at the terminals of the straight line segments is concerned, is limited only by the number of increments of frequency selected for the summation.

In order to determine the actual magnitude of errors to be expected $\delta_1 B$ was computed for $x_c = .4$ and $\Delta x = .02$ and found to be only .000015 degree. Since the total number of .02 intervals needed to be used between previously computed values of B is 5, the total cumulative error in this region for increments of this magnitude will not be greater than .0001 degree, which is entirely satisfactory, since the accuracy being sought is $\pm$ .0005 degree in B. For $x_c = .9$ and $\Delta x = .005$ the $\delta_1 B$ error proves to be only .00001 degree and since in this region the value of B has already been determined at .01 intervals by the more accurate series expansion technique referred to above, only two increments are necessary between known values of B and therefore the $\delta_1 B$ error is sufficiently small.

Having determined the order of magnitude of intervals necessary to keep $\delta_1 B$ errors small, let us examine the errors due to the departure of the straight line approximation from the true curve in the interval between x_c and $x_c + \Delta x$. Since $\delta_1 B$ will be very small it is anticipated that the maximum value

of $\delta_2 B$ (see Fig. 3) will occur in the vicinity of $x_c + \frac{\Delta x}{2}$. $\delta_2 B$ at this point may be determined as shown below.

$$\delta_2 B = B\left(x_c + \frac{\Delta x}{2}\right) - B(x_c) - \frac{dB}{dx}\left(x_c + \frac{\Delta x}{2}\right)\frac{\Delta x}{2} \tag{5}$$

where:

$$B\left(x_c + \frac{\Delta x}{2}\right) - B(x_c) = \frac{2}{\pi}\left[\Delta x \sum_{n=1}^{n=\infty} \frac{x_c^{2n-2}}{2(2n-1)} + \Delta x^2 \sum_{n=1}^{n=\infty} \frac{n x_c^{2n-1}}{4(2n+1)} + \cdots\right]$$

$$\frac{dB}{dx}\left(x_c + \frac{\Delta x}{2}\right)\frac{\Delta x}{2} = \frac{2}{\pi}\left[\Delta x \sum_{n=1}^{n=\infty} \frac{x_c^{2n-2}}{2(2n-1)} + \Delta x^2 \sum_{n=1}^{n=\infty} \frac{n x_c^{2n-1}}{2(2n+1)} + \cdots\right].$$

Again retaining only the first term of the error function and dropping all higher order terms of Δx

$$\begin{aligned}\delta_2 B &\doteq \frac{2}{\pi}\left[\Delta x^2 \sum_{n=1}^{n=\infty} \frac{n x_c^{2n-1}}{4(2n+1)} - \Delta x^2 \sum_{n=1}^{n=\infty} \frac{n x_c^{2n-1}}{2(2n+1)}\right] \\ &= -\frac{\Delta x^2}{2\pi} \sum_{n=1}^{n=\infty} \frac{n x_c^{2n-1}}{2n+1}.\end{aligned} \tag{6}$$

$\delta_2 B$ proves to be negative and considerably larger than $\delta_1 B$ for the same magnitude of interval. Therefore the computed B will always exceed the true phase in the interval x_c to $x_c + \Delta x$ except above a value of x very near to $x_c + \Delta x$ where the straight line approximation crosses the true phase curve. When $x_c = .35$ and $\Delta x = .02$, $\delta_2 B$ is found to be $-.0005$ degree from (6) above, and for $x_c = .91$ and $\Delta x = .005$, $\delta_2 B$ is also found to be $-.0005$ degree. The $\delta_2 B$ errors are therefore found to be much more important than the $\delta_1 B$ errors. $\delta_2 B$ errors are not accumulative, however, and therefore increments of Δx of the above order of magnitude prove to be sufficiently small to give the accuracy being sought, namely $\pm$ .0005 degree in B.

An evaluation of the $\delta_1 B$ and $\delta_2 B$ errors for values of x_c greater than .9 is difficult due to the slowness of convergence of the series giving these errors. For values of x_c between .9 and unity, however, the frequency of known values of B determined from (1) above and available as check points is sufficient to check the adequacy of intervals insofar as $\delta_1 B$ errors are concerned. Furthermore an analysis similar to that given above for the determination of the $\delta_1 B$ and $\delta_2 B$ errors shows that an interpolation of the slopes computed for construction of the tables in question, to give the intervening slopes necessary to cut the increments of Δx in half will give check points at $x_c + \frac{\Delta x}{2}$ frequencies, with a $\delta_1 B$ error ($x_c + \frac{\Delta x}{2}$ is then the termination of a straight

line segment since the Δx interval has been halved) of comparable order of magnitude to the $\delta_1 B$ error for the original interval selected and therefore small in comparison to the $\delta_2 B$ error for the original Δx interval. This technique was therefore used in checking the adequacy of the intervals in so far as $\delta_2 B$ errors are concerned in the region $x_c = .9$ to $x_c = 1.0$.

Using the procedure outlined above the phase associated with the semi-infinite unit slope of attenuation of Fig. 1 was computed for values of f less than f_0 and is given as a function of f/f_0 in Table I in degrees and in Table III in radians. For values of f greater than f_0 the phase was computed as a function of f_0/f utilizing the odd symmetry behavior of the phase characteristic of Fig. 2 on opposite sides of $f/f_0 = 1$, and this phase is tabulated in Table II in degrees and in Table IV in radians. For the other type of semi-infinite unit slope of attenuation in which the attenuation slope is constant and equal to unity at all frequencies below f_0 and the attenuation is constant for all frequencies above f_0 (with the constant slope of attenuation intersecting the f_0 axis at the same point as the constant attenuation line) the same tables can be used by reading the values of phase for $f/f_0 < 1$ from the f_0/f tables and the values of phase for $f_0/f < 1$ from the f/f_0 tables.

The intervals over which the straight line approximation to the true phase was assumed are given below:

Δx			x_c	
.02	from	.00	to	.40
.01	"	.40	"	.70
.005	"	.70	"	.92
.002	"	.92	"	.98
.001	"	.98	"	.996
.0005	"	.996	"	.998
.0002	"	.998	"	.999
.0001	"	.999	"	.9998
.00005	"	.9998	"	1.0000

The points at which the cumulative sum of the straight line increments of phase was corrected to the phase as determined from (1) above are listed below:

Every	.1	from	.00	to	.40
"	.05	"	.40	"	.80
"	.02	"	.80	"	.90
"	.01	"	.90	"	.99

and at .996, .998, .999, and 1.000

A study of the errors based on the error analysis discussed above indicates that the computed values of B in degrees are accurate to $\pm$ .0005 degree and since there is an additional possibility of $\pm$ .0005 degree error in dropping all figures beyond the third decimal place, the over-all reliability of the degree tables is $\pm$ .001 degree. Similarly the computed values of B in radians are accurate to $\pm$ .00001 radian and since there is an additional possibility of $\pm$ .000005 radian error in dropping all figures beyond the fifth decimal

place, the over-all reliability of the radian tables is ± .000015 radian. Since the function tabulated was constructed by a series of straight line approximations to the true phase, interpolation to get the phase for values of f/f_0 or f_0/f between those given in the tables in problems where this is necessary, will result in the same accuracy as that given for the tabulated values.

Murlan S. Corrington[7] of Radio Corporation of America has computed the phase in radians for the semi-infinite unit slope of attenuation of Fig. 1 for approximately 100 values of f/f_0 using equations 15-9 and 15-11 of Bode's "Network Analysis and Feedback Amplifier Design" and has given a table of these values to five decimal places. Where the values of Table III differ from Corrington's values, his value is given as a superscript. Since his approach is the more exact one, it is assumed that where a difference exists, his value is correct. The differences have a maximum value of one figure in the fifth decimal place which is consistent with the accuracy of ± .000015 radian given for Table III. However, linear interpolation of Corrington's values to get the function to three figures in f/f_0, which precision in f/f_0 is really needed to utilize five figure accuracy in B, will result in errors considerably larger than those of Table III for the higher values of f/f_0.

ACKNOWLEDGMENT

The writer wishes to thank Miss J. D. Goeltz who carried out the calculations of the basic Tables and of the illustrative examples of this paper.

APPENDIX

USE OF TABLES I TO IV IN DETERMINING PHASE FROM ATTENUATION OR REACTANCE FROM RESISTANCE

The first step in determining the phase associated with a given attenuation characteristic using the tables described in the basic paper is to plot the attenuation as a function of log frequency to a suitable scale. Such an attenuation characteristic is illustrated in Fig. 4a. The attenuation characteristic is then approximated by a series of straight lines such as are shown in dotted form. The number of straight lines used will depend upon the accuracy desired in the resultant phase. As a rule, an approximation to the attenuation which does not depart by more than ± .5 *db* will give a resultant phase which does not depart by more than ± 3° from the true phase.

If we now examine the straight line attenuation approximation of Fig. 4a,

[7] Murlan S. Corrington, "Table of the Integral $\frac{2}{\pi}\int_0^x \frac{\tanh^{-1} t}{t}\,dt$" *R.C.A. Review* September, 1946, page 432.

we see that it can be constructed by adding a number of semi-infinite constant slopes of attenuation as shown in Fig. 4b. The first of these will be a semi-infinite slope of magnitude k_1 commencing at the first critical frequency

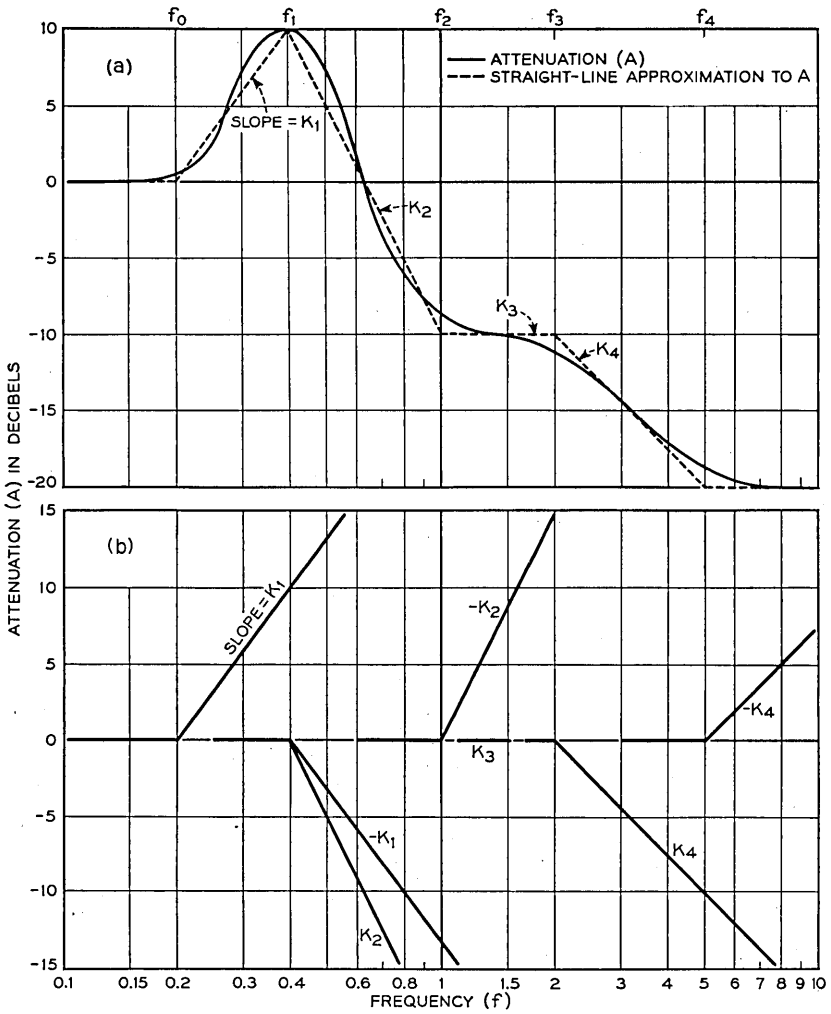

Fig. 4—(a) Straight line approximation to attenuation characteristic. (b) Individual semi-infinite constant slopes of attenuation which add to produce the straight line approximation of Fig. 4(a).

f_0. The second will be a semi-infinite slope of magnitude $-k_1$ commencing at the critical frequency f_1 which must be added to correct for the fact that the first straight line of slope $+k_1$ does not extend to infinity, but terminates at the critical frequency f_1, where the straight line approximation assumes a

new slope. In order to achieve this new slope a semi-infinite slope of magnitude k_2, commencing at frequency f_1, must be added. This process is continued up the frequency scale until the entire straight line approximation is constructed.

The total phase $\theta(f)$ at a particular frequency f is then given by the sum of the phase at frequency f associated with each of the semi-infinite constant slopes of attenuation which together make up the straight line approxmation.

Thus:

$$\theta(f) = k_1\theta_0 - k_1\theta_1 + k_2\theta_1 - k_2\theta_2 + k_3\theta_2 - k_3\theta_3 + k_4\theta_3 - k_4\theta_4$$

or for the general straight line approximation having slopes

$$k_1 , k_2 , \cdots k_n$$

$$\theta(f) = k_1 (\theta_0 - \theta_1) + k_2 (\theta_1 - \theta_2) + \cdots k_n (\theta_{n-1} - \theta_n)$$

where:

θ_n is the phase at frequency f associated with the semi-infinite unit slope of attenuation commencing at frequency f_n and extending to $f = \infty$ and is read from Tables I or III for $f < f_n$ and Tables II or IV for $f > f_n$,

and

k_n is the slope of the straight line approximation between f_{n-1} and f_n given by:

$$k_n = \frac{A_n - A_{n-1}}{20 \log \frac{f_n}{f_{n-1}}}$$

where:

A_n is the attenuation at frequency f_n on the straight line approximation.

Note that in Fig. 4a the attenuation is constant from zero frequency to the first critical frequency f_0. In many problems, there is a constant slope below frequency f_1 to frequency zero. In that event, the initial critical frequency, f_0, will be zero, and θ_0 will be 90°. ($f_0/f = 0$ at all finite frequencies.) When this occurs, k_1 must be determined by choosing a finite frequency f_0' and taking the ratio of attenuation change between f_0' and f_1 to 20 log of the ratio of f_1 to f_0'. Similarly, the attenuation is constant in the illustration from the top critical frequency f_4 to infinity, whereas in many problems the attenuation will have a constant slope extending from the top critical frequency to infinity. In these cases, the top critical frequency will be infinity and the final angle θ_n will, of course, be zero. Here again the final slope k_n must be determined over a finite portion of this infinite slope.

It will also be noted that in the illustration given the characteristic is approximated, commencing at zero frequency, by a series of semi-infinite slopes, each of which is a constant times the characteristic of Fig. 1 of the basic paper, for which Tables I to IV were computed. The characteristic could have been approximated just as well with a series of semi-infinite constant slopes, commencing at $f = \infty$ and going down in frequency, each having a flat attenuation above a critical frequency f_n and constant slope at frequencies below. In summing the phase for such an approximation Tables I to IV may be used by reading the angles for f/f_n from the f_0/f tables and vice versa as indicated in the basic paper.

As an illustration of the above procedure, consider the determination of the phase associated with the characteristic given by 20 log | Z | shown in Fig. 5. The characteristic is first approximated by a series of straight lines as shown in dotted form. The critical frequencies and values of $A = 20$ log | Z | at these critical frequencies are then read from the straight line approximation[8] and the slopes of the various straight line segments determined as illustrated in Table V.

Having determined the slopes of the various segments of the straight line approximation, the phase at any desired frequency is summed as illustrated in Table VI where the phase for $f = 1.5$ is summed.

The mesh computed value of θ for the network in question is plotted in Fig. 6 and it will be noted that the phase summation of Table VI checks the true value to within the accuracy to which the phase can be read from the curve. The identical procedure is followed in determining the phase at any other frequency. As an illustration of the accuracy of the method, the phase was determined at a considerable number of frequencies and the results shown as individual points in Fig. 6. The straight line approximation to 20 log | Z | of Fig. 5 was of the order of $\pm$ .25 *db* and, in accordance with the estimated accuracy of the method given above, the maximum departure of the phase summation from the true phase is approximately $\pm$ 1.5°.

A much simpler approximation than that of Fig. 5 may be used without a great loss in accuracy. For instance, a five-line approximation determined by the critical frequencies of Table VII will match 20 log | Z | to within approximately $\pm$ .5 *db* and therefore should give a phase summation within $\pm$ 3° of the true phase. The phase was actually summed at 12 frequencies chosen at random for this five-line approximation and the maximum departure of the summed phase from the true phase was 3.2°. With experience in use of the method, simpler approximations can be used and the phase determined more accurately than the limits of accuracy of the summation at individual frequencies by plotting the individual summations

[8] The original plot was expanded and had much greater scale detail than can be shown with clarity on a single page plate.

TABLE I—DEGREES PHASE (±.001°) FOR SEMI-INFINITE ATTENUATION SLOPE $k = 1 f < f_0$

f/f_0	0	1	2	3	4	5	6	7	8	9
.00	.000	.036	.073	.109	.146	.182	.219	.255	.292	.328
.01	.365	.401	.438	.474	.511	.547	.584	.620	.657	.693
.02	.730	.766	.803	.839	.875	.912	.948	.985	1.021	1.058
.03	1.094	1.131	1.167	1.204	1.240	1.277	1.313	1.350	1.386	1.423
.04	1.459	1.496	1.532	1.569	1.605	1.642	1.678	1.715	1.751	1.788
.05	1.824	1.861	1.897	1.934	1.970	2.007	2.043	2.080	2.116	2.153
.06	2.189	2.226	2.262	2.299	2.335	2.372	2.409	2.445	2.482	2.518
.07	2.555	2.591	2.628	2.664	2.701	2.737	2.774	2.810	2.847	2.884
.08	2.920	2.957	2.993	3.030	3.066	3.103	3.140	3.176	3.213	3.249
.09	3.286	3.322	3.359	3.396	3.432	3.469	3.505	3.542	3.578	3.615
.10	3.652	3.688	3.725	3.762	3.798	3.835	3.871	3.908	3.945	3.981
.11	4.018	4.054	4.091	4.128	4.164	4.201	4.238	4.274	4.311	4.347
.12	4.384	4.421	4.457	4.494	4.531	4.568	4.604	4.641	4.678	4.714
.13	4.751	4.788	4.824	4.861	4.898	4.934	4.971	5.008	5.044	5.081
.14	5.118	5.155	5.191	5.228	5.265	5.302	5.338	5.375	5.412	5.449
.15	5.485	5.522	5.559	5.596	5.632	5.669	5.706	5.743	5.779	5.816
.16	5.853	5.890	5.927	5.963	6.000	6.037	6.074	6.111	6.148	6.184
.17	6.221	6.258	6.295	6.332	6.369	6.405	6.442	6.479	6.516	6.553
.18	6.590	6.626	6.663	6.700	6.737	6.774	6.811	6.848	6.885	6.922
.19	6.959	6.996	7.033	7.070	7.106	7.143	7.180	7.217	7.254	7.291
.20	7.328	7.365	7.402	7.439	7.476	7.513	7.550	7.587	7.624	7.661
.21	7.698	7.735	7.772	7.809	7.846	7.883	7.920	7.957	7.994	8.032
.22	8.069	8.106	8.143	8.180	8.217	8.254	8.291	8.329	8.366	8.403
.23	8.440	8.477	8.514	8.551	8.589	8.626	8.663	8.700	8.737	8.774
.24	8.811	8.849	8.886	8.923	8.960	8.998	9.035	9.072	9.109	9.147
.25	9.184	9.221	9.259	9.296	9.333	9.370	9.408	9.445	9.482	9.519
.26	9.557	9.594	9.631	9.669	9.706	9.744	9.781	9.818	9.856	9.893
.27	9.931	9.968	10.006	10.043	10.080	10.118	10.155	10.193	10.230	10.267
.28	10.305	10.342	10.380	10.417	10.455	10.492	10.530	10.568	10.605	10.643
.29	10.680	10.718	10.755	10.793	10.830	10.868	10.906	10.943	10.981	11.018
.30	11.056	11.094	11.131	11.169	11.207	11.244	11.282	11.320	11.358	11.395
.31	11.433	11.471	11.508	11.546	11.584	11.622	11.659	11.697	11.735	11.772
.32	11.810	11.848	11.886	11.924	11.962	12.000	12.037	12.075	12.113	12.151
.33	12.189	12.227	12.265	12.303	12.341	12.379	12.416	12.454	12.492	12.530
.34	12.568	12.606	12.644	12.682	12.720	12.758	12.797	12.835	12.873	12.911
.35	12.949	12.987	13.025	13.063	13.101	13.139	13.177	13.215	13.254	13.292
.36	13.330	13.368	13.406	13.445	13.483	13.521	13.559	13.598	13.636	13.674
.37	13.713	13.751	13.789	13.827	13.866	13.904	13.942	13.981	14.019	14.057
.38	14.096	14.134	14.173	14.211	14.250	14.288	14.327	14.365	14.404	14.442
.39	14.481	14.519	14.558	14.596	14.635	14.673	14.712	14.750	14.789	14.827
.40	14.866	14.905	14.943	14.982	15.021	15.059	15.098	15.137	15.175	15.214
.41	15.253	15.292	15.330	15.369	15.408	15.447	15.486	15.525	15.563	15.602
.42	15.641	15.680	15.719	15.758	15.797	15.836	15.875	15.914	15.953	15.991
.43	16.030	16.070	16.109	16.148	16.187	16.226	16.265	16.304	16.343	16.382
.44	16.421	16.460	16.500	16.539	16.578	16.617	16.657	16.696	16.735	16.774
.45	16.813	16.853	16.892	16.931	16.971	17.010	17.050	17.089	17.128	17.168
.46	17.207	17.247	17.286	17.326	17.365	17.405	17.444	17.484	17.523	17.563
.47	17.602	17.642	17.681	17.721	17.761	17.800	17.840	17.880	17.919	17.959
.48	17.999	18.039	18.078	18.118	18.158	18.198	18.238	18.277	18.317	18.357
.49	18.397	18.437	18.477	18.517	18.557	18.597	18.637	18.677	18.717	18.757
.50	18.797	18.837	18.877	18.917	18.958	18.998	19.038	19.078	19.118	19.158
.51	19.198	19.239	19.279	19.320	19.360	19.400	19.441	19.481	19.521	19.562
.52	19.602	19.642	19.683	19.723	19.764	19.804	19.845	19.885	19.926	19.967
.53	20.007	20.048	20.088	20.129	20.170	20.211	20.251	20.292	20.333	20.373
.54	20.414	20.455	20.496	20.537	20.578	20.619	20.660	20.701	20.741	20.782

TABLE I—*Continued*

f/f_0	0	1	2	3	4	5	6	7	8	9
.55	20.823	20.864	20.906	20.947	20.988	21.029	21.070	21.111	21.152	21.193
.56	21.234	21.276	21.317	21.358	21.400	21.441	21.482	21.524	21.565	21.606
.57	21.648	21.689	21.731	21.772	21.814	21.855	21.897	21.939	21.980	22.022
.58	22.063	22.105	22.147	22.189	22.230	22.272	22.314	22.356	22.397	22.439
.59	22.481	22.523	22.565	22.607	22.649	22.691	22.733	22.775	22.817	22.859
.60	22.901	22.943	22.986	23.028	23.070	23.112	23.155	23.197	23.239	23.281
.61	23.324	23.366	23.409	23.451	23.494	23.536	23.579	23.621	23.664	23.706
.62	23.749	23.792	23.834	23.877	23.920	23.963	24.006	24.048	24.091	24.134
.63	24.177	24.220	24.263	24.306	24.349	24.392	24.435	24.478	24.521	24.564
.64	24.607	24.651	24.694	24.738	24.781	24.824	24.868	24.911	24.954	24.998
.65	25.041	25.085	25.128	25.172	25.216	25.259	25.303	25.347	25.390	25.434
.66	25.478	25.522	25.566	25.610	25.654	25.698	25.742	25.786	25.830	25.873
.67	25.917	25.962	26.006	26.050	26.095	26.139	26.183	26.228	26.272	26.316
.68	26.361	26.405	26.450	26.494	26.539	26.584	26.628	26.673	26.718	26.762
.69	26.807	26.852	26.897	26.942	26.987	27.032	27.077	27.122	27.167	27.212
.70	27.257	27.302	27.348	27.393	27.438	27.484	27.529	27.574	27.620	27.665
.71	27.711	27.757	27.802	27.848	27.894	27.939	27.985	28.031	28.077	28.123
.72	28.169	28.215	28.261	28.307	28.353	28.399	28.445	28.492	28.538	28.584
.73	28.631	28.677	28.724	28.770	28.817	28.863	28.910	28.957	29.003	29.050
.74	29.097	29.144	29.191	29.238	29.285	29.332	29.379	29.426	29.473	29.521
.75	29.568	29.615	29.663	29.710	29.757	29.805	29.853	29.900	29.948	29.996
.76	30.043	30.091	30.139	30.187	30.235	30.283	30.331	30.379	30.428	30.476
.77	30.524	30.572	30.621	30.669	30.718	30.766	30.815	30.864	30.913	30.961
.78	31.010	31.059	31.108	31.157	31.206	31.255	31.305	31.354	31.403	31.453
.79	31.502	31.551	31.601	31.651	31.700	31.750	31.800	31.850	31.900	31.950
.80	32.000	32.050	32.100	32.150	32.201	32.251	32.301	32.352	32.403	32.453
.81	32.504	32.555	32.606	32.657	32.707	32.758	32.810	32.861	32.912	32.963
.82	33.015	33.066	33.118	33.170	33.221	33.273	33.325	33.377	33.429	33.481
.83	33.533	33.586	33.638	33.690	33.743	33.795	33.848	33.901	33.954	34.006
.84	34.059	34.113	34.166	34.219	34.272	34.325	34.379	34.433	34.486	34.540
.85	34.594	34.648	34.702	34.756	34.810	34.865	34.919	34.974	35.028	35.083
.86	35.138	35.193	35.248	35.303	35.358	35.413	35.469	35.524	35.580	35.636
.87	35.691	35.747	35.804	35.860	35.916	35.972	36.029	36.086	36.142	36.199
.88	36.256	36.313	36.370	36.428	36.485	36.542	36.600	36.658	36.716	36.774
.89	36.832	36.891	36.949	37.008	37.067	37.125	37.184	37.244	37.303	37.362
.90	37.422	37.482	37.542	37.602	37.662	37.722	37.783	37.844	37.904	37.965
.91	38.026	38.088	38.149	38.211	38.273	38.334	38.397	38.459	38.522	38.584
.92	38.647	38.710	38.773	38.837	38.901	38.965	39.029	39.093	39.157	39.222
.93	39.287	39.352	39.418	39.483	39.549	39.615	39.681	39.748	39.815	39.882
.94	39.949	40.017	40.085	40.153	40.221	40.290	40.359	40.428	40.497	40.567
.95	40.638	40.708	40.779	40.850	40.921	40.993	41.066	41.138	41.211	41.285
.96	41.358	41.432	41.507	41.582	41.657	41.733	41.809	41.887	41.964	42.042
.97	42.120	42.199	42.278	42.359	42.439	42.521	42.603	42.686	42.769	42.854
.98	42.938	43.024	43.111	43.199	43.288	43.378	43.469	43.561	43.655	43.750
.99	43.846	43.945	44.045	44.148	44.253	44.361	44.473	(refer to table below)		

.9960	44.473	.9984	44.763	.9992	44.871
.9965	44.530	.9985	44.776	.9993	44.886
.9970	44.589	.9986	44.789	.9994	44.900
.9975	44.649	.9987	44.802	.9995	44.915
.9980	44.711	.9988	44.816	.9996	44.931
.9981	44.724	.9989	44.829	.9997	44.946
.9982	44.737	.9990	44.843	.9998	44.963
.9983	44.750	.9991	44.857	.9999	44.980
				1.0000	45.000

TABLE II—DEGREES PHASE (±.001°) FOR SEMI-INFINITE ATTENUATION SLOPE $k = 1$
$f > f_0$

f_0/f	0	1	2	3	4	5	6	7	8	9
.00	90.000	89.964	89.927	89.891	89.854	89.818	89.781	89.745	89.708	89.672
.01	89.635	89.599	89.562	89.526	89.489	89.453	89.416	89.380	89.343	89.307
.02	89.270	89.234	89.197	89.161	89.125	89.088	89.052	89.015	88.979	88.942
.03	88.906	88.869	88.833	88.796	88.760	88.723	88.687	88.650	88.614	88.577
.04	88.541	88.504	88.468	88.431	88.395	88.358	88.322	88.285	88.249	88.212
.05	88.176	88.139	88.103	88.066	88.030	87.993	87.957	87.920	87.884	87.847
.06	87.811	87.774	87.738	87.701	87.665	87.628	87.591	87.555	87.518	87.482
.07	87.445	87.409	87.372	87.336	87.299	87.263	87.226	87.190	87.153	87.116
.08	87.080	87.043	87.007	86.970	86.934	86.897	86.860	86.824	86.787	86.751
.09	86.714	86.678	86.641	86.604	86.568	86.531	86.495	86.458	86.422	86.385
.10	86.348	86.312	86.275	86.238	86.202	86.165	86.129	86.092	86.055	86.019
.11	85.982	85.946	85.909	85.872	85.836	85.799	85.762	85.726	85.689	85.653
.12	85.616	85.579	85.543	85.506	85.469	85.432	85.396	85.359	85.322	85.286
.13	85.249	85.212	85.176	85.139	85.102	85.066	85.029	84.992	84.956	84.919
.14	84.882	84.845	84.809	84.772	84.735	84.698	84.662	84.625	84.588	84.551
.15	84.515	84.478	84.441	84.404	84.368	84.331	84.294	84.257	84.221	84.184
.16	84.147	84.110	84.073	84.037	84.000	83.963	83.926	83.889	83.852	83.816
.17	83.779	83.742	83.705	83.668	83.631	83.595	83.558	83.521	83.484	83.447
.18	83.410	83.374	83.337	83.300	83.263	83.226	83.189	83.152	83.115	83.078
.19	83.041	83.004	82.967	82.930	82.894	82.857	82.820	82.783	82.746	82.709
.20	82.672	82.635	82.598	82.561	82.524	82.487	82.450	82.413	82.376	82.339
.21	82.302	82.265	82.228	82.191	82.154	82.117	82.080	82.043	82.006	81.968
.22	81.931	81.894	81.857	81.820	81.783	81.746	81.709	81.671	81.634	81.597
.23	81.560	81.523	81.486	81.449	81.411	81.374	81.337	81.300	81.263	81.226
.24	81.189	81.151	81.114	81.077	81.040	81.002	80.965	80.928	80.891	80.853
.25	80.816	80.779	80.741	80.704	80.667	80.630	80.592	80.555	80.518	80.481
.26	80.443	80.406	80.369	80.331	80.294	80.256	80.219	80.182	80.144	80.107
.27	80.069	80.032	79.994	79.957	79.920	79.882	79.845	79.807	79.770	79.733
.28	79.695	79.658	79.620	79.583	79.545	79.508	79.470	79.432	79.395	79.357
.29	79.320	79.282	79.245	79.207	79.170	79.132	79.094	79.057	79.019	78.982
.30	78.944	78.906	78.869	78.831	78.793	78.756	78.718	78.680	78.642	78.605
.31	78.567	78.529	78.492	78.454	78.416	78.378	78.341	78.303	78.265	78.228
.32	78.190	78.152	78.114	78.076	78.038	78.000	77.963	77.925	77.887	77.849
.33	77.811	77.773	77.735	77.697	77.659	77.621	77.584	77.546	77.508	77.470
.34	77.432	77.394	77.356	77.318	77.280	77.242	77.203	77.165	77.127	77.089
.35	77.051	77.013	76.975	76.937	76.899	76.861	76.823	76.785	76.746	76.708
.36	76.670	76.632	76.594	76.555	76.517	76.479	76.441	76.402	76.364	76.326
.37	76.287	76.249	76.211	76.173	76.134	76.096	76.058	76.019	75.981	75.943
.38	75.904	75.866	75.827	75.789	75.750	75.712	75.673	75.635	75.596	75.558
.39	75.519	75.481	75.442	75.404	75.365	75.327	75.288	75.250	75.211	75.173
.40	75.134	75.095	75.057	75.018	74.979	74.941	74.902	74.863	74.825	74.786
.41	74.747	74.708	74.670	74.631	74.592	74.553	74.514	74.475	74.437	74.398
.42	74.359	74.320	74.281	74.242	74.203	74.164	74.125	74.086	74.047	74.009
.43	73.970	73.930	73.891	73.852	73.813	73.774	73.735	73.696	73.657	73.618
.44	73.579	73.540	73.500	73.461	73.422	73.383	73.343	73.304	73.265	73.226
.45	73.187	73.147	73.108	73.069	73.029	72.990	72.950	72.911	72.872	72.832
.46	72.793	72.753	72.714	72.674	72.635	72.595	72.556	72.516	72.477	72.437
.47	72.398	72.358	72.319	72.279	72.239	72.200	72.160	72.120	72.081	72.041
.48	72.001	71.961	71.922	71.882	71.842	71.802	71.762	71.723	71.683	71.643
.49	71.603	71.563	71.523	71.483	71.443	71.403	71.363	71.323	71.283	71.243
.50	71.203	71.163	71.123	71.083	71.042	71.002	70.962	70.922	70.882	70.842
.51	70.802	70.761	70.721	70.680	70.640	70.600	70.559	70.519	70.479	70.438
.52	70.398	70.358	70.317	70.277	70.236	70.196	70.155	70.115	70.074	70.033
.53	69.993	69.952	69.912	69.871	69.830	69.789	69.749	69.708	69.667	69.627
.54	69.586	69.545	69.504	69.463	69.422	69.381	69.340	69.299	69.259	69.218

TABLE II—*Continued*

f_0/f	0	1	2	3	4	5	6	7	8	9
.55	69.177	69.136	69.094	69.053	69.012	68.971	68.930	68.889	68.848	68.807
.56	68.766	68.724	68.683	68.642	68.600	68.559	68.518	68.476	68.435	68.394
.57	68.352	68.311	68.269	68.228	68.186	68.145	68.103	68.061	68.020	67.978
.58	67.937	67.895	67.853	67.811	67.770	67.728	67.686	67.644	67.603	67.561
.59	67.519	67.477	67.435	67.393	67.351	67.309	67.267	67.225	67.183	67.141
.60	67.099	67.057	67.014	66.972	66.930	66.888	66.845	66.803	66.761	66.719
.61	66.676	66.634	66.591	66.549	66.506	66.464	66.421	66.379	66.336	66.294
.62	66.251	66.208	66.166	66.123	66.080	66.037	65.994	65.952	65.909	65.866
.63	65.823	65.780	65.737	65.694	65.651	65.608	65.565	65.522	65.479	65.436
.64	65.393	65.349	65.306	65.262	65.219	65.176	65.132	65.089	65.046	65.002
.65	64.959	64.915	64.872	64.828	64.784	64.741	64.697	64.653	64.610	64.566
.66	64.522	64.478	64.434	64.390	64.346	64.302	64.258	64.214	64.170	64.127
.67	64.083	64.038	63.994	63.950	63.905	63.861	63.817	63.772	63.728	63.684
.68	63.639	63.595	63.550	63.506	63.461	63.416	63.372	63.327	63.282	63.238
.69	63.193	63.148	63.103	63.058	63.013	62.968	62.923	62.878	62.833	62.788
.70	62.743	62.698	62.652	62.607	62.562	62.516	62.471	62.426	62.380	62.335
.71	62.289	62.243	62.198	62.152	62.106	62.061	62.015	61.969	61.923	61.877
.72	61.831	61.785	61.739	61.693	61.647	61.601	61.555	61.508	61.462	61.416
.73	61.369	61.323	61.276	61.230	61.183	61.137	61.090	61.043	60.997	60.950
.74	60.903	60.856	60.809	60.762	60.715	60.668	60.621	60.574	60.527	60.479
.75	60.432	60.385	60.337	60.290	60.243	60.195	60.147	60.100	60.052	60.004
.76	59.957	59.909	59.861	59.813	59.765	59.717	59.669	59.621	59.572	59.524
.77	59.476	59.428	59.379	59.331	59.282	59.234	59.185	59.136	59.087	59.039
.78	58.990	58.941	58.892	58.843	58.794	58.745	58.695	58.646	58.597	58.547
.79	58.498	58.449	58.399	58.349	58.300	58.250	58.200	58.150	58.100	58.050
.80	58.000	57.950	57.900	57.850	57.799	57.749	57.699	57.648	57.597	57.547
.81	57.496	57.445	57.394	57.343	57.293	57.242	57.190	57.139	57.088	57.037
.82	56.985	56.934	56.882	56.830	56.779	56.727	56.675	56.623	56.571	56.519
.83	56.467	56.414	56.362	56.310	56.257	56.205	56.152	56.099	56.046	55.994
.84	55.941	55.887	55.834	55.781	55.728	55.675	55.621	55.567	55.514	55.460
.85	55.406	55.352	55.298	55.244	55.190	55.135	55.081	55.026	54.972	54.917
.86	54.862	54.807	54.752	54.697	54.642	54.587	54.531	54.476	54.420	54.364
.87	54.309	54.253	54.196	54.140	54.084	54.028	53.971	53.914	53.858	53.801
.88	53.744	53.687	53.630	53.572	53.515	53.458	53.400	53.342	53.284	53.226
.89	53.168	53.109	53.051	52.992	52.933	52.875	52.816	52.756	52.697	52.638
.90	52.578	52.518	52.458	52.398	52.338	52.278	52.217	52.156	52.096	52.035
.91	51.974	51.912	51.851	51.789	51.727	51.666	51.603	51.541	51.478	51.416
.92	51.353	51.290	51.227	51.163	51.099	51.035	50.971	50.907	50.843	50.778
.93	50.713	50.648	50.582	50.517	50.451	50.385	50.319	50.252	50.185	50.118
.94	50.051	49.983	49.915	49.847	49.779	49.710	49.641	49.572	49.503	49.433
.95	49.362	49.292	49.221	49.150	49.079	49.007	48.934	48.862	48.789	48.715
.96	48.642	48.568	48.493	48.418	48.343	48.267	48.191	48.113	48.036	47.958
.97	47.880	47.801	47.722	47.641	47.561	47.479	47.397	47.314	47.231	47.146
.98	47.062	46.976	46.889	46.801	46.712	46.622	46.531	46.439	46.345	46.250
.99	46.154	46.055	45.955	45.852	45.747	45.639	45.527	(refer to table below)		

.9960	45.527	.9984	45.237	.9992	45.129
.9965	45.470	.9985	45.224	.9993	45.114
.9970	45.411	.9986	45.211	.9994	45.100
.9975	45.351	.9987	45.198	.9995	45.085
.9980	45.289	.9988	45.184	.9996	45.069
.9981	45.276	.9989	45.171	.9997	45.054
.9982	45.263	.9990	45.157	.9998	45.037
.9983	45.250	.9991	45.143	.9999	45.020
				1.0000	45.000

TABLE III—RADIANS PHASE (±.000015) FOR SEMI-INFINITE ATTENUATION SLOPE $k = 1 f < f_0$

f/f_0	0	1	2	3	4	5	6	7	8	9
.00	0.00000	0.00064	0.00127	0.00191	0.00255	0.00318	0.00382	0.00446	0.00509	0.00573
.01	0.00637	0.00700	0.00764	0.00828	0.00891	0.00955	0.01019	0.01082	0.01146	0.01210
.02	0.01273	0.01337	0.01401	0.01464	0.01528	0.01592	0.01655	0.01719	0.01783	0.01846
.03	0.01910	0.01974	0.02037	0.02101	0.02165	0.02228	0.02292	0.02356	0.02419	0.02483
.04	0.02547	0.02611	0.02674	0.02738	0.02802	0.02865	0.02929	0.02993	0.03057	0.03120
.05	0.03184	0.03248	0.03311	0.03375	0.03439	0.03503	0.03566	0.03630	0.03694	0.03757
.06	0.03821	0.03885	0.03949	0.04012	0.04076	0.04140	0.04204	0.04267	0.04331	0.04395
.07	0.04459	0.04523	0.04586	0.04650	0.04714	0.04778	0.04841	0.04905	0.04969	0.05033
.08	0.05097	0.05160	0.05224	0.05288	0.05352	0.05416	0.05479	0.05543	0.05607	0.05671
.09	0.05735	0.05799	0.05862	0.05926	0.05990	0.06054	0.06118	0.06182	0.06245	0.06309
.10	0.06373	0.06437	0.06501	0.06565	0.06629	0.06693	0.06757	0.06821	0.06885	0.06949
.11	0.07013[2]	0.07076	0.07140	0.07204	0.07268	0.07332	0.07396	0.07460	0.07524	0.07588
.12	0.07652	0.07716	0.07780	0.07844	0.07908	0.07972	0.08036	0.08100	0.08164	0.08228
.13	0.08292	0.08356	0.08420	0.08484	0.08548	0.08612	0.08676	0.08740	0.08804	0.08868
.14	0.08932	0.08996	0.09061	0.09125	0.09189	0.09253	0.09317	0.09381	0.09445	0.09509
.15	0.09574[3]	0.09638	0.09702	0.09766	0.09830	0.09894	0.09959	0.10023	0.10087	0.10151
.16	0.10215	0.10279	0.10344	0.10408	0.10472	0.10537	0.10601	0.10665	0.10729	0.10794
.17	0.10858	0.10922	0.10987	0.11051	0.11115	0.11179	0.11244	0.11308	0.11372	0.11437
.18	0.11501	0.11565	0.11630	0.11694	0.11759	0.11823	0.11888	0.11952	0.12016	0.12081
.19	0.12145	0.12210	0.12274	0.12339	0.12403	0.12468	0.12532	0.12596	0.12661	0.12725
.20	0.12790	0.12854	0.12919	0.12984	0.13048	0.13113	0.13178	0.13242	0.13307	0.13371
.21	0.13436	0.13501	0.13565	0.13630	0.13695	0.13759	0.13824	0.13888	0.13953	0.14018
.22	0.14082	0.14147	0.14212	0.14277	0.14342	0.14406	0.14471	0.14536	0.14601	0.14666
.23	0.14730	0.14795	0.14860	0.14925	0.14990	0.15055	0.15119	0.15184	0.15249	0.15314
.24	0.15379	0.15444	0.15509	0.15574	0.15639	0.15704	0.15769	0.15834	0.15899	0.15964
.25	0.16029	0.16094	0.16159	0.16224	0.16289	0.16354	0.16419	0.16484	0.16549	0.16615
.26	0.16680	0.16745	0.16810	0.16875	0.16941	0.17006	0.17071	0.17137	0.17202	0.17267
.27	0.17332	0.17398	0.17463	0.17528	0.17593	0.17659	0.17724	0.17789	0.17855	0.17920
.28	0.17985	0.18051	0.18116	0.18182	0.18247	0.18313	0.18378	0.18444	0.18509	0.18575
.29	0.18641[0]	0.18706	0.18772	0.18837	0.18903	0.18968	0.19034	0.19099	0.19165	0.19230
.30	0.19296	0.19362	0.19428	0.19493	0.19559	0.19625	0.19691	0.19757	0.19823	0.19888
.31	0.19954	0.20020	0.20086	0.20152	0.20218	0.20283	0.20349	0.20415	0.20481	0.20547
.32	0.20613	0.20679	0.20745	0.20811	0.20877	0.20943	0.21009	0.21076	0.21142	0.21208
.33	0.21274[3]	0.21340	0.21406	0.21472	0.21538	0.21605	0.21671	0.21737	0.21803	0.21869
.34	0.21935	0.22002	0.22068	0.22135	0.22201	0.22268	0.22334	0.22401	0.22467	0.22534
.35	0.226[5]0[9]0[9]	0.22666	0.22733	0.22799	0.22866	0.22932	0.22999	0.23065	0.23132	0.23198
.36	0.23265	0.23332	0.23398	0.23465	0.23532	0.23599	0.23666	0.23732	0.23799	0.23866
.37	0.23933[2]	0.24000	0.24067	0.24134	0.24200	0.24267	0.24334	0.24401	0.24468	0.24534
.38	0.24601	0.24669	0.24736	0.24803	0.24870	0.24937	0.25005	0.25072	0.25139	0.25206
.39	0.25274[3]	0.25341	0.25408	0.25475	0.25542	0.25610	0.25677	0.25744	0.25811	0.25879
.40	0.25946	0.26013	0.26081	0.26148	0.26216	0.26284	0.26351	0.26419	0.26486	0.26554
.41	0.26621	0.26689	0.26757	0.26824	0.26892	0.26960	0.27028	0.27095	0.27163	0.27231
.42	0.27299	0.27367	0.27435	0.27503	0.27571	0.27639	0.27706	0.27774	0.27842	0.27910
.43	0.27978	0.28047	0.28115	0.28183	0.28251	0.28319	0.28388	0.28456	0.28524	0.28592
.44	0.28660[1]	0.28729	0.28797	0.28866	0.28934	0.29003	0.29071	0.29140	0.29208	0.29276
.45	0.29345	0.29414	0.29482	0.29551	0.29620	0.29688	0.29757	0.29826	0.29894	0.29963
.46	0.30032	0.30101	0.30170	0.30239	0.30308	0.30377	0.30446	0.30515	0.30584	0.30652
.47	0.30721[2]	0.30791	0.30860	0.30929	0.30998	0.31068	0.31137	0.31206	0.31275	0.31344
.48	0.31414	0.31483	0.31553	0.31622	0.31692	0.31761	0.31831	0.31900	0.31970	0.32039
.49	0.32109	0.32179	0.32248	0.32318	0.32388	0.32458	0.32527	0.32597	0.32667	0.32737
.50	0.32807	0.32877	0.32947	0.33017	0.33087	0.33157	0.33227	0.33297	0.33368	0.33438
.51	0.33508	0.33578	0.33648	0.33719	0.33789	0.33860	0.33930	0.34000	0.34071	0.34141
.52	0.34212	0.34282	0.34353	0.34424	0.34495	0.34565	0.34636	0.34707	0.34777	0.34848
.53	0.34919	0.34990	0.35061	0.35132	0.35203	0.35274	0.35345	0.35416	0.35487	0.35558
.54	0.35629	0.35701	0.35772	0.35844	0.35915	0.35986	0.36058	0.36129	0.36201	0.36272

Superscripts—Corrington's values.

TABLE III—*Continued*

f/f_0	0	1	2	3	4	5	6	7	8	9
.55	0.36343	0.36415	0.36487	0.36559	0.36631	0.36702	0.36774	0.36846	0.36918	0.36989
.56	0.37061	0.37133	0.37205	0.37277	0.37350	0.37422	0.37494	0.37566	0.37638	0.37710
.57	0.37782	0.37855	0.37927	0.38000	0.38072	0.38145	0.38217	0.38290	0.38362	0.38435
.58	0.38507	0.38580	0.38653	0.38726	0.38799	0.38872	0.38945	0.39018	0.39091	0.39164
.59	0.39237	0.39310	0.39383	0.39457	0.39530	0.39603	0.39677	0.39750	0.39823	0.39897
.60	0.39970	0.40044	0.40117	0.40191	0.40265	0.40339	0.40413	0.40486	0.40560	0.40634
.61	0.40708	0.40782	0.40856	0.40930	0.41004	0.41079	0.41153	0.41227	0.41301	0.41375
.62	0.41450	0.41524	0.41599	0.41674	0.41748	0.41823	0.41898	0.41972	0.42047	0.42122
.63	0.42197	0.42272	0.42347	0.42422	0.42497	0.42572	0.42647	0.42723	0.42798	0.42873
.64	0.42948	0.43024	0.43100	0.43175	0.43251	0.43327	0.43402	0.43478	0.43554	0.43629
.65	0.43705	0.43781	0.43857	0.43934	0.44010	0.44086	0.44162	0.44238	0.44315	0.44391
.66	0.44467	0.44544	0.44620	0.44697	0.44774	0.44851	0.44927	0.45004	0.45081	0.45158
.67	0.45234	0.45312	0.45389	0.45466	0.45544	0.45621	0.45698	0.45776	0.45853	0.45930
.68	0.46008	0.46086	0.46164	0.46242	0.46319	0.46397	0.46475	0.46553	0.46631	0.46709
.69	0.46787	0.46866	0.46944	0.47023	0.47101	0.47180	0.47258	0.47337	0.47415	0.47494
.70	0.47573	0.47652	0.47731	0.47810	0.47889	0.47968	0.48047	0.48127	0.48206	0.48285
.71	0.48365	0.48444	0.48524	0.48604	0.48684	0.48763	0.48843	0.48923	0.49004	0.49084
.72	0.49164	0.49244	0.49325	0.49405	0.49485	0.49566	0.49647	0.49727	0.49808	0.49889
.73	0.49970	0.50051	0.50132	0.50213	0.50295	0.50376	0.50457	0.50539	0.50621	0.50702
.74	0.50784	0.50866	0.50948	0.51030	0.51112	0.51194	0.51276	0.51358	0.51441	0.51523
.75	0.51605	0.51688	0.51771	0.51854	0.51937	0.52019	0.52103	0.52186	0.52269	0.52352
.76	0.52436	0.52519	0.52603	0.52686	0.52770	0.52854	0.52938	0.53022	0.53106	0.53190
.77	0.53274[5]	0.53359	0.53444	0.53528	0.53613	0.53697	0.53783	0.53868	0.53953	0.54038
.78	0.54123	0.54208	0.54294	0.54380	0.54465	0.54551	0.54637	0.54723	0.54809	0.54895
.79	0.54981	0.55068	0.55154	0.55241	0.55327	0.55414	0.55501	0.55588	0.55676	0.55763
.80	0.55850	0.55938	0.56025	0.56113	0.56201	0.56288	0.56377	0.56465	0.56553	0.56642
.81	0.56730	0.56819	0.56908	0.56996	0.57085	0.57174	0.57264	0.57353	0.57443	0.57532
.82	0.57622	0.57712	0.57802	0.57892	0.57982	0.58072	0.58163	0.58254	0.58345	0.58436
.83	0.58526	0.58618	0.58709	0.58801	0.58892	0.58984	0.59076	0.59168	0.59260	0.59353
.84	0.59445	0.59538	0.59631	0.59723	0.59816	0.59909	0.60003	0.60097	0.60190	0.60284
.85	0.60378	0.60472	0.60567	0.60661	0.60756	0.60850	0.60945	0.61041	0.61136	0.61231
.86	0.61327	0.61423	0.61519	0.61615	0.61711	0.61808	0.61905	0.62002	0.62099	0.62196
.87	0.62293	0.62391	0.62489	0.62587	0.62685	0.62783	0.62882	0.62981	0.63080	0.63179
.88	0.63278	0.63378	0.63478	0.63578	0.63678	0.63779	0.63880	0.63981	0.64082	0.64183
.89	0.64284	0.64387	0.64489	0.64591	0.64693	0.64796	0.64899	0.65003	0.65106	0.65210
.90	0.65313	0.65418	0.65523	0.65628	0.65733	0.65837	0.65943	0.66050	0.66156	0.66262
.91	0.66368	0.66476	0.66583	0.66691	0.66798	0.66906	0.67015	0.67124	0.67233	0.67343
.92	0.67452	0.67562	0.67672	0.67783	0.67894	0.68006	0.68118	0.68230	0.68342	0.68456
.93	0.68569	0.68683	0.68797	0.68911	0.69026	0.69141	0.69257	0.69373	0.69490	0.69607
.94	0.69724	0.69843	0.69961	0.70080	0.70199	0.70319	0.70439	0.70560	0.70681	0.70804
.95	0.70926	0.71049	0.71172	0.71297	0.71421	0.71547	0.71673	0.71800	0.71927	0.72055
.96	0.72183	0.72313	0.72443	0.72574	0.72706	0.72838	0.72971	0.73106	0.73240	0.73377
.97	0.73513	0.73651	0.73790	0.73930	0.74070	0.74213	0.74356	0.74501	0.74646	0.74794
.98	0.74942	0.75092	0.75243	0.75397	0.75552	0.75709[8]	0.75867	0.76028	0.76192	0.76358
.99	0.76527	0.76698	0.76874[3]	0.77053	0.77236	0.77425	0.77620	(refer to table below)		

.9960	0.77620	.9984	0.78125	.9992	0.78315
.9965	0.77720	.9985	0.78148	.9993	0.78340
.9970	0.77822	.9986	0.78171	.9994	0.78366
.9975	0.77928	.9987	0.78195	.9995	0.78392
.9980	0.78036	.9988	0.78218	.9996	0.78419
.9981	0.78058	.9989	0.78242	.9997	0.78446
.9982	0.78080	.9990	0.78266	.9998	0.78475
.9983	0.78103	.9991	0.78290	.9999	0.78505
				1.0000	0.78540

TABLE IV—RADIANS PHASE (±.000015) FOR SEMI-INFINITE ATTENUATION SLOPE $k = 1$
$f > f_0$

f_0/f	0	1	2	3	4	5	6	7	8	9
.00	1.57080	1.57016	1.56952	1.56889	1.56825	1.56761	1.56698	1.56634	1.56570	1.56507
.01	1.56443	1.56379	1.56316	1.56252	1.56188	1.56125	1.56061	1.55997	1.55934	1.55870
.02	1.55806	1.55743	1.55679	1.55615	1.55552	1.55488	1.55424	1.55361	1.55297	1.55233
.03	1.55170	1.55106	1.55042	1.54979	1.54915	1.54851	1.54787	1.54724	1.54660	1.54596
.04	1.54533	1.54469	1.54405	1.54342	1.54278	1.54214	1.54150	1.54087	1.54023	1.53959
.05	1.53896	1.53832	1.53768	1.53704	1.53641	1.53577	1.53513	1.53450	1.53386	1.53322
.06	1.53258	1.53195	1.53131	1.53067	1.53003	1.52940	1.52876	1.52812	1.52748	1.52685
.07	1.52621	1.52557	1.52493	1.52430	1.52366	1.52302	1.52238	1.52174	1.52111	1.52047
.08	1.51983	1.51919	1.51855	1.51792	1.51728	1.51664	1.51600	1.51536	1.51472	1.51409
.09	1.51345	1.51281	1.51217	1.51153	1.51089	1.51026	1.50962	1.50898	1.50834	1.50770
.10	1.50706	1.50642	1.50578	1.50515	1.50451	1.50387	1.50323	1.50259	1.50195	1.50131
.11	1.50067	1.50003	1.49939	1.49875	1.49811	1.49748	1.49684	1.49620	1.49556	1.49492
.12	1.49428	1.49364	1.49300	1.49236	1.49172	1.49108	1.49044	1.48980	1.48916	1.48852
.13	1.48788	1.48724	1.48660	1.48596	1.48532	1.48468	1.48404	1.48339	1.48275	1.48211
.14	1.48147	1.48083	1.48019	1.47955	1.47891	1.47827	1.47763	1.47698	1.47634	1.47570
.15	1.47506	1.47442	1.47378	1.47314	1.47249	1.47185	1.47121	1.47057	1.46993	1.46929
.16	1.46864	1.46800	1.46736	1.46672	1.46607	1.46543	1.46479	1.46414	1.46350	1.46286
.17	1.46222	1.46157	1.46093	1.46029	1.45964	1.45900	1.45836	1.45772	1.45707	1.45643
.18	1.45579	1.45514	1.45450	1.45385	1.45321	1.45257	1.45192	1.45128	1.45063	1.44999
.19	1.44934	1.44870	1.44805	1.44741	1.44677	1.44612	1.44548	1.44483	1.44419	1.44354
.20	1.44290	1.44225	1.44161	1.44096	1.44031	1.43967	1.43902	1.43837	1.43773	1.43708
.21	1.43644	1.43579	1.43514	1.43450	1.43385	1.43320	1.43256	1.43191	1.43127	1.43062
.22	1.42997	1.42933	1.42868	1.42803	1.42738	1.42673	1.42608	1.42544	1.42479	1.42414
.23	1.42349	1.42284	1.42219	1.42155	1.42090	1.42025	1.41960	1.41895	1.41831	1.41766
.24	1.41701	1.41636	1.41571	1.41506	1.41441	1.41376	1.41311	1.41246	1.41181	1.41116
.25	1.41050	1.40985	1.40920	1.40855	1.40790	1.40725	1.40660	1.40595	1.40530	1.40465
.26	1.40400	1.40335	1.40270	1.40204	1.40139	1.40074	1.40008	1.39943	1.39878	1.39813
.27	1.39747	1.39682	1.39617	1.39551	1.39486	1.39421	1.39356	1.39290	1.39225	1.39160
.28	1.39094	1.39029	1.38963	1.38898	1.38832	1.38767	1.38701	1.38636	1.38570	1.38505
.29	1.38439	1.38374	1.38308	1.38242	1.38177	1.38111	1.38046	1.37980	1.37915	1.37849
.30	1.37784	1.37718	1.37652	1.37586	1.37520	1.37455	1.37389	1.37323	1.37257	1.37191
.31	1.37125	1.37060	1.36994	1.36928	1.36862	1.36796	1.36730	1.36665	1.36599	1.36533
.32	1.36467	1.36401	1.36335	1.36269	1.36203	1.36136	1.36070	1.36004	1.35938	1.35872
.33	1.35806	1.35740	1.35673	1.35607	1.35541	1.35475	1.35409	1.35343	1.35277	1.35210
.34	1.35144	1.35078	1.35011	1.34945	1.34878	1.34812	1.34745	1.34679	1.34613	1.34546
.35	1.34480	1.34413	1.34347	1.34280	1.34214	1.34147	1.34081	1.34014	1.33948	1.33881
.36	1.33815	1.33748	1.33681	1.33614	1.33548	1.33481	1.33414	1.33347	1.33280	1.33213
.37	1.33147	1.33080	1.33013	1.32946	1.32879	1.32812	1.32746	1.32679	1.32612	1.32545
.38	1.32478	1.32411	1.32344	1.32277	1.32209	1.32142	1.32075	1.32008	1.31941	1.31873
.39	1.31806	1.31739	1.31672	1.31604	1.31537	1.31470	1.31403	1.31336	1.31268	1.31201
.40	1.31134	1.31066	1.30999	1.30931	1.30864	1.30796	1.30729	1.30661	1.30594	1.30526
.41	1.30458	1.30391	1.30323	1.30255	1.30187	1.30120	1.30052	1.29984	1.29916	1.29849
.42	1.29781	1.29713	1.29645	1.29577	1.29509	1.29441	1.29373	1.29305	1.29237	1.29169
.43	1.29101	1.29033	1.28965	1.28897	1.28828	1.28760	1.28692	1.28624	1.28556	1.28487
.44	1.28419	1.28351	1.28282	1.28214	1.28145	1.28077	1.28008	1.27940	1.27872	1.27803
.45	1.27735	1.27666	1.27597	1.27529	1.27460	1.27391	1.27323	1.27254	1.27185	1.27116
.46	1.27048	1.26979	1.26910	1.26841	1.26772	1.26703	1.26634	1.26565	1.26496	1.26427
.47	1.26358	1.26289	1.26220	1.26150	1.26081	1.26012	1.25943	1.25874	1.25804	1.25735
.48	1.25666	1.25596	1.25527	1.25457	1.25388	1.25318	1.25249	1.25179	1.25110	1.25040
.49	1.24971	1.24901	1.24831	1.24762	1.24692	1.24622	1.24552	1.24482	1.24413	1.24343
.50	1.24273	1.24203	1.24133	1.24063	1.23992	1.23922	1.23852	1.23782	1.23712	1.23642
.51	1.23572	1.23502	1.23431	1.23361	1.23290	1.23220	1.23150	1.23079	1.23009	1.22938
.52	1.22868	1.22797	1.22726	1.22656	1.22585	1.22514	1.22444	1.22373	1.22302	1.22231
.53	1.22161	1.22090	1.22019	1.21948	1.21876	1.21805	1.21734	1.21663	1.21592	1.21521
.54	1.21450	1.21379	1.21307	1.21236	1.21165	1.21093	1.21022	1.20950	1.20879	1.20808

TABLE IV—*Continued*

f_0/f	0	1	2	3	4	5	6	7	8	9
.55	1.20736	1.20664	1.20593	1.20521	1.20449	1.20377	1.20306	1.20234	1.20162	1.20090
.56	1.20019	1.19946	1.19874	1.19802	1.19730	1.19658	1.19586	1.19514	1.19442	1.19369
.57	1.19297	1.19225	1.19152	1.19080	1.19007	1.18935	1.18862	1.18790	1.18717	1.18645
.58	1.18572	1.18499	1.18426	1.18353	1.18280	1.18208	1.18135	1.18062	1.17989	1.17916
.59	1.17843	1.17770	1.17696	1.17623	1.17550	1.17476	1.17403	1.17330	1.17256	1.17183
.60	1.17110	1.17036	1.16962	1.16888	1.16815	1.16741	1.16667	1.16593	1.16519	1.16446
.61	1.16372	1.16298	1.16224	1.16149	1.16075	1.16001	1.15927	1.15853	1.15778	1.15704
.62	1.15630	1.15555	1.15481	1.15406	1.15331	1.15257	1.15182	1.15107	1.15032	1.14958
.63	1.14883	1.14808	1.14733	1.14658	1.14582	1.14507	1.14432	1.14357	1.14282	1.14207
.64	1.14131	1.14056	1.13980	1.13904	1.13829	1.13753	1.13677	1.13602	1.13526	1.13450
.65	1.13375	1.13298	1.13222	1.13146	1.13070	1.12994	1.12917	1.12841	1.12765	1.12689
.66	1.12613	1.12536	1.12459	1.12382	1.12306	1.12229	1.12152	1.12075	1.11999	1.11922
.67	1.11845	1.11768	1.11690	1.11613	1.11536	1.11459	1.11381	1.11304	1.11227	1.11149
.68	1.11072	1.10994	1.10916	1.10838	1.10760	1.10682	1.10604	1.10526	1.10448	1.10371
.69	1.10293	1.10214	1.10135	1.10057	1.09978	1.09900	1.09821	1.09743	1.09664	1.09586
.70	1.09507	1.09428	1.09349	1.09270	1.09191	1.09112	1.09032	1.08953	1.08874	1.08794
.71	1.08715	1.08635	1.08556	1.08476	1.08396	1.08316	1.08236	1.08156	1.08076	1.07996
.72	1.07916	1.07836	1.07755	1.07675	1.07594	1.07514	1.07433	1.07352	1.07271	1.07191
.73	1.07110	1.07029	1.06947	1.06866	1.06785	1.06704	1.06622	1.06541	1.06459	1.06378
.74	1.06296	1.06214	1.06132	1.06050	1.05968	1.05886	1.05804	1.05721	1.05639	1.05557
.75	1.05474	1.05391	1.05309	1.05226	1.05143	1.05060	1.04977	1.04894	1.04811	1.04727
.76	1.04644	1.04560	1.04477	1.04393	1.04309	1.04226	1.04142	1.04058	1.03973	1.03889
.77	1.03805	1.03721	1.03636	1.03551	1.03467	1.03382	1.03297	1.03212	1.03127	1.03042
.78	1.02957	1.02871	1.02786	1.02700	1.02615	1.02529	1.02443	1.02357	1.02271	1.02185
.79	1.02099	1.02012	1.01925	1.01839	1.01752	1.01666	1.01578	1.01491	1.01404	1.01317
.80	1.01230	1.01142	1.01054	1.00967	1.00879	1.00791	1.00703	1.00615	1.00526	1.00438
.81	1.00350	1.00261	1.00172	1.00083	.99994	.99905	.99816	.99726	.99637	.99547
.82	.99458	.99368	.99278	.99188	.99097	.99007	.98916	.98826	.98735	.98644
.83	.98553	.98462	.98370	.98279	.98187	.98096	.98004	.97912	.97819	.97727
.84	.97635	.97542	.97449	.97356	.97263	.97170	.97077	.96983	.96889	.96796
.85	.96702	.96607	.96513	.96418	.96324	.96229	.96134	.96039	.95944	.95848
.86	.95753	.95657	.95561	.95464	.95368	.95272	.95175	.95078	.94981	.94884
.87	.94787	.94689	.94591	.94493	.94395	.94297	.94198	.94099	.93999	.93900
.88	.93801	.93701	.93601	.93501	.93401	.93301	.93200	.93099	.92998	.92896
.89	.92795	.92693	.92591	.92488	.92386	.92284	.92180	.92077	.91973	.91870
.90	.91766	.91662	.91557	.91452	.91347	.91242	.91136	.91030	.90924	.90818
.91	.90712	.90604	.90496	.90389	.90281	.90174	.90064	.89955	.89846	.89737
.92	.89628	.89518	.89407	.89296	.89185	.89074	.88962	.88850	.88737	.88624
.93	.88511	.88397	.88283	.88168	.88054	.87938	.87823	.87706	.87590	.87473
.94	.87355	.87237	.87119	.87000	.86881	.86761	.86641	.86519	.86398	.86276
.95	.86154	.86031	.85907	.85783	.85658	.85533	.85407	.85280	.85153	.85025
.96	.84896	.84766	.84637	.84505	.84374	.84241	.84108	.83974	.83839	.83703
.97	.83567	.83428	.83290	.83150	.83009	.82867	.82724	.82579	.82434	.82286
.98	.82138	.81988	.81836	.81683	.81528	.81371	.81212	.81051	.80888	.80722
.99	.80553	.80381	.80206	.80027	.79844	.79655	.79460	(refer to table below)		

.9960	0.79460	.9984	0.78954	.9992	0.78765	
.9965	0.79360	.9985	0.78931	.9993	0.78739	
.9970	0.79257	.9986	0.78908	.9994	0.78714	
.9975	0.79152	.9987	0.78885	.9995	0.78688	
.9980	0.79044	.9988	0.78862	.9996	0.78661	
.9981	0.79022	.9989	0.78838	.9997	0.78633	
.9982	0.78999	.9990	0.78814	.9998	0.78605	
.9983	0.78977	.9991	0.78789	.9999	0.78575	
				1.0000	0.78540	

of phase versus frequency and drawing a smooth curve weighting the points in accordance with the errors known by experience to occur for various types

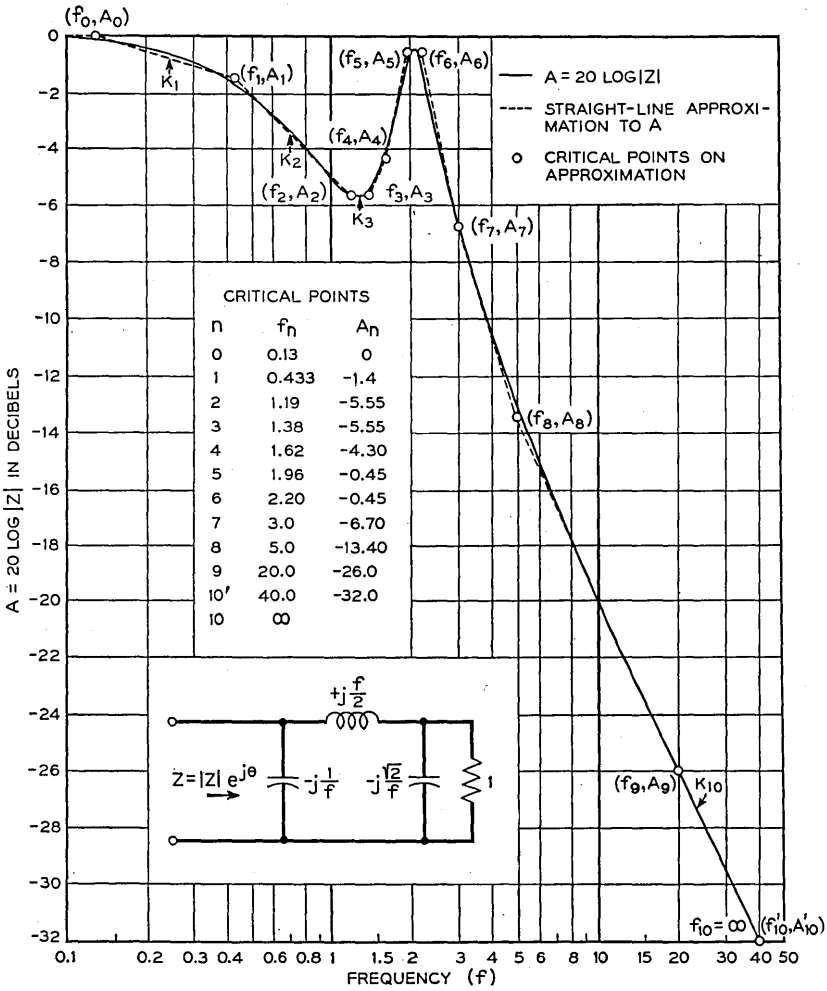

Fig. 5—20 log | Z |.

of departures of the straight line approximation from the exact characteristic.

Although the degree and *db* relationship is applicable to attenuation and phase computations, nepers and radians are proper theoretical units which can be used in other problems[9]. For instance, Tables III and IV give the

[9] Bode, "Network Analysis and Feedback Amplifier Design," Chapter XV, page 340.

reactance in ohms associated with a semi-infinite unit slope of resistance where a unit slope of resistance is one in which a one-ohm change in resistance

TABLE V

TABULATION OF CRITICAL POINTS AND DETERMINATION OF SLOPES OF STRAIGHT LINES APPROXIMATING CHARACTERISTIC OF FIG. 5

n	f_n	A_n	$A_n - A_{n-1}$	$20 \log \frac{f_n}{f_{n-1}}$	k_n
0	.13	0	—	—	—
1	.433	−1.40	−1.40	10.45	−.134
2	1.19	−5.55	−4.15	8.78	−.473
3	1.38	−5.55	.00	1.287	0
4	1.62	−4.30	+1.25	1.393	+.897
5	1.96	−.45	+3.85	1.655	+2.326
6	2.20	−.45	.00	1.003	0
7	3.00	−6.70	−6.25	2.694	−2.320
8	5.00	−13.40	−6.70	4.437	−1.510
9	20.0	−26.00	−12.60	12.04	−1.046
10′	40.0	−32.0	−6.0	6.02	
10	∞				−1.0

Note that $f'_{10} = 40.0$ is chosen to get k_{10} over a finite section of the semi-infinite slope extending to $f = \infty$.

TABLE VI

SUMMATION OF PHASE ASSOCIATED WITH 20 LOG $|Z|$ OF FIG. 5 AT $f = 1.5$

n	f_n from Table V	$\frac{f_n}{f}$	$\frac{f}{f_n}$	θ_n Degrees	$\theta_{n-1} - \theta_n$ Degrees	k_n from Table V	$k_n(\theta_{n-1} - \theta_n)$ Degrees
0	.13	.087		86.824			
1	.433	.289		79.357	7.467	−.134	−1.00
2	1.19	.793		58.349	21.008	−.473	−9.94
3	1.38	.920		51.353	6.996	0	
4	1.62		.926	39.029	12.324	+.897	+11.05
5	1.96		.765	30.283	8.746	+2.326	+20.34
6	2.20		.682	26.450	3.833	0	
7	3.00		.5	18.797	7.653	−2.320	−17.75
8	5.00		.3	11.056	7.741	−1.510	−11.69
9	20.0		.075	2.737	8.319	−1.046	−8.70
10	∞		0	.000	2.737	−1.00	−2.74
						$\Sigma k_n (\theta_{n-1} - \theta_n)$	= −20.43
						$\theta (f = 1.5)$	= −20.4°

Note that for f_0 to f_3 the ratio of f to f_n must be taken f_n/f to be less than unity and θ_n is therefore read from Table II, whereas for f_4 to f_{10} the ratio must be taken f/f_n and θ_n is therefore read from Table I.

occurs between frequencies which are in the ratio $e = 2.7183$. The same technique described above for the determination of the phase associated

TABLE VII
CRITICAL POINTS FOR FIVE LINE APPROXIMATION TO CHARACTERISTIC OF FIG. 5

n	f_n	A_n
0	.25	0
1	1.40	−5.8
2	2.10	0
3	3.00	−7.0
4	10.0	−20.0
5′	40.0	−32.0
5	∞	

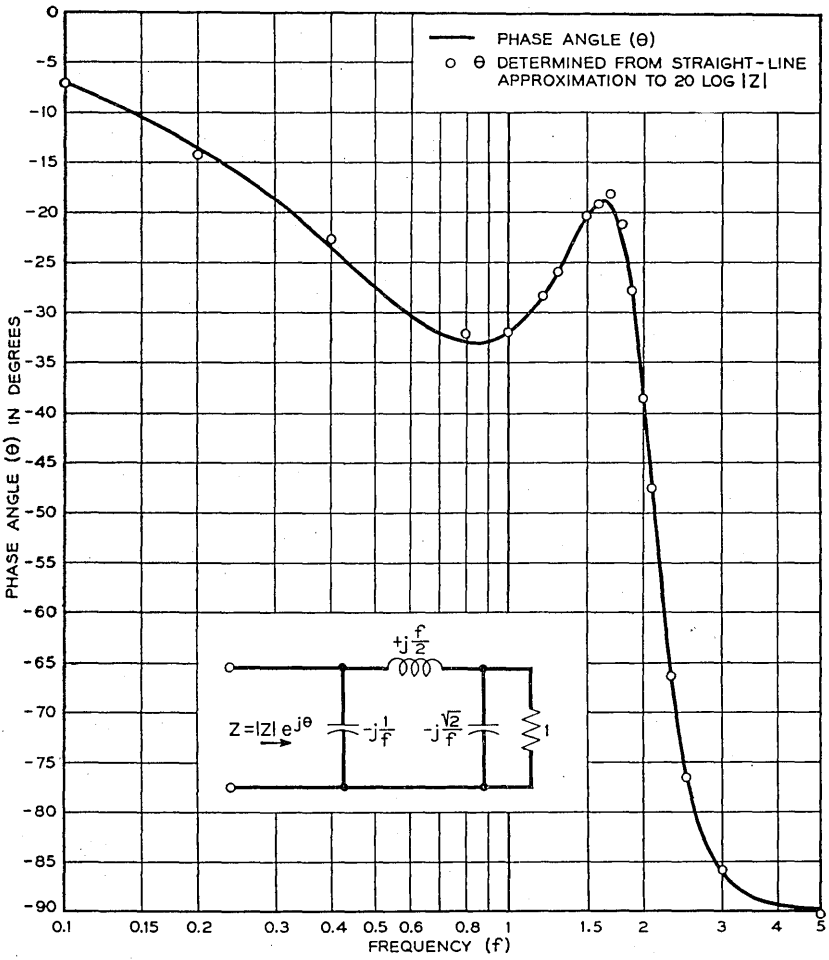

Fig. 6—Phase associated with 20 log | Z | of Fig. 5.

with a given attenuation characteristic may therefore be used to determine the reactance associated with a given resistance characteristic. The only

TABLE VIII
TABULATION OF CRITICAL POINTS AND DETERMINATION OF SLOPES OF STRAIGHT LINES APPROXIMATING RESISTANCE CHARACTERISTIC OF FIG. 7

n	f_n	R_n	$R_n - R_{n-1}$	$2.303 \log \frac{f_n}{f_{n-1}}$	k_n
0	.078	1.000	0		
1	.185	.912	−.088	.864	−.102
2	.290	.805	−.107	.450	−.238
3	.900	.400	−.405	1.133	−.357
4	1.20	.400	0	−	
5	1.50	.547	+.147	.2231	+.659
6	1.67	.840	+.293	.1074	+2.728
7	1.84	1.280	+.440	.0969	+4.54
8	1.92	1.280	0		
9	2.20	.335	−.945	.1361	−6.94
10	2.45	.094	−.241	.1076	−2.24
11	2.85	.015	−.079	.1512	−.52
12	5.00	.000	−.015	.562	−.027

TABLE IX
SUMMATION OF REACTANCE ASSOCIATED WITH RESISTANCE OF FIG. 7 AT $f = 1.0$

n	f_n (From Table VIII)	$\frac{f_n}{f}$	$\frac{f}{f_n}$	X_n Ohms	$X_{n-1} - X_n$ Ohms	k_n (From Table VIII)	$k_n (X_{n-1} - X_n)$ Ohms
0	.078	.078		1.52111			
1	.185	.185		1.45257	.06854	−.102	−.0070
2	.290	.290		1.38439	.06818	−.238	−.0162
3	.90	.900		.91766	.46673	−.357	−.1666
4	1.20		.833	.58801	.32965		
5	1.50		.667	.45004	.13797	+.659	+.0909
6	1.67		.599	.39897	.05107	+2.728	+.1393
7	1.84		.543	.35844	.04053	+4.54	+.1840
8	1.92		.521	.34282	.01562		
9	2.20		.455	.29688	.04594	−6.94	−.3188
10	2.45		.408	.26486	.03202	−2.24	−.0717
11	2.85		.351	.22666	.03820	−.52	−.0199
12	5.00		.200	.12790	.09876	−.027	−.0027
					$\Sigma k_n (X_{n-1} - X_n) = -.1887$		
					$X (f = 1.0) = -.189$ Ohm		

difference is that the slopes of the straight lines approximating the resistance plotted on a log frequency scale are determined by the expression below:

$$k_n = \frac{R_n - R_{n-1}}{\log_e \frac{f_n}{f_{n-1}}} = \frac{R_n - R_{n-1}}{2.303 \log \frac{f_n}{f_{n-1}}}$$

where:

R_n is the resistance at f_n on the straight line approximation to R.

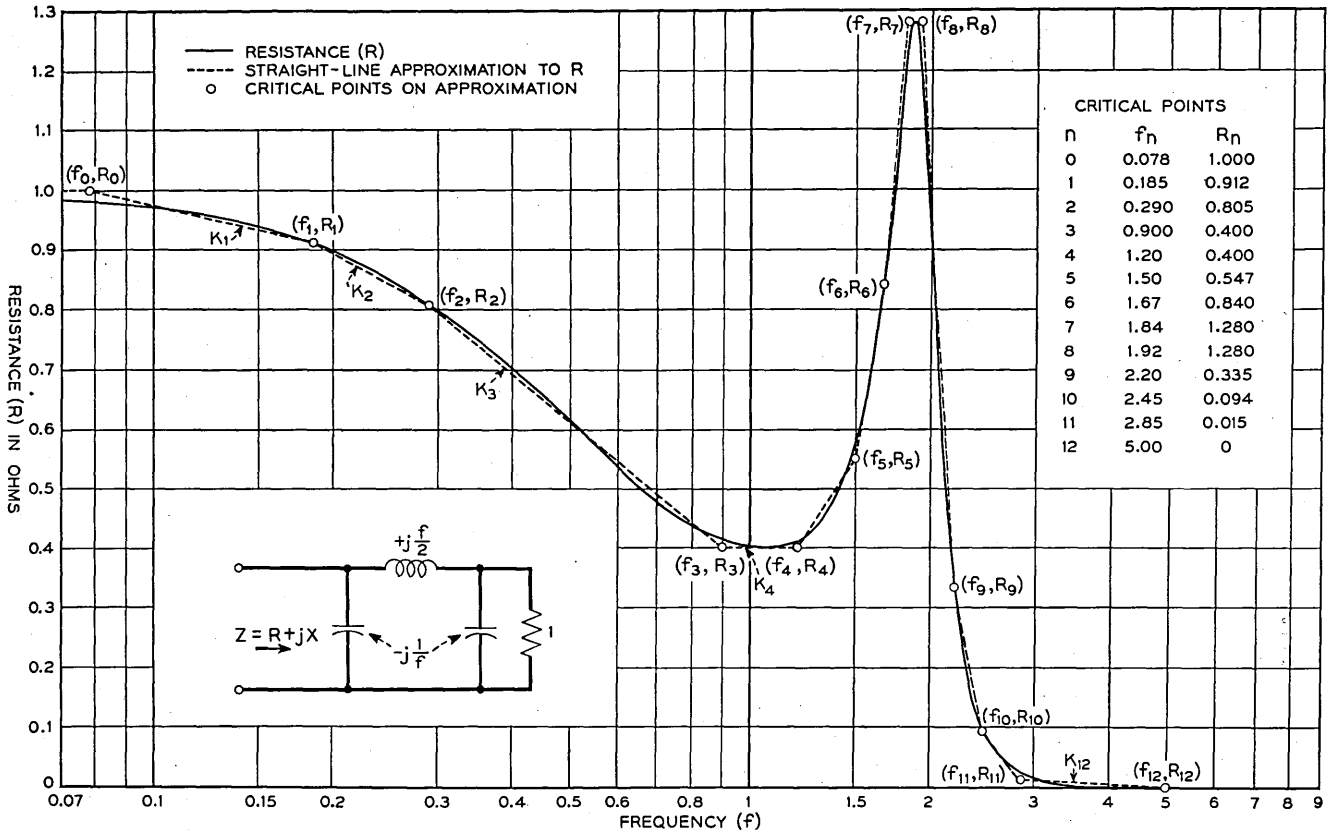

Fig. 7—Resistance characteristic.

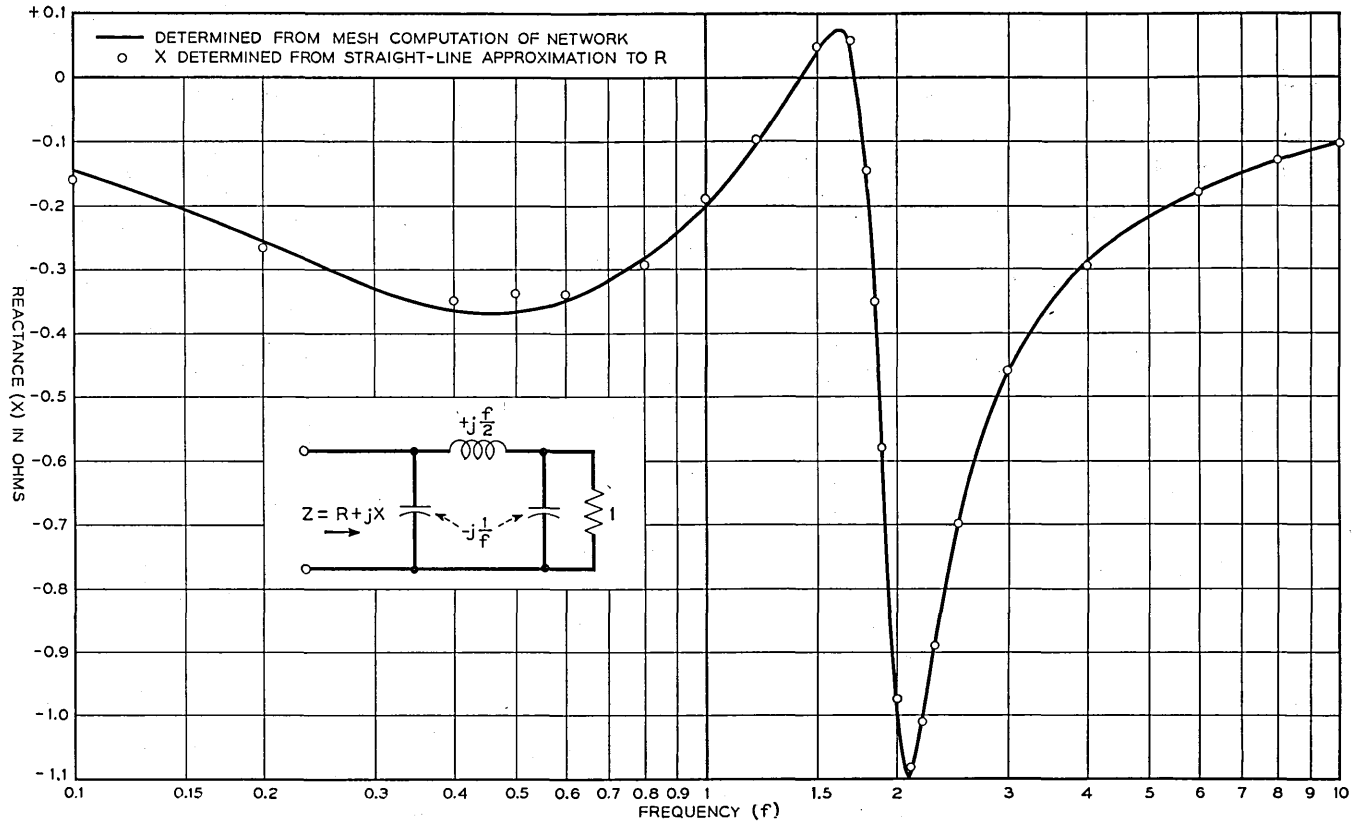

Fig. 8—Reactance associated with resistance characteristic of Fig. 7.

As an example of the determination of the reactance associated with a given resistance characteristic, consider the resistance characteristic of Fig. 7 and the straight line approximation shown in dotted form. The slopes of the straight lines are determined as illustrated in Table VIII.
Having determined the slopes of the various straight lines of the approximation, the reactance can be summed at any desired frequency. As an illustration the reactance is summed at $f = 1.0$, in Table IX.

The mesh computed reactance of the network of Fig. 7 is plotted in Fig. 8 and the reactance summed for $f = 1.0$ is seen to be within .01 ohm of the true reactance. The reactance was summed at a considerable number of frequencies and the results plotted as individual points in Fig. 8. The degree of approximation to the true reactance should be similar to the

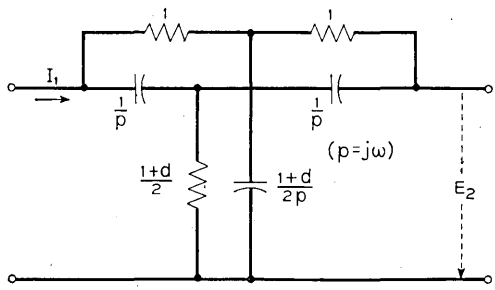

Fig. 9—Parallel T network.

degree of approximation to the original resistance and this is borne out by the example where the straight line approximation to the resistance characteristic is within $\pm$ .03 ohm and the maximum departure of the reactance determined from the straight line approximation is $\pm$ .025 ohm.

As was pointed out in the attenuation example a much simpler straight line approximation to the resistance characteristic would have resulted in a reactance determination without too much greater error than the determination of the illustration.

A word of caution is necessary in connection with the use of the straight line approximation method discussed above. The true phase or reactance is reliably obtained only in those cases where the problem in question is a minimum phase one. In order to illustrate the failure of the method in those problems in which non-minimum phase conditions exist consider the parallel T network of Fig. 9. The transfer impedance Z_{012} defined by the

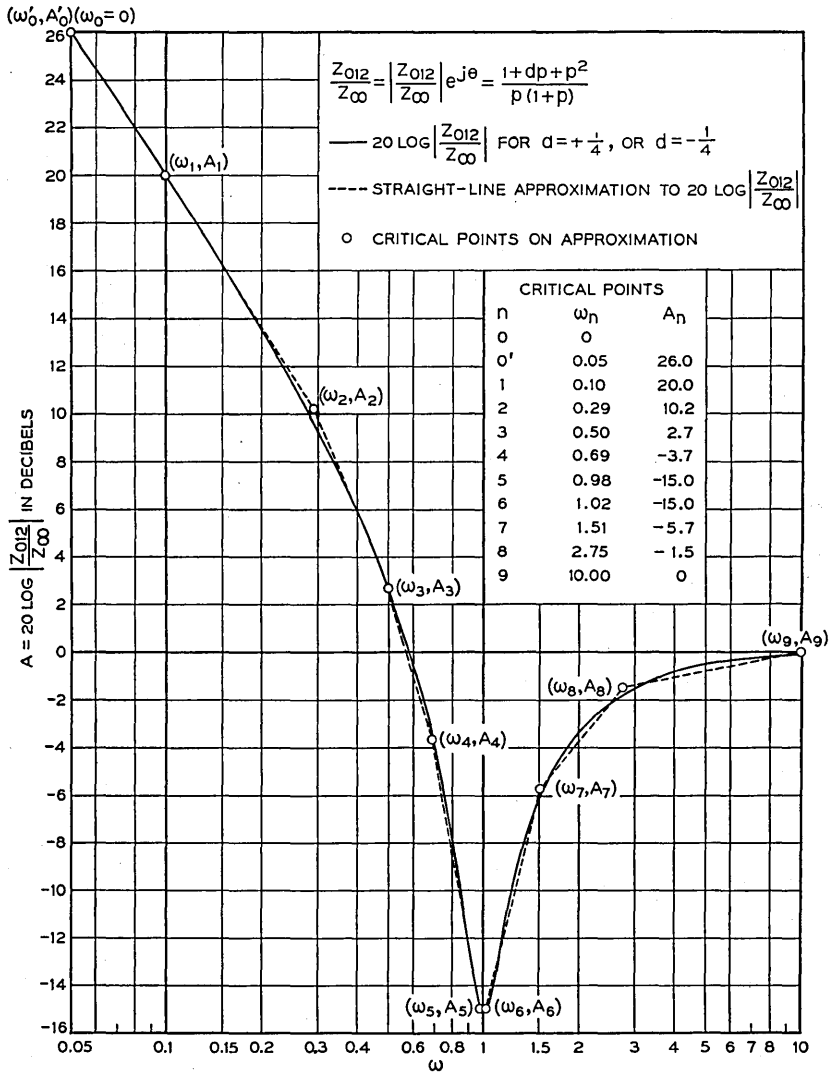

Fig. 10—20 log $\left|\frac{Z_{012}}{Z_\infty}\right|$ for network of Fig. 9.

ratio of the open circuit voltage E_2 to the open circuit driving current I_1 is given by:

$$Z_{012} = \frac{1}{2}\frac{1+d}{2+d}\frac{1+dp+p^2}{p(1+p)}.$$

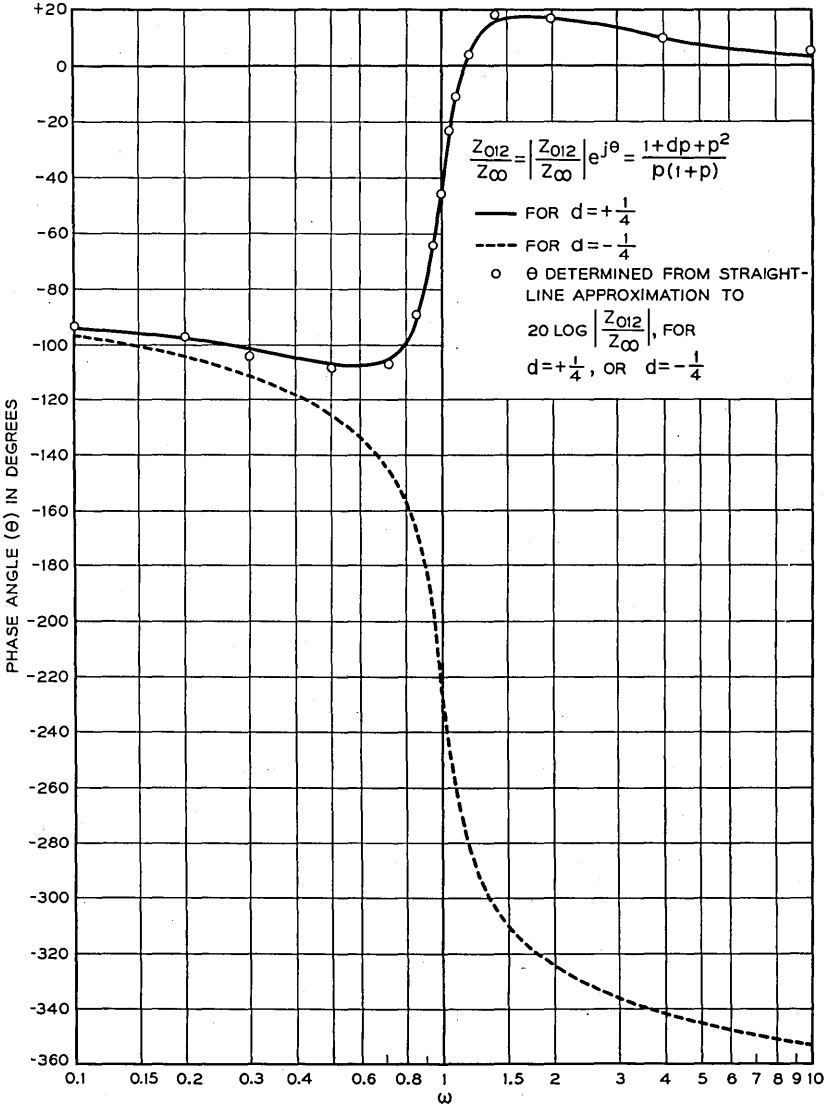

Fig. 11—Phase angle of $\frac{Z_{012}}{Z_\infty}$ for network of Fig. 9.

If we take the ratio of Z_{012} to its value for $\omega = \infty$ then:

$$\frac{Z_{012}}{Z_\infty} = \left|\frac{Z_{012}}{Z_\infty}\right| e^{j\theta} = \frac{1 + dp + p^2}{p(1 + p)}.$$

$20 \log \left| \frac{Z_{012}}{Z_\infty} \right|$ is plotted in Fig. 10 for $d = +1/4$ and it is apparent than $20 \log \left| \frac{Z_{012}}{Z_\infty} \right|$ for $d = -1/4$ is identical. This identity does not hold for θ, however. This is shown in Fig. 11 where θ for $d = +1/4$ and θ for $d = -1/4$ are plotted.

The real characteristic of Fig. 10 was then approximated by a series of straight lines determined by the critical points listed and the phase associated with this straight line approximation summed. The phase so determined is plotted as individual points in Fig. 11. It is seen that this summation determined the phase of the function in question for $d = +1/4$ but completely failed to do so for $d = -1/4$. The function for $d = -1/4$ is an example of a non-minimum phase function for which the above technique fails to determine the phase of the function from its attenuation characteristic.[10]

There are certain instances where the above technique can be usefully applied in connection with non-minimum phase systems in spite of the failure of the method to predict the total phase.[11] However, the necessity of checking for non-minimum phase conditions and, if such exist, determining whether the above method of computing phase is at all applicable, is illustrated by the non-minimum phase example above.

[10] This is the anticipated result since the function is identified as a non-minimum phase function by the fact that it has two zeros falling in the right half p plane.

[11] Bode, "Network Analysis and Feedback Amplifier Design," Chap. XIV, page 309.

Abstracts of Technical Articles by Bell System Authors

Television Network Facilities.[1] L. G. ABRAHAM and H. I. ROMNES. Television networks, like sound broadcasting networks, must be available to make distribution of high quality programs economical. For television circuits interconnecting studios in different cities, coaxial cable and radio relay are the most suitable methods. For short distance transmission balanced wire pairs also may be used. Local conditions will control the type circuit selected.

Protective Coatings on Bell System Cables.[2] V. J. ALBANO and ROBERT POPE. The practice of placing some Bell System cables directly in the ground without the use of conduit was introduced in about 1929. Since bare cable thus installed would be subject to the corrosive action of soils, or damage from lightning or gophers, suitable protective coatings to guard against these hazards had to be developed. Seven types of such coverings are described, and their particular field of application is indicated.

Surface States and Rectification at a Metal Semi-Conductor Contact.[3] JOHN BARDEEN. Localized states (Tamm levels), having energies distributed in the "forbidden" range between the filled band and the conduction band, may exist at the surface of a semi-conductor. A condition of no net charge on the surface atoms may correspond to a partial filling of these states. If the density of surface levels is sufficiently high, there will be an appreciable double layer at the free surface of a semi-conductor formed from a net charge from electrons in surface states and a space charge of opposite sign, similar to that at a rectifying junction, extending into the semi-conductor. This double layer tends to make the work function independent of the height of the Fermi level in the interior (which in turn depends on impurity content). If contact is made with a metal, the difference in work function between metal and semi-conductor is compensated by surface states charge, rather than by a space charge as is ordinarily assumed, so that the space charge layer is independent of the metal. Rectification characteristics are then independent of the metal. These ideas are used to explain results of Meyerhof and others on the relation between contact potential differences and rectification.

[1] *Electrical Engineering*, May 1947.
[2] *Corrosion*, May 1947.
[3] *Phys. Rev.*, May 15, 1947.

Plating on Aluminum.[4] R. A. EHRHARDT* and J. M. GUTHRIE. This article describes tests made to develop a satisfactory process for producing adherent electrodeposits on aluminum alloys using a zincate immersion pretreatment.

Since the major interest was the fabrication of aluminum structures by the use of lead-tin solders the adherence of the deposit was determined by measuring the strength of soldered joints.

Excellent results were obtained with commercially pure aluminum and copper bearing alloys and satisfactory results with magnesium and silicon bearing alloys.

Corrective Networks.[5] F. L. HOPPER. A type of fully compensated constant resistance network is described which provides a larger family of equalization characteristics particularly suited to corrective use in rerecording as determined by aural monitoring.

Spectrochemical Analysis of Ceramics and Other Non-Metallic Materials.[6] EDWIN K. JAYCOX. The procedure described is applicable to the quantitative spectrochemical analysis of ceramics, ashes, ores, paints, and other non-metallic materials for the determination of most of the common metals and their oxides. These include: aluminum, boron, barium, beryllium, calcium, copper, chromium, iron, lithium, magnesium, manganese, sodium, lead, silicon, titanium, zinc, and zirconium, in the general range of 0.30–70.0 per cent. Samples in the form of a fine powder are mixed one part of sample to 10–100 parts of a suitable metal oxide which serves as a buffer, diluent, and internal control. Carbon dust is added to this mixture for its additional buffering effect. Spectra are obtained of the samples and of an appropriate series of standards. Determinations of the amount of element sought are made, in most cases by the well known internal standard technique, in others by the simple comparison standard procedure.

The Spectrochemical Analysis of Nickel Alloys.[7] EDWIN K. JAYCOX. A procedure is described for the analysis of nickel alloys for copper, iron, lead, magnesium, manganese, silicon, titanium, and zinc in the range 0.005–0.30 per cent and for boron in the range 0.0003–0.03 per cent. Samples are taken into solution with dilute nitric acid, evaporated to dryness, and baked at 400°C. The resulting dry nitrate-oxide powder is mixed with pure carbon dust which acts as a buffer and diluent. Aliquots of each sample and of a

[4] *The Monthly Review, American Electroplaters Society,* April 1947.
* Of Bell Tel. Labs.
[5] *Jour. Soc. Motion Pic. Engrs.,* March 1947.
[6] *Jour. Optical Soc. Amer.,* March 1947.
[7] *Jour. Optical Soc. Amer.,* March 1947.

series of standards are excited in the direct current arc, and their spectra recorded on the same plate. Determinations of the amounts of constituent elements present in the sample are made by measuring the logarithm of the ratio of the relative intensities of a line of the element sought to that of a nickel control line by the general internal control technique.

Measurement of the Viscosity and Shear Elasticity of Liquids by Means of a Torsionally Vibrating Crystal.[8] W. P. MASON. This paper describes a method of measuring viscosities of liquids at high frequencies by means of oscillating cylinders, in which a torsionally vibrating crystal generates a viscous wave in the medium to be measured. Both a reactance and a resistance loading occur in the crystal which lowers its frequency and raises the measured resistance at resonance. The viscosity may then be determined by measuring the changes in the properties of the crystal. By varying the voltage on the crystal, the shearing displacement can be varied and hence the viscosity can be measured as a function of shearing stress. Measurements on light oils over a viscosity range from 0.01 poise to 10 poises check within a few per cent when made with rough temperature-control conditions.

Considerations in the Design of Centimeter-Wave Radar Receivers.[9] STEWART E. MILLER. A review of the radar duplexer and receiver, as developed during the war, is presented. Attention is devoted to the principles of operation and typical circuit arrangements employed in the duplexer, the crystal converter, the local-oscillator injection circuits, the intermediate-frequency amplifier, and the automatic-tuning unit. Emphasis is placed on methods found advantageous in the 1-centimeter and 3-centimeter wavelength regions. The interrelation between the various receiver components in determining the over-all receiver noise figure is shown analytically, and typical performance numbers are given.

Experimental Rural Radiotelephony.[10] J. HAROLD MOORE, PAUL K. SEYLER and S. B. WRIGHT. The first rural party-line telephone service utilizing radio installations operating on the subscribers' premises was undertaken experimentally in the vicinity of Cheyenne Wells, near the eastern border of Colorado. Radio links have been used to supply regular telephone service to eight ranches since August 20, 1946. The development of a standard rural radiotelephone system will be aided materially by the experience gained from these experiments.

[8] *Transactions A.S.M.E.*, May 1947.
[9] *Proc. I.R.E.*, April 1947.
[10] *Electrical Engineering*, April 1947.

Alkaline Earth Porcelains Possessing Low Dielectric Loss.[11] M. D. RIGTERINK and R. O. GRISDALE. Alkaline earth porcelains have been prepared from mixtures of clay, flint, and synthetic fluxes consisting of clay calcined with at least three alkaline earth oxides. These porcelains possess excellent dielectric properties, have low coefficients of thermal expansion, are white, and are especially valuable as bases for deposited carbon resistors for which they were developed. Their characteristics make it probable that other uses will be found for materials of this type.

An illustrative composition is 50.0% Florida kaolin, 15.0% flint (325 mesh), 35.0% calcine (200 mesh). The composition of the calcine is 40.0% Florida kaolin, 15.0% $MgCO_3$, 15.0% $CaCO_3$, 15.0% $SrCO_3$, 15.0% $BaCO_3$, calcined at 1200°C. The electrical properties of this body at 1 mc. are Q at 25°C., 2160; Q at 250°C., 280; Q at 350°C., 90; specific resistance at 150°C., $10^{13.5}$ ohm-cm. and at 300°C., $10^{10.7}$ ohm-cm.

Attenuation of Drainage Effects on a Long Uniform Structure with Distributed Drainage.[12] J. M. STANDRING, JR. This paper discusses the general behavior of forced drainage currents on long uniform underground communication cables with particular regard to the case where drainage is applied at regular intervals. Expressions are developed for the structure-to-earth potential which is caused by uniformly spaced drainers when the power supply is from variable e.m.f. sources, such as rectifiers, and also for the case where fixed e.m.f.'s, such as galvanic anodes, are employed.

[11] *Jour. Amer. Ceramic Society*, March 1, 1947.
[12] *Corrosion*, June 1947.

Contributors to this Issue

CLIFFORD E. FAY, B.S. in Electrical Engineering, Washington University, 1925; M.S., 1927. Bell Telephone Laboratories, 1927–. Mr. Fay has been engaged principally in the development of power vacuum tubes for radio purposes.

LAURENCE W. MORRISON, B.S. in Electrical Engineering, University of Wisconsin, 1930. Graduate work, 1930–31. Bell Telephone Laboratories, 1931–. Mr. Morrison was engaged in the development of telephone and television terminal equipment for the coaxial system to 1941. During the past war he was concerned with the development of various radar systems as project engineer. Since 1945 he has been in charge of a group concerned with the development of television transmission over wire facilities.

G. E. MUELLER, B.S., Missouri School of Mines and Metallurgy, 1939; M.S., Purdue University, 1940. Bell Telephone Laboratories, 1940–46. Mr. Mueller was engaged in television and radio research. During the war he worked on radar antenna development. Mr. Mueller is now Assistant Professor of Electrical Engineering at the Ohio State University.

SLOAN D. ROBERTSON, B.E.E., University of Dayton, 1936; M.Sc., Ohio State University, 1938; Ph.D., 1941, Instructor of Electrical Engineering, University of Dayton, 1940. Bell Telephone Laboratories, 1940–. Dr. Robertson was engaged in microwave radar work in the Radio Research Department during the war. He is now engaged in fundamental microwave radio research.

D. E. THOMAS, B.S. in Electrical Engineering, Pennsylvania State College, 1929; M.A., Columbia University, 1932. Bell Telephone Laboratories, 1929–. On Military leave from 1942–46 with U. S. Army Signal Corps and U. S. Army Air Forces. Mr. Thomas has been engaged in investigations of submarine telephone cable systems.

W. A. TYRRELL, B.S., Yale University, 1935; Ph.D., 1939. Bell Telephone Laboratories, 1939–. Dr. Tyrrell has been engaged in waveguide research, principally in the field of microwave loss measurements. During the war he developed a number of waveguide components for Navy radar.